Neural and Molecular Mechnanisms Underlying Mechanotransduction, Thermosensation and Nociception in *Caenorhabditis elegans*.

Marios Chatzigeorgiou

MRC-Laboratory of Molecular Biology

Homerton College

This dissertation is submitted for the degree of Doctor of Philosophy at the University of Cambridge

2011

Preface

I certify that this dissertation is the result of my own work and includes nothing which is the outcome of work done in collaboration except where specifically indicated in the text. No part of this dissertation has been or is currently being submitted for a degree or diploma or any other qualification at any other university. The total length of this dissertation does not exceed 60,000 words.

The text of Chapter Two is a modified version of the work as it appears in Chatzigeorgiou M, Yoo S, Watson JD, Lee WH, Spencer WC, Kindt KS, Hwang SW, Miller DM 3rd, Treinin M, Driscoll M, Schafer WR (2010) Specific roles for DEG/ENaC and TRP channels in touch and thermosensation in *C. elegans* nociceptors. Nature Neuroscience 13(7):861-8. I am the first author in this publication. The contribution of the co-authors is documented at the "Experimental Contributions" section of Chapter 2.

The text of Chapter Three is a modified version of the work as it appears in Chatzigeorgiou M, Grundy L, Kindt KS, Lee WH, Driscoll M, Schafer WR (2010) Spatial asymmetry in the mechanosensory phenotypes of the *C. elegans* DEG/ENaC gene *mec-10* J Neurophysiol 104(6):3334-44. I am the first author in this publication. The contribution of the co-authors is documented at the "Experimental Contributions" section of Chapter 3.

The text of Chapter Four is a modified version of the work as it appears in Chatzigeorgiou M, Schafer WR (2010) Lateral facilitation between primary mechanosensory neurons controls nose touch perception in *C. elegans*. Neuron (In press) I am the first author in this publication. William Schafer supervised the work.

Acknowledgments

I would first like to thank my supervisor Bill Schafer for all his support, advice and enthousiasm during my PhD. Bill has provided me with the trust and freedom to initiate new projects and develop my scientific skills.

I would like to thank my second supervisor Mario de Bono for our fruitful discussions. Robyn Branicky for teaching me a lot of what I know about worms and for editing all of my papers. I shared for two years the calcium imaging scope with James Cregg and I thank him for his help with my imaging experiments. Marina Ezcurra was the person who taught me the basics of calcium imaging and I am grateful for this. I shared a bench with Denise Walker, Victoria Butler and Laura Grundy. I had great fun interacting with them. I spent a lot of time in the lab discussing scientific and non-scientific matters with my friends and colleagues Henrik Bringmann, Eiji Kodama-Namba, Patrick Laurent, Emanuel Busch, Kate Weber and Andre Brown. I would like to thank all my collaborators and in particular the group leaders that supported fruitful collaborations, Monica Driscoll, Millet Treinin, David M Miller and Sun Wook Hwang. I would also like to thank Ithai Rabinowitch for a great project that we are running together over the last few months. I have been lucky to supervise two very talented undergraduates, Buyun Zhao and Stelios Serghiou.

I would like to thank my family, who have always supported me in all of my decisions and my endeavours far away from my country for the past nine years. I am most grateful to my partner Eleni Fistikaki who has seen me through my BSc and PhD. I doubt I could have managed without her!

Finally, I would like to thank Basil Papachristidis, who gave me a chance to open my wings, by leaving Greece as a young teenager and Neil Vargesson, who believed in my potential and supported every scientific step I took.

Summary

The nematode *Caenorhabditis elegans* has a simple nervous system comprised of 302 neurons with known connectivity, displaying a wide range of behaviours with surprising complexity. A major goal of this dissertation has been to understand how genes act in mechanosensory and nociceptive neural circuits to generate behaviour.

Polymodal nociceptors are able to detect noxious stimuli, including harsh touch and extremes of heat and cold. The molecular pathways by which nociceptors sense multiple qualitatively distinct stimuli are poorly understood. I have found that the *C. elegans* PVD neurons are mulitidendritic nociceptors capable of responding to cold shock and harsh touch. Responses to cold require the TRPA-1 channel. Conversely, harsh touch requires the DEG/ENaC proteins MEC-10 and DEGT-1, which are putative components of a harsh touch mechanotransduction complex.

DEG/ENaC channels have been broadly implicated in mechanosensation, yet how these proteins contribute to different mechanosensory modalities remains unclear.

Following the harsh touch study, I examined two different mechanosensory behaviours. Initially, I investigated the response to gentle touch. In *C. elegans*, two DEG/ENaC channel subunits contribute to the gentle touch transduction complex: MEC-4, which is essential for gentle touch sensation, and MEC-10, whose importance is poorly defined. By characterizing a *mec-10* deletion mutant, I found that MEC-10 is important, but not essential, for gentle touch responses in the body touch neurons. Surprisingly, the requirement for MEC-10 is spatially asymmetric, indicating that MEC-10 may contribute only to a subset of gentle touch mechanotransducer complexes.

Finally, I investigated the molecules and multiple classes of mechanoreceptor neurons that are required by *C. elegans* in order to sense head and nose touch. Using

in vivo neuroimaging, I found that one sensory neuron class, the multidendritic FLP nociceptors, respond to harsh touch using DEG/ENaC channels throughout their receptive field but respond to gentle touch only at the tip of the nose. Interestingly, FLP nose touch responses require the activities of additional neurons, which are connected to FLP through a gap junction network and sense mechanical stimuli using TRP channels. More so, I showed that information flow across the network is bidirectional. Thus, nose touch perception involves a hub-and-spoke network that allows individual sensory neurons to integrate information from multiple interconnected mechanoreceptors.

Table of Contents

List of Figures

Chapter 1

Introduction

1.1 *Caenorhabditis elegans*: a model to study neurobiology

Sydney Brenner initiated the scientific use of the nematode worm *Caenorhabditis elegans* in the 1960s (Brenner S, 1974; Brenner S, 1988). Brenner reasoned that given the animal's small size, ease of cultivation, short lifecycle and the powerful genetics one could ask fundamental biological questions in a large spectrum of biological research areas like cellular and molecular biology, developmental biology and neurobiology. *C. elegans* has exceeded Sydney Brenner's expectations, providing researchers with important insight into enigmatic biological phenomena like programmed cell death (apoptosis), aging and RNA interference. Notably *C. elegans* was the first multi-cellular organism with a completely sequenced genome. Two Nobel Prizes have recognized some of the contributions of the worm to basic biology in 2003 and 2006. However, our knowledge of the cellular and molecular basis of *C. elegans* behaviour proceeded more slowly than Sydney Brenner perhaps anticipated. Over the last few years due to further advancements in genetics, electrophysiology and *in vivo* imaging techniques, the worm's full potential in neurobiology is now being realised.

Caenorhabditis elegans is a small, free-living soil nematode, found in a multitude of locations around the world. It has two sexes, hemaphrodites and males both of which are approximately one millimetre long. The adult hemaphrodite has a generation time of 3 days and its body is made of 959 somatic cells of invariant lineage (Brenner S, 1988; Riddle DL et al., 1997). Of these cells, 302 are neurons and 56 are glial cells accounting for 37% of the somatic cells (Sulston JE, Horvitz HR, 1977; Sulston JE et al., 1983).

The nervous system of the worm is composed of the nerve ring in the head, a dorsal and a ventral nerve cord and a number of neurons proximal to the tail. The nerve ring is composed of most interneurons as well as sensory neurons together with their axonal projections. The dorsal and ventral nerve cords are located to the posterior of the nerve ring and run all the way to the tail. The neurons found in the nerve cord are largely motor neurons, while the ventral nerve cord contains the processes of a number of sensory and interneurons located in the middle of the body or close to the tail. The 302 neurons of the adult hemaphrodie fall into 118 classes using morphological and other criteria (White JG et al., 1986). Structurally each neuron is nearly identical between individual animals. This applies also to the neuron cell bodies, which are invariantly positioned (Sulston JE et al., 1983).

Serial electron micrographs have enabled a better understanding of the nematode's nervous system by providing the complete connectivity of all neural cells. This wiring diagram consists of 5,000 chemical synapses, 700 gap junctions and 2,000 neuromuscular junctions (White JG et al., 1986). In comparison, the human brain is composed of around 100 billion neurons, each making on average 7,000 synaptic connections to other partner neurons, yielding a total of up to 500 trillion synapses in the brain (Drachman DA, 2005).

C. elegans neurons differentiate, send out neural processes that migrate to their target neurons, form synapses with the proper targets and synthesize, package and release neurotransmitters. Metabotropic and ionotropic receptors on the postsynaptic neurons act in a direct or indirect fashion in order to activate ion channels, which transmit the signal to their terminals. Higher organisms and worms share common means of chemical neurotransmission (Rankin CH, 2002). Neurotransmitter receptors,

neurotransmitter synthesis and release are highly conserved between *C. elegans* and mammals in contrast to gap junctions and chemosensory receptors which have independently evolved from their vertebrate counterparts. Ion channels are similar to their mammalian homologues but there are no predicted voltage-activated sodium channels in the worm's genome (Bargmann CI, 1998). *C. elegans* uses classical neurotransmitter systems like acetylcholine (Ach), glutamate, GABA (γ-amunobutyric acid), serotonin, dopamine and octopamine, while the neurotransmitter receptors it contains are homologous to their metabotropic and ionotropic counterparts in higher organisms (Brownlee DJ et al., 2000; Brownlee DJ, Fairweather I, 1999). A further important component of the nervous system of the worm is neuropeptide modulation of neurons and other tissues, which generates a wireless network superimposed on the existing wiring diagram (Bargmann CI, 1998). There are at least 28 precursor genes from FMRF-amide-related peptides and at least a further 20 genes that encode apparent neuropeptides (Kim K, Li C, 2004; Nathoo AN et al., 2001).

Despite having a particularly simple nervous system, *C. elegans* can perform a wide range of behaviours, including mating between hemaphrodites and males, chemotaxis to bacterial food sources and chemicals, targeted deposition of eggs by evaluating a number of environmental cues, thermotaxis to cultivation temperatures, avoidance of noxious mechanical, thermal and chemical stimuli, habituation to repeated application of mechanical or chemical stimuli and associative learning where it can pair ions with the presence or absence of food (Bounoutas A, Chalfie M, 2007; Wicks SR, Rankin CH, 1996; Driscoll M, Kaplan J, 1997; Garrity PA et al., 2010).

1.2 Genetics of *Caenorhabditis elegans*

C. elegans is not only an attractive organism due to the easily accessible nervous system that it is equipped with. The worm is particularly amenable to genetic dissection of the mechanisms of neuronal development and function both of which are essential for behaviour. Forward genetic screens in *C. elegans* have been a potent tool to identify novel genes that are important for biological processes like aging, mitosis, axon guidance and behaviour (Bargmann CI, 1998; Dillin A et al., 2002; Wu W et al., 1999). For example, screens for gentle touch insensitive mutants have identified a set of genes that are required for both touch receptor neuron development and function (Chalfie M, Au M, 1989; Chalfie M, Sulston J, 1981; Sulston J et al., 1975). The ability to conduct germline transformations allows the generation of transgenic animals that transmit extrachromosomal arrays in a stable fashion to their offsprings (Mello CC et al., 1991). Thus, one can generate transgenic animals that express a gene of interest in a defined subset of neurons, or suppress the expression of genes by means of cell-specific knockdown with RNAi in neurons, or to express a genetically encoded indicator.

The sequencing of the *C. elegans* genome has revealed a genome size of 97MB and approximately 20,000 genes. The completion of sequencing of numerous other eukaryotic genomes has allowed homology searches, which demonstrate the high degree of conservation between the genes of higher organisms and *C. elegans*. For example, homology searches have revealed C. elegans homologues to mammalian TRP channels like the *C. elegans* TRPA-1 a homologue of TRPA1 (Kindt KS et al., 2007a), OSM-9, which is a homologue of the mammalian TRPV1 (Colbert HA et al., 1997) and TRP-4, which is a TRPN homologue (Li W et al., 2006).

1.3 Mechanosensation in *C. elegans*

Our senses are the physiological means by which stimuli from both outside and inside the body are perceived. The traditional senses are thought to be sight, smell, taste, hearing and touch. The Greek philosopher Aristotle classified the five senses in the ancient times. It is well known that smell, sight and to a large extent taste are mediated by ligands that bind to G-protein coupled receptors. In contrast we know relatively little about the molecular basis of mechanosensation and heat.

The detection of mechanical forces is a fundamental sense present in all organisms. Mammals and insects can hear, when touched worms respond by changing their direction and speed while the Venus Flytrap closes its tentacles when it feels a mechanical stimulus. Bacteria are capable of sensing osmotic pressure, plants are capable of sensing gravity and regulate the direction of their growth with respect to it. Animals can be equipped with a range of mechanosensors that are located in the ears, the skin, or the circumventricular organs, which sample the systemic osmolarity. Mechanosensors is muscle cell spindles can sense muscular stretch and generate proprioreceptive signals, which allow the brain to calculate the position of limbs. Similarly, bones are capable of sensing stress during growth or recovery/regeneration.

The difficulties of understanding mechanosensation in higher organisms arise mostly from the low abundance of the mechanotransducers making their biochemical isolation extremely hard. Researchers turned their attention to genetics to identify candidate molecules that are involved in mechanotransduction. This approach was pioneered in *Caenorhabditis elegans*. In particular the worm exhibits a range of mechanosensory-related behaviours that are amenable to genetic dissection. These

include responses to gentle touch, harsh touch, and nose touch, osmotic avoidance, food-mediated slowing response and male-mating (O'Hagan R, Chalfie M, 2006).

A gentle touch stimulus is delivered to the worm using an eyebrow hair attached to a toothpick. Strokes to the anterior half of the worm's body result in the animals reversing, while stimulation of the posterior half causes the animals to move forwards usually with a strong acceleration (Chalfie M, Sulston J, 1981). Nose touch is also delivered using an eyebrow hair positioned perpendicularly to the direction of movement of the worm. When a worm's nose comes into contact with the eyebrow hair the worm reverses and moves backward. Harsh touch is a more intense stimulus, delivered by a platinum wire and it is mediated by a set of neurons that largely overlaps with the neurons sensing gentle body touch (Chalfie M, Sulston J, 1981; White JG et al., 1986).

The worm has six touch receptor neurons capable of sensing gentle touch. Two bilaterally symmetric pairs of cells are found in the anterior part (ALMR and ALML) and the tail (PLMR and PLML). These cells appear at the embryonic stage and have a single laterally-directed process. Two other neurons (AVM and PVM) appear post-embryonically and are located mid anterior and posterior of the worm with processes projecting to the ventral nerve cord, following the migration of their precursors (Sulston JE, Horvitz HR, 1977).

The morphology of the touch receptor neurons is very simple. They are bipolar cells with a single anteriorly directed process. All the cells branch at the anterior end of the process and occasionally they have a short posterior process extending from the cell body. The touch receptor processes are adjacent to the cuticle which serves their primary function, to sense external mechanical stimuli, resulting in a deflection of the

cuticle. In addition the processes make a number of synaptic and gap junction connections with sensory neurons or interneurons. Two defining characteristics of the gentle touch neurons are the significantly higher amounts of extracellular matrix and the large-diameter, 15-protofilament microtubules that run along their processes (Chalfie M, Sulston J, 1981; Savage C et al., 1989, Du H et al., 1996).

1.4 The building blocks of the mechanosensory channel

The touch receptor neurons, express a number of genes that are required to sense gentle mechanical forces. These include the subunits required to make the mechanosensory channel complex, the molecules required to make the extracellular matrix, two types of tubulin required to make the 15-protofilament microtubules and a few other genes with products of unknown function. Work primarily in the lab of Marty Chalfie has identified five proteins that are needed to transduce gentle touch stimuli. The *mec-4* and *mec-10* genes encode the pore forming subunits. MEC-4 and MEC-10 are degenerins. Degenerins belong to the degenerin/epithelial sodium channel (DEG/ENaC) protein superfamily. Its members can be found both in invertebrates and vertebrates (Alvarez de la Rosa D et al., 2000; Kellenberger S, Schild L, 2002). Gain-of-function alleles of these ion channels cause neuronal degeneration phenotypes (Chalfie M, Wolinsky E, 1990; Driscoll M, Chalfie M, 1991; Huang M, Chalfie M, 1994). A distinctive pharmacological characteristic of the DEG/ENaC channels is that they can be blocked by amiloride (Hamill OP, McBride DW Jr, 1996). *C. elegans* degenerins are thought to function in mechanosensation (Suzuki H et al., 2003; O'Hagan R et al., 2005), and possibly in learning (Voglis G, Tavernarakis N, 2008) and proprioception (Tavernarakis et al., 1997), whereas their

vertebrate counterparts have been shown to underlie processes like nociception, homeostasis of tissues, as well as memory and learning (Wemmie JA et al., 2003; reviewed in Julius D, Basbaum AI, 2001; Chalfie M, 2009; Arnadóttir J, Chalfie M, 2010).

DEG/ENaC proteins have a well-studied topology containing cytoplasmic C- and N-termini, two transmembrane (TM) domains and an extracellular loop with two cystein-rich domains (CRDs). Some, including six out of a total twenty-three C. elegans degenerins have an extra CRD in addition to an extracellular regulatory domain (ERD) that is located in between CRDI and CRDII (Kellenberger S, Schild L, 2002). Analysis of numerous mutations in the *mec-4* gene as well as some in the *mec-10* gene has revealed that the second transmembrane domain (TMII) and the sequence N-terminal to it contribute to the pore of the channel. Mutations in these regions result in a constitutively active channel, inhibit the constitutive activity or change the ion selectivity of the channel (Hong K, Driscoll M, 1994; Hong K et al. 2000, O'Hagan R et al., 2005). Mutations causing a constitutively active channel have been shown to cause neurodegeneration (Chalfie M, Wolinsky E, 1990; Driscoll M, Chalfie M, 1991; Huang M, Chalfie M, 1994). When an alanine scan was performed in the region preceding TMII it was found that substitutions of large side-chain amino acids caused hyperactivation of the channel and a detrimental influx of ions (Driscoll M, Chalfie M, 1991; Hong K, Driscoll M, 1994; Snyder PM et al., 2000). In a similar effort to identify more mutations that cause degeneration, a number of mutations affecting the ERD were identified, indicating that the extracellular loop gates channel activity (Garcia-Anoveros J et al., 1995; Tavernarakis N. et al., 2000). Another interesting observation one can make is that CRDIII is highly conserved between species with

a significant similarity to venom neurotoxin. This observation together with analysis of mutations located in this region of *mec-4* suggests that CRDIII may modulate DEG/ENaC channel gating (Hong K et al., 2000; Vogel BE, Hedgecock EM, 2001). There is a strong body of evidence that supports the model that MEC-4 and MEC-10 transduce gentle touch. Worms that carry mutations in either *mec-4* or *mec-10* are insensitive to gentle touch (Chalfie M, Sulston J, 1981). Gain-of-function mutations have a detrimental phenotype for the gentle touch cells, which degenerate (Chalfie M, Wolinsky E, 1990; Driscoll M, Chalfie M, 1991; Garcia-Anoveros J et al., 1995; Huang M, Chalfie M, 1994). In addition both *mec-10* and *mec-4* are expressed in the six gentle touch neurons. A question that has also been partly addressed is where the gentle touch complex localizes in the gentle touch neurons. In particular MEC-4 localizes to discrete puncta along the touch neuron process where mechanosensory proteins are believed to exist as a complex (Chelur DS et al., 2002). When expressed in heterologous systems, MEC-4 and MEC-10 immunoprecipitate together as well as with other candidate subunits of the mechanosensory complex (Chelur DS et al., 2002; Goodman MB et al., 2002). Interestingly expression of MEC-4d (the product of a gain-of-function allele that causes degeneration) in *Xenopus* oocytes can induce amiloride-sensitive sodium currents. In contrast MEC-10d alone cannot induce a current, but when co-expressed with MEC-4d it modifies the properties of the currents (Goodman MB et al., 2002). This data is complementary with *in vivo* experiments where *mec-4(d)* causes a strong degeneration independent of *mec-10*, in contrast to *mec-10(d)* which causes degeneration with a lower frequency and requires the presence of *mec-4*. More so, *in vivo* electrophysiological and/or calcium imaging

recordings from the gentle touch neurons show that MEC-4 and MEC-10 transduce gentle touch stimuli (Suzuki H et al., 2003; O'Hagan et al., 2005). These observations suggest that MEC-4 and MEC-10 are part of the same mechanotransduction complex but also highlight that there must be functional differences between the two.

MEC-4 and MEC-10 are thought to form the pore of the mechanotransducer, but it has been shown that more proteins are required to form a functional complex. These are encoded by *mec-2*, *unc-24* and *mec-6*. MEC-2 and UNC-24 are encoded by genes, which belong to the family of PHB (prohibitin homology)-domain membrane proteins (Barnes TM et al., 1996; Huang M et al., 1995). The PHB domain is defined by a series of 150 amino acid residues and it is found in a number of proteins such as stomatin, prohibitin, podocin and flotillin in vertebrate organisms. Stomatin has attracted medical interest because loss of stomatin function in red blood cells in individuals with hereditary stomatocytosis results in cell lysis, thus suggesting a potential role for stomatin in ion permeability regulation (Stewart GW et al., 1993). MEC-2, UNC-24 as well as other PHB-domain proteins have a hydrophobic region adjacent to the PHB domain, which allows them to bind to cholesterol, multimerize to form a mechanorecptor complex and localize to the inner layer of the plasma membrane (Barnes TM et al., 1996; Boute N et al., 20000; Huang M et al., 1995; Hubert TB et al., 2006; reviewed in Bounoutas A, Chalfie M, 2007).

While MEC-2 expression is restricted to the six touch receptor neurons, UNC-24 is expressed in a larger set of neurons including many cells in the ventral cord and thus it comes as no surprise that it is required for proper movement and coordination (Barnes TM et al., 1996; Huang M et al., 1995).

Both MEC-2 and UNC-24 colocalize with MEC-4 and coimmunoprecipitate with other subunits of the mechanotransducer (Chelur DS et al., 2002; Goodman MB et al., 2002; Zhang Y et al., 2004). Nonetheless, MEC-2 and UNC-24 affect differently the ability of the worms to sense mechanical stimuli. Examination of *mec-2* null animals shows that their ability to respond to gentle touch stimuli is greatly diminished (Chalfie M, Sulston J, 1981). This is in contrast to *unc-24* mutants. These animals display only a mild touch insensitivity phenotype (Zhang S et al., 2004). Moreover *Xenopus* oocyte electrophysiological recordings have shown that expression of MEC-2 alongside MEC-4d increases currents by forty-fold, while UNC-24 in the presence of MEC-4d has no phenotype, and in the presence of MEC-2 reduces MEC-4d derived currents by as much as 30% (Goodman MB et al., 1998).

MEC-6 is a homologue of the mammalian paraoxonosases and has a broad expression pattern including expression in the touch neurons. MEC-6 colocalizes with MEC-4 puncta in the gentle touch process, while *mec-6* null alleles eliminate the MEC-4 puncta (Chelur DS et al., 2002). Notably, *mec-6* mutant animals are gentle touch insensitive (Chalfie M, Sulston J, 1981), and null alleles suppress the detrimental effects of *mec-4(d)* and *mec-10(d)* induced degeneration in the touch neurons (Chalfie M, Wolinsky E, 1990; Huang M, Chalfie M, 1994). Finally in the *Xenopus* oocyte electrophysiological assays it was shown that MEC-6 has the ability to increase the MEC-4d currents (Chelur DS et al., 2002). The current evidence suggests that MEC-6 has an important role for the proper localization, formation and function of the mechanotransducer complex. Given that it is broadly expressed in the *C. elegans* nervous system it is possible that it can associate with other DEG/ENaC channels in different neurons.

In screens for touch-insensitivite mutants a significant number of genes identified were responsible for forming the mechanotransducing channel complex at the membrane of the touch neurons. Additionally, a number of mutant alleles were isolated and mapped to genes encoding components of the extracellular matrix (ECM). These were *mec-1*, *mec-5* and *mec-9*. Both *mec-1* and *mec-9* are expressed in the touch neurons and encode proteins with EGF- and Kunitz-like domains that are secreted by the touch neurons. MEC-5 is a collagen produced by the epidermal cells located around the touch cells (Du H et al. 1996). MEC-1 and MEC-5 colocalize with MEC-4 puncta all along the process of the touch neuron, providing some evidence for their participation in the mechanotransduction channel complex (Emtage L et al., 2004).

Studies have revealed that the puncate distribution of the mechanosensory complex requires *mec-1*, *mec-5* and *mec-9*. Mutations in any one of these genes lead to an abnormal localization of the pore subunit MEC-4 as well as of the PHB-domain membrane protein MEC-2. In addition the ECM proteins MEC-1 and MEC-5 fail to localize to the mechanotransducing complex in a *mec-9* background (Emtage L et al., 2004, Zhang S, 2004; Bounoutas A, Chalfie M, 2007). Conversely, loss-of-function mutations in *mec-4* or *mec-10* do not affect the proper localization of MEC-1 and MEC-5 (Emtage L et al., 2004). Interestingly, Emtage L et al noted that the puncta localized with the periodic folds of the cuticle termed annuli. These are formed by the hypodermis and this led to the hypothesis that the hypodermis may contribute to the distribution of the mechanotransducing complex. Even more intriguingly mutations in *mec-1* appear to affect touch neurons and the mechanotransducing complex in a various ways. A null mutation of *mec-1* results in animals lacking touch sensitivity

and whose touch neuron processes are stripped of the ECM that attaches them to the body wall (Chalfie M, Sulston J, 1981, Emtage L et al., 2004). In contrast partial loss-of-function alleles of *mec-1* lead to animals showing complete gentle touch insensitivity but have wild type ECM appearance and normal localization of the mechanotransducing complex puncta.

A unique feature of touch receptor neurons is the 15-protofilament microtubules in contrast to the 11-protofilament microtubules found in other cells types (Chalfie M, Thomson JN, 1982). *mec-7* and *mec-12* encode the β-tubulin and the α-tubulin subunits of these 15-protofilament microtubules respectively. (Savage C et al., 1989; Fukushige T et al., 1999). Analysis of *mec-7* and *mec-12* mutant alleles as well as the use of drugs that depolimerize the specialized microtubules like colchicine revealed that animals lacking these cellular components are touch insensitive (Chalfie M, Sulston J, 1981; Chalfie M, Thomson JN, 1982; Bounoutas et al., 2009a). In these mutants the processes of the touch receptor neurons are still intact and they have the ability to grow and extend given that the 11-protofilament microtubules substitute the 15-protofilament microtubules (Chalfie M, Thomson JN, 1982). It has been thought that MEC-7 and MEC-12 have multiple roles in the touch receptor neurons, but it remains unclear what is their precise role in mechanotransduction. Mutations in *mec-7* and *mec-12* can disrupt the punctate pattern of MEC-2 and MEC-4 restricting their presence to the cell body and the proximal region of the process hinting to a potential role of the microtubules in the transport of the mechanotransduction complex along the process (Emtage L et al., 2004; Huang M et al., 1995, Bounoutas et al., 2009a).

Recent work by Bounoutas et al has shown that when the 15-protofilament microtubules are disrupted at the adult stage using late stage treatment with 1mM

Colchicine, the animals have a normal distribution of puncta but are touch insensitive (Bounoutas A, Chalfie M, 2007; Bounoutas et al., 2009a). This led Bounoutas et al to support the idea of a specific role of the microtubules in mechanotransduction.

Similarly, work done by the Goodman lab combining high-pressure freezing and serial-section immunoelectron microscopy determined the position of the mechanotransducing channels with the respect to the putative gating tethers the 15-protofilament microtubules. The mechanotransducing channels visualized using antibodies against MEC-4 and MEC-2 were found to occupy all sides of the touch receptor process but they were shown not to be associated with the distal endpoints of 15-protofilament microtubules. MEC-7 and MEC-12 composed microtubules were found to assemble into a cross-linked bundle linked by kinked filaments to the cell membrane of the process (Cueva JG et al., 2007). Cueva JG et al, suggested that the 15-protofilament microtubules transduced external point forces into membrane stretch thus facilitating mechanotransduction channel activation.

Finally, further proteins that are required for gentle touch sensitivity were identified in screens. Alleles for *mec-14*, *mec-15*, *mec-17* and *mec-18* have been cloned. *mec-14* codes for an oxido-reductase-like protein which is expressed in the six touch receptor neurons (Chalfie et al., unpublished data; Gu G et al., 1996; Bounoutas A, Chalfie M, 2007). MEC-14 has a level of homology to the β-subunit of the *Drosophila shaker* K+ channel. This led Bounoutas A and Chalfie M to speculate that it regulates the mechanotransducer channel complex (Bounoutas A, Chalfie M, 2007).

mec-15 encodes an F-box protein with WD repeats, which is required for the development and function of the *C. elegans* touch receptor neurons (Bounoutas A et al., 2009b). The exact mechanism by which the *mec-15* touch insensitivity phenotype

is derived is yet unclear but it may be atrributed to developmental defects or overexpression of target proteins involved in cytoskeletal organization of the 15 protofilament microtubules.

The product of *mec-17* was identified as aN α-tubulin acetyltransferase that is required for the proper function of touch receptor neurons via MEC-12 acetylation. MEC-17 adapts the α-tubulin MEC-12 for its specific function by acetylation of the ε-amino group of K40 (Akella JS et al., 2010). Failure to do so results in the touch insensitivity phenotype observed in *mec-17* null alleles. Finally, *mec-18* encodes a protein similar to the plant firefly luciferase and plant CoA ligase (reviewed in Bounoutas A, Chalfie M, 2007).

1.5 Other mechanosensory modalities

Although gentle touch sensation is the best-understood mechanosensory modality in *Caenorhabditis elegans*, other mechanosensory-related behaviours have been the subject of intense research. These behaviours include an escape reflex in response to nose touch (Kaplan, J.M., Horvitz, H.R, 1993; Croll NA, 1976), harsh touch to the body (Chalfie M, Sulston J, 1981), food texture-mediated slowing response (Sawin ER et al., 2000), responses to proprioceptive signals from body stretching (Li W et al., 2006; Tavernarakis et al., 1997) and mechanical detection of the vulva by males during mating (Liu KS, Sternberg PW, 1995). These behaviours are mediated at the molecular level either by DEG/ENaC channels or transient receptor potential (TRP) channels.

As described above when an eyelash is placed in the direction of a forward-moving animal it evokes a reversal upon collision. This behaviour is mostly dependent on the

ASH pair of nociceptive neurons as well as a further two neuron classes the OLQ and the FLP neurons (Kaplan JM, Horvitz HR, 1993). OSM-9 and OCR-2, two members of the vanilloid subfamily of transient receptor potential (TRPV), are required for nose touch and for escape responses to several noxious stimuli, they are coexpressed and could potentially interact in the ASH neurons (Colbert HA et al., 1997; Tobin D et al., 2002). OSM-9 is expressed also in the FLP and OLQ neurons. In addition the OLQ neurons express TRPA-1, which is the homologue of the mammalian TRPA1 that has been implicated in many nociceptive functions. *trpa-1* mutants have a behavioural nose touch defect and calcium imaging has a revealed significant reduction in responses following repeated mechanical stimulation of the nose (Kindt KS et al., 2007a). A number of DEG/ENaC channels are expressed in the nose touch neurons. In particular UNC-8 is expressed in ASH and FLP neurons, DEL-1 and MEC-10 in FLP neurons but their role if any was not known (Huang M, Chalfie M, 1994; Tavernarakis N et al., 1997).

The sensation of harsh body touch is mediated by the PVD neurons (Way JC, Chalfie M, 1989). These are a pair of nonciliated neurons, located between the midbody and the tail, extending long anterior and posterior processes that run the entire length of the animal (White JG et al., 1976). As the animals age the PVD processes develop an elaborate dendritic branching pattern that covers most of the surface area of the worm, showing great morphological similarity to the multridendritic neurons of higher organisms (Tsalik EL et al., 2003; Smith CJ et al., 2010; Albeg A et al., 2011). The molecular machinery underlying the sensation of harsh touch stimuli is unknown. Previous work had shown that the DEG/ENaC channel MEC-10 and the TRPV channel OSM-9 are expressed in PVD (Way JC,

Chalfie M, 1989; Colbert HA et al., 1997). Recently, a paper reported microarray data from the PVD neurons. Besides MEC-10 and OSM-9 a number of DEG/ENaC and TRP channels were enriched in PVD. These included DEG/ENaC/ASIC channels DEL-1, ASIC-1, F25D1.4 and the TRP channels TRP-2, GON-2 and GTL-1 (Smith CJ et al., 2010). The effects of their loss-of-function on harsh touch have not been previously investigated.

When *C. elegans* encounters a bacterial lawn or alternatively a patch of Sephadex beads with a size similar to that of bacteria, they slow in response to surface texture. This behaviour requires the presence of eight dopaminergic neurons ADE, CEP and PDE (Sawin ER et al., 2000). The four CEP neurons are located in the head along with the pair of ADE neurons while the pair of PDE neurons are positioned at the posterior midbody sending ciliated processes along the body's lateral midlines (Sulston JE et al., 1980; White JG et al., 1986). These neurons express the TRPN channel TRP-4 (Li et al., 2006). *trp-4* is a homologue of the *Drosophila* and zebrafish *nompC* genes (Sidi S et al., 2003; Walker RG et al., 2000). *trp-4* mutant worms do not slow upon encountering a bacterial lawn (Sidi S et al., 2003). This led to the hypothesis that the dopaminergic neurons might use TRP-4 in order to transduce textural stimuli. Recently, two studies using electrophysiology and calcium imaging have shown that *trp-4* mutations result in irresponsive CEP neurons when presented with a mechanical stimulus (Kang L et al., 2010; Kindt KS et al., 2007b).

Male mating is a complex behaviour that requires a number of orchestrated moves of the male tail, in order to make contact with the hemaphrodite, to sense the vulva, to insert the spicules into the vulva and finally to release sperm (Liu KS, Sternberg PW, 1995). This behaviour is mediated by 87 neurons that are exclusive to the male of

which 42 are ciliated neurons inervating the tail with some being candidate mechanoreceptors (Sulston JE et al.,1980). It has been shown that some of these tail neurons express two TRPP proteins namely LOV-1 and PKD-2, which colocalize (Barr MM et al., 2001; Barr MM, Sternberg PW, 1999; Montell C et al., 2002). The human homologues of these polycystins are PC-1 and PC-2 respectively. They have been involved in inherited polycystic kidney disease (Igarashi P, Somlo S, 2002; Nauli SM et al., 2003). They are localized at the primary cilium of kidney epithelial cells and are though to sense fluid sheer stress.

C. elegans moves in solid substrates by bending its body in a sinusoidal wave. The sinusoidal waveform can be altered by a number of mutations in a set of critical genes that are thought to be involved with proprioception. *trp-4* mutations result in animals that bend their bodies deeper and with higher frequency than wild type (Li W et al., 2006). *trp-4* is not only expressed in the dopaminergic neurons but also in the DVA interneuron (Walker RG et al, 2000). DVA is located in the midbody and extends a process that covers both the anterior and posterior parts of the animal (White JG et al, 1986). The proprioceptive defects of *trp-4* mutants can be rescued by the expression of TRP-4 in DVA (Li W et al., 2006). These results are supported by calcium imaging data showing that body bends generate calcium transients in DVA (Li W et al., 2006).

Yet another candidate for sensing proprioceptive forces is the UNC-8 degenerin. UNC-8 is expressed in a number of neurons including the VA and VB motor neurons. These cells have long, undifferentiated process that may act as proprioceptors (Tavernarakis N et al.,1997; White JG et al., 1986). In addition they express the degenerin DEL-1 that is thought to interact with UNC-8 to form heterologous mechanotransducing channels (Tavernarakis N et al.,1997). *unc-8* mutants have

shallower body bends in comparison to *trp-4* mutants (Tavernarakis N et al.,1997). This has led to the hypothesis that UNC-8 in combination with the VA, VB motorneurons might act opposite to the TRP-4 and DVA combination in order to promote rather than inhibit *C. elegans* body bending (discussed in Schafer WR, 2006; Bounoutas A, Chalfie M, 2007).

1.6 Temperature sensation in animals

1.6.1 Temperature sensation in vertebrates

Temperature is an important environmental cue that affects the rate at which chemical reactions happen, thus affecting animal physiology is a striking manner. Exposure to extreme heat or cold causes dramatic alterations in cellular physiology that can rapidly result in a malfunctioning nervous system and serious tissue damage. Thus thermal nociception -the capacity of an organism to sense and respond to noxious heat and noxious cold- is of great importance for its survival (Tominaga M, Caterina MJ, 2004). Even at milder temperatures, thermal variations can affect animal physiology. Therefore thermotaxis can also make a critical contribution to the animal's fitness. Endotherms, like mammals have developed multiple means of maintaining a fairly constant internal temperature irrespective of the ambient temperature such as behavioural modifications and a central regulation of autonomic nervous system functions (Hensel H,1973; Simon E et al., 1986).

Temperatures over 43°C and about 15°C in mammals not only evoke a thermal sensation, but also a feeling of discomfort and pain (LaMotte RH, Campbell JN, 1978; Tillman et al., 1995a). Researchers have identified the peripheral neurons of the dorsal root ganglia (DRG) and the trigeminal root ganglia as the receptor cells that

sense thermal and mechanical stimuli within the skin (Hensel H, 1981). Notably, a population of such neurons can exhibit great heterogeneity (McKemy DD et al., 2002; Reid G, Flonta ML, 2001b; Story GM et al., 2003). The molecular basis of thermosensation and mechanosensation in the DRG neurons remains largely unknown. A number of candidates have been implicated in cold sensation in DRG neurons. For example, TREK-1 could be closed by cold, causing a depolarization and activation of the DRG neurons (Maingret F et al., 2000; Reid G, Flonta M, 2001a; Viana F et al., 2002). Further candidates in the form of DEG/ENaC channels have also been suggested to play a role in cold transduction (Askwith et al., 2001; Voets T et al., 2007). Generation of knockout animals in mice for TREK-1 and DEG/ENaC channels have not confirmed that they are required for cold sensation (Alloui A et al., 2006; Price MP et al., 2000; Price MP et al., 2001).

More recent lines of evidence implicate a subset of Transient Receptor Potential (TRP) cation channels in vertebrate thermosensation. In particular a total of four TRPV (Vanilloid) family members have been shown to be involved in sensing innocuous and noxious heat (Caterina MJ et al., 1997; Caterina MJ et al., 1999; Caterina MJ et al., 2000; Guler AD et al., 2002; Peier AM et al.,2002b; Smith GD et al., 2002; Xu H et al., 2002; reviewed in Patapoutian A et al., 2003; Dhaka A et al., 2006). Two channels have been shown to be involved in cold sensing. TRPM8 is activated by innocuous cooling (<30°C) and has been shown to be the receptor for menthol and icilin (McKemmy DD et al, 2002; Peier AM et al., 2002a). A knockout mouse provided evidence suggesting that TRPM8 is required *in vivo* to sense unpleasant cold and mediate the effects of cold analgesia (Dhaka et al., 2007). However, TRPM8 knockout animals have wild type responses to subzero

temperatures (Dhaka et al., 2007). The other channel implicated in cold sensation is TRPA1. TRPA1 is activated by noxious cold (<17°C), icilin and pungent chemicals (Bandell M et al., 2007; Jordt SE et al., 2004; Macpherson LJ et al., 2005; Story GM et al. 2003). A number of animal studies have investigated the role of TRPA1 in rats and mice. Knockdown of TRPA1 in rats demonstrated that they are required for inflammation or nerve injury induced cold allodynia (a mode of nociceptive response to an innocuous stimulus) (Obata K et al., 2005) giving strong support for a role of TRPA1 in noxious cold perception. Experiments using a knockout TRPA1 mouse model showed a modest decrement in their ability to respond to noxious cold (Kwan K.Y et al., 2006). Interestingly, there is some ambiguity over TRPA1 activation by cold and its importance in mice for sensing noxious cold (Bautista DM et al., 2004; Jordt SE et al., 2004; also reviewed in Reid G, 2005; Dhaka A et al., 2006).

1.6.2 Temperature sensation in invertebrates

Body temperature in ectotherms like *Caenorhabditis elegans* or *Drosophila melanogaster* varies in accordance with ambient temperature. These organisms use behavioural strategies mediated by temperature transducers located in neurons as their primary mechanism for regulating and maintaining optimal internal temperature (Stevenson RD, 1985; Huey RB et al., 2003).

Distantly related members of the temperature sensing TRP channels have been identified in the popular invertebrate models *Caenorhabditis elegans* and *Drosophila melanogaster* (Dhaka A et al., 2006). Their activation by high or low temperatures as well as their *in vivo* contribution to thermosensation remains unclear. Phylogenetic analysis of the *C. elegans* and *D. melanogaster* genome did not reveal any

orthologues of 4 mammalian TRPVs (TRPV 1-4) (reviewed in Dhaka A et al., 2006). There are no literature reports suggesting the involvement of *Drosophila* or *C. elegans* TRPVs in thermosensation. However, it does seem like they do have a functional role in other sensory modalities. Indeed in *C. elegans* the TRPV channels OSM-9 and OCR-2 are required for chemosensation and mechanosensation. Studies have shown that animals carrying mutations in osm-9 as well as in ocr-2 have severe defects in osmotic avoidance, response to nose touch and to noxious chemical repellents in the polymodal nociceptor neuron ASH (Colbert HA et al., 1997; Tobin D et al., 2002; Hilliard MA et al., 2005; Ezak MJ et al., 2010). Liedtke et al. were able to substitute TRPV4 for OSM-9 in the ASH, thus demonstrate the compatability between the TRPV4 and OSM-9 signaling cascade (Liedtke W et al., 2003). On the contrary expression of TRPV1 in ASH failed to rescue the nociceptive defects of the *osm-9* mutants. However, the TRPV1 worms were able to respond to capsaicin (Liedtke W et al., 2003). In *Drosophila melanogaster* the TRPV4 homologues *nanchung* and *inactive* were found to be activated by osmotic shock and to mediate hearing (Gong Z et al., 2004; Kim J et al 2003).

The single member of the vertebrate TRPA family TRPA1 has attracted a great deal of interest and there is an ongoing debate as to its function in vertebrates. The TRPA family in invertebrates includes four *D. melanogaster* and two *C. elegans* members (reviewed in Dhaka A et al., 2006). The *Drosophila* TRPA1 orthologue, dTRPA1 is activated by a warming stimulus instead of cooling stimulus when tested in *Xenopus* oocytes and it has been shown to control temperature preference in Drosophila by acting as an internal warm sensor (Viswanath V et al., 2003; Hamada FN et al., 2008; Rosenzweig M et al., 2005). dTRPA1 is expressed also in *Drosophila* larvae. It is

expressed in two groups of neurons that regulate normal thermotaxis. However, the body wall neurons that show an increase in intracellular calcium levels in response to warm and cold stimuli do not express dTRPA1 (Liu L et al., 2003). These are multidendritic neurons that express a more distal relative of dTRPA1 called *painless* (Tracey WD Jr et al.. 2003). *painless* was identified in a reverse genetic screen that searched for molecules involved in nociception. *painless* was found to be required both for thermal and mechanical responses. However, a heterologous expression study showed that painless responds directly only to thermal stimuli (Sokabe T et al., 2008). It is important to note that dTRPA1 does not affect noxious heat responses while painless does not affect *Drosophila* larval thermotaxis. Further search for mutants defective in heat responses identified another dTRPA channel named pyrexia (Lee Y et al., 2005). *pyrexia* senses temperatures from 40°C upwards as observed in *Xenopus* oocytes and HEK cells heterologous expression (Lee Y et al., 2005). A striking observation is that *Drosophila* TRPA channels are heat sensitive, which is in contrast to mammalian TRPA1 that is cold activated. The mechanism by which this difference occurs is unknown.

Most research efforts in *C. elegans* thermosensation have focused in the molecular and neural mechanisms regulating thermotaxis. *C. elegans* uses specialized sensory neurons (AFD and AWC) to detect minute changes in temperature through a cGMP-dependent molecular network (reviewed in Garrity PA et al., 2010). The sensory neurons in turn modulate the activity of neural circuits that control migration to preferred temperatures (reviewed in Garrity PA et al., 2010). Only one study has been published looking into how the nematode *C. elegans* responds to noxious thermal stimuli. In particular, Wittenburg N and Baumeister R showed that *C. elegans*

responds to an acute heat stimulus with a reflexive withdrawal reaction. They concluded that thermal avoidance response uses distinct molecular mechanisms from thermotaxis, the thermal nociceptors are located in the head and the tail of the worm and finally that thermal avoidance is modulated by glutamate and neuropeptides (Wittenburg N, Baumeister R, 1999). The identity of the neurons mediating the noxious heat response remains unknown. Similarly the molecules that mediate thermal transduction in these neurons are also unknown. Moreover, there are no published studies, which examine the avoidance response of the worm to noxious cold.

1.7 *In vivo* calcium imaging

The traditional tool in neuroscience for monitoring the activity of neurons is electrophysiology. In *C. elegans* there have been some attempts to take this approach despite the small size and the inaccessibility of neurons. Nonetheless it has remained particularly hard to record neural responses in living animals in response to one or more stimuli. The solution to these difficulties came from genetically-encoded sensors that can be targeted to a subset of neurons under the control of cell-specific promoters in order to monitor *in vivo* responses. Cameleon, a genetically encoded calcium indicator, uses fluorescence resonance energy transefer (FRET) in order to monitor calcium influxes (Miyawaki et al., 1999; Miyawaki et al., 1997). When the cytoplasmic concentrations of calcium are high, like in the case of a neuronal depolarization, the two fluorophores YFP and CFP, which are separated by calmodulin-binding domain, are brought together in order to give a ratiometric measure of calcium response. This tool has now been extensively used to study

neuronal responses in *C. elegans*, including the response properties of neurons responding to touch, chemical, heat and oxygen stimuli.

1.8 Thesis Aims

The aim of this thesis is to investigate the molecular basis of mechanosensation and thermosensation at the level of molecules and neural circuits. In particular my research addresses the following objectives:

- To develop and apply behavioural and in vivo neuroimaging assays to investigate the behaviour of worms and the responses of candidate neurons to harsh mechanical stimuli and noxious cold.
- To determine the identities of the harsh touch mechanotransduction channel components.
- To determine the identity of the cold sensing channel in the putative cold sensing neuron.
- To obtain a better understanding of how the DEG/ENaC channel MEC-10 contributes to mechanosensory transduction in the gentle touch neurons.
- To investigate the molecules and multiple classes of mechanoreceptor neurons that are required by *C. elegans* in order to sense head and nose touch.

1.9 References

Akella JS, Wloga D, Kim J, Starostina NG, Lyons-Abbott S, Morrissette NS, Dougan ST, Kipreos ET, Gaertig J (2010) MEC-17 is an alpha-tubulin acetyltransferase. Nature 467(7312):218-22

Albeg A, Smith CJ, Chatzigeorgiou M, Feitelson DG, Hall DH, Schafer WR, Miller DM 3rd, Treinin M (2011) *C. elegans* multi-dendritic sensory neurons: morphology and function. Mol Cell Neurosci. 46(1):308-317

Alloui A, Zimmermann K, Mamet J, Duprat F, Noel J, Chemin J, Guy N, Blondeau N, Voilley N, Rubat-Coudert C, Borsotto M, Romey G, Heurteaux C, Reeh P, Eschalier A, Lazdunski M (2006) TREK-1, a K+ channel involved in polymodal pain perception. EMBO J. 25, 2368–2376

Alvarez de la Rosa D, Canessa CM, Fyfe GK, Zhang P (2000) Structure and regulation of amiloride-sensitive sodium channels. Annu Rev Physiol 62:573–594

Arnadóttir J, Chalfie M (2010) Eukaryotic mechanosensitive channels. Annu Rev Biophys. 39:111-37

Askwith CC, Benson CJ, Welsh MJ, Snyder PM (2001) DEG/ENaC ion channels involved in sensory transduction are modulated by cold temperature. Proc. Natl. Acad. Sci. USA 98, 6459–6463

Bandell M, Story GM, Hwang SW, Viswanath V, Eid SR, Petrus MJ, Earley TJ, Patapoutian A (2004) Noxious cold ion channel TRPA1 is activated by pungent compounds and bradykinin. Neuron 41(6):849-57

Bargmann, C. I. (1998). Neurobiology of the *Caenorhabditis elegans* genome. Science *282*, 2028-2033

Barnes TM, Jin Y, Horvitz HR, Ruvkun G, Hekimi S (1996) The *Caenorhabditis elegans* behavioral gene unc-24 encodes a novel bipartite protein similar to both erythrocyte band 7.2 (stomatin) and nonspecific lipid transfer protein. J Neurochem 67:46–57

Barr MM, DeModena J, Braun D, Nguyen CQ, Hall DH, Sternberg PW (2001) The *Caenorhabditis* elegans autosomal dominant polycystic kidney disease gene homologs *lov-1* and *pkd-2* act in the same pathway. Curr Biol 11:1341–1346

Barr MM, Sternberg PW (1999) A polycystic kidney-disease gene homologue required for male mating behaviour in *C. elegans*. Nature 401:386–389

Bautista DM, Jordt SE, Nikai T, Tsuruda PR, Read AJ, Poblete J, Yamoah EN, Basbaum AI, Julius D (2006) TRPA1 mediates the inflammatory actions of environmental irritants and proalgesic agents. Cell 124(6):1269-82

Bounoutas A, Chalfie M (2007) Touch sensitivity in *Caenorhabditis elegans* Pflugers Arch – Eur J Physiol 454:691-702

Bounoutas A, O'Hagan R, Chalfie M (2009a) The Multipurpose 15-protofilament Microtubules in *C. elegans* Have Specific Roles in Mechanosensation Current Biol; 19(16):1362-1367

Bounoutas A, Zheng Q, Nonet ML, Chalfie M (2009b) *mec-15* encodes an F-box protein required for touch receptor neuron mechanosensation, synapse formation and development. Genetics 183(2):607-17

Boute N, Gribouval O, Roselli S, Benessy F, Lee H, Fuchshuber A, Dahan K, Gubler MC, Niaudet P, Antignac C (2000) NPHS2, encoding the glomerular protein podocin, is mutated in autosomal recessive steroid-resistant nephrotic syndrome. Nat Genet 24:349–354

Brenner, S. (1974). The genetics of *Caenorhabditis elegans*. Genetics 77,71-94

Brenner, S. (1988). In The Nematode *Caenorhabditis elegans*, W.B. Wood ed (Cold Spring Harbor, New York: Cold Spring Harbor Laboratory Press.)

Brownlee, D., Holden-Dye, L., and Walker, R. (2000). The range and biological activity of FMRFamide-related peptides and classical neurotransmitters in nematodes. Adv Parasitol *45*, 109-180

Brownlee, D. J., and Fairweather, I. (1999) Exploring the neurotransmitter labyrinth in nematodes. Trends Neurosci *22*, 16-24

Caterina MJ, Leffler A, Malmberg AB, Martin WJ, Trafton J, et al. 2000. Impaired nociception and pain sensation in mice lacking the capsaicin receptor. Science 288(5464):306–13

Caterina MJ, Rosen TA, Tominaga M, Brake AJ, Julius D (1999) A capsaicin-receptor homologue with a high threshold for noxious heat. Nature 398(6726):436–41

Caterina MJ, Schumacher MA, Tominaga M, Rosen TA, Levine JD, Julius D (1997) The capsaicin receptor: a heat-activated ion channel in the pain pathway. *Nature* 389(6653):816–24

Chalfie M, (2009) Neurosensory mechanotransduction. Nat Rev Mol Cell Biol. 10(1):44-52

Chalfie M, Au M (1989) Genetic control of differentiation of the *Caenorhabditis elegans* touch receptor neurons. Science 243:1027–1033

Chalfie M, Thomson JN (1982) Structural and functional diversity in the neuronal microtubules of *Caenorhabditis elegans*. J Cell Biol 93:15–23

Chalfie M, Sulston J (1981) Developmental genetics of the mechanosensory neurons of *Caenorhabditis elegans*. Dev Biol 82:358–370

Chalfie M, Wolinsky E (1990) The identification and suppression of inherited neurodegeneration in *Caenorhabditis elegans*. Nature 345:410–416

Chelur DS, Ernstrom GG, Goodman MB, Yao CA, Chen L, ROH, Chalfie M (2002) The mechanosensory protein MEC-6 is a subunit of the *C. elegans* touch-cell degenerin channel. Nature 420:669–673

Colbert HA, Smith TL, Bargmann CI (1997) OSM-9, a novel protein with structural similarity to channels, is required for olfaction, mechanosensation, and olfactory adaptation in *Caenorhabditis elegans*. J Neurosci 17:8259–8269

Croll NA (1976) When *Caenorhabditis elegans* (Nematoda:Rhabditdae) bumps into a bead. Can J Zool 54:566–570

Cueva JG, Mulholland A, Goodman MB (2007) Nanoscale Organization of the MEC-4 DEG/ENaC Sensory Mechanotransduction Channel in *Caenorhabditis elegans* Touch Receptor Neurons J. Neurosci 27(51):14089-14098

Dhaka A, Murray AN, Mathur J, Earley TJ, Petrus MJ, Patapoutian A (2007) TRPM8 is required for cold sensation in mice. Neuron 54(3):345-7

Dhaka A, Viswanath V, Patapounian A (2006) TRP Ion Channels and Temperature Sensation Annu. Rev. Neurosci. 29:135-61

Dillin, A., Hsu, A. L., Arantes-Oliveira, N., Lehrer-Graiwer, J., Hsin, H., Fraser, A. G., Kamath, R. S., Ahringer, J., and Kenyon, C. (2002). Rates of behavior and aging specified by mitochondrial function during development. Science *298*, 2398-2401

Drachman, D. A. (2005). Do we have brain to spare? Neurology *64*, 2004-2005

Driscoll M, Chalfie M (1991) The *mec-4* gene is a member of a family of *Caenorhabditis elegans* genes that can mutate to induce neuronal degeneration. Nature 349:588–593

Driscoll M, Kaplan J (1997) , Mechanosensation and neurodegeneration. In: D Riddle, Editor, *C. elegans* **II**, Cold Spring Harbor Press, Cold Spring Harbor

Du H, Gu G,William CM, Chalfie M (1996) Extracellular proteins needed for *C. elegans* mechanosensation. Neuron 16:183–194

Emtage L, Gu G, Hartwieg E, Chalfie M (2004) Extracellular proteins organize the mechanosensory channel complex in *C. elegans* touch receptor neurons. Neuron 44:795–807

Ezak MJ, Hong E, Chaparro-Garcia A, Ferkey DM (2010) *Caenorhabditis elegans* TRPV channels function in a modality-specific pathway to regulate response to aberrant sensory signaling. Genetics 185(1):233-244

Fukushige T, Siddiqui ZK, Chou M, Culotti JG, Gogonea CB, Siddiqui SS, Hamelin M (1999) MEC-12, an alpha-tubulin required for touch sensitivity in *C. elegans*. J Cell Sci 112(Pt3):395–403

Garcia-Anoveros J, Ma C, Chalfie M (1995) Regulation of *Caenorhabditis elegans* degenerin proteins by a putative extracellular domain. Curr Biol 5:441–448

Garrity PA, Goodman MB, Samuel AD, Sengupta P (2010) Running hot and cold: behavioral strategies, neural circuits, and the molecular machinery for thermotaxis in *C. elegans* and *Drosophila*. Genes Dev. 24(21):2365-82

Gong Z, Son W, Chung YD, Kim J, Shin DW, McClung CA, Lee Y, Lee HW, Chang DJ, Kaang BK, Cho H, Oh U, Hirsh J, Kernan MJ, Kim C (2004) Two interdependent TRPV channel subunits, inactive and Nanchung, mediate hearing in *Drosophila*. J Neurosci. 24(41):9059-66

Goodman MB, Ernstrom GG, Chelur DS, O'Hagan R, Yao CA, Chalfie M (2002) MEC-2 regulates *C. elegans* DEG/ENaC channels needed for mechanosensation. Nature 415:1039–1042

Gu G, Caldwell GA, Chalfie M (1996) Genetic interactions affecting touch sensitivity in *Caenorhabditis elegans*. Proc Natl Acad Sci U S A; 93(13):6577-82

Guler AD, Lee H, Iida T, Shimizu I, Tominaga M, Caterina M (2002). Heat-evoked activation of the ion channel, TRPV4. J. Neurosci. 22(15):6408–14

Hamada FN, Rosenzweig M, Kang K, Pulver SR, Ghezzi A, Jegla TJ, Garrity PA (2008) An internal thermal sensor controlling temperature preference in *Drosophila*. Nature 454(7201):217-20

Hamill OP, McBride DW Jr (1996) The pharmacology of mechanogated membrane ion channels. Pharmacol Rev 48:231– 252

Hensel H (1973). Neural processes in thermoregulation. Physiol Rev 53: 948–1017

Hensel, H (1981). Thermoreception and temperature regulation. Monogr. Physiol. Soc. 38, 1–321

Hilliard MA, Apicella AJ, Kerr R, Suzuki H, Bazzicalupo P, Schafer WR (2005) In vivo imaging of *C. elegans* ASH neurons: cellular response and adaptation to chemical repellents. EMBO J. 24(7):1489

Hong K, Driscoll M (1994) A transmembrane domain of the putative channel subunit MEC-4 influences mechanotransduction and neurodegeneration in *C. elegans*. Nature 367:470–473

Hong K, Mano I, Driscoll M (2000) In vivo structure-function analyses of *Caenorhabditis elegans* MEC-4, a candidate mechanosensory ion channel subunit. J Neurosci 20:2575–2588

Huang M, Chalfie M (1994) Gene interactions affecting mechanosensory transduction in *Caenorhabditis elegans*. Nature 367:467–470

Huang M, Gu G, Ferguson EL, Chalfie M (1995) A stomatin like protein necessary for mechanosensation in *C. elegans*. Nature 378:292–295

Huber TB, Schermer B, Muller, RU, Hohne, M, Bartram, M, Hagmann H, Reinhardt C, Calixto A, Koos F, Kunelmann K, Shirokova E, Krautwurst D, Harteneck C, Simons M, Pavenstadt H, Kerjaschki D, Thiele C, Walz G, Chalfie M, Benzing T (2006) Podocin and MEC-2 bind cholesterol to regulate the activity of associated ion channels. Proc Natl Acad Sci USA 103:17079–17086

Huey RB, Hertz PE, Sinervo B. 2003. Behavioral drive versus behavioral inertia in evolution: A null model approach. Am Nat 161: 357–366

Jordt SE, Bautista DM, Chuang HH, McKemy DD, Zygmunt PM, Högestätt ED, Meng ID, Julius D (2004) Mustard oils and cannabinoids excite sensory nerve fibres through the TRP channel ANKTM1. Nature 427(6971): 260-5

Julius D, Basbaum AI (2001) Molecular mechanisms of nociception. Nature 413(6852):203-10

Igarashi P, Somlo S (2002) Genetics and pathogenesis of polycystic kidney disease. J Am Soc Nephrol 13:2384–2398

Kang L, Gao J, Schafer WR, Xie Z, Xu XZ (2010) *C. elegans* TRP family protein TRP-4 is a pore-forming subunit of a native mechanotransduction channel. Nature 67(3):349-51

Kaplan, JM, Horvitz HR (1993) A dual mechanosensory and chemosensory neuron in *Caenorhabditis elegans*. Proc. Natl. Acad. Sci. USA 90, 2227–2231

Kellenberger S, Schild L (2002) Epithelial sodium channel/degenerin family of ion channels: a variety of functions for a shared structure. Physiol Rev 82:735–767

Kim J, Chung YD, Park DY, Choi S, Shin DW, Soh H, Lee HW, Son W, Yim J, Park CS, Kernan MJ, Kim C (2003) A TRPV family ion channel required for hearing in *Drosophila*. Nature 424(6944):81-4

Kim K, Li C (2004) Expression and regulation of an FMRFamide-related neuropeptide gene family in *Caenorhabditis elegans*. J Comp Neurol 475(4):540-50

Kindt KS, Viswanath V, Macpherson L, Quast K, Hu H, Patapoutian A, Schafer WR (2007a) *Caenorhabditis elegans* TRPA-1 functions in mechanosensation. Nature Neurosci. 10: 568-577

Kindt KS, Quast KB, Giles AC, De S, Hendrey D, Nicastro I, Rankin CH, Schafer WR (2007b) Dopamine mediates context-dependent modulation of sensory plasticity in *C. elegans*. Neuron 55(4):662-76

Kwan KY, Allchorne AJ, Vollrath MA, Christensen AP, Zhang DS, Woolf CJ, Corey DP (2006) TRPA1 contributes to cold, mechanical, and chemical nociception but is not essential for hair-cell transduction. Neuron 50(2):177-80

LaMotte RH, Campbell JN. (1978) Comparison of responses of warm and nociceptive C-fiber afferents in monkey with human judgments of thermal pain. J Neurophysiol 41:509 –528

Lee Y, Lee Y, Lee J, Bang S, Hyun S, Kang J, Hong ST, Bae E, Kaang BK, Kim J (2005) Pyrexia is a new thermal transient receptor potential channel endowing tolerance to high temperatures in *Drosophila melanogaster*. Nat. Genet. 37(3):305-10

Li W, Feng Z, Sternberg PW, Xu XZ (2006) A *C. elegans* stretch receptor neuron revealed by a mechanosensitive TRP channel homologue. Nature 440:684–687

Liedtke W, Tobin DM, Bargmann CI, Friedman JM (2003) Mammalian TRPV4 (VR-OAC) directs behavioral responses to osmotic and mechanical stimuli in *Caenorhabditis elegans*. Proc Natl Acad Sci USA 2:14531-6

Liu KS, Sternberg PW (1995) Sensory regulation of male mating behavior in *Caenorhabditis elegans*. Neuron 14:79–89

Liu L, Yermolaieva O, Johnson WA, Abboud FM, Welsh MJ (2003) Identification and function of thermosensory neurons in *Drosophila* larvae. Nat Neurosci. (3):267-73

Macpherson LJ, Geierstanger BH, Viswanath V, Bandell M, Eid SR, Hwang S, Patapoutian A (2005) The pungency of garlic: activation of TRPA1 and TRPV1 in response to allicin. Curr Biol. 15(10):929-34

Maingret F, Lauritzen I, Patel AJ, Heurteaux C, Reyes R, Lesage F, Lazdunski M, and Honore E (2000) TREK-1 is a heatactivated background K(+) channel. EMBO J. 19, 2483–2491

McKemy DD, Neuhausser WM, Julius D (2002). Identification of a cold receptor reveals a general role for TRP channels in thermosensation. Nature 416, 52–58

Mello, C. C., Kramer, J. M., Stinchcomb, D., and Ambros, V. (1991). Efficient gene transfer in *C. elegans:* extrachromosomal maintenance and integration of transforming sequences. EMBO J *10*, 3959-3970

Miyawaki, A., Griesbeck, O., Heim, R., and Tsien, R. Y. (1999). Dynamic and quantitative Ca2+ measurements using improved cameleons. Proc Natl Acad Sci U S A *96*, 2135-2140

Miyawaki, A., Llopis, J., Heim, R., McCaffery, J. M., Adams, J. A., Ikura, M., and Tsien, R. Y. (1997). Fluorescent indicators for Ca2+ based on green fluorescent proteins and calmodulin. Nature *388*, 882-887

Montell C, Birnbaumer L, Flockerzi V, Bindels RJ, Bruford EA, Caterina MJ, Clapham DE, Harteneck C, Heller S, Julius D, Kojima I, Mori Y, Penner R, Prawitt D, Scharenberg AM, Schultz G, Shimizu N, Zhu MX (2002) A unified nomenclature for the superfamily of TRP cation channels. Mol Cell 9:229–231

Nathoo AN, Moeller RA, Westlund BA, Hart AC (2001) Identification of neuropeptide-like protein gene families in *Caenorhabditis elegans* and other species. Proc Natl Acad Sci U S A. 98(24):14000-5

Nauli SM, Alenghat FJ, Luo Y, Williams E, Vassilev P, Li X, Elia AE, Lu W, Brown EM, Quinn SJ, Ingber DE, Zhou J (2003) Polycystins 1 and 2 mediate mechanosensation in the primary cilium of kidney cells. Nat Genet 33:129–137

Obata K, Katsura H, Mizushima T, Yamanaka H, Kobayashi K, Dai Y, Fukuoka T, Tokunaga A, Tominaga M, Noguchi K (2005) TRPA1 induced in sensory neurons contributes to cold hyperalgesia after inflammation and nerve injury. J Clin Invest. 115(9):2393-401

O'Hagan R, Chalfie M (2006) Mechanosensation in *Caenorhabditis elegans*. Int Rev Neurobiol 69:169–203

O'Hagan R, Chalfie M, Goodman MB (2005) The MEC-4 DEG/ENaC channel of *Caenorhabditis elegans* touch receptor neurons transduces mechanical signals. Nat Neurosci 8:43–50

Patapoutian A, Peier AP, Story GM, Viswanath V (2003) ThermoTRPs and beyond: mechanisms of temperature sensation. Nat. Rev. Neurosci. 4(7):529–39

Peier AM, Moqrich A, Hergarden AC, Reeve AJ, Andersson DA, Story GM, Earley TJ, Dragoni I, McIntyre P, Bevan S, Patapoutian A (2002a) A TRP channel that senses cold stimuli and menthol. Cell 108, 705–715

Peier AM, Reeve AJ, Andersson DA, Moqrich A, Earley TJ, Hergarden AC, Story GM, Colley S, Hogenesch JB, McIntyre P, Bevan S, Patapoutian A (2002b) A heat-sensitive TRP channel expressed in keratinocytes. Science 296(5575):2046-9

Price MP, Lewin GR, McIlwrath SL, Cheng C, Xie J, Heppenstall PA, Stucky CL, Mannsfeldt AG, Brennan TJ, Drummond HA, Qiao J, Benson CJ, Tarr DE, Hrstka RF, Yang B, Williamson RA, Welsh MJ (2000) The mammalian sodium channel BNC1 is required for normal touch sensation. Nature 407(6807):1007-11

Price MP, McIlwrath SL, Xie J, Cheng C, Qiao J, Tarr DE, Sluka KA, Brennan TJ, Lewin GR, Welsh MJ (2001) The DRASIC cation channel contributes to the detection of cutaneous touch and acid stimuli in mice. Neuron 32(6):1071-83

Rankin, C.H. (2002). From gene to identified neuron to behaviour in *Caenorhabditis elegans*. Nat Rev Genet 3, 622-630

Reid G (2005) ThermoTRP channels and cold sensing: What are they really up to? Pflugers Arch. 451(1):250–63

Reid G, Flonta, M (2001a). Cold transduction by inhibition of a background potassium conductance in rat primary sensory neurones. Neurosci. Lett. 297, 171–174

Riddle, D.L., Blumenthal, T., Meyer, B.J., and Price J.R. (1997). Introduction to *C. elegans*. In *C. elegans* II, Riddle, D.L., Blumenthal, T., Meyer, B.J., and Price J.R., eds. (Cold Spring Harbor, NY: Cold Spring Harbor Laboratory Press)

Rosenzweig M, Brennan KM, Tayler TD, Phelps PO, Patapoutian A, Garrity PA (2005) The *Drosophila* ortholog of vertebrate TRPA1 regulates thermotaxis. Genes Dev. 19(4):419-24

Savage C, Hamelin M, Culotti JG, Coulson A, Albertson DG, Chalfie M (1989) mec-7 is a beta-tubulin gene required for the production of 15-protofilament microtubules in *Caenorhabditis elegans*. Genes Dev 3:870–881

Sawin ER, Ranganathan R, Horvitz HR (2000) *C. elegans* locomotory rate is modulated by the environment through a dopaminergic pathway and by experience through a serotonergic pathway. Neuron 26:619–631

Schafer WR (2006) Proprioception: a channel for body sense in the worm. Curr Biol 16:R509–R511

Sidi S, Friedrich RW, Nicolson T (2003) NompC TRP channel required for vertebrate sensory hair cell mechanotransduction. Science 301:96–99

Simon E, Pierau FK, Taylor DC. 1986. Central and peripheral thermal control of effectors in homeothermic temperature regulation. Physiol Rev 66: 235–300

Smith CJ, Watson JD, Spencer WC, O'Brien T, Cha B, Albeg A, Treinin M, Miller DM 3rd (2010) Time-lapse imaging and cell-specific expression profiling reveal dynamic branching and molecular determinants of a multi-dendritic nociceptor in *C. elegans*. Dev Biol. 345(1):18-33

Smith GD, Gunthorpe MJ, Kelsell RE, Hayes PD, Reilly P, Facer P, Wright JE, Jerman JC, Walhin JP, Ooi L, Egerton J, Charles KJ, Smart D, Randall AD, Anand P, Davis JB (2002) TRPV3 is a temperature-sensitive vanilloid receptor-like protein. Nature 418(6894):186-90

Snyder PM, Bucher DB, Olson DR (2000) Gating induces a conformational change in the outer vestibule of ENaC. JGen Physiol 116:781–790

Sokabe T, Tsujiuchi S, Kadowaki T, Tominaga M (2008) *Drosophila* painless is a Ca^{2+}-requiring channel activated by noxious heat. J Neurosci 28(40):9929-38

Stevenson RD. 1985. The relative importance of behavioral and physiological adjustments controlling body temperature interrestrial ectotherms. Am Nat 126: 362–386

Stewart GW, Argent AC, Dash BC (1993) Stomatin: a putative cation transport regulator in the red cell membrane. Biochim Biophys Acta 1225:15–25

Story GM, Peier AM, Reeve AJ, Eid SR, Mosbacher J, Hricik TR, Earley TJ, Hergarden AC, Andersson DA, Hwang SW, et al. (2003) ANKTM1, a TRP-like Channel Expressed in Nociceptive Neurons, Is Activated by Cold Temperatures. Cell 112, 819–829

Sulston J, Dew M, Brenner S (1975) Dopaminergic neurons in the nematode *Caenorhabditis elegans*. J Comp Neurol 163:215–226

Sulston JE, Albertson DG, Thomson JN (1980) The *Caenorhabditis elegans* male: postembryonic development of nongonadal structures. Dev Biol 78:542–57

Sulston, J. E., and Horvitz, H. R. (1977). Post-embryonic cell lineages of the nematode *Caenorhabditis elegans*. Dev Biol *56*, 110-156

Sulston, J. E., Schierenberg, E., White, J. G., and Thomson, J. N. (1983). The embryonic cell lineage of the nematode *Caenorhabditis elegans*. Dev Biol *100*, 64-119

Suzuki H, Kerr R, Bianchi L, Frokjaer-Jensen C, Slone D, Xue J, Gerstbrein B, Driscoll M, Schafer WR (2003) In vivo imaging of *C. elegans* mechanosensory neurons demonstrates a specific role for the MEC-4 channel in the process of gentle touch sensation. Neuron 39:1005–1017

Tavernarakis N, Shreffler W, Wang S, Driscoll M (1997) unc-8, a DEG/ENaC family member, encodes a subunit of a candidate mechanically gated channel that modulates *C. elegans* locomotion. Neuron 18:107–119

Tillman DB, Treede RD, Meyer RA, Campbell JN (1995a) Response of C fibre nociceptors in the anaesthetized monkey to heat stimuli: correlation with pain threshold in humans. J Physiol 485(Pt 3):767–774

Tobin D, Madsen D, Kahn-Kirby A, Peckol E, Moulder G, Barstead R, Maricq A, Bargmann C (2002) Combinatorial expression of TRPV channel proteins defines their sensory functions and subcellular localization in *C. elegans* neurons. Neuron 35:307–318

Tominaga M, Caterina MJ. 2004. Thermosensation and pain. J Neurobiol 61: 3–12

Tracey WD Jr, Wilson RI, Laurent G, Benzer S (2003) painless, a *Drosophila* gene essential for nociception. 113(2):261-73

Tsalik EL, Niacaris T, Wenick AS, Pau K, Avery L, Hobert O (2003) LIM homeobox gene-dependent expression of biogenic amine receptors in restricted regions of the *C. elegans* nervous system. Dev Biol 263:81–102

Viana F, de la Pena E, Belmonte C (2002) Specificity of cold thermotransduction is determined by differential ionic channel expression. Nat. Neurosci. 5, 254–260

Viswanath V, Story GM, Peier AM, Petrus MJ, Lee VM, Hwang SW, Patapoutian A, Jegla T (2003) Opposite thermosensor in fruitfly and mouse. Nature 423(6942):822-3

Voets T, Owsianik G, Janssens A, Talavera K, Nilius B (2007) TRPM8 voltage sensor mutants reveal a mechanism for integrating thermal and chemical stimuli. Nat Chem Biol. 2007 (3):174-82

Voglis G and Tavernarakis N (2008) A synaptic DEG/ENaC ion channel mediates learning in *C. elegans* by facilitating dopamine signalling. The EMBO Journal 27, 3288 - 3299

Vogel BE, Hedgecock EM (2001) Hemicentin, a conserved extracellular member of the immunoglobulin superfamily, organizes epithelial and other cell attachments into oriented line-shaped junctions. Development 128:883–894

Walker RG, Willingham AT, Zuker CS (2000) A *Drosophila* mechanosensory transduction channel. Science 287:2229–2234

Watanabe H, Vriens J, Suh SH, Benham CD, Droogmans G, Nilius B (2002) Heat-evoked activation of TRPV4 channels in a HEK293 cell expression system and in native mouse aorta endothelial cells. J NBiol Chem 277(49):47044-51

Way JC, Chalfie M (1989) The *mec-3* gene of *Caenorhabditis elegans* requires its own product for maintained expression and is expressed in three neuronal cell types. Genes Dev 3:1823–1833

Wemmie JA, Askwith CC, Lamani E, Cassell MD, Freeman Jr JH, Welsh MJ (2003) Acid-sensing ion channel 1 is localized in brain regions with high synaptic density and contributes to fear conditioning. J Neurosci 23: 5496-5502

White JG, Southgate E, Thomson JN, Brenner S (1986) The structure of the nervous system of the nematode *Caenorhabditis elegans.* Philos Trans R Soc Lond 314:1–340

White JG, Southgate E, Thomson JN, Brenner S (1976) The structure of the ventral cord of *Caenorhabditis elegans.* Philos Trans R Soc Lond (Biol) 275:327–348

Wicks SR, Rankin CH, (1996) The integration of antagonistic reflexes revealed by laser ablation of identified neurons determines habituation kinetics of the *Caenorhabditis elegans* tap withdrawal response. *J Comp Physiol A Sens Neural Behav Physiol* 179: 675–685

Wittenburg N, Baumeister R (1999) Thermal avoidance in *Caenorhabditis elegans*: An approach to the study of nociception. Proc Natl Acad Sci USA 96(18):10477-82

Wood WB (1988). Introduction to *C. elegans* biology. In The Nematode *Caenorhabditis elegans*, W.B. Wood ed (Cold Spring Harbor, New York: Cold Spring Harbor Laboratory Press.)

Wu W, Wong K, Chen J, Jiang Z, Dupuis S, Wu JY, Rao Y (1999) Directional guidance of neuronal migration in the olfactory system by the protein Slit. Nature *400*, 331-336

Xu H, Ramsey IS, Kotecha SA, Moran MM, Chong JA, Lawson D, Ge P, Lilly J, Silos-Santiago I, Xie Y, DiStefano PS, Curtis R, Clapham DE (2002) TRPV3 is a calcium-permeable temperature-sensitive cation channel. Nature 418(6894):181-6

Zhang S (2004) Stomatin gene family in *Caenorhabditis elegans*. Ph.D. thesis, Department of Biological Sciences, Columbia University, New York, New York

Zhang S, Arnadottir J, Keller C, Caldwell GA, Yao CA, Chalfie M (2004) MEC-2 is recruited to the putative mechanosensory complex in *C. elegans* touch receptor neurons through its stomatin-like domain. Curr Biol 14:1888–1896

Chapter 2

Specific roles for DEG/ENaC and TRP channels in mechanical and thermal sensation in *C. elegans* polymodal nociceptors

2.1 Abstract

Polymodal nociceptors are sensory neurons that detect noxious stimuli including harsh touch, toxic chemicals, and extremes of heat and cold. The molecular mechanisms by which nociceptors are able to sense multiple qualitatively distinct stimuli are not well-understood. I show here that the *C. elegans* PVD neurons are mulitidendritic nociceptors that respond to harsh touch as well as cold temperatures. The harsh touch modality specifically requires the MEC-10 and DEGT-1 proteins, which are members of the DEG/ENaC family of ion channel subunits. MEC-10 and DEGT-1 protein fusions colocalize in PVD dendritic puncta, implicating them as putative components of a harsh touch mechanotransduction complex. By contrast, responses to cold require the TRPA-1 channel and are MEC-10- and DEGT-1-independent. Heterologous expression of *C. elegans* TRPA-1 can confer cold responsiveness to other *C. elegans* neurons or to mammalian cells, indicating that TRPA-1 is itself a cold sensor. These results show that *C. elegans* nociceptors respond to thermal and mechanical stimuli through distinct molecular mechanisms, and identify DEG/ENaC channels as potential receptors for mechanical pain.

2.2 Introduction

Polymodal nociceptors are sensory neurons that detect aversive stimuli generally perceived as painful. For example, nociceptors respond to harsh touch, extremes of cold and heat, acidic pH, and a variety of toxic chemicals. Although individual nociceptors do not necessarily detect all of these stimuli, the ability to respond to multiple qualitatively distinct aversive cues is a hallmark of both vertebrate and invertebrate nociceptor neurons. Understanding the basis for this polymodality is a

fundamental question: are responses to different stimuli mediated by distinct molecular pathways, or do all responses involve a common polymodal sensory transduction mechanism?

Information about the molecular basis of nociceptive sensory transduction has come primarily from studies of two protein superfamilies: the TRP channels and the DEG/ENaC channels (Patapoutian A et al., 2009; Wemmie JA et al., 2006). TRP channels are non-specific cation channels composed of subunits with six transmembrane α-helices. Several members of the TRP family have been implicated in nociception. For example, TRPV1, the capsaicin receptor, is expressed in mammalian nociceptor neurons and appears to be important for responses to heat, acid, and vanilloid toxins (Caterina MJ et al, 1997; Tominaga et al., 1998). Another TRP channel, TRPM8, is important for sensing cooling as well as cool-mimetic compounds such as menthol (McKemy DD et al., 2002; Peier et al., 2002). Finally, TRPA1, a channel often coexpressed in nociceptors with TRPV1, has been implicated in sensation of noxious cold and a number of chemical irritants as well as non-painful touch, though conflicting results have been obtained for some of these modalities (Story GM et al., 2003; Bandell M et al., 2004; Bautista DM et al., 2006). At least some TRP channels appear to be sufficient by themselves to produce depolarizing currents in response to thermal, chemical or mechanical stimuli, implicating them as potential primary sensory transducers (Christensen et al., 2007; Kahn-Kirby AH, Bargmann CI, 2006).

A second family of candidate nociceptive transduction channels are the DEG/ENaC channels. DEG/ENaC channel subunits have two transmembrane α-helices and the heterotrimeric channels they form are permeable to sodium and in

some cases calcium (Bounoutas A, Chalfie M, 2007). Various members of this family have been linked to sensory transduction processes, including detection of touch, temperature, and acidic pH (Garcia-Anoveros J, Corey DP, 1997). The ASIC subfamily in particular has been implicated in the sensation of pain related to tissue acidification (Price MP et al., 2001). Clear links have also been established between vertebrate and invertebrate DEG/ENaC channels and non-painful mechanosensory processes such as gentle touch (Driscoll M, Chalfie M 1991; O'Hagan R et al., 2005).

Despite significant progress, important questions remain about how painful stimuli are sensed. In particular, the receptor for mechanical pain has not been convincingly identified. Recently, attention has turned to addressing these questions in genetically-tractable invertebrates, such as the nematode *C. elegans*. *C. elegans* contain several neurons with similarities to mammalian polymodal nociceptors. The best characterized are the ASH neurons, ciliated sensory neurons with exposed endings in the animal's nose. The ASH neurons are required for behavioural responses to a variety of aversive stimuli, including noxious chemicals, nose touch, high osmolarity, and acidic pH (Kaplan JM, Horvitz HR, 1993; Hilliard MA et al., 2004). Calcium imaging experiments indicate that each of these stimuli leads to cell-autonomous activation of neural activity in ASH (Hilliard MA et al., 2005). Homologues of TRPV (OSM-9) and TRPA (TRPA-1) are expressed in ASH, and mutations in the former lead to defects in ASH responses to most aversive stimuli (Colbert HA et al., 1997; Tobin D et al., 2002; Kindt KS et al., 2007). *C. elegans* also contain multidendritic neurons (for example the PVDs) that morphologically resemble mammalian nociceptors (Yassin L et al., 2002) and express the OSM-9 (TRPV) and TRPA-1 proteins (Colbert HA et al., 1997; Kindt KS et al., 2007). In addition, the

PVD neurons express the DEG/ENaC protein MEC-10 (Huang M, Chalfie M, 1994) which contributes to a channel complex that is important for mechanotransduction in body touch neurons (Chelur DS et al., 2002; O'Hagan R et al., 2005). Cell ablation experiments have implicated the PVD neurons in sensation and avoidance of harsh body touch (Way JC, Chalfie M, 1989); roles for the PVD neurons in sensation of other noxious stimuli have not been described.

In this study, I investigated the molecular basis for nociceptive transduction in *C. elegans* multidendritic neurons. I found that the PVD neurons respond to harsh touch as well as cold shock, and are required for avoidance responses to these noxious stimuli. The DEG/ENaC protein MEC-10 is essential for responses to harsh body touch, but is not required for responses to cold. A second DEG/ENaC protein, DEGT-1, is also required specifically for harsh touch responses, and may function with MEC-10 in a harsh touch mechanosensory complex. In contrast, responses to acute cold require the TRPA-1 protein, which appears uninvolved in sensing harsh touch. These findings demonstrate that *C. elegans* nociceptors sense harsh touch and noxious cold using distinct molecular mechanisms, and identify the MEC-10 DEG/ENaC channel as a candidate receptor for mechanical pain.

2.3 Results

2.3.1 PVD mutlidendritic nociceptors sense harsh touch and cold

The left and right PVD neurons are located on either side of the animal and envelop the body with multidendritic processes similar to those of mammalian nociceptive neurons (Figure 2.1a, b, c). The PVD neurons have been shown to be important for

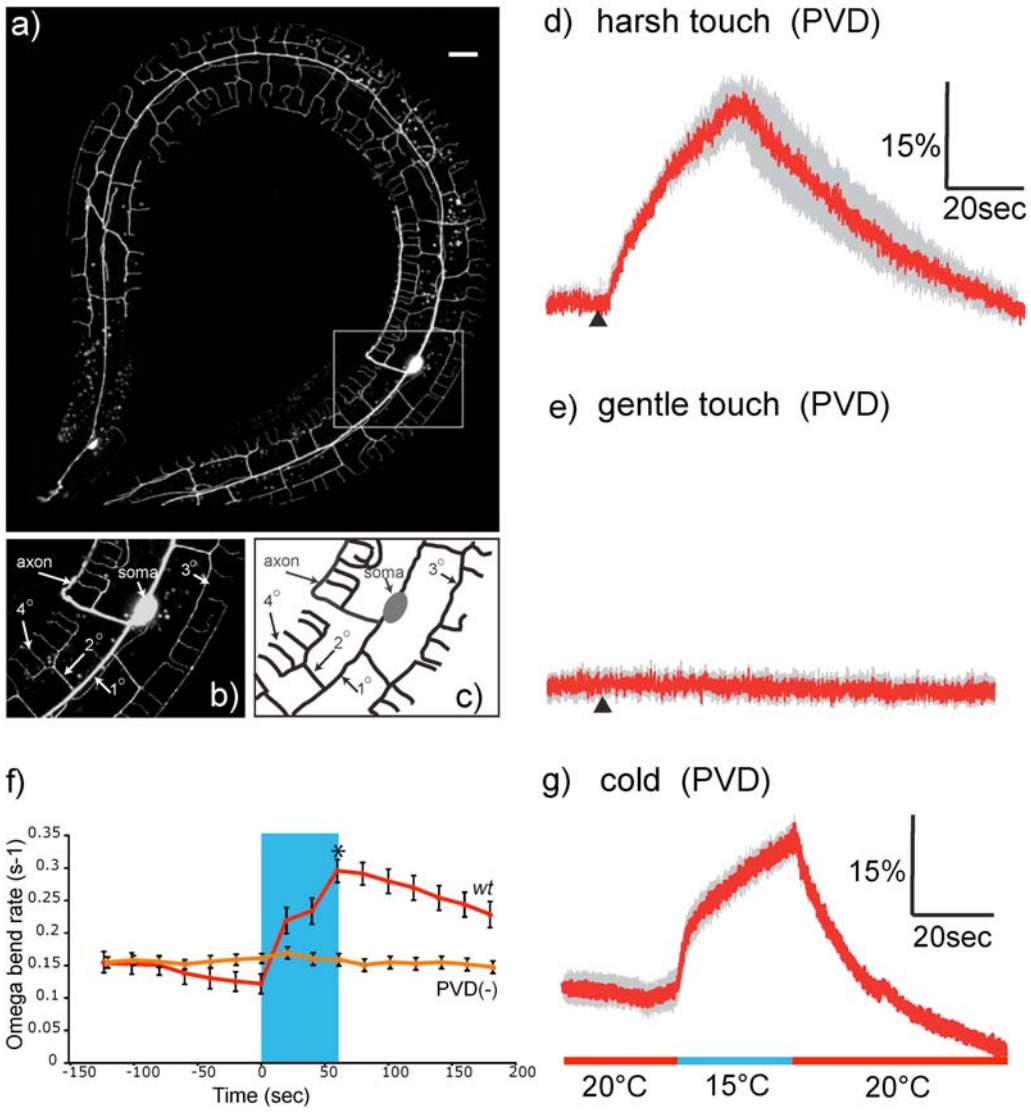

Figure 2.1: PVD neurons respond to harsh touch and cold temperature.

Figure 2.1: PVD neurons respond to harsh touch and cold temperature.

(a–c) PVD neurons display complex dendritic arbours that envelop the worm. Confocal z projection of an adult worm (left side) showing PVDL labelled with a F49H12.4::GFP marker (anterior to left, ventral side corresponds to inside surface of looped worm). PVDR on the right side is excluded from this confocal series. Insets show enlarged view of posterior-lateral location of PVDL cell soma with ventrally projecting axon and orthogonal array of dendritic branches. Scale bar represents 15 μm.

(d,e) Calcium responses to harsh (d) and gentle (e) touch. Each red trace represents the average percentage change in normalized yellow fluorescent protein (YFP)/cyan fluorescent protein (CFP) ratio (R/R_0) for 20 individual recordings. The black triangle indicates the time at which the mechanical stimulus was applied. Grey shading indicates s.e.m. of the mean response.

(f) Behavioural responses to cold shock. Shown are percentages of worms (n = 30) displaying avoidance behaviour (omega bends) during a recording of worms experiencing acute temperature change (15–20 °C). The blue box indicates a 50-s interval during which the buffer temperature was 15 °C; temperature was 20 °C for the remainder of the recording. Error bars indicate s.e.m. Worms in which both PVD neurons were ablated by laser microsurgery (PVD-) were significantly less responsive than intact worms (*$P < 0.05$) according to the Student's t test.

(g) Calcium response to cold shock. Red trace represents the average percentage change in R/R0 for 20 individual recordings; grey shading indicates s.e.m. of the mean response. The lower line indicates the buffer temperature during the recording.

behavioural responses to harsh body touch; in animals lacking the body touch neurons (ALM, AVM, PLM and PVM), PVD ablation significantly compromises escape responses evoked by touching the body with a platinum wire (Way JC, Chalfie M, 1989). To test directly whether these neurons respond to harsh touch, a transgenic line expressing the calcium-sensitive fluorescent protein YC2.3 under the control of the *egl-46* promoter was generated. These animals, designated *ljEx19*, expressed the calcium indicator in the PVD neurons as well as another class of multidendritic neurons, the FLPs. Using this line, I observed that calcium transients could be evoked by a harsh mechanical stimulus of large displacement and high velocity (Figure 1d). In contrast, gentle touch stimuli that activate calcium influx in body touch neurons (e.g. ALM and PLM) did not evoke calcium transients in PVD (Figure 2.1e). Thus, the PVD neurons respond specifically to noxious harsh touch.

To determine whether PVD is involved in sensing other noxious stimuli, I ablated the PVD neurons and assayed responses to various conditions that evoke escape behaviour. In this way, I found that acute cold shock, administered by changing the buffer temperature from 20º to 15º, triggered a robust increase in the frequency of omega turns (Figure 2.1f), a characteristic avoidance response in which animals change their direction of movement by deep body bending (Croll NA, 1975; Gray et al., 2005; Srivastava N et al., 2009). PVD-ablated animals were defective in this response to cold, indicating that the PVD neurons are important for cold-shock avoidance (Figure 2.1f). I also used the *ljEx19* line to determine whether cold shock induced calcium transients in PVD. I observed that temperature downsteps from 20º to 15º led to large calcium transients in PVD (Figure 2.1g). Calcium changes were not observed in response to smaller temperature downsteps, to 15º to 20º upsteps, or

to temperature upsteps from 20º to higher temperatures (Figure 2.2a). Ablations of other neurons, including the AFD thermosensory cells, did not abolish escape responses to 20-15º cold downsteps (Figure 2.2b, c). Thus, the PVD neuron specifically responds to acute cold shock as well as to harsh body touch.

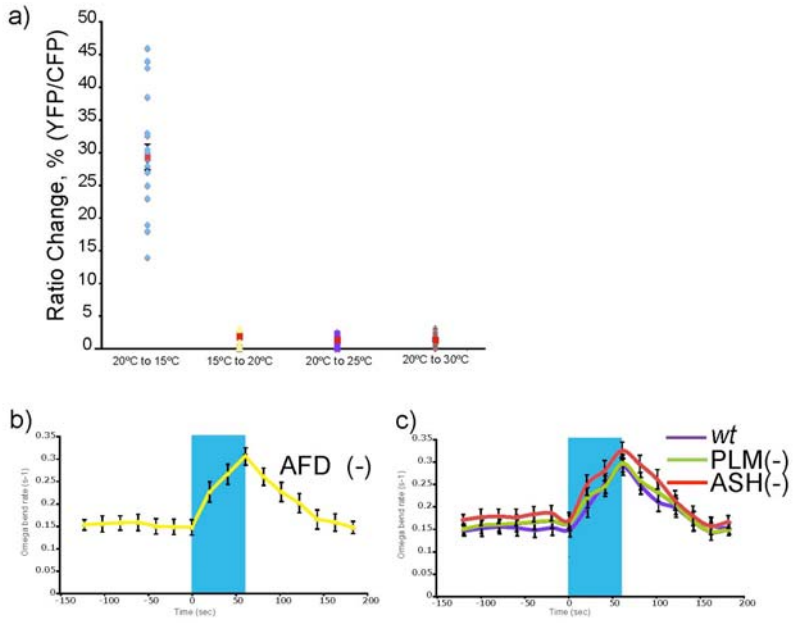

Figure 2.2: Additional data on the thermosensory properties of PVD.

(a) PVD neurons do not respond to temperature upsteps. Scatter plots for peak calcium responses for PVD responses to indicated temperature changes. Calcium recordings from PVD in wild-type *ljEx19* animals were conducted as described in Figure 2.1. 16 animals were recorded for each condition.

(**b–c) Ablations of neurons other than PVD do not affect cold avoidance behaviour.** Shown are percentages of n>20 animals displaying avoidance behaviour (omega bends) during a recording of worms experiencing acute temperature change (20-15º C). For each panel, the blue box indicates a 50 second interval during which the buffer temperature was 15º; temperature was 20º during the remainder of the recording. Error bars indicate SEM.

2.3.2 MEC-10 is required for harsh touch mechanosensation in PVD

To explore the molecular basis for mechanical and thermal nociception in the PVD neurons, I tested the effects of candidate sensory transduction mutants on calcium transients evoked in response to these stimuli. I first investigated the importance of the DEG/ENaC channel protein MEC-10 in harsh touch mechanosensation. After crossing the *ljEx19* array into a *mec-10(tm1552)* deletion mutant background, I observed that *mec-10(tm1552)* mutants exhibited no detectable calcium transients in response to harsh touch stimulation (Figure 2.3a, b). This harsh touch response defect could be rescued by introducing a *mec-10(+)* transgene expressed under the control of the PVD-specific *ser-2prom3* or *egl-46* promoter (Figure 2.3c, f; Figure 2.4a). Harsh touch did not evoke calcium transients in neurons not implicated in harsh touch escape behaviours (Figure 2.4b). To further evaluate the importance of *mec-10* for harsh touch sensation in PVD, I measured harsh touch avoidance behaviour. To focus specifically on the contribution of PVD, I used a *mec-4(u231)* genetic background in which the ALM, AVM and PLM body touch neurons, which respond to gentle as well as harsh touch, were absent (Driscoll M, Chalfie M, 1991). I observed (Figure 2.4c) that in this *mec-4(u231)* background, loss of *mec-10* function caused a significant defect in harsh touch avoidance. This harsh touch behavioural defect was rescued by expression of a *mec-10(+)* transgene in the PVD neurons (Figure 2.4c). Thus, *mec-10* appears to act cell-autonomously in PVD to facilitate a harsh touch response.

I also tested the harsh touch responses of mutants defective in TRP channels expressed in PVD. In contrast to what I had observed for *mec-10* animals, I found that loss-of-function mutants defective in the TRPA channel *trpa-1* or in the TRPV channel *osm-9* showed robust behavioural and PVD calcium responses to harsh touch

stimulation (Figure 2.3d-f; Figure 2.4c). Thus, MEC-10 appears to be specifically essential for harsh touch mechanosensation in PVD, while OSM-9 and TRPA-1 are not required for this process.

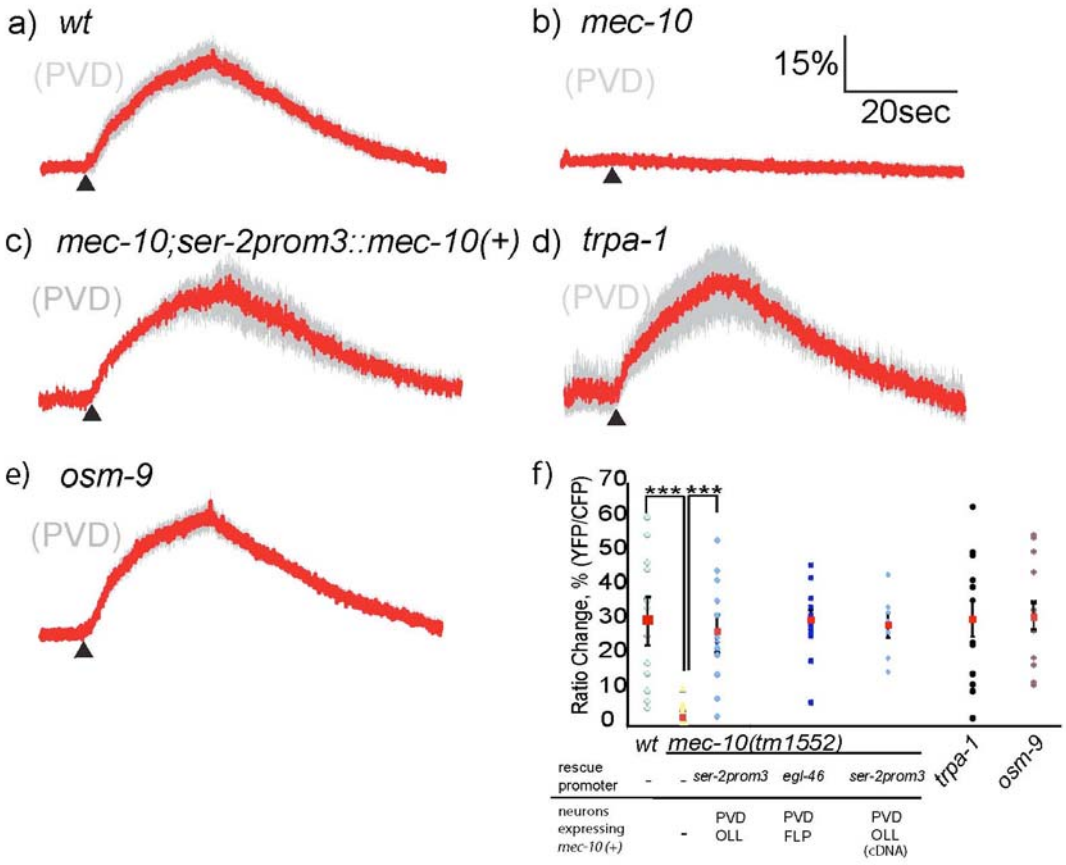

Figure 2.3: *mec-10* is required for harsh touch in PVD.

Figure 2.3: *mec-10* is required for harsh touch in PVD.

(a,b) *mec-10(tm1552)* worms are defective in harsh touch response in PVD. Shown are averaged responses of 17 wild-type (a) and 14 *mec-10(tm1552)* mutant (b) worms to harsh body touch. The red traces represent the average percentage change in normalized YFP/CFP ratio (R/R_0) and the grey shading represents the s.e.m. of the mean response. The triangle indicates the time of the stimulus.

(c) PVD-specific rescue of the *mec-10* harsh touch phenotype. The averaged calcium response of 13 *mec-10(tm1552); ljEx*221 *[pser-2prom-3::mec-10(+)]* worms is shown. Rescue was also observed with a *mec-10* cDNA and with a second PVD-specific promoter, *pegl-46* (see f).

(d,e) *trpa-1* and *osm-9* are not required for harsh touch in PVD. Shown are averaged traces for 13 *trpa-1(ok999)* (d) and 17 *osm-9(ky10)* (e) worms.

(f) Scatter plot of peak calcium responses for each genotype. Statistical significance (***$P < 0.0005$) was determined by the Mann-Whitney rank sum test. Additional genotypes shown include *mec-10(tm1552); ljEx220 [pegl-46::mec-10(+)]* (13 recordings) and *mec-10(tm1552); ljEx230 [pser-2prom-3::mec-10(cDNA)]* (12 recordings).

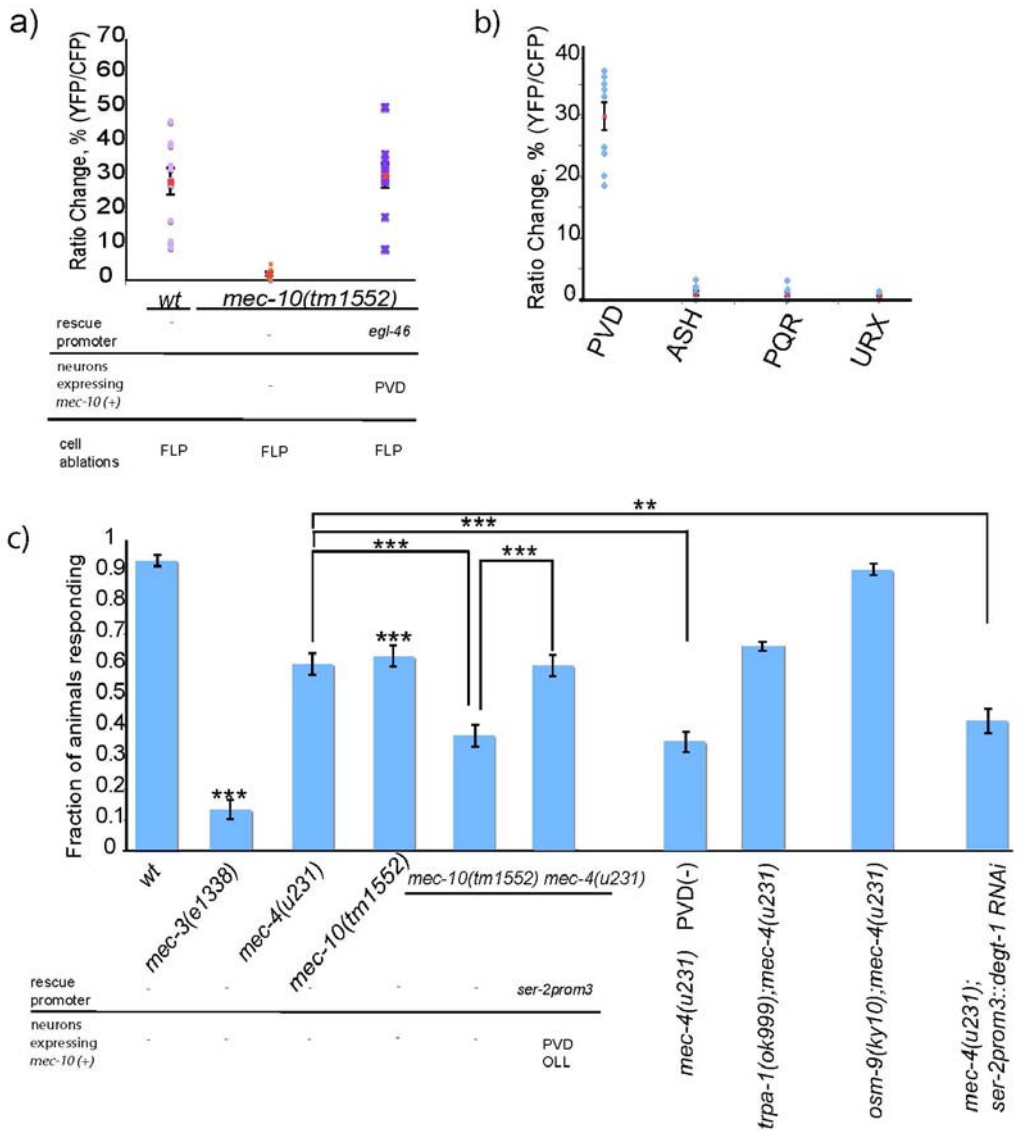

Figure 2.4: Additional data on harsh body touch response in wild-type and mutant animals.

Figure 2.4: Additional data on harsh body touch response in wild-type and mutant animals.

(a) PVD harsh touch response and *mec-10* phenotypes do not depend on the FLP neurons. Shown is a scatter plot of PVD peak calcium responses to harsh touch stimulation for FLP ablated worms. Ablation of FLP in wild-type, *mec-10(tm1552)* and *mec-10(tm1552); ljEx220 [pegl-46::mec-10(+)]* does not affect PVD responses. 12 animals were recorded for each genotype.

(b) Harsh touch does not generally activate *C.elegans* neurons. Shown are scatter plots of wild-type animals expressing cameleon in the indicated neurons. 9 animals were imaged for PVD responses using *ljEx19*, 14 were imaged for ASH responses using *ljEx95[psra-6::YC2.12]* (Hilliard MA et al., 2005) and 13 animals were imaged for PQR and URX responses using a *pgcy-32::YC3.60* line (Persson A et al.,2009).

(c) Effects of *mec-10* and TRP channel genes on PVD-dependent harsh body touch avoidance. Animals were touched on the body with a platinum wire as described; escape responses (reversals) were scored as described. *mec-4(u231)* is a dominant allele that kills touch receptor neurons; the remaining touch response depends largely on PVD. At least 100 animals were tested for each genotype. Statistical significance (***P* < .005, *** *P <0* .0005) is according to the Student's t test; *mec-3(e1338)* and *mec-10(tm1552)* are statistically-different from wild-type (*P* < .0005).

2.3.3 DEGT-1 encodes a second DEG/ENaC subunit required for harsh touch response in nociceptor neurons

What other proteins might contribute to harsh touch mechanosensation in the multidendritic neurons? In contrast to gentle touch, which has been subjected to intense genetic and physiological study, relatively little is known about the molecular basis for harsh touch in *C. elegans.* Since expression of activated MEC-10 without MEC-4 does not produce functional channels in *Xenopus* oocytes (Goodman MB et al., 2002; Bianchi L et al., 2004) MEC-10 may not be able to form homomeric channels. *C. elegans* contains at least 28 DEG channel genes (Goodman MB, 2006), most with uncharacterized expression patterns. Thus, I reasoned that another DEG/ENaC channel protein might function along with MEC-10 in harsh touch mechanoreceptors.

To identify such a protein, the results of expression profiling experiments identifying genes with transcripts that are enriched in PVD were analyzed (Smith CJ et al., 2010). Among the PVD-enriched genes were four DEG/ENaC channels: *mec-10, del-1, asic-1*, and an uncharacterized gene, F25D1.4 (Table 2.1). *del-1* and *asic-1* deletion alleles had no measurable abnormalities in harsh touch escape behaviour or harsh touch-evoked calcium transients in PVD (Figure 2.5), so I focused our attention on F25D1.4.

Gene name	Sequence name	Fold Enriched	FDR
mec-10	F16F9.5	1.7x	< 1 %
mec-4	T01C8.7	1.1	> 10%
del-1	E02H4.1	4.3	< 1 %
asic-1	ZK770.1	1.9	< 1 %
degt-1	F25D1.4	1.7	< 1 %

Table 2.1: DEG/ENaC channel genes showing significant enrichment in PVD/OLL.

Shown are the fold enrichment and false discovery rate (FDR) for the four DEG/ENaC channels with a false discovery rate <1%. Data for *mec-4*, which was not significantly enriched, is shown for comparison. None of the other DEG/ENaC genes showed significant (<10%) enrichment (Smith CJ et al., 2010).

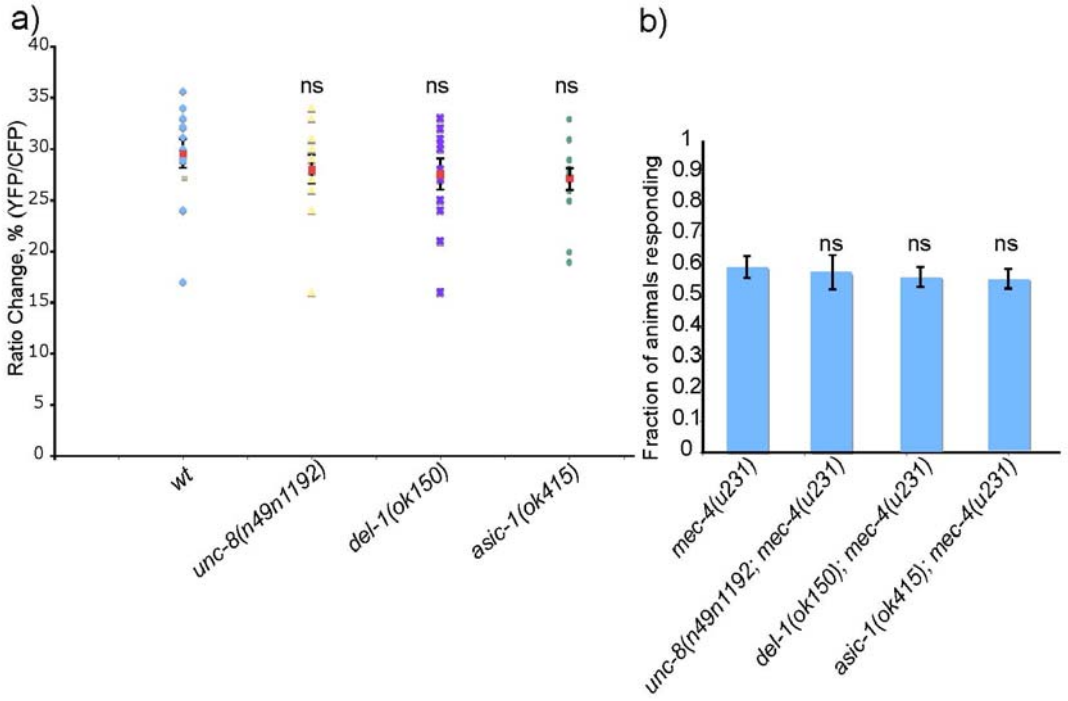

Figure 2.5: Effects of other DEG/ENaC channels on harsh touch.

(a) Scatter plot of peak calcium responses for each genotype. Animals expressing cameleon in PVD neurons (array *ljEx19*) were given a harsh touch stimulus on the body, as described in Experimental Procedures. In response to the stimulus 12 wild-type animals gave an average R/R_0 = 29.5%, 12 *unc-8(n491n1192)* animals responded with an average R/R_0= 28%, 12 *del-1(ok150)* gave an average R/R_0= 27.5% and 12 *asic-1(ok415)* gave an average R/R_0 of 27.2 %. Statistical significance (ns=not significant) is according to the Mann-Whitney rank sum test.

(**b) Effect on harsh touch avoidance behaviour.** Animals were touched on the body with a platinum wire as described; escape responses (reversals) were scored as described (n>100 for each genotype). Statistical significance (ns=not significant) is according to Student's t-test.

Since no deletion allele was available for F25D1.4, I used cell-specific RNAi (Esposito G et al., 2007) to eliminate its expression in PVD and assess its effect on harsh touch mechanosensation. I generated multiple transgenic lines (*ljEX224, ljEx225, ljEx258, ljEx264*) that expressed sense and antisense F25D1.4 sequences cell-specifically in the PVD neurons (Figure 2.6; Figure 2.7). For the RNAi transgenes, I used two different promoters (*egl-46* and *ser-2prom3*) whose expression domains overlap only in the PVD neurons (Tsalik EL., 2003; Wu J et al., 2001). I targeted the F25D1.4 gene using two different segments of the open reading frame, which did not overlap in sequence (Figure 2.7b).

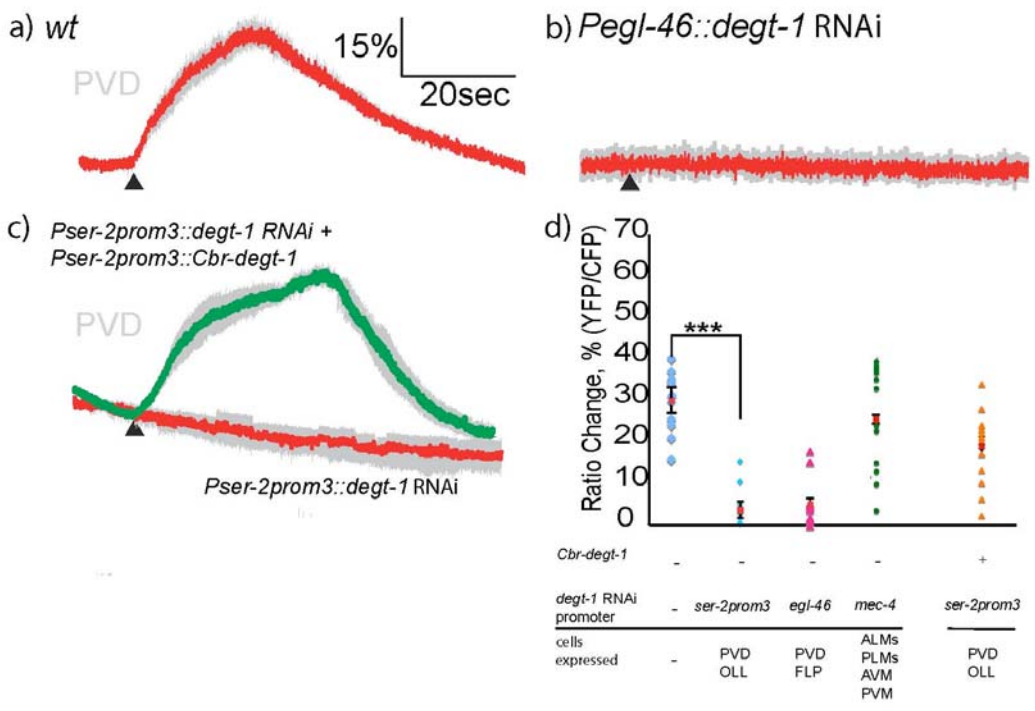

Figure 2. 6: DEGT-1 is required for harsh touch responses in PVD

Figure 2. 6: DEGT-1 is required for harsh touch responses in PVD

(a–c) Calcium responses of wild-type and *degt-1* RNAi worms to harsh body touch in PVD. Each red trace represents the average percentage change in normalized YFP/CFP ratio (R/R_0) for the indicated genotype and the grey shading represents the s.e.m. of the mean response. The wild-type response (13 worms recorded) is shown in a. Harsh touch response was lost in lines expressing *degt-1* RNAi under the PVD-specific promoters *pegl-46* (*ljEx224*, 14 worms) and *pser-2prom3* (*ljEx225*, 17 worms) (b,c). In c, the upper line shows rescue of the *pser-2::degt-1RNAi* (*ljEx225*) phenotype by the *C. briggsae* ortholog *Cbr-degt-1* expressed cell-specifically in PVD under the control of the *pser-2prom3* promoter (*ljEx261*; 14 worms). *Cbr-degt-1* shares less than 5% sequence identity with *C. elegans degt-1* over the region targeted by *ljEx225*.

(d) Scatter plot of peak calcium responses for each genotype. Statistical significance (***$P < 0.001$) was determined by the Mann-Whitney rank sum test. Also shown are responses of the off-target control in which a *degt-1* RNAi transgene was expressed outside PVD under the touch neuron promoter *pmec-4* (*ljEx240*; 14 worms recorded). Responses of additional on-target and off-target RNAi control strains are shown in Figure 2.7

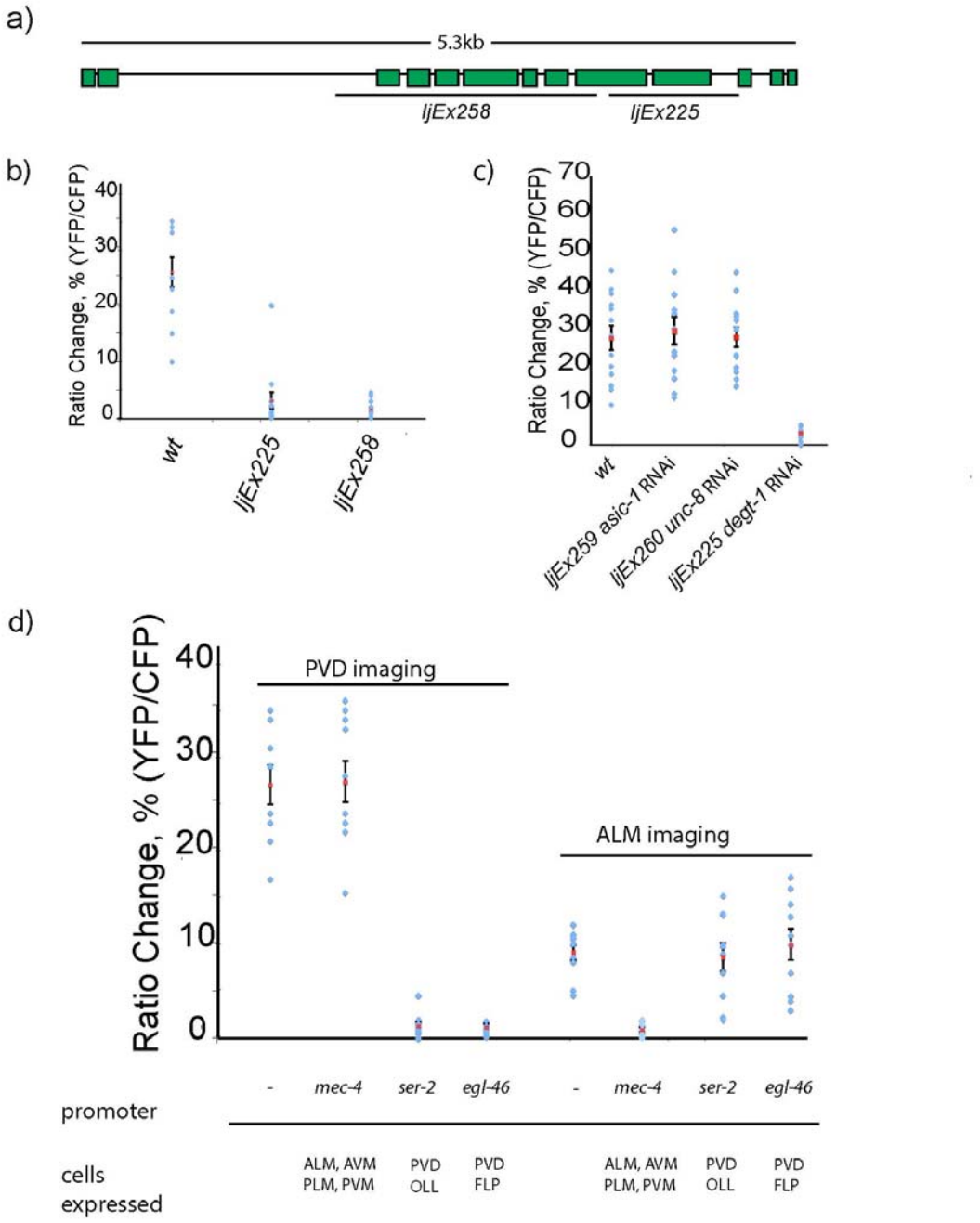

Figure 2.7: Design and controls for *degt-1* RNAi.

Figure 2.7: Design and controls for *degt-1* RNAi

(a) Diagram of RNAi constructs. Shown are the regions of the *degt-1* coding sequence used for the *ljEx258* and *ljEx225* RNAi transgenes. Both constructs were driven by the *ser-2prom3* promoter; *degt-1* RNAi lines in Figures 4 and 5 containing other promoters (e.g. *pegl-46*(*ljEx224*) and *pmec-4*(*ljEx240*)) used the same fragment as in *ljEx225*. Parallel constructs (*pegl-46=ljEx264* and *pmec-4=ljEx265*) using the same fragment as in *ljEx258* showed similar phenotypes (data not shown). (**b) RNAi with non-overlapping *degt-1* fragments inhibits harsh touch response in PVD.** Shown is a scatter plot of PVD peak calcium responses to harsh touch stimulation for lines expressing non overlapping *degt-1* dsRNA fragments under the *ser-2prom3* promoter. Lines using the same fragments driven by the *egl-46* promoter–*ljEx224* and *ljEx264* (data not shown)–gave similar phenotypes.

(c) Effects of RNAi in PVD for DEG/ENaC genes with sequence similarity to *degt-1.* Scatter plot shows peak harsh touch responses of *asic-1(ljEx259)*, and *unc-8*(*ljEx260*) RNAi lines, in which sense and antisense gene fragments were expressed under the *ser-2prom3* promoter as described in Methods. Neither line showed significant reduction in peak responses.

(d) Cell-specificity of *degt-1* RNAi harsh touch defects. Scatter plot shows peak harsh touch responses of indicated RNAi lines compared to wild-type controls in PVD (left) or ALM (right). RNAi arrays used were *ljEx240* (*pmec-4*), *ljEx225* (*ser-2prom3*) and *ljEx224* (*pegl-46*). For PVD imaging, all strains contained the *ljEx19* cameleon array; for ALM imaging, all strains contained the *bzIs17* integrated array and were carried out in a *mec-4(u253)* background.

Strains carrying any of these PVD-directed F25D1.4 RNAi arrays completely lacked harsh touch-induced calcium transients as reported by cameleon in PVD (Figure 2.6a-d; Figure 2.7b) and exhibited significant defects in harsh touch escape behaviour in a *mec-4(u231)* background (Figure 2.4c). Both the calcium imaging and behavioural phenotypes of F25D1.4 RNAi animals could be rescued by transgenic expression of the *C. briggsae* F25D1.4 orthologue (here designated *Cbr-degt-1)* in the PVD neurons (Figure 2.6c,d). RNAi constructs targeting other PVD-expressed DEG/ENaC channels did not cause a harsh touch defect in PVD, indicating that the harsh touch phenotype resulted from loss of F25D1.4 and not from off-target knockdown of another DEG/ENaC channel (Figure 2.7c). Expression of F25D1.4 RNAi constructs in other neurons did not cause a harsh touch defect in PVD (Figure 2.6e; Figure 2.7c), nor did the PVD-directed constructs confer harsh touch defects in cells outside the expression domains of their promoters (Figure 2.7d); thus, the effect of F25D1.4 appeared to be cell-specific. Together, these data indicate that F25D1.4 functions specifically in the PVD multidendritic neurons in harsh touch mechanosensation. I have designated F25D1.4 *degt-1*, for DEG/ENaC protein involved in touch.

To learn more about the role of DEGT-1 in the PVD neurons, I investigated its intracellular localization using GFP- and RFP-tagged transgenes (Figure 2.8a). I observed that both DEGT-1::GFP and DEGT-1::RFP proteins labelled the PVD cell body as well as the PVD dendritic branches in a punctate distribution (Figure 2.9a). I also analyzed the localization of a MEC-10::GFP fusion protein (Figure 2.8b), which rescued the harsh touch defect of the *mec-10(tm1552)* deletion (Figure 2.8d). I observed a subcellular distribution similar to that of the DEGT-1 fusion proteins, with fluorescence observed in a punctate pattern throughout the dendrite (Figure 2.9b).

Colabeling experiments in animals expressing both *degt-1::rfp* and *mec-10::gfp* transgenes in PVD indicated that the DEGT-1 and MEC-10 dendritic puncta colocalize (Figure 2.9c-e). These results suggest that the MEC-10 and DEGT-1 proteins are clustered in the PVD dendrites, and are consistent with the possibility that MEC-10 and DEGT-1 are components of the same harsh touch mechanosensory complex.

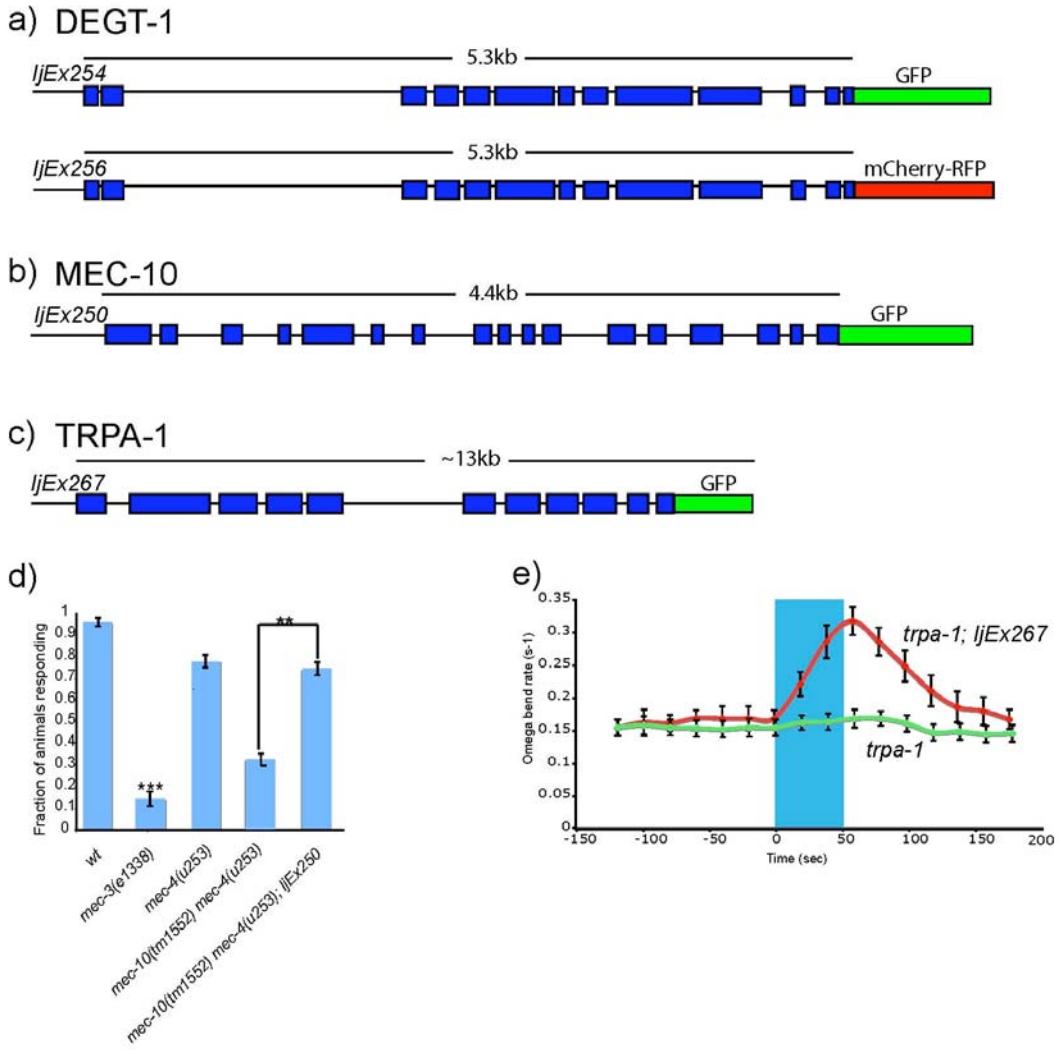

Figure 2.8: Design and rescue experiments for DEGT-1, MEC-10 and TRPA-1 protein fusions.

Figure 2.8: Design and rescue experiments for DEGT-1, MEC-10 and TRPA-1 protein fusions.

(a–c) Structures of fusion transgenes. Shown are diagrams of fusion transgene structures; boxes indicate exons and thin lines indicate introns. Fusion transgenes were constructed as described in Methods and expressed under the *ser-2prom3* promoter. Fluorescence was not observed outside the *ser-2prom3* expression domain.

(d) Expression of *mec-10::GFP* in PVD rescues the *mec-10* harsh touch behavioural defect. Animals were touched on the body with a platinum wire as described; escape responses (reversals) were scored as described. At least 100 animals were scored for each genotype. Statistical significance (*** $P < .001$; ** $P < .005$) is according to the Student's t test (*mec-3(e1338)* is compared to wild-type).

(e) Expression of *trpa-1::GFP* in PVD rescues the *trpa-1* cold avoidance defect. Shown are percentages of n > 20 animals displaying avoidance behaviour (omega bends) during a recording of worms experiencing acute temperature change (20-15º). The blue box indicates a 50 second interval during which the buffer temperature was 15º; the temperature was 20º during the remainder of the recording. Error bars indicate SEM.

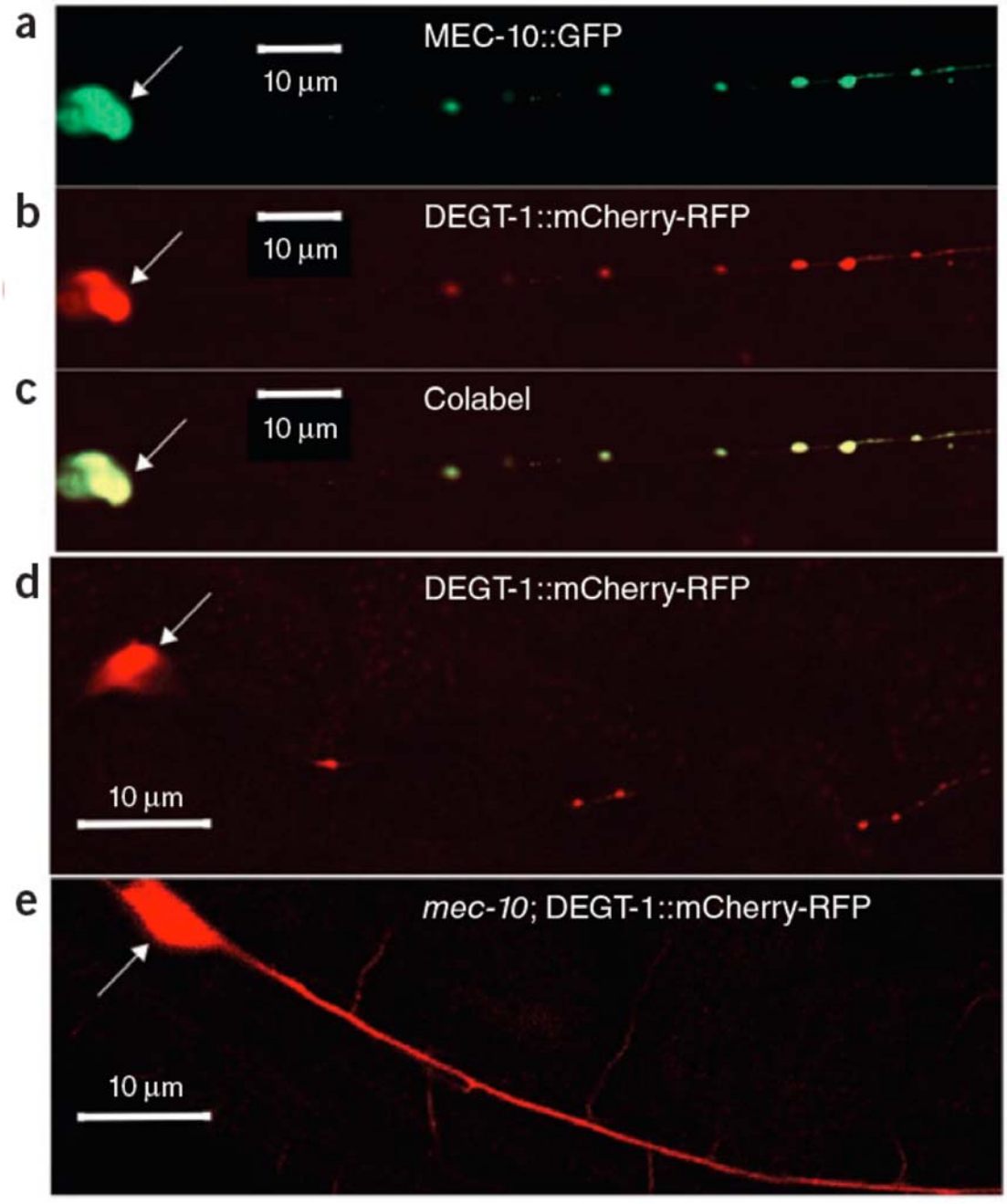

Figure 2.9: Localization patterns of DEGT-1 and MEC-10 fusion proteins in PVD.

Figure 2.9: Localization patterns of DEGT-1 and MEC-10 fusion proteins in PVD.

The large arrows indicate the PVD soma. (**a–c**) **Colocalization of MEC-10::GFP and DEGT-1::RFP in PVD dendritic puncta.** Shown are green, red and dual wavelength images of a single confocal section of AQ2427 *ljEx250[pser-2prom3::mec-10::GFP; pmyo-2::GFP]; ljEx256[pser-2prom3::degt-1::mCherry-RFP pmyo-2::GFP]* worms, which express both MEC-10::GFP and DEGT-1::RFP in PVD. AQ2427 was generated by crossing AQ2396 *ljEx250* and AQ2402 *lj256* and selecting for the presence of both arrays. These images all show the primary PVD dendrite; similar results were observed in higher-order dendritic branches (Figure 2.10).

(**d,e) Punctate localization of DEGT-1::RFP is *mec-10* dependent.** Shown are single confocal sections of PVD processes expressing the *ljEx256* DEGT-1::RFP transgene in a wild-type (d**)** or *mec-10(tm1552)* mutant (e) background. *degt-1* RNAi did not abolish punctate expression of MEC-4::GFP (Figure 2.10).

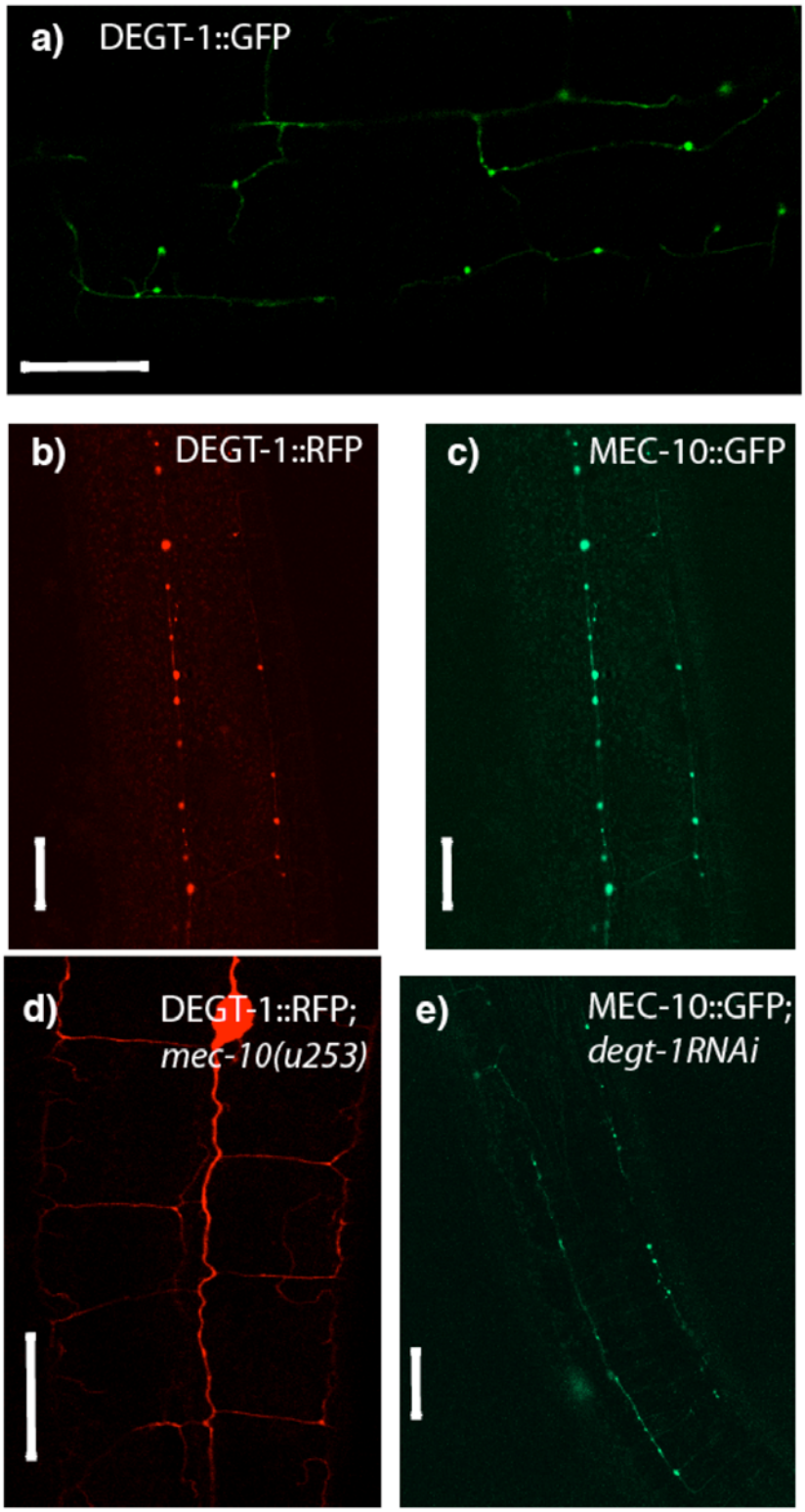

Figure 2.10: Additional images of DEGT-1 and MEC-10 protein fusion localization patterns in PVD.

Figure 2.10: Additional images of DEGT-1 and MEC-10 protein fusion localization patterns in PVD.

In all figures, scale bar is 10 μM. (**a) Subcellular localization of a full-length DEGT-1::GFP fusion protein in PVD.** Shown is a confocal section of an adult AQ2400 *ljEx254[ser-2prom3::degt-1::GFP; pmyo-2::GFP]* animal, which expresses the DEGT-1::GFP fusion protein in PVD.

(**b–c) Punctate distribution of MEC-10::GFP and DEGT-1::RFP in higher-order PVD dendritic branches.** Shown are red (b) and green (c) wavelength images of a single confocal section of AQ2427 *ljEx250[ser-2prom3::mec-10::GFP; pmyo-2::GFP]; ljEx256[ser-2prom3::degt-1::mCherry; pmyo-2::GFP]* animals, which express both MEC-10::GFP and DEGT-1::RFP in PVD.

(d–e) MEC-10::GFP distribution remains punctate in a *degt-1 RNAi* background. Shown are single confocal sections of PVD processes expressing the *ljEx256* DEGT-1::RFP transgene in a *mec-10(tm1552)* mutant background (d) or the *ljEx250* MEC-10::GFP transgene in an *ljEx225 degt-1* RNAi background (e).

2.3.4 MEC-10 and DEGT-1 are essential for harsh touch responses in ALM

In addition to its role in harsh touch, *mec-10* has a well-defined role in gentle touch sensation. Specifically, *mec-10* is important for the responses of body touch neurons such as ALM to low-threshold mechanical stimuli; these responses are also dependent on the DEG/ENaC protein MEC-4 (O'Hagan R et al., 2005; Huang M, Chalfie M, 1994). ALM neurons respond to harsh touch as well as to gentle touch; while the gentle touch response requires MEC-4, the harsh touch response is MEC-4-independent (Suzuki H et al., 2003). This raises the question of whether the role of *mec-10* in harsh touch mechanosensation is a feature of the cell in which it is expressed (PVD instead of ALM) or alternatively a feature of the other molecules with which it associates (DEGT-1 instead of MEC-4).

To address this question, I investigated the effect of *mec-10* on harsh touch responses in the ALM neurons. To determine the importance of MEC-10 for MEC-4-independent harsh touch, I measured the harsh touch-evoked calcium transients in a *mec-4(u253)* null mutant background, in which the ALM neurons are morphologically normal and respond to harsh touch but not gentle touch (Suzuki H et al., 2003). I found (Figure 2.11a, b, e; Figure 12a) that the ALM calcium responses observed in *mec-4(u253)* single mutants were absent in the *mec-10(tm1552) mec-4(u253)* double mutants. Expression of a wild-type *mec-10(+)* transgene under a touch-neuron-specific promoter restored harsh touch calcium responses (Figure 2.11c, e) and partially restored harsh touch avoidance behaviour (Figure 2.12b) to the *mec-10(tm1552) mec-4(e253)* double mutant, indicating that MEC-10 acts cell-autonomously in the ALM neurons. Thus, MEC-10 appears to be essential for harsh touch mechanosensation in ALM as well as PVD.

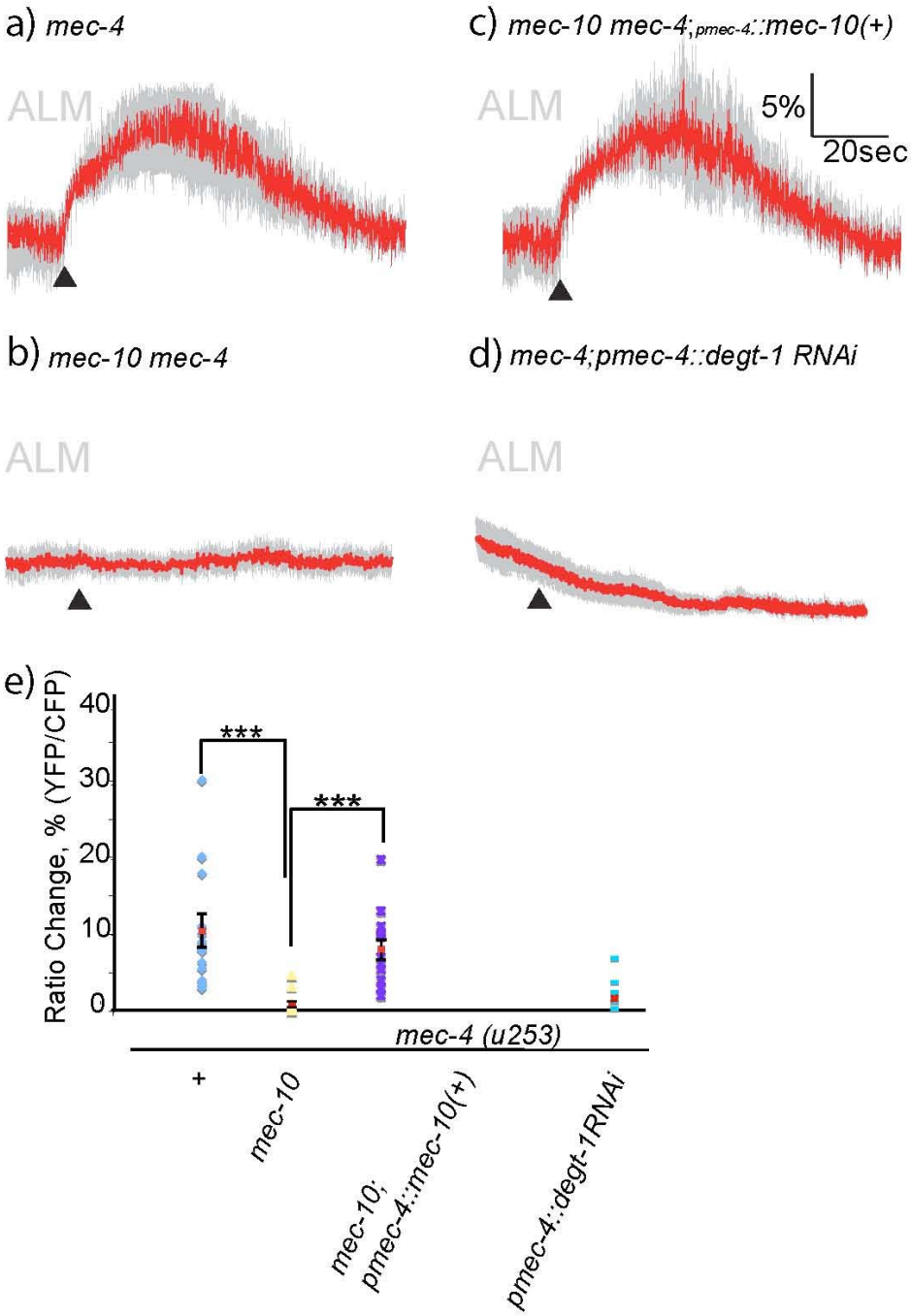

Figure 2.11: Effect of *mec-10* on harsh touch responses in ALM.

Figure 2.11: Effect of *mec-10* on harsh touch responses in ALM.

(a,b) ***mec-10* is required for *mec-4*–independent harsh touch response in ALM.** Shown are calcium responses in ALM to fast large-displacement stimulation in *mec-4(u253)* single mutant **(**a**)** and *mec-10(tm1552) mec-4(u253)* double mutant **(**b**)**. Each red trace represents the average percentage change in R/R_0 and the grey shading represents the s.e.m. of the mean response. The triangle indicates the application of the harsh touch stimulus. The averaged response of 13 *mec-4(u253*) worms are shown in a and the response of 13 *mec-10(tm1552) mec-4(u253)* worms are shown in b.

(c) *mec-10* functions in the body touch neurons to promote ALM harsh touch response. Shown is the averaged response of 17 *mec-10(tm1552) mec-4(u253); pmec-4::mec-10(+)* worms, in which *mec-10* was specifically rescued in the body touch neurons. Similar results were seen when the PVD neurons were eliminated by laser ablation (Figure 2.12).

(d) *degt-1* was required for ALM harsh touch responses. Shown is the averaged response of 19 *mec-4(u253); ljEx240[pmec-4::degt-1RNAi]* worms, in which *degt-1* was specifically eliminated in the ALM neurons by RNAi. Additional off-target RNAi controls are shown in Figure 2.7.

(e) Scatter plot of peak calcium responses for each genotype. Statistical significance (***$P < 0.001$) was determined by the Mann-Whitney rank sum test.

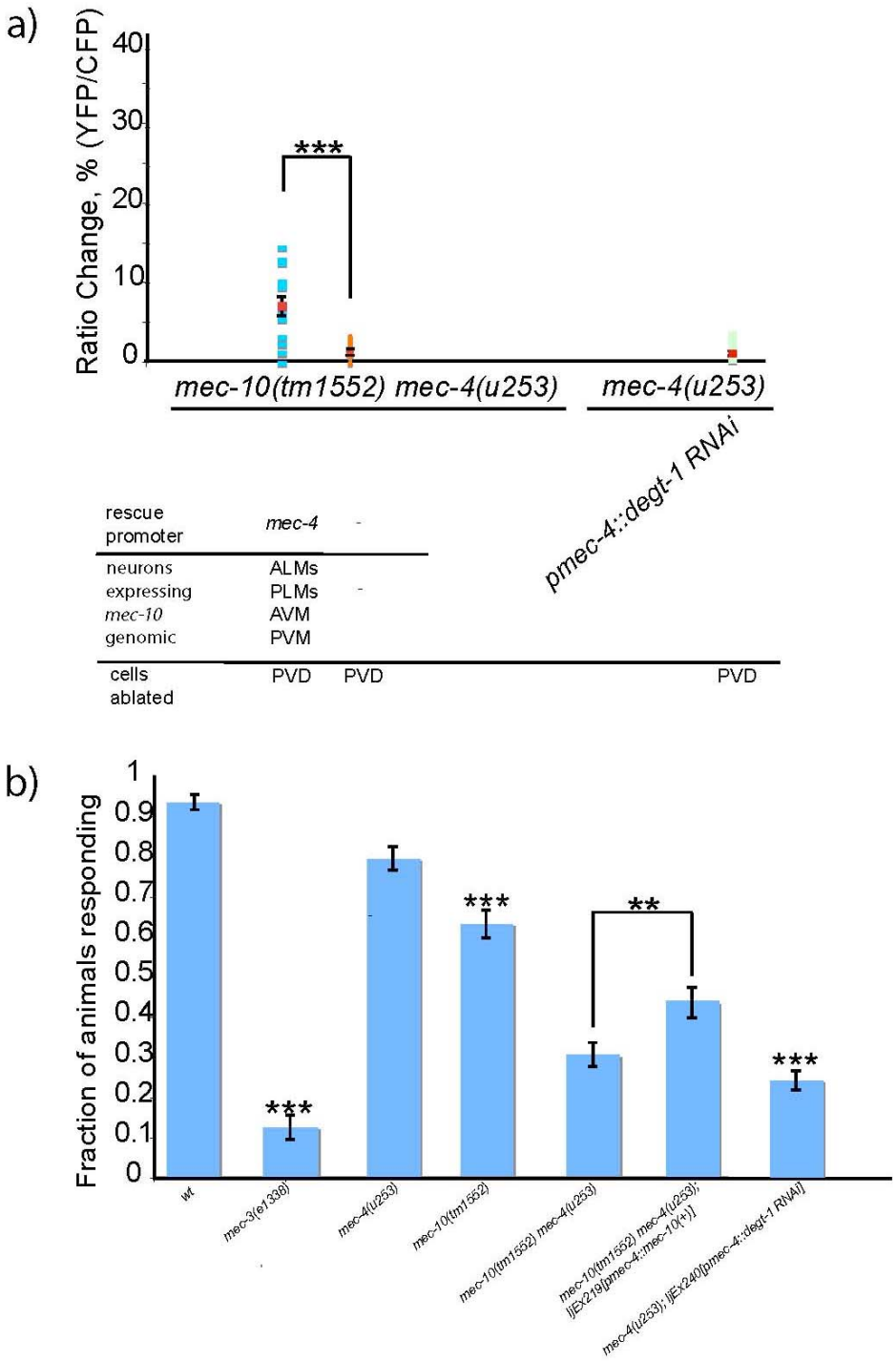

Figure 2.12: Additional data on the effect of *mec-10* and *degt-1* on harsh touch responses in ALM.

Figure 2.12: Additional data on the effect of *mec-10* and *degt-1* on harsh touch responses in ALM.

a. *mec-10* and *degt-1* effects on ALM harsh touch-evoked calcium transients do not require PVD. Shown is a scatter plot of ALM peak calcium responses to harsh touch stimulation in animals in which the PVD neurons have been ablated. The following number of animals were imaged for each genotype: *mec-10(tm1552) mec-4(u253); ljEx219[pmec-4::mec-10]*—15*, mec-10(tm1552)mec-4(u253)*—15, *mec-4(u253);ljEx240[pmec-4::degt-1 RNAi]*—13*.* Statistical significance (*** *P* < .001) is according to the Mann-Whitney rank sum test.

b. Body touch neuron-related effects of *mec-10* and *degt-1* on harsh body touch avoidance behaviour. Histogram shows cell-specific partial rescue of the harsh touch defect of the *mec-10(tm1552) mec-4(u253)* double mutant (in which touch cells are present but non-responsive; see Figure 5b) by a *pmec-4*-driven *mec-10(+)* transgene (compare 5th and 6th histogram bars; statistically different at ***P* <.005). Also shown is the harsh touch defect of a strain expressing *pmec-4*-driven *degt-1* RNAi in a *mec-4(u253)* mutant background (statistically different from *mec-4(u253)* at ****P*<.0005). *mec-3* and *mec-10* single mutants are shown for reference (statistically different from wild-type at ****P* <.0005). For all genotypes, animals were touched on the body with a platinum wire and escape responses (reversals) scored as described in Methods (n > 100 for each genotype). Statistical significance is according to Student's t-test.

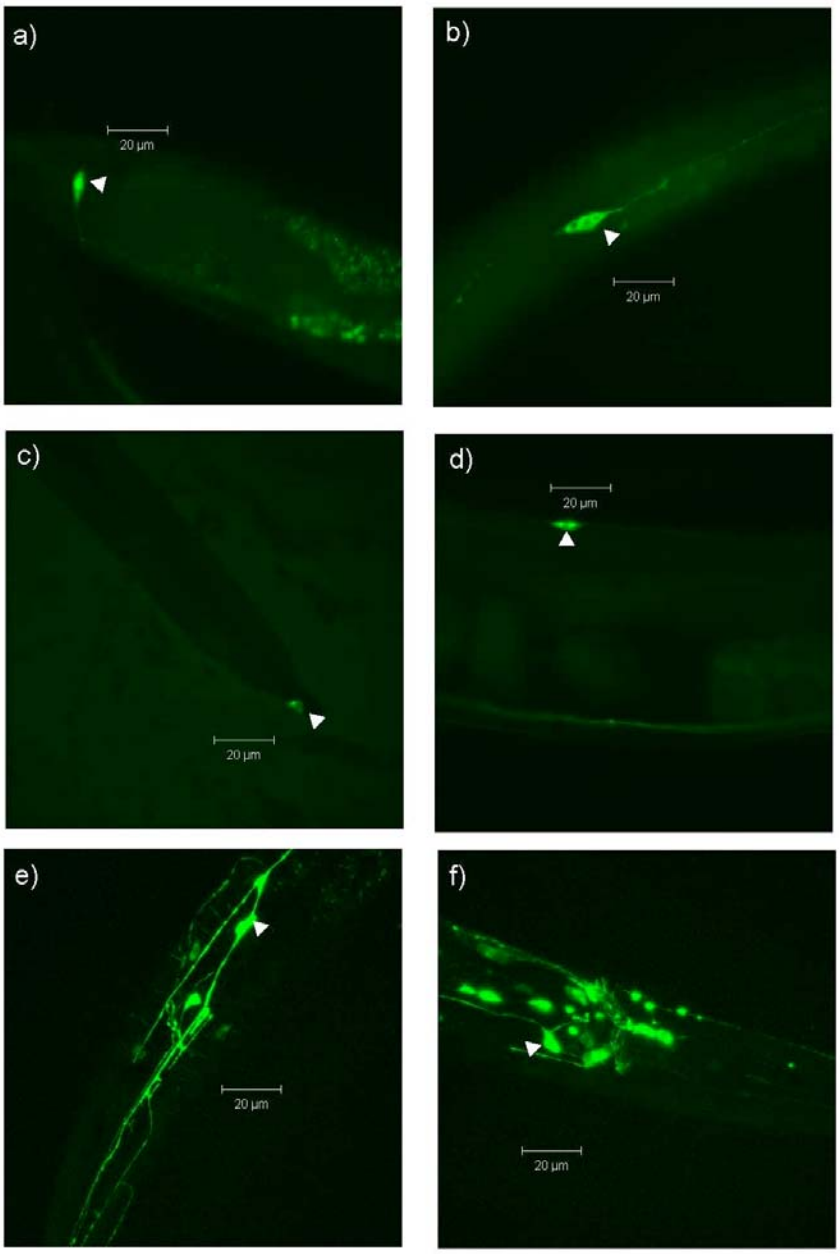

Figure 2.13: Expression pattern of a *pdegt-1*::GFP reporter.

Shown are images of transgenic animals expressing a full-length *degt-1::gfp* fusion under the control of the *degt-1* promoter. Panels a-d represent single confocal sections; panels e-f are Z-stack projection**s.** Triangles indicates the soma of the indicated cell. **a.** Expression in unidentified tail neuron. **b.** Expression in PVD. **c.** Expression in PLM. **d.** Expression in ALM. **e-f.** Expression in FLP (triangle) as well as other head neurons.

Based on reporter transgene experiments (Figure 2.13), *degt-1* is expressed in the ALM neurons; therefore, I also tested the role of DEGT-1 in ALM harsh touch sensation by expressing *degt-1* double-stranded RNA under the control of the *mec-4* promoter. I observed that *degt-1* RNAi largely eliminated harsh touch responses in ALM (Figure 2.11d), but did not affect gentle touch responses (Figure 2.9a, b, d). Thus, while MEC-10 contributes to both the gentle touch and harsh touch modalities of ALM, DEGT-1 appears to be required only for harsh touch. These findings are consistent with the possibility that gentle touch mechanoreceptors contain MEC-4 and MEC-10 subunits, whereas harsh touch mechanoreceptors contain MEC-10 and DEGT-1. Such a model would predict that overexpression of DEGT-1 might compete with MEC-4 for association with MEC-10, thereby inhibiting gentle touch. In fact, I observed that a multicopy *degt-1* transgene under the control of the *mec-4* promoter significantly compromised gentle touch avoidance and gentle touch-evoked calcium transients in ALM (Figure 2.14c, d, e). These results are consistent with the possibility that MEC-10 and DEGT-1 interact in a harsh touch mechanosensory complex.

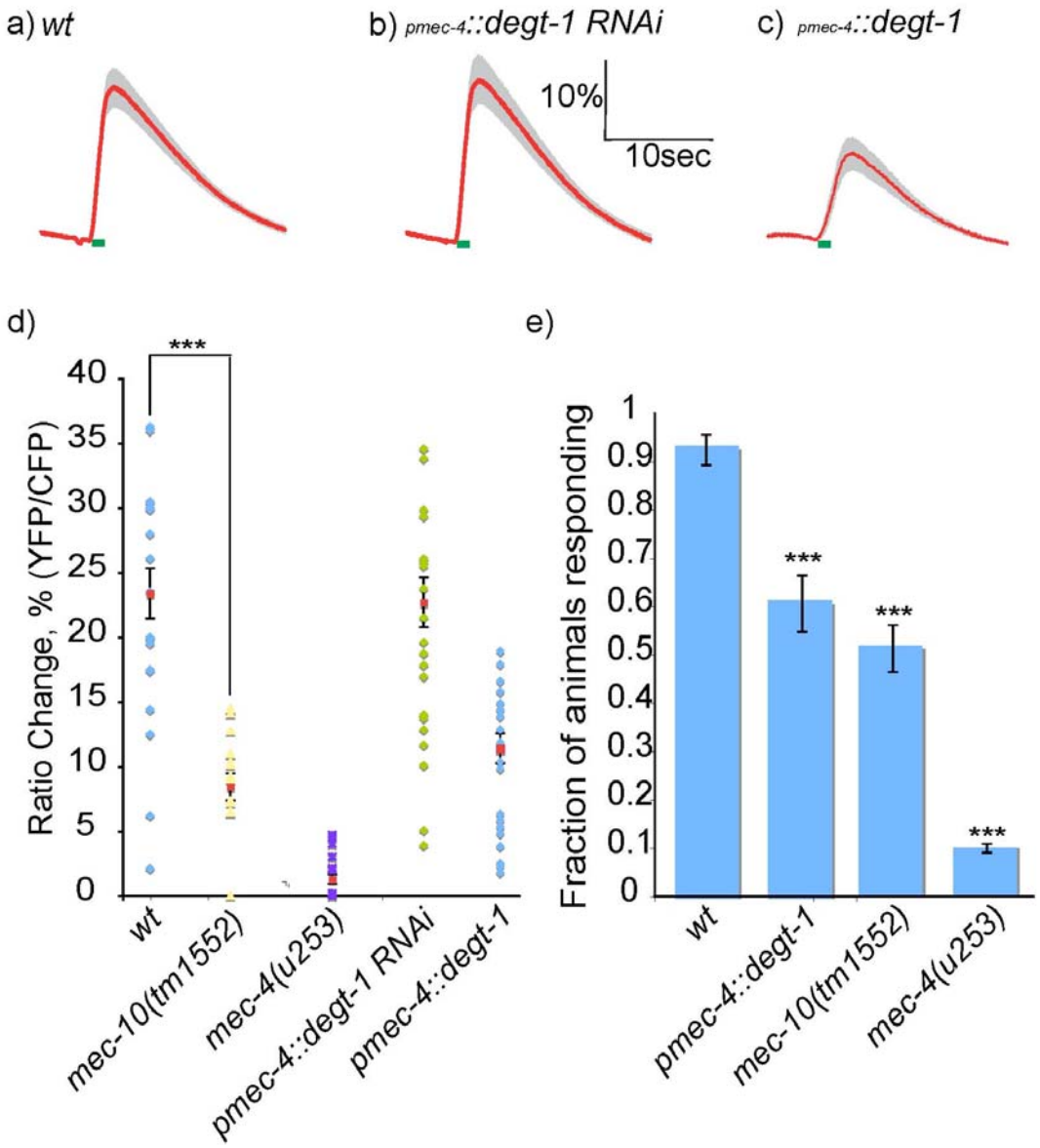

Figure 2.14: Effects of *degt-1* RNAi and *degt-1* overexpression on ALM gentle touch responses.

Figure 2.14: Effects of *degt-1* RNAi and *degt-1* overexpression on ALM gentle touch responses.

(a–b) *degt-1* RNAi does not inhibit gentle touch responses in ALM. Shown are averaged calcium responses of wild-type (a) and *ljEx240[pmec-4::degt-1RNAi]* (b) in response to gentle touch stimulation. Each red trace represents the average percentage change in R/R_0 for 22 animals of the indicated genotype; green bars indicate the time of the stimulus. Grey shading indicates SEM. Scale bars are indicated in upper right.

(**c) *degt-1* overexpression in body touch neurons inhibits gentle touch response.** Shown is the averaged response of 22 *ljEx268[pmec-4::degt-1(+)]* animals. ALM neuronal morphology (visualized by the *ljEx19* cameleon reporter) appears normal in these animals.

(d) Scatter plot of peak calcium responses for each genotype. Statistical significance (*** $P < .005$) is according to the Mann-Whitney rank sum test. Also shown are data for 22 *mec-10(tm1552)* and 10 *mec-4(u253)* mutant animals.

(e) Effects on gentle touch avoidance behaviour. Animals were touched on the body with an eyelash as described; escape responses (reversals) were scored as described. Indicated genotypes are statistically different from wild-type (*** $P < .001$) according to the Student's t test.

2.3.5 PVD responses to acute cold shock require TRPA-1

I next investigated whether MEC-10 and DEGT-1 are required for PVD responses to other noxious stimuli. In particular, I tested whether loss of either DEG/ENaC channel protein affects responses to cold shock. Calcium imaging experiments in *mec-10* loss-of-function mutant animals revealed no measurable defect in PVD responses to cold downsteps (Figure 2.15a, g). Likewise, *degt-1* RNAi lines showed normal cold-evoked calcium transients in PVD (Figure 2.15b, g). Cold-evoked escape behaviour was also unaffected by loss of function in either gene (Figure 15d, e). Thus, the DEG/ENaC channel proteins do not affect cold sensation in PVD and appear to be required specifically for responses to noxious touch.

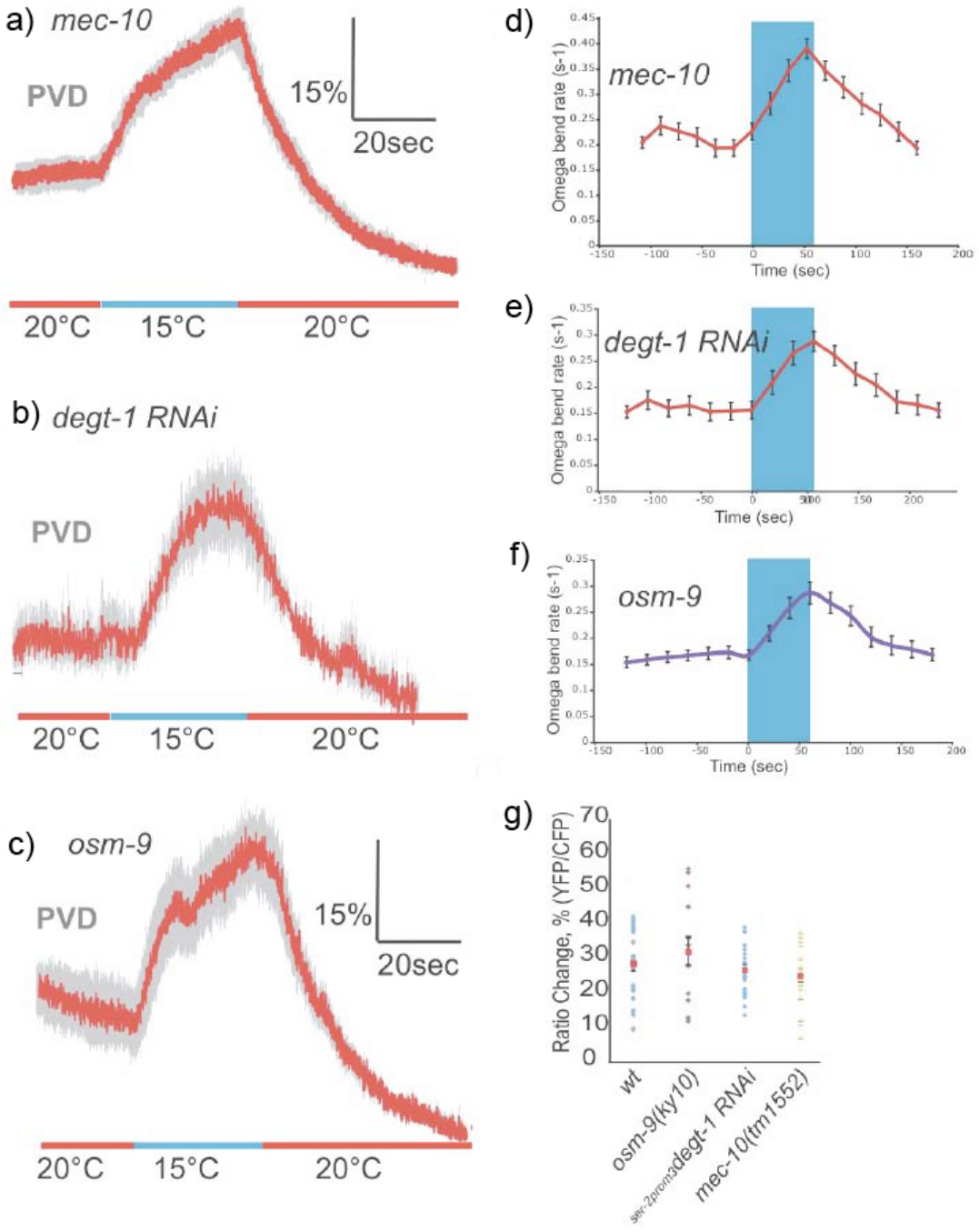

Figure 2.15: Effects of *degt-1* and *osm-9* on cold responses in PVD.

Figure 2.15: Effects of *degt-1* and *osm-9* on cold responses in PVD.

(a) *mec-10* is not required for cold responses in PVD. Shown is the averaged change in R/R_0 of *mec-10(tm1552)* animals in response to cold. For this and other calcium imaging panels, the red trace represents the average R/R_0 and grey shading indicates SEM. Scale bars are indicated in upper right. This trace represents the average of 14 *mec-10(tm1552)* animals.

(b) *degt-1* is not required for cold responses in PVD. Panel shows the averaged PVD calcium response of 17 *ljEx225[ser-2prom3::degt-1RNAi]* animals to cold stimulation.

(c) *osm-9* is not required for PVD responses to cold shock. Panel shows the averaged PVD calcium response of 13 *osm-9(ky10)* animals to cold stimulation.

(**d) *mec-10* is not required for cold shock avoidance behaviour.** Shown are percentages of >20 *mec-10(tm1552)* animals displaying avoidance behaviour (omega turns) following acute temperature change (20-15º). In this and panels e and f, the blue box indicates a 50 second interval during which the buffer temperature was 15º; the temperature was 20º during the remainder of the recording. Error bars indicate SEM.

(**e) *degt-1* RNAi in PVD does not affect cold shock avoidance.** Shown are percentages of n>20 *ljEx225[ser-2prom3::degt-1RNAi]* animals displaying cold avoidance behaviour.

(**f) *osm-9* is not required for cold shock avoidance.** Shown are percentages of n>20 *osm-9(ky10)* animals displaying cold avoidance behaviour).

(g) Scatter plot of peak calcium responses to cold shock. Data from panels a-c and Figure 1g (wild-type).

What molecules might be responsible for cold sensation in PVD? Two candidates are TRPA-1 and OSM-9, TRP channels that are expressed in PVD (Kindt KS et al., 2007; Colbert HA et al., 1997). To determine the effects of these molecules on cold shock responses, I measured behavioural and calcium imaging responses of *trpa-1(ok999)* and *osm-9(ky10)* animals to temperature downsteps. *osm-9(ky10)* animals responded normally to cold shock (Figure 2.15c, f, g), indicating that OSM-9 is not required for cold sensation by PVD. However, I observed no cold-evoked calcium transients (Figure 2.16a) and no cold-evoked escape behaviour (Figure 2.16b) in *trpa-1(ok999)* animals. Expression of wild-type *trpa-1(+)* under the control of PVD-specific promoters rescued these cold response defects, indicating that TRPA-1 functions cell-autonomously in the PVD neurons (Figure 2.16a, b, d). Since the PVD neurons of *trpa-1* mutants respond normally to harsh touch stimulation (Figure 2.3d, f), the TRPA-1 protein appears to be specifically required for sensation of noxious cold by PVD. These data identify TRPA-1 as a candidate noxious cold thermosensor.

The modality-specific phenotypes of *mec-10, degt-1* and *trpa-1* suggested that mechanosensation and thermosensation occur through functionally distinct pathways in the PVD neurons. To gain further insight into this possibility, I then investigated the intracellular localization of a rescuing (Figure 2.8e) TRPA-1::GFP fusion protein (Kindt KS et al., 2007) in PVD. I observed that in contrast to MEC-10 and DEGT-1, whose fusion proteins were found in puncta throughout the PVD dendrite, TRPA-1::GFP was restricted to the cell body and the most proximal portion of the dendrite (Figure 2.16 e, f). This observation suggests that the harsh touch and cold-sensing mechanisms may not only involve different molecular components but might also be localized differently within the PVD neurons.

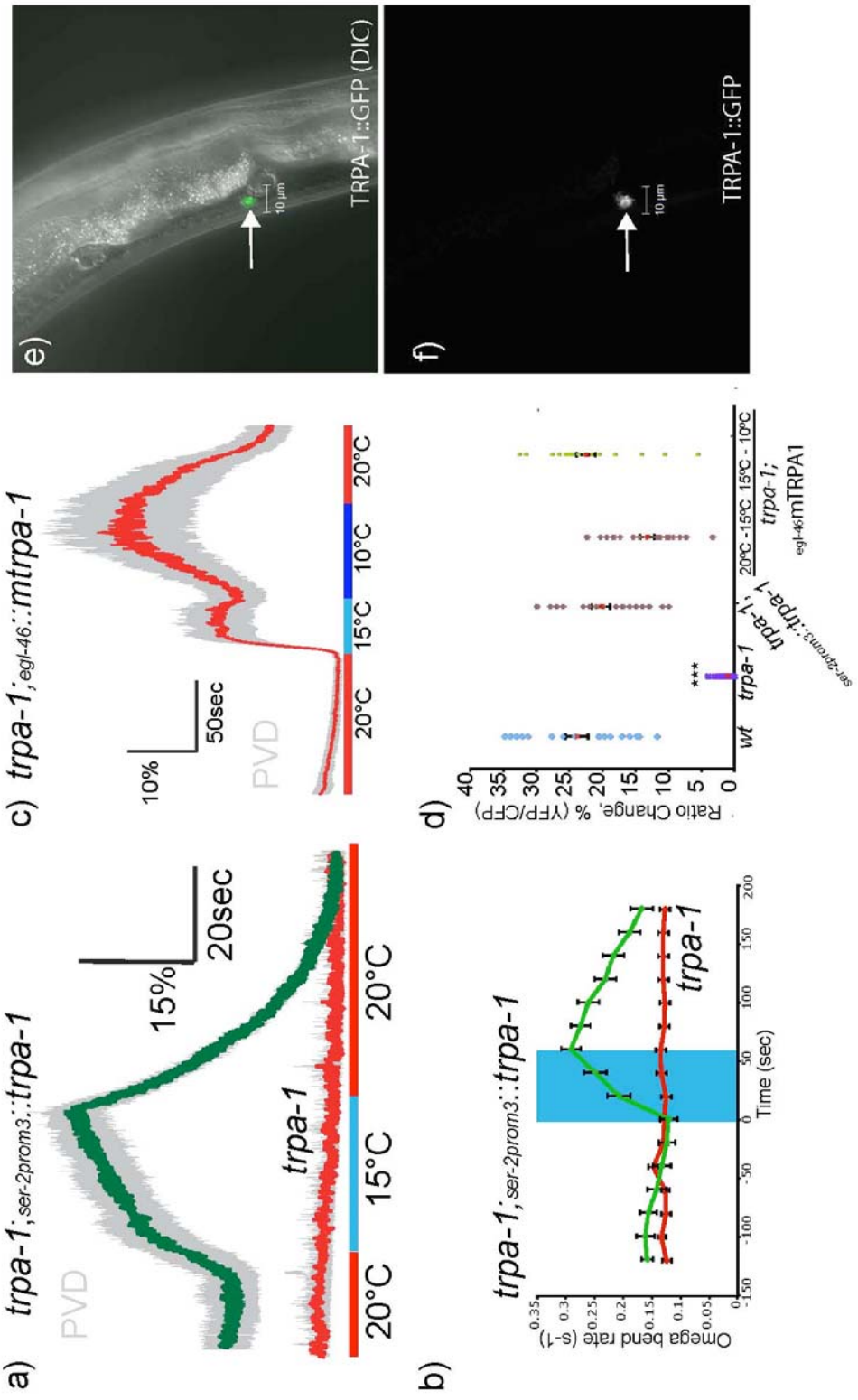

Figure 2.16: TRPA-1 is specifically required for cold responses in PVD.

Figure 2.16 TRPA-1 is specifically required for cold responses in PVD.

(a) *trpa-1* was required for PVD cold response. Lower trace indicates the averaged percentage change in R/R_0 of 17 *trpa-1(ok999)* worms; the upper trace is the response of 13 *trpa-1(ok999); ljEx*245 *[ser-2prom3::trpa-1(+)]* worms in which a wild-type *trpa-1(+)* transgene cell-specifically rescued the null phenotype in PVD. The temperature changes during the recording are shown below; grey shading indicates s.e.m. of the mean response.

(b) *trpa-1* is required in PVD for cold shock avoidance behaviour. Shown are percentages of *trpa-1(ok999)* and PVD-rescued worms displaying avoidance behaviour (omega turns) following acute temperature change (20 °C to 15 °C). Blue box indicates the duration of the 15 °C cold shock; error bars indicate s.e.m.

(c) Mammalian mTRPA1 confers cold responses in PVD. Red trace indicates the averaged response of 13 *trpa-1(ok999); ljEx262 [pegl-46::mTRPA1]* worms.

(d) Scatter plot of peak calcium responses for each genotype. Statistical significance (***$P < 0.001$) was determined by the Mann-Whitney rank sum test.

(e,f) Subcellular localization of a rescuing full-length TRPA-1::GFP fusion in PVD. Fluorescence images of AQ2428 *ljEx267[pser-2prom3::trpa-1::GFP pmyo-2::GFP]*, which express a rescuing full-length TRPA-1::GFP fusion protein in PVD. A single confocal section with differential interference contrast optics is shown in e and a *z* stack confocal projection in darkfield is shown in f. Phenotypic rescue of the *trpa-1* cold avoidance phenotype is shown in Figure 2.8.

2.3.6 Functional conservation between *C. elegans* and mammalian TRPAs

C. elegans TRPA-1 is related to the mammalian mTRPA1 protein, which has been implicated as a potential cold sensor in nociceptor neurons (Story GM et al., 2003). To assess the functional conservation between *C. elegans* TRPA-1 and its mammalian counterpart, I generated a transgenic line, *ljEx247* that expressed a mouse mTRPA1 cDNA in the PVD neurons under the control of the *egl-46* promoter. I observed robust calcium transients in response to cold temperature in the PVD neurons of *trpa-1(ok999); ljEx247* animals (Figure 2.16c), indicating that mouse mTRPA1 partially rescues the cold-insensitive phenotype of the *trpa-1* deletion mutant. Consistent with the known properties of the mammalian channel, larger responses were seen following a further temperature downshift to 10º (Figure 2.16c, d). Thus, the mammalian protein can functionally substitute for *C. elegans* TRPA-1 in nematode neurons.

To further investigate the sufficiency of TRPA-1 for cold sensation, I tested whether heterologous expression of *C. elegans* TRPA-1 could confer cold responsiveness to other cell types. I first expressed *trpa-1* in the *C. elegans* FLP neurons. The FLPs are multidendritic cells with morphological similarities to the PVDs (Hall D, Altun ZF, 2008); however, unlike the PVDs, they do not express reporters for *trpa-1* (Kindt KS et al., 2007) and are activated by heat rather than cold (Figure 2.17a, b, f). When I expressed a *trpa-1* transgene in FLP under the *egl-46* promoter, I observed robust cold-evoked calcium transients (Figure 2.17c, f), indicating that the TRPA-1 protein is sufficient to confer cold responsiveness on the FLP neurons. I also expressed TRPA-1 in the gentle body touch neurons under the control of the *mec-4* promoter. Again, heterologous *trpa-1(+)* expression conferred

robust calcium responses to cold shock in the normally cold-insensitive ALM neurons (Figure 2.17d-f). These results indicate that TRPA-1 can confer ectopic cold sensing properties on at least two classes of *C. elegans* neurons.

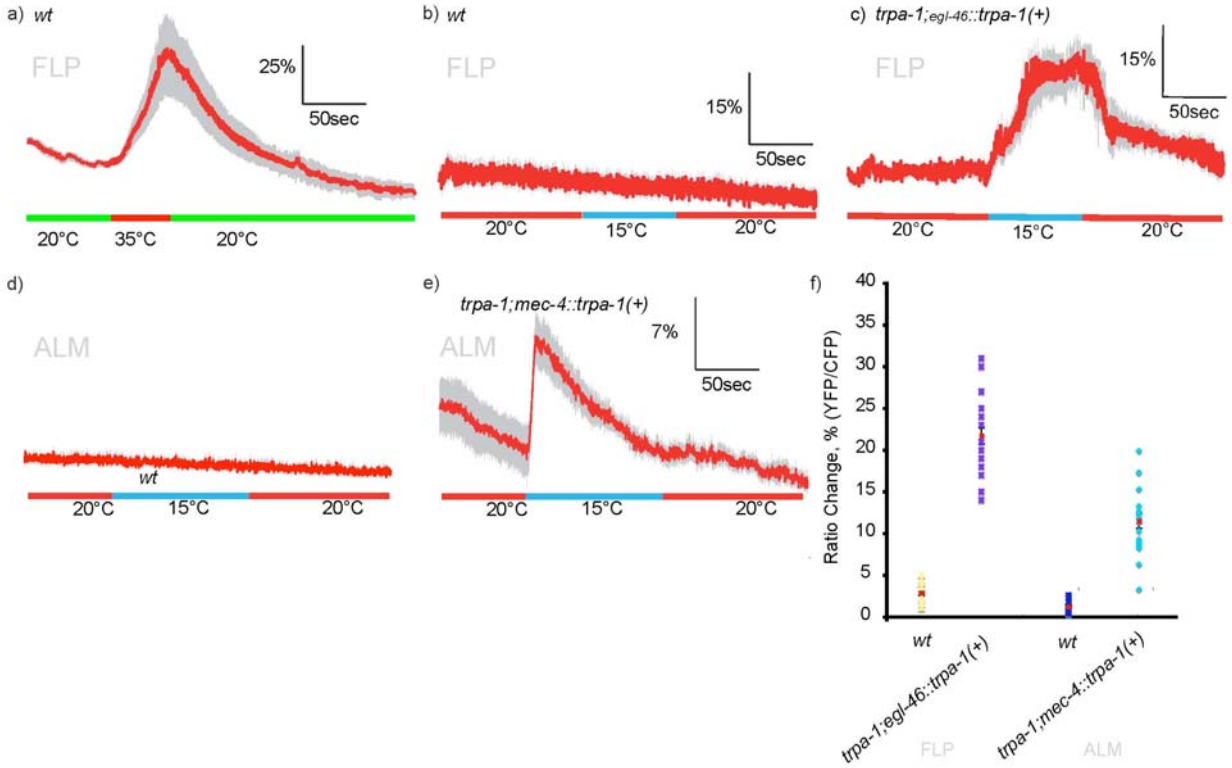

Figure 2.17 Heterologous expression of TRPA-1 in *C. elegans* neurons confers cold sensitivity.

Figure 2.17 Heterologous expression of TRPA-1 in *C. elegans* neurons confers cold sensitivity.

(a) Normal response of FLP to noxious heat shock. Shown is an averaged calcium trace of wild-type FLP neurons expressing the *ljEx19* transgene. The red trace represents the average percentage change in R/R_0 for 20 individual worms. Grey shading indicates s.e.m. of the mean response and the lower line indicates temperature changes during the recording.

(b) FLP does not respond to cold shock in wild-type worms. Shown is an averaged trace of 20 wild-type *ljEx19* worms in response to 20 °C to 15 °C cold shock.

(c) Worms expressing *trpa-1(+)* ectopically in FLP respond to cold shock. Trace shows the averaged response of 20 *trpa-1(ok999); ljEx246[pegl-46::trpa-1(+)]; ljEx19* worms, which express *trpa-1(+)* heterologously in FLP.

(d) Wild-type ALM neurons do not respond to cold. Shown is the averaged response of 20 *bzIs17[pmec-4::YC2.12]* worms, which express cameleon in the body touch neurons.

(e) Worms expressing *trpa-1(+)* ectopically in ALM respond to cold shock. Shown is the averaged response of 20 *trpa-1(ok999); ljEx223 [pmec-4::trpa-1(+)]; bzIs17* worms, in which *trpa-1(+)* is expressed heterologously in ALM and other the body touch neurons.

(f) Scatter plot of peak calcium responses for each genotype. Statistical significance (***$P < 0.001$) was determined by the Mann-Whitney rank sum test.

HEK293T cells transiently transfected with *C. elegans* TRPA-1 were tested to determine whether they could be activated by cold stimulation. In whole-cell recordings, robust currents were observed in response to cold stimuli in TRPA-1–expressing HEK cells (n = 9), but not in naive cells (n = 26) (Figure 2.18a, c). The average current density evoked by 15ºC at +60 mV was 40.34±19.38pA/pF (± s.e.m.) in TRPA-1 expressing HEK cells, and 1.78±0.33pA/pF (± s.e.m.) in untransfected cells (Figure 2.18c). Current responses were not observed in response to upstep temperature changes to the room temperature. The currents evoked by cold stimuli in TRPA-1–expressing cells are blocked by gadolinium ions (Figure 19) and show the current-voltage relationship similar to those observed previously (Figure 18b; Figure 19) (Kindt KS et al., 2007). These results suggest that the TRPA-1 protein is itself sufficient to produce cold-activated cation currents.

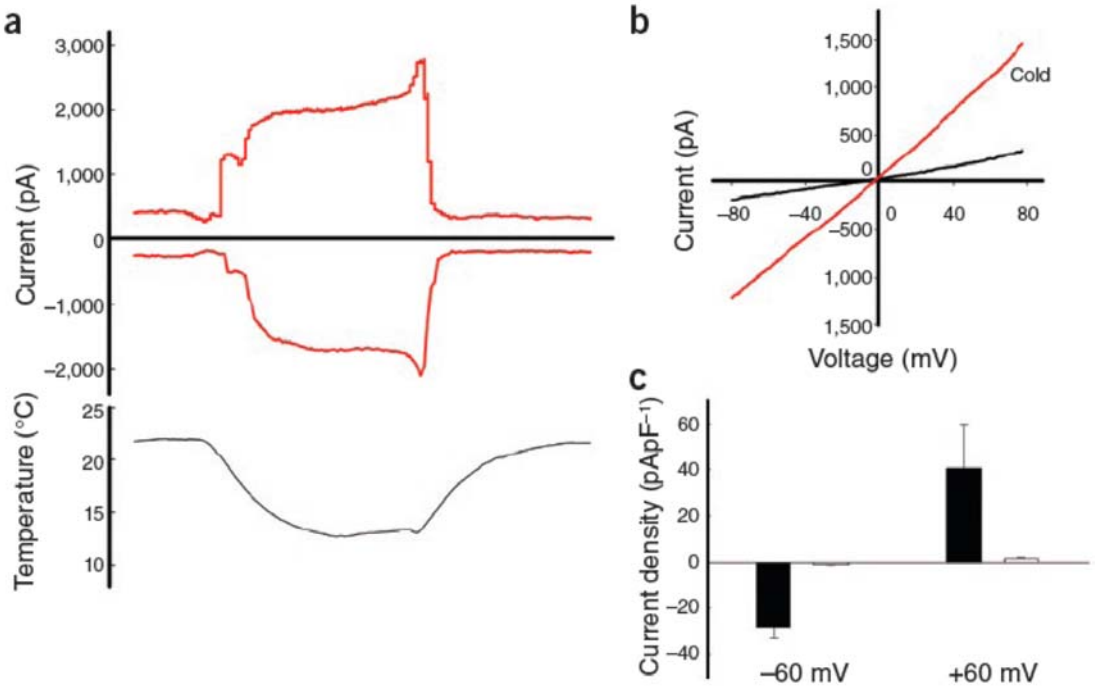

Figure 2.18: Cold stimuli activate TRPA-1 expressing HEK293T cells.

Figure 2.18: Cold stimuli activate TRPA-1–expressing HEK293T cells.

(a) TRPA-1–expressing HEK cells respond to cold in whole-cell configuration. Perfusion of the cold bath solution activates a representative TRPA-1–expressing HEK cell (*n* = 9). Currents are shown at holding potentials of +60 and –60 mV. As previously observed in CHO cells23, currents were also activated by pressure (Figure 2.19).

(b) Instantaneous current voltage relationships of the TRPA-1–expressing HEK cell. Voltages were ramped from –80 to +80 mV. Responses are shown before and during application of 15 °C cold temperature in the bath.

(c) Average current densities evoked by a cold temperature of 15 °C. Current densities of the cold responses of TRPA-1–transfected (filled bars) and untransfected HEK cells (open bars) at ± 60 mV (*n* = 9 for cold response, *n* = 26 for no response). Error bars represent ± s.e.m.

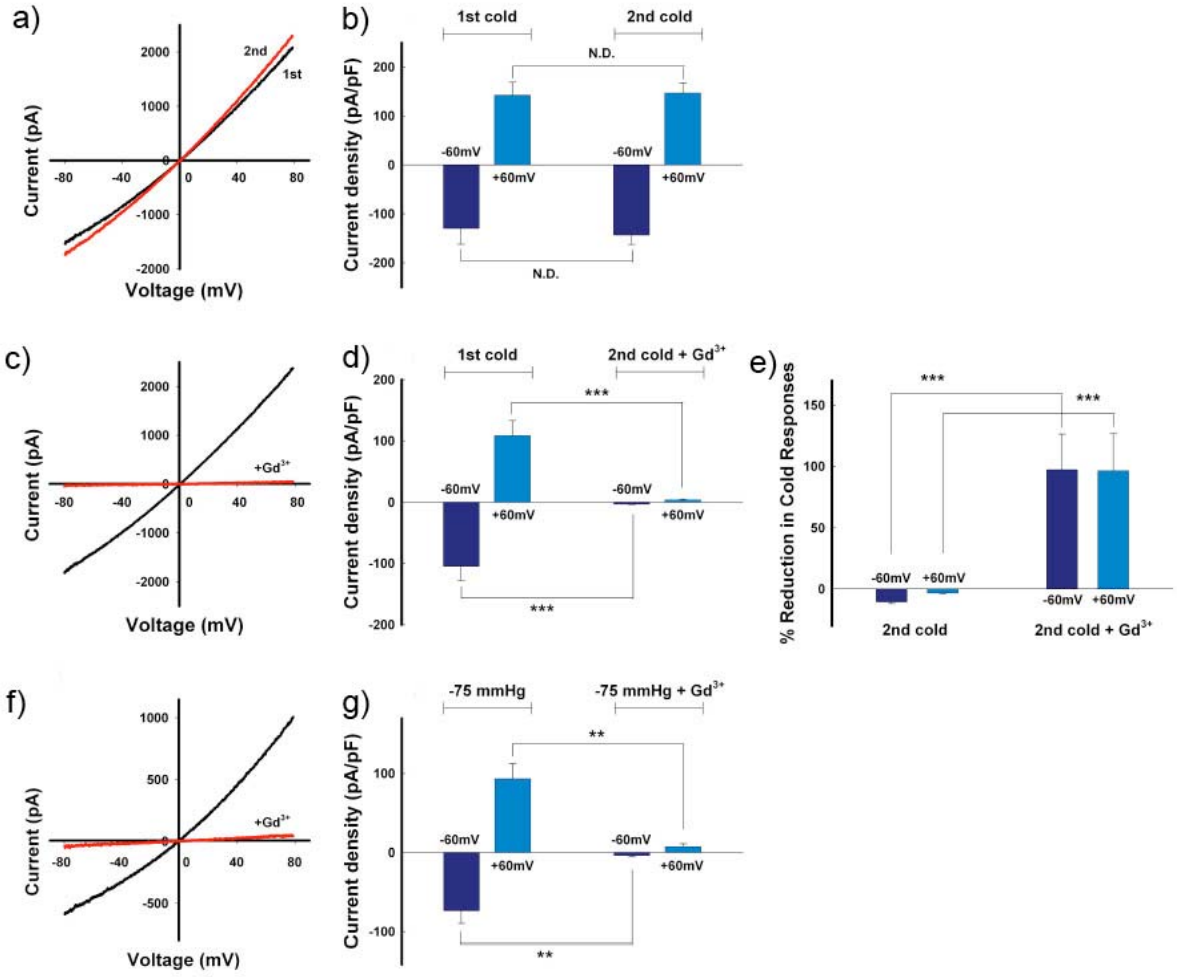

Figure 2.19: Gd^{3+} inhibits TRPA-1 activation.

Figure 2.19: Gd^{3+} inhibits TRPA-1 activation.

(a–b) TRPA-1 activation by repeated cold stimulation. Panel (a) shows representative current-voltage relationships of the TRPA-1 responses in the same HEK cells expressing TRPA-1 upon the initial exposure (black) and the second exposure (red) to cold temperatures (13ºC). The second cold stimulation was applied ~30 s after the end of the first cold response. Panel (b) shows averaged current densities of the cold responses of TRPA-1-HEK cells at ± 60 mV (n=6).

(**c–e) TRPA-1 response to cold temperature was attenuated by extracellular 500 μM Gd^{3+}.** Panel (c) shows representative current-voltage relationships of the TRPA-1 responses upon the initial cold exposure without Gd^{3+} (black) and the second exposure with Gd^{3+} (red). Panel (d) shows averaged current densities of the cold responses of TRPA-1-expressing HEK cells at ± 60 mV (n=6). Panel (e) shows a summary of the percent (%) reduction in the cold responses by Gd^{3+} treatment. The mean percent reductions of cold responses by Gd^{3+} were 97.3 ± 0.8% at -60 mV and 96.4 ± 1.1% at +60 mV. The data were compared to those of 2nd cold responses without Gd^{3+} in (b). Error bars, ± SEM. (*** p< .001; N.D., no statistically significant difference; Student's t-test).

(**f–g) TRPA-1 activation by mechanical stimulation.** As in previous CHO cell expression experiments (Kindt KS et al.,2007), *C. elegans* TRPA-1 mechanosensitivity was also observed in HEK cell experiments. Panel f shows representative current-voltage relationships of the TRPA-1 responses upon the pressure application (-75 mmHg of suction) with (red) or without 500 μM Gd^{3+} (black). Panel g shows averaged current densities of the pressure responses of TRPA-1-expressing HEK cells at ± 60 mV (n=4 with Gd^{3+}, n=7 without Gd3+). Error bars, ± SEM. (** *P* < .001).

2.4 Discussion

In this study, I have characterized the sensory transduction mechanisms of a new class of polymodal nociceptors in the nematode *C. elegans*, the multidendritic PVD neurons. These neurons were previously shown to be important for behavioural responses to harsh touch (Way JC, Chalfie M, 1989); the results presented here demonstrate that the PVD neurons are also required for acute behavioural responses to cold, and that both types of noxious stimuli evoke cell autonomous activation of PVD calcium transients. I showed that responses to noxious touch and temperature require distinct molecular pathways: touch sensation requires the DEG/ENaC proteins MEC-10 and DEGT-1, whereas temperature sensation requires the TRP channel TRPA-1. Thus, polymodal nociception in the *C. elegans* multidendritic neurons appears to involve parallel sensory transduction mechanisms.

The evidence from my work strongly implicates *C. elegans* TRPA-1 as the thermosensor for cold in the PVD neurons. The effects of the *trpa-1* deletion on the PVD neurons are highly specific to cold responses; moreover, *C. elegans* TRPA-1 protein expressed in mammalian cultured cells is sufficient to produce cold-activated depolarizing currents. These results contrast with previous observations in the OLQ nose touch mechanosensory neurons, in which *trpa-1* was shown to affect touch responses. Why might TRPA-1 affect mechanosensation in one cell type but affect only thermosensation in another? One possibility is that the ability of TRPA-1 channels to function in mechanosensation may depend on the morphology of the cell in which it is expressed. While TRPA-1 channels can be activated by stretch *in vitro*, the mechanical gating of TRPA channels *in vivo* may depend on structural features that the PVD neurons lack. Alternatively, TRPA-1 may play an indirect role in

mechanosensation in OLQ, and this function may not be required in other touch-sensing neurons. Interestingly, although heterologous expression of TRPA-1 can confer cold sensitivity on the normally non-responding FLP and ALM neurons, some cells that normally express TRPA1 (e.g. OLQ; data not shown) do not respond to cold. Thus, the ability of TRPA-1 to respond mediate neural responses to cold may also depend on additional cell-specific factors.

I have also identified a DEG/ENaC channel that functions specifically in noxious mechanosensation in PVD. I observed that strong mechanical stimuli evoked calcium transients in PVD that were absent in *mec-10* mutants or animals in which a second DEG/ENaC gene, *degt-1*, was knocked down by cell-specific RNAi. MEC-10 and DEGT-1 fusion proteins colocalize in puncta throughout the PVD dendrite, consistent with the two DEG/ENaC proteins participating in the same multimeric complex. DEGT-1 and MEC-10 may therefore represent essential components of the harsh touch mechanotransducer in PVD. The identity of the receptor for mechanical pain in human polymodal nociceptors is still unknown; based on my results, as well as recent evidence from *Drosophila* (Zhong L et al., 2010) it is reasonable to speculate that it may be a DEG/ENaC channel.

My results suggest that subunit composition of DEG/ENaC channels may play an important role in distinguishing harsh touch receptors from gentle touch receptors. Previous work has shown that the ALM body touch neurons contain distinct gentle touch and harsh touch modalities (Suzuki H et al., 2003), with gentle touch completely dependent on the DEG/ENaC protein MEC-4 and largely dependent on MEC-10 (O'Hagan R et al., 2005). In contrast, the harsh touch response in ALM requires MEC-10 and DEGT-1, but is independent of MEC-4. Thus, MEC-4/MEC-

10 channels may mediate low-threshold responses in the ALM neurons, whereas MEC-10/DEGT-1 channels may mediate high threshold responses within the same cells.

While these findings are a first step toward identifying the components of the harsh touch mechanotransduction machinery, additional subunits and accessory proteins almost certainly remain to be identified. In particular, stomatin proteins seem to be important components of known DEG/ENaC channel complexes. While MEC-2, the stomatin associated with the gentle touch mechanoreceptor, is not present in the multidendritic neurons, at least two uncharacterized stomatin genes were identified in the PVD expression profile (Smith CJ et al., 2010). It will be interesting to test the involvement of these proteins in harsh touch-evoked neural activity and behaviour. Since harsh touch receptor function can be straightforwardly assessed through both behavioural and neuroimaging assays, it should be possible to identify additional components of the harsh touch mechanoreceptor by assaying candidate gene knockouts or by conducting forward mutant screens.

2.5 Methods

Generation of FLP/PVD cameleon line ljEx19.

The *egl-46* promoter region was obtained from plasmid TU#307 (Tsalik EL et al., 2003), a gift from M. Chalfie. A 3-kb HinDIII/NotI fragment was fused to cameleon YC2.3 in the vector pPD95.75 (A. Fire, Stanford University). Transgenic lines were obtained by germline injection of a lin-15(n765) mutant strain with the *egl-46::YC2.3* plasmid at a concentration of 50 ng µl−1 along with *lin-15(+)* genomic DNA (30 ng µl−1) as a co-injection marker. Once a stable transgenic line was obtained, the *lin-15(n765)* allele was removed by backcrossing to wild-type worms.

Transgenic rescue lines.

For all rescue plasmids, I used the MultiSite Gateway Three Fragment Vector Construction Kit. Individual PCR products were cloned into the appropriate pDONOR vector generating pENTRY clones. Subsequently, pENTRY vectors with the promoter and gene of interest as well as an *unc-54* 3′ UTR–containing vector were recombined with a pDEST vector to generate an expression vector.

For rescue arrays *ljEx219*, *ljEx220* and *ljEx221*, a 4.4-kb *mec-10* genomic DNA was amplified using Phusion High-Fidelity DNA Polymerase F-530S from adult genomic DNA using the primers 5′-GTA CAA AAT TCA AAA AAT GAA TCG-3′ and 5′-GAA ATA AGA AAT TTA TTT TCC G-3′. For *ljEx261* and *ljEx266*, a 4.4-kb region coding for *C. briggsae degt-1* ortholog *Cbr-degt-1* was amplified from adult genomic DNA with the primers 5′-ATG CCC CGA AAA CGA AGG TCT G-3′ and 5′-CAC ATC ATA TTG ATG GGT TGG TG-3′. For array *ljEx230*, a 2.2-kb *mec-10* cDNA

was amplified using Qiagen OneStep RT-PCR Kit from an RNA library using the primers 5′-ATG AAT CGA AAC CCG CGA ATG-3′ and 5′-TCA ATA CTC ATT TGC AGC ATT TTC-3′. For array *ljEx246*, a *trpa-1* 3.6-kb cDNA fragment was amplified from a plasmid generated previously (Kindt KS et al., 2007) using the primers 5′-ATG TCG AAG AAA TCA TTA GG-3′ and 5′-TCA GTT ATC TTT CTC CTC AAG T-3′. A 1-kb *mec-4* promoter region was obtained from plasmid pIR13, a gift from I. Rabinowitch (MRC-LMB, Cambridge). The 1.7-kb *ser-2prom-3* was obtained from plasmid pWCS8, from the Miller laboratory. I used the same *egl-46* promoter fragment described above in the creation of the *egl-46*::cameleon plasmid.

The *pmec-4::mec10* construct was injected in *mec-10(tm1552); ljEx19 [pegl-46::YC2.3]* worms at 72 ng µl−1 with *punc122::GFP* at 20 ng µl−1 to generate array *ljEx219[pmec-4::mec-10 punc122::GFP]*. The same *pmec-4::mec10* construct was injected in *mec-10(tm1552); bzIs17* worms at 70 ng µl−1 with *pmyo-2::GFP* at 20 ng µl−1 to generate array *ljEx228[pmec-4::mec-10 pmyo-2::GFP]*. This was crossed into the *mec-10(tm1552); mec-4(u253)* double mutant to generate strain AQ2436. I injected *mec-10(tm1552); ljEx19[pegl-46::YC2.3]* worms with *pegl-46::mec-10* at 80 ng µl−1 and with *punc122::GFP* at 20 ng µl−1 to generate array *ljEx220 [pegl-46::mec-10 punc122::GFP]*. To generate cell-specific rescue of *mec-10* in the PVD cells, I injected *mec-10(tm1552); ljEx19[pegl-46::YC2.3]* worms with *ser-2prom-3::mec-10* at 80 ng µl−1 with *punc122::GFP* at 20 ng µl−1 to generate array *ljEx221* transgenic worms. A *pegl-46::trpa-1* construct was injected into wild-type worms at 70 ng µl−1 with *punc122::GFP* at 20 ng µl−1 to generate array *ljEx246*. A *pser-2prom3::trpa-1* construct was injected into wild-type *ljEx19[pegl-46::YC2.3]* worms at 70 ng µl−1 with *pmyo-2::GFP* at 11 ng µl−1 to generate array *ljEx245*. These

worms were crossed into the *degt-1RNAi* strains AQ2282 and AQ2404.

Cell ablations

Laser ablations were carried out using MicroPoint laser system. The FLPs and AFDs, PLMs, and ASHs were ablated in the early L1 stage, usually 3–4 h post hatching; the PVD cells were ablated at early L2. As an additional control, I also ablated V5 precursor cells at early L1 stage, which removes the PVD/PDE cells (data not shown). No apparent difference in the effects of the two different ablations was noted. All ablations were confirmed by observing loss of cameleon fluorescence in the adult worm.

Generation of *degt-1* and control RNAi lines

Transgenes for cell-specific knockdown were constructed as described previously (Esposito G et al., 2007). *ljEx224[pegl-46::degt-1RNAi]* and *ljEx225[ser-2prom-3::degt-1RNAi]* expressed a *degt-1(RNAi)* in the FLP and PVD or OLL and PVD neurons, respectively. Transgene *ljEx240[pmec-4::degt-1 RNAi]* expressed a *degt-1* RNAi transgene in the gentle body touch neurons (ALM, AVM, PLM, PVM). For these constructs, the same exon-rich region of degt-1 that was used as an insert for a previously reported RNAi feeding library (Kamath RS et al., 2001) was amplified using the primers 5′-CGG TTG TAA ACA TGA CGC TG-3′ and 5′-CCA CGG ATG AAT CGA GTT TT-3′. A second set of RNAi lines against *degt-1* targeting a different region of the gene was generated by using the exon rich region of *degt-1* that was used as an insert for a previously reported RNAi feeding library (Sönnichsen, B. *et al*., 2005). The following primers: 5′-CTA ACC CAC CAT TTC CGC TA-3′ and 5′-TTG CGT GGT TAT TCT TTC CC-3′ amplified a 1.7-kb fragment from which

three different transgenes were generated*: ljEx265[pmec-4::degt-1 RNAi]*, *ljEx258[pegl-46::degt-1RNAi]* and *ljEx225[ser-2prom-3::degt-1RNAi]* expressed a *degt-1(RNAi)* in the body touch neurons, FLP and PVD or OLL and PVD neurons, respectively. For all RNAi transgenes, both sense and antisense expression clones were microinjected at 100 ng μl−1 together with 50 ng μl−1 *pmyo-2::gfp* as a co-injection marker.

PVD expression profiling

A 1.6-kb region of the *ser-2prom3* promoter (Tsalik EL et al., 2003) was inserted into the 3XFLAG::PAB-1 plasmid pSV15 (Von Stetina SE et al., 2007) to produce the ser-2prom3B::3XFLAG::PAB-1 mRNA tagging construct pWCS8. A transgenic line (NC221) was generated by microparticle bombardment and specific expression in PVD and OLL neurons was confirmed by FLAG immunostaining. The mRNA tagging method was used to isolate PVD/OLL transcripts from synchronized L3-L4 larvae (Von Stetina SE et al., 2007). A reference sample of total RNA from all larval cells was obtained from L3-L4 larval lysates by trizol extraction. Triplicate samples were applied to the Affymetrix Gene Chip array and transcripts showing relative enrichment (>1.5×; false discovery rate < 1%) in PVD/OLL versus the reference were identified using previously described methods (Fox RM et al., 2005; Watson JD et al., 2008). Four DEG/ENaC channel transcripts (*mec-10*, *del-1*, *asic-1*, *degt-1*) satisfied these criteria (Smith CJ et al., 2010), whereas *mec-4* showed only slight enrichment (1.1×) at relaxed stringency (<10% false discovery rate) (Table 1.1).

Generation of DEGT-1, MEC-10 and TRPA1 fusion protein transgenes

Fusion transgenes were expressed under the control of the *ser-2prom3* promoter described above. Primers to PCR amplify the genomic regions coding for MEC-10, DEGT-1 and TRPA-1 were altered to allow in frame fusion with the C-terminal tag. pENTRY clones for GFP and the RFP-variant *mCherry* were generated by I. Rabinowitch (unpublished data). Transgenic lines were generated by injecting the constructs into the *N2* strain; each line was compared with multiple additional independently-derived transgenic lines with the same transgene to confirm the reproducibility of the expression pattern. The *mec-10::GFP* construct was injected at 95 ng μl−1 with *pmyo-2::GFP* at 11 ng μl−1, giving *ljEx250*. The *degt-1::gfp* construct was injected at 86 ng μl−1 with *pmyo-2::GFP* at 15 ng μl−1, giving ljEx254. The *degt-1::mCherry-RFP* construct was injected at 100 ng μl−1 with *pmyo-2::gfp* at 15 ng μl−1, giving *ljEx256*. The *trpa-1::gfp* construct was injected at 60 ng μl−1 with *pmyo-2::GFP* at 15 ng μl−1, giving *ljEx267*. To test for functional rescue, the transgenic lines were crossed into the corresponding mutant background and subsequently tested for touch or cold responses.

Calcium imaging

Optical recordings were performed essentially as described previously (Kerr R et al., 2000; Kerr RA, 2006) on a Zeiss Axioskop 2 upright compound microscope equipped with a Dual View beam splitter and a Uniblitz Shutter. Fluorescence images were acquired using MetaVue 6.2. Filter-dichroic pairs were excitation, 400–440; excitation dichroic 455; CFP emission, 465–495; emission dichroic 505; YFP emission, 520–550. Individual adult worms (~24h past L4) were glued with Nexaband

S/C cyanoacrylate glue to pads composed of 2% agarose in extracellular saline (145 mM NaCl, 5 mM KCl, 1 mM CaCl2, 5 mM MgCl2, 20 mM D-glucose and 10 mM HEPES buffer, pH 7.2). Worms used for calcium imaging had similar levels of cameleon expression in sensory neurons as inferred from initial fluorescence intensity. Acquisitions were taken at 28 Hz (35-ms exposure time) with 4 × 4 or 2 × 2 binning, using a 63× Zeiss Achroplan water-immersion objective.

Gentle body touch stimulation was performed as described Suzuki H et al., 2003), with a standard probe displacement of ~10 μm. Harsh stimuli were delivered using a glass needle with a sharp end (the outcome of these experiments was the same if a piece of platinum wire was used), which was driven into the worm ~30 to 50 μm at speed of 2.8 μm s−1. Stimulus duration was ~50 ms.

For thermal stimulation, a circular metal stage (Microscope Thermal Stage MTS-1, Techne, Proton-Wilten) was fitted with four 80 W peltier elements controlled by a National Instruments controller and custom-made Labview software. A T-junction thermocoupler located inside the chamber where the worm is positioned provides a continuous stream of readings to the temperature controller and adjusts the temperature using a feedback system. A worm grown at 20 °C was glued on an agar pad (2%) in a buffer-filled chamber with an approximate volume of 0.5 ml. The acquisition rate was 28 Hz; the recordings lasted 2 min with a 30-s stimulus.

Behavioural assays

For harsh body touch, worms were touched at the midsection of the body with a platinum wire and scored for reversal behaviour. Worms were tested on nematode growth medium with ten worms per plate; ten pokes were applied per assay with a 3-min interval between each stimulus to avoid stimulating the same worm twice before it had recovered. For each genotype, at least ten plates (>100 worms stimulated) were tested. For statistical analysis, the measurements (percent response) for individual plates were averaged to compute the overall mean as well as used to calculate s.e.m. and to conduct t test comparisons.

Thermal avoidance was assayed essentially as described (Srivastava N et al, 2009). I used the same thermal controller system described for the calcium imaging experiments. To improve the contrast, I provided dark-field illumination using a paired fiber-optic gooseneck lamp set at an oblique angle. The worm swam freely in a microdroplet sandwiched between a cover slip below and a round sapphire window above. A typical microdroplet contained ~0.6 μl of neuronal buffer flattening to a circular droplet containing a young adult worm. Using a 20× air objective, I recorded for 350 s at 10 frames per s. Worms cultivated at 20 °C were recorded initially for 150 s at 20 °C; the stimulus (a fast drop in temperature to 15 °C) lasted 60 s followed by a return to 20 °C. Image stacks were loaded on ImageJ and were scored blindly for omega turns according to the criteria described previously30. Events following a previous event within 0.3 s were rejected.

TRPA-1 expression in mammalian cells

HEK293T cells were maintained in DMEM containing 10% fetal bovine serum (vol/vol) and 1% penicillin/streptomycin (wt/vol). The HEK cells were transiently transfected with 3 μg of TRPA-1 channel plasmid DNA per 35-mm dish using Fugene 6 (Roche Diagnostics) as described23. Cells were plated onto poly-D-lysine–coated coverslips for recording purposes, and recordings were made 10–24 h after transfection.

Whole-cell voltage-clamp recordings were performed with protocols slightly modified from those described previously (Kindt KS et al., 2007). Briefly, the bath solution contained 140 mM NaCl, 5 mM KCl, 2 mM CaCl2, 1 mM MgCl2 and 10 mM HEPES, titrated to pH 7.4 with NaOH. The pipette solution contained 140 mM CsCl, 5 mM EGTA, 10 mM HEPES, 2.0 mM MgATP and 0.2 mM NaGTP titrated to pH 7.2 with CsOH. The holding potential was –60 mV and for the current-voltage analysis, 800-ms voltage-ramp pulses from -80 to +80 mV were used. For cold temperature stimulation, a Bipolar Temperature Controller CL-100 (Warner Instruments) was used. The temperature was measured using a temperature probe (TA-29, Warner Instruments) located ~5 mm distant from the cells under recording.

Confocal microscopy

PVDL labeled with F49H12.4::GFP48 was imaged in a Zeiss LSM 510 Meta confocal microscope with a 40× objective. The MEC-10::GFP, DEGT-1::GFP, DEGT-1::mCherry and TRPA-1::GFP lines were imaged in a Zeiss LSM 510 Meta confocal microscope with a 60× objective.

2.6 Experimental Contributions

The TRPA-1 expression in HEK cells and the electrophysiology experiments were conducted by Sungjae Yoo under the supervision of Sun Wook Hwang. Joseph D Watson generated the microarray data for PVD expression profiling using an mRNA tagging strain constructed by W Clay Spencer, David Miller III and Millet Treinin. Katie Kindt generated the cameleon line for PVD and FLP imaging. Wei-Hsiang Lee characterized the harsh touch behaviour of mec-10 (none of his data are included in the paper or my dissertation) and generated the *mec-10 mec-4* double mutants under the guidance of Monica Driscoll. I conducted the rest of the experiments under the supervision of William R Schafer.

2.7 References

Bandell M, Story GM, Hwang SW, Viswanath V, Eid SR, Petrus MJ, Earley TJ, Patapoutian A (2004) Noxious cold ion channel TRPA1 is activated by pungent compounds and bradykinin. Neuron 41(6):849-57

Bautista DM, Jordt SE, Nikai T, Tsuruda PR, Read AJ, Poblete J, Yamoah EN, Basbaum AI, Julius D (2006) TRPA1 mediates the inflammatory actions of environmental irritants and proalgesic agents. Cell 124(6):1269-82

Bianchi L, Gerstbrein B, Frøkjaer-Jensen C, Royal DC, Mukherjee G, Royal MA, Xue J, Schafer WR, Driscoll M (2004) The neurotoxic MEC-4(d) DEG/ENaC sodium channel conducts calcium: implications for necrosis initiation. Nat Neurosci 7(12):1337-44

Bounoutas A, Chalfie M (2007) Touch sensitivity in *Caenorhabditis elegans* Pflugers Arch – Eur J Physiol 454:691-702

Caterina MJ, Schumacher MA, Tominaga M, Rosen TA, Levine JD, Julius D (1997) The capsaicin receptor: a heat-activated ion channel in the pain pathway. *Nature* 389(6653):816–24

Chelur DS, Ernstrom GG, Goodman MB, Yao CA, Chen L, ROH, Chalfie M (2002) The mechanosensory protein MEC-6 is a subunit of the *C. elegans* touch-cell degenerin channel. Nature 420:669–673

Christensen AP, Corey DP (2007) TRP channels in mechanosensation: direct or indirect activation? Nat. Rev. Neurosci. 8(7):510–521

Colbert HA, Smith TL, Bargmann CI (1997) OSM-9, a novel protein with structural similarity to channels, is required for olfaction, mechanosensation, and olfactory adaptation in *Caenorhabditis elegans*. J Neurosci 17:8259–8269

Croll NA (1975) Components and patterns in the behaviour of the nematode, *Caenorhabditis elegans*. J. Zool. 176:159–76

Driscoll M, Chalfie M (1991) The *mec-4* gene is a member of a family of *Caenorhabditis elegans* genes that can mutate to induce neuronal degeneration. Nature 349:588–593

Esposito G, Di Schiavi E, Bergamasco C, Bazzicalupo P (2007) Efficient and cell specific knock-down of gene function in targeted *C. elegans* neurons. Gene 395(1-2):170-6

Fox RM, Von Stetina SE, Barlow SJ, Shaffer C, Olszewski KL, Moore JH, Dupuy D, Vidal M, Miller DM 3rd (2005) A gene expression fingerprint of *C. elegans* embryonic motor neurons. 21;6(1):42

Garcia-Anoveros J, Corey DP (1997) The molecules of mechanosensation. Annu Rev Neurosci. 20:567-94

Goodman MB, (2006) Mechanosensation. in WormBook (ed. The *C. elegans* Research Community) doi:10.1895/wormbook.1.62.1 <http://www.wormbook.org/>

Goodman MB, Ernstrom GG, Chelur DS, O'Hagan R, Yao CA, Chalfie M (2002) MEC-2 regulates *C. elegans* DEG/ENaC channels needed for mechanosensation. Nature 415:1039–1042

Gray JM, Hill JJ, Bargmann CI (2005) A circuit for navigation in *Caenorhabditis elegans*. Proc Natl Acad Sci U S A 102(9):3184-91

Hall D, Altun ZF, C. elegans Atlas (2008) Cold Spring Harbor Laboratory Press, Cold Spring Harbor, New York

Hilliard MA, Apicella AJ, Kerr R, Suzuki H, Bazzicalupo P, Schafer WR (2005) In vivo imaging of C. elegans ASH neurons: cellular response and adaptation to chemical repellents. EMBO J 24(1):63-72

Hilliard MA, Bergamasco C, Arbucci S, Plasterk RH, Bazzicalupo P (2004) Worms taste bitter: ASH neurons, QUI-1, GPA-3 and ODR-3 mediate quinine avoidance in *Caenorhabditis elegans*. EMBO J. 23(5):1101-11

Huang M, Chalfie M (1994) Gene interactions affecting mechanosensory transduction in *Caenorhabditis elegans*. Nature 367:467–470

Kahn-Kirby AH, Bargmann CI (2006) TRP channels in C. elegans. Annu. Rev. Physiol. 68:719–36 (2006)

Kammath RS, Martinez-Campos M, Zipperlen P, Fraser AG, Ahringer J (2001) Effectiveness of specific RNA-mediated interference through ingested double-stranded RNA in *Caenorhabditis elegans*. Genome Biol 2, 2

Kang K, Pulver SR, Panzano VC, Chang EC, Griffith LC, Theobald DL, Garrity PA (2010) Analysis of Drosophila TRPA1 reveals an ancient origin for human chemical nociception. Nature 464(7288):597-600

Kaplan, JM, Horvitz HR (1993) A dual mechanosensory and chemosensory neuron in *Caenorhabditis elegans*. Proc. Natl. Acad. Sci. USA 90, 2227–2231

Kerr R, Lev-Ram V, Baird G, Vincent P, Tsien RY, Schafer WR (2000) Optical imaging of calcium transients in neurons and pharyngeal muscle of *C. elegans*. Neuron 26(3):583-94

Kerr RA (2006) Imaging the activity of neurons and muscles. In WormBook (ed. The *C. elegans* Research Community) doi:10.1895/wormbook.1.113.1 <http://www.wormbook.org/>

Kindt KS, Viswanath V, Macpherson L, Quast K, Hu H, Patapoutian A, Schafer WR (2007a) *Caenorhabditis elegans* TRPA-1 functions in mechanosensation. Nature Neurosci. 10: 568-577

McKemy DD, Neuhausser WM, Julius D (2002). Identification of a cold receptor reveals a general role for TRP channels in thermosensation. Nature 416, 52–58

O'Hagan R, Chalfie M, Goodman MB (2005) The MEC-4 DEG/ENaC channel of *Caenorhabditis elegans* touch receptor neurons transduces mechanical signals. Nat Neurosci 8:43–50

Patapoutian A, Tate S, Woolf CJ (2009) Transient receptor potential channels: targeting pain at the source. Nat Rev Drug Discov. 8(1):55-68

Peier AM, Moqrich A, Hergarden AC, Reeve AJ, Andersson DA, Story GM, Earley TJ, Dragoni I, McIntyre P, Bevan S, Patapoutian A (2002a) A TRP channel that senses cold stimuli and menthol. Cell 108, 705–715

Persson A, Gross E, Laurent P, Busch KE, Bretes H, de Bono M (2009) Natural variation in a neural globin tunes oxygen sensing in wild *Caenorhabditis elegans*. Nature 458(7241):1030-3

Price MP, McIlwrath SL, Xie J, Cheng C, Qiao J, Tarr DE, Sluka KA, Brennan TJ, Lewin GR, Welsh MJ (2001) The DRASIC cation channel contributes to the detection of cutaneous touch and acid stimuli in mice. Neuron 32(6):1071-83

Smith CJ, Watson JD, Spencer WC, O'Brien T, Cha B, Albeg A, Treinin M, Miller DM 3rd (2010) Time-lapse imaging and cell-specific expression profiling reveal dynamic branching and molecular determinants of a multi-dendritic nociceptor in *C. elegans*. Dev Biol. 345(1):18-33

Sönnichsen, B. et al., (2005) Full-genome RNAi profiling of early embryogenesis in *Caenorhabditis elegans*. Nature 434, 462–469

Srivastava N, Clark DA, Samuel AD (2009) Temporal analysis of stochastic turning behavior of swimming *C. elegans*. J Neurophysiol 102(2):1172-9

Story GM, Peier AM, Reeve AJ, Eid SR, Mosbacher J, Hricik TR, Earley TJ, Hergarden AC, Andersson DA, Hwang SW, et al. (2003) ANKTM1, a TRP-like Channel Expressed in Nociceptive Neurons, Is Activated by Cold Temperatures. Cell 112, 819–829

Suzuki H, Kerr R, Bianchi L, Frokjaer-Jensen C, Slone D, Xue J, Gerstbrein B, Driscoll M, Schafer WR (2003) In vivo imaging of *C. elegans* mechanosensory neurons demonstrates a specific role for the MEC-4 channel in the process of gentle touch sensation. Neuron 39:1005–1017

Tobin D, Madsen D, Kahn-Kirby A, Peckol E, Moulder G, Barstead R, Maricq A, Bargmann C (2002) Combinatorial expression of TRPV channel proteins defines their sensory functions and subcellular localization in *C. elegans* neurons. Neuron 35:307–318

Tominaga M, Caterina MJ, Malmberg AB, Rosen TA, Gilbert H, Skinner K, Raumann BE, Basbaum AI, Julius D (1998) The cloned capsaicin receptor integrates multiple pain-producing stimuli. Neuron 21(3):531-543

Tsalik EL, Niacaris T, Wenick AS, Pau K, Avery L, Hobert O (2003) LIM homeobox gene-dependent expression of biogenic amine receptors in restricted regions of the *C. elegans* nervous system. Dev Biol. 1;263(1):81-102

Watson JD, Wang S, Von Stetina SE, Spencer WC, Levy S, Dexheimer PJ, Kurn N, Heath JD, Miller DM 3rd (2008) Complementary RNA amplification methods enhance microarray identification of transcripts expressed in the *C. elegans* nervous system. BMC Genomics 19;9:84

Way JC, Chalfie M (1989) The *mec-3* gene of *Caenorhabditis elegans* requires its own product for maintained expression and is expressed in three neuronal cell types. Genes Dev 3:1823–1833

Wemmie JA, Price MP, Welsh MJ (2006) Acid-sensing ion channels: advances, questions and therapeutic opportunities. Trends Neurosci. (10):578-86

Wu J, Duggan A, Chalfie M (2001) Inhibition of touch cell fate by *egl-44* and *egl-46* in *C. elegans*. Genes Dev. 15(6):789-802

Von Stetina SE, Fox RM, Watkins KL, Starich TA, Shaw JE, Miller DM 3rd (2007) UNC-4 represses CEH-12/HB9 to specify synaptic inputs to VA motor neurons in *C. elegans*. Genes Dev 21(3):332-46

Yassin L, Samson AO, Halevi S, Eshel M, Treinin M (2002) Mutations in the extracellular domain and in the membrane-spanning domains interfere with nicotinic acetylcholine receptor maturation. Biochemistry 41(41):12329-35

Zhong L, Hwang RY, Tracey WD (2010) Pickpocket is a DEG/ENaC protein required for mechanical nociception in *Drosophila* larvae. *Curr. Biol.* 20:429-434

Chapter 3

Spatial Asymmetry in the Mechanosensory Phenotypes of the *C. elegans* DEG/ENaC Gene *mec-10*

3.1 Abstract

DEG/ENaC channels have been broadly implicated in mechanosensory transduction, yet many questions remain about how these proteins contribute to complexes that sense mechanical stimuli. In *C. elegans*, two DEG/ENaC channel subunits are thought to contribute to a gentle touch transduction complex: MEC-4, which is essential for gentle touch sensation, and MEC-10, whose importance is less well defined. By characterizing a *mec-10* deletion mutant, I have found that MEC-10 is important, but not essential, for gentle touch responses in the body touch neurons ALM, PLM, and PVM. Surprisingly, the requirement for MEC-10 in ALM and PLM is spatially asymmetric; *mec-10* animals show significant behavioural and physiological responses to stimulation at the distal end of touch neuron dendrites, but respond poorly to stimuli applied near the neuronal cell body. The subcellular distribution of a rescuing MEC-10::GFP translational fusion was found to be restricted to the neuronal cell body and proximal dendrite, consistent with the hypothesis that MEC-10 protein is asymmetrically distributed within the touch neuron process. These results suggest that MEC-10 may contribute to only a subset of gentle touch mechanosensory complexes found preferentially at the proximal dendrite.

3.2 Introduction

The senses of touch, hearing, and balance depend on sensory neurons that generate receptor potentials in response to mechanical force. Most, if not all, mechanosensory neurons sense force using ion channels that are directly mechanically gated. The structural subunits of these channels appear to come primarily from one of two protein superfamilies: the TRP (transient receptor potential) channels and the DEG/ENaC (degenerin/epithelial Na channel) channels (Garcia-Anoveros J, Corey

DP, 1997; Goodman MB et al., 2004). TRP channels are nonspecific cation channels composed of subunits with six transmembrane α-helices. At least some TRP channels appear to be sufficient by themselves to produce touch- or stretch evoked currents (Christensen AP, Corey DP, 2007). In addition,TRP channels can be activated by G protein signaling, which has been implicated in other sensory transduction processes including taste, vision, and olfaction (Kahn-Kirby AH, Bargmann CI, 2006). In contrast, DEG channel subunits have two transmembrane α-helices and form channels permeable to sodium and, in some cases, calcium (Bounoutas A, Chalfie M, 2007). Relatively little is known about how DEG channels are activated by mechanical or other stimuli.

Perhaps the best-studied case of DEG channel–mediated mechanosensation involves the gentle body touch neurons of *C. elegans*. Three gentle touch neurons (ALML, ALMR, and AVM) have processes extending from the midbody to the pharynx and are required for escape responses to light mechanical stimulation to the anterior body (Chalfie M et al., 1985). Two additional neurons (PLML and PLMR) have processes extending from the tail to the midbody and are required for escape responses to posterior gentle touch. Screens for mutants defective in gentle touch avoidance have identified over a dozen *mec* genes whose products are specifically required for the function of these neurons (Chalfie M, Au M, 1989). Among the *mec* genes are two that encode DEG/ENaC channel proteins, MEC-4 (Driscoll M, Chalfie M,1991) and MEC-10 (Huang M, Chalfie M, 1994), and two that encode DEG channel accessory subunits, MEC-2 (Huang M et al. ,1995) and MEC-6 (Chelur DS et al., 2002). Additional *mec* genes encode extracellular or intracellular structures thought to be important for coupling external forces to channel gating; however, the

mechanisms by which this might occur are not known (Bounoutas A, Chalfie M, 2007; Goodman MB, Schwarz EM, 2003). The importance of each of the *mec* genes for mechanosensation in the gentle touch neurons has been investigated at the cellular level through in vivo imaging and electrophysiology. Wild-type *C. elegans* exhibit robust calcium transients in the gentle touch neurons in response to mechanical stimulation; null mutations in *mec-4*, *mec-2*, and *mec-6* abolish these responses (Suzuki H et al., 2003). Likewise, *mec-4*, *mec-2*, and *mec-6* null mutant neurons lack mechanoreceptor potentials measured by electrophysiology (O'Hagan R et al., 2005). Previously characterized *mec-10* alleles are missense mutations (Huang M, Chalfie M, 1994) that reduce, but do not eliminate, mechanoreceptor potentials evoked by mechanical stimulation (O'Hagan R et al., 2005). I have analyzed a *mec-10* deletion allele and showed that MEC-10, along with a second DEG/ENaC protein known as DEGT-1, is required for harsh touch responses in the ALMs. However, the effect of the *mec-10* deletion allele on gentle touch responses has not been reported.

In addition to the gentle body touch neurons, MEC-10 is expressed in several additional neurons, where its function has not been established. The PVM neurons express not only *mec-10*, but also most of the other *mec* genes (Huang M, Chalfie M, 1994), and their overall morphology is very similar to that of the gentle touch neurons. However, unlike the gentle touch neurons, PVM is not sufficient to mediate an escape response to gentle touch and its role in mechanosensory behaviour in general is not known (Chalfie M, Sulston J, 1981; Chalfie M et al. 1985). Unlike the gentle touch neurons, PVM expresses another DEG channel gene, *unc-8*, which has been hypothesized to encode a stretch receptor potentially involved in proprioception (Tavernarakis N, Driscoll M, 1997). Another class of neurons

expressing *mec-10* are the FLPs, which play a role in escape responses to nose touch. The FLPs have highly branched multidendritic arbors that surround the animal's head, which are thought to be mechanosensory (Huang M, Chalfie M, 1994). *mec-4* is not expressed in the FLPs, although these neurons do express the TRP channel OSM-9, which is required for nose touch responses by the polymodal ASH neurons (Colbert HA et al., 1997). Finally, *mec-10* is expressed in the PVD neurons, which have been implicated in responses to harsh body touch (Way JC, Chalfie M, 1989). Similar to the FLPs, the PVDs have multidendritic arbors that cover the animal's body. Likewise, the PVDs do not express MEC-4, but express OSM-9, a TRP channel that is involved in mechanosensation in other *C. elegans* neurons (Colbert HA et al. 1997). I have shown that MEC-10 and DEGT-1 are required for harsh touch responses in PVD.

In this study, I have investigated the role of MEC-10 in the *C. elegans* gentle touch mechanosensory neurons. By analyzing a loss-of-function *mec-10* deletion mutant, I find that MEC-10 is important for responses to gentle touch applied near the mechanoreceptor neuron's cell body, but is less important for touch applied near the distal end of the touch receptor process. Consistent with this, MEC-10::GFP translational fusions are restricted to the ALM cell body and proximal dendrite, whereas MEC-4::GFP fusions are distributed in puncta all along the ALM process. These results suggest that the touch neurons may contain both MEC-10–dependent and MEC-10– independent mechanotransduction complexes, with the MEC-10–containing complexes specifically important for gentle touch near the cell body.

3.3 Results

3.3.1 Effects of *mec-10* mutations on anterior gentle touch responses

To investigate the contribution of MEC-10 to gentle touch, I studied three mutant alleles: *e1515*, a recessive missense mutation affecting a highly conserved region near the first transmembrane domain (Huang and Chalfie 1994); *u20*, a missense mutation that encodes a functional channel with altered reversal potential; and a deletion, *tm1552* (Zhang et al. 2008), which removes exon 5 and part of exon 6 (Figure 3.1). To determine the effects of these mutations on gentle touch avoidance behaviour, I scored the reversal responses of *mec-10* mutants to a light eyelash stroke across the anterior body (Fig. 3.2). I observed that when *mec-10(tm1552)* animals were touched near the midbody, they exhibited a strong touch-insensitive (Mec) phenotype. Interestingly, when the animals were stimulated at locations along the ALM process that were more distal to the cell body, I observed that *mec-10* mutants showed significantly greater touch sensitivity. This spatial asymmetry in the severity of the *mec-10* touch phenotype contrasted with *mec-4* null mutants, which were strongly touch-insensitive throughout the anterior body (Figure 3.2). A similar phenotype was observed for the other two *mec-10* mutations (Figure 3.2, Figure 3.3), indicating that the stronger proximal defect is related to the function of the MEC-10 protein rather than to specific features of particular mutant alleles.

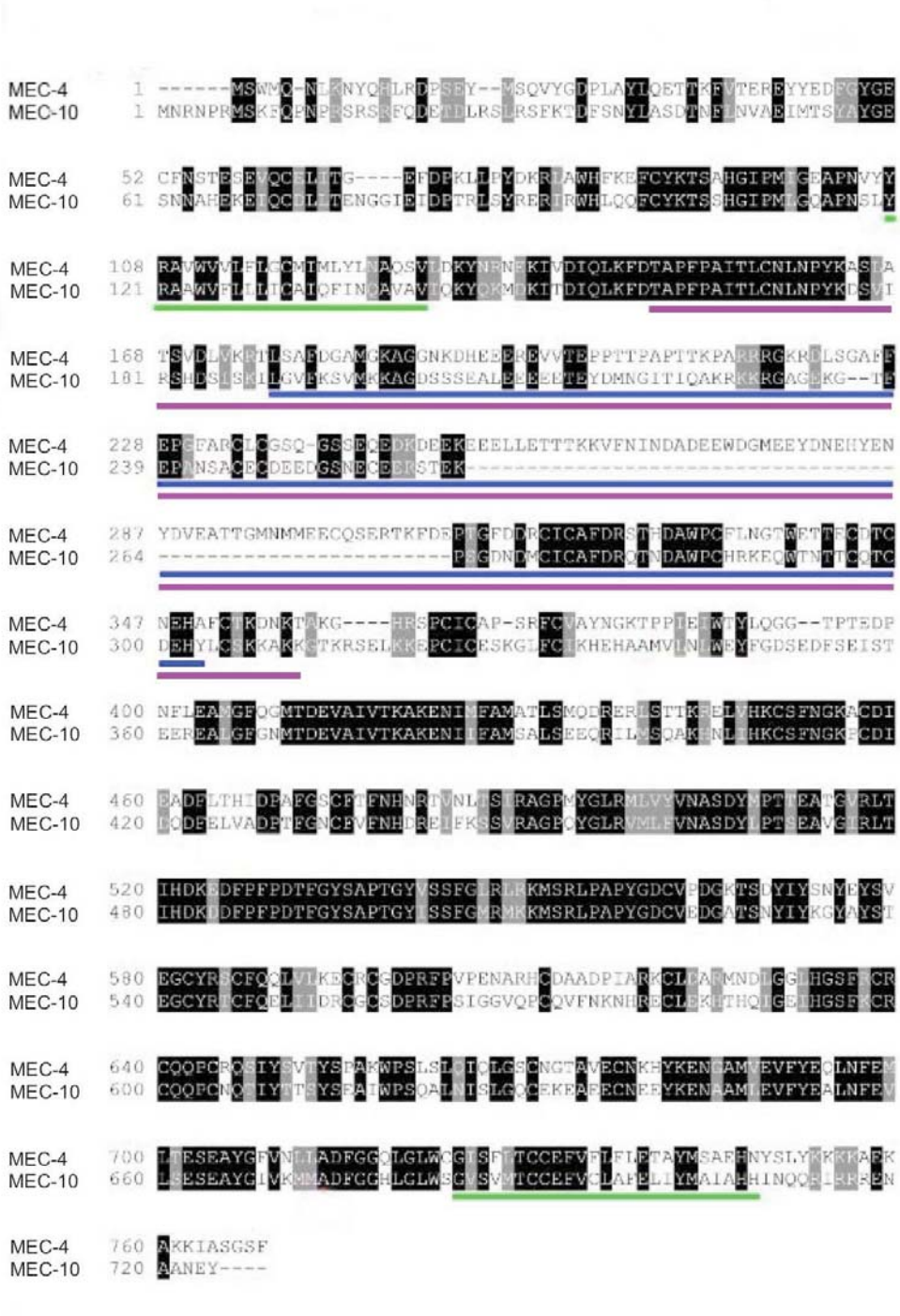

Figure 3.1: *mec-10(tm1552)* deletion structure and potential deleted translation product.

Figure 3.1: *mec-10(tm1552)* deletion structure and potential deleted translation product.

mec-10(tm1552) deletes 448 bp and removes exon 5 and part of exon 6, which encode part of the conserved extracellular domain (the amino acids encoded by the deleted nucleotides are indicated by blue underline). Normal translation of the mutant sequence would induce a frameshift with three premature stop codons (the first one is TAA at the end of the sequence below) close to the deletion site (…tctattcatattttt-deletion-TTTATGCAGCAAAAAAAGCTAA) such that if the theoretical transcript were translated, most of the extracellular domain and the pore-forming 2nd transmembrane domain of MEC-10 would be missing. However, an alternatively spliced transcript that joins exon 3 in-frame to exon 7 (detected in RT/PCR experiments with multiple primer sets) would, if translated, encode a MEC-10 protein lacking 153 amino acids from the extracellular domain (indicated by purple underline). Since the deleted region includes highly conserved sequences known to be essential for MEC-4 function, *tm1552* is likely to be a loss-of-function allele. Primers designed to avoid the homologous sequences between *mec-4* and *mec-10* and identify the deletion were: 5'GTAGGGTCTGCAACTAGCTC-3' and 5'-TGGGAGGGAGCTTCATCTTA-3'. Green lines indicate the 1st and 2nd transmembrane domains.

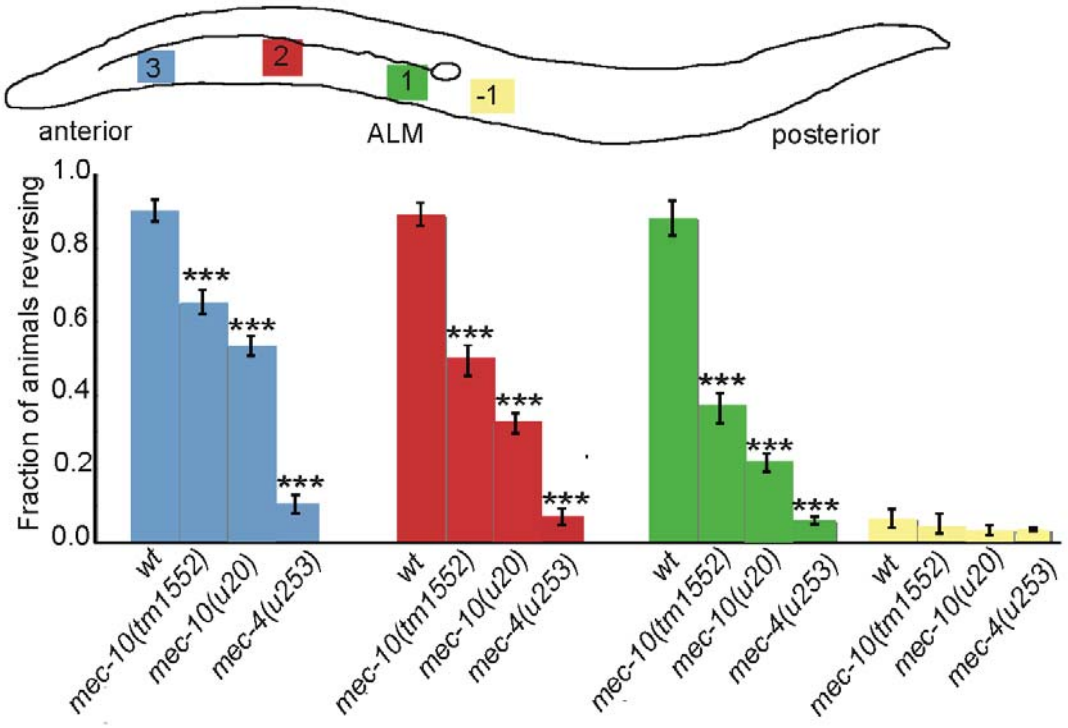

Figure 3.2: *mec-10* is important, but not essential, for anterior gentle touch avoidance.

Animals were touched with an eyelash at the indicated positions; escape responses (reversals) were scored as described. *mec-10(tm1552)* and *mec-10(u20)* animals were significantly less responsive than wild-type at all positions (***$P < 0.001$) according to the Student's *t*-test (n =100 for each genotype over 5 different days). One-way ANOVA demonstrated a statistically significant difference in the responses of *mec-10(tm1552)* and *mec-10(u20)* animals at different positions along the anteroposterior axis ($P < 0.001$).

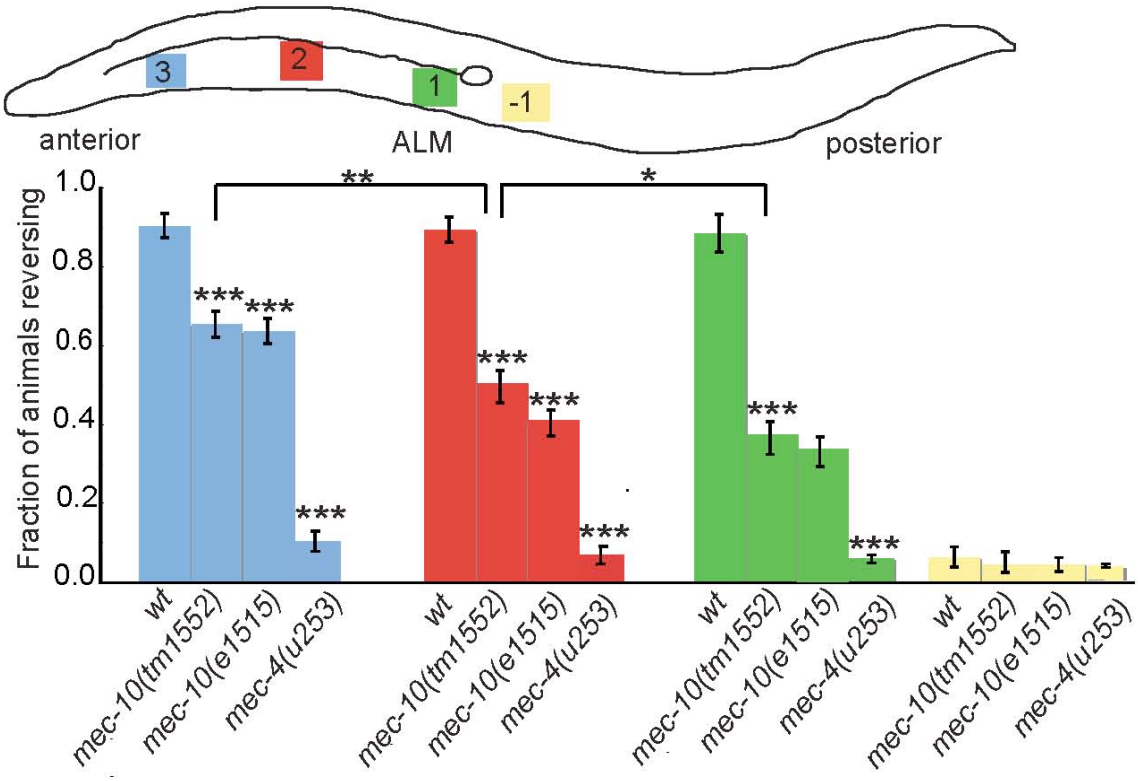

Figure 3.3: Effect of *mec-10(e1515)* on anterior touch gentle touch avoidance behaviour.

Animals were touched with an eyelash at the indicated positions; escape responses (reversals) were scored as described. *mec-10(e1515)* animals were significantly less responsive than wild-type at all positions (***p<.001) according to the Student's t test (n= 100 for each genotype over five different days). One-way analysis of variance (ANOVA) demonstrated a statistically significant difference in the responses of *mec-10(e1515)* animals at different positions along the anteroposterior axis (p<.001).

The distal dendrites of the ALM and AVM anterior touch receptors are closer to their synaptic outputs in the nerve ring than their proximal dendrites; thus one explanation for the more severe proximal defect in *mec-10* mutants is that weak proximal responses propagate less effectively to ALM/AVM synapses than weak distal responses (Savage C et al., 1989). Alternatively, *mec-10* mutations might have asymmetric defects in touch response per se. To distinguish between these possibilities, I measured calcium transients evoked in ALM by mechanical stimulation across the anterior body. I used a transgenic line, *bzIs17*, which expresses the calcium-sensitive protein cameleon from the touch neuron-specific *mec-4* promoter, to image touch-evoked calcium transients in the ALM cell body. As observed previously, wild-type animals generated calcium transients of similar size in response to gentle stimulation at various points along the anterior cell body (Suzuki H et al., 2003). When I conducted similar experiments in a *mec-10(tm1552)* or *mec 10(e1515)* background, I observed that the magnitude of the touch-evoked calcium influx was significantly reduced compared with wild-type (Figure 3.4).

Moreover, as in the behavioural experiments, I observed a spatial asymmetry in the magnitude of the ALM response to touch: responses to stimulations near the ALM cell body were more strongly defective than to those applied near the head (Figure 3.4, Figure 3.5). Recordings from *mec-10(u20)* mutants showed altered response dynamics compared with those from wild-type and other mutant strains, presumably because of altered properties of the mutant mechanoreceptor complex; however, the *u20* mutant responses were nonetheless stronger to distal stimuli than to proximal ones. For all mutants, the asymmetry in the severity of the touch response defect was observed not only across the population of animals tested, but also in individual

animals (Figure 3.4f, Figure 3.5b). Thus *mec-10* mutants appear to be less sensitive to gentle touch stimuli applied near the ALM cell body than to stimuli applied to the distal dendrite.

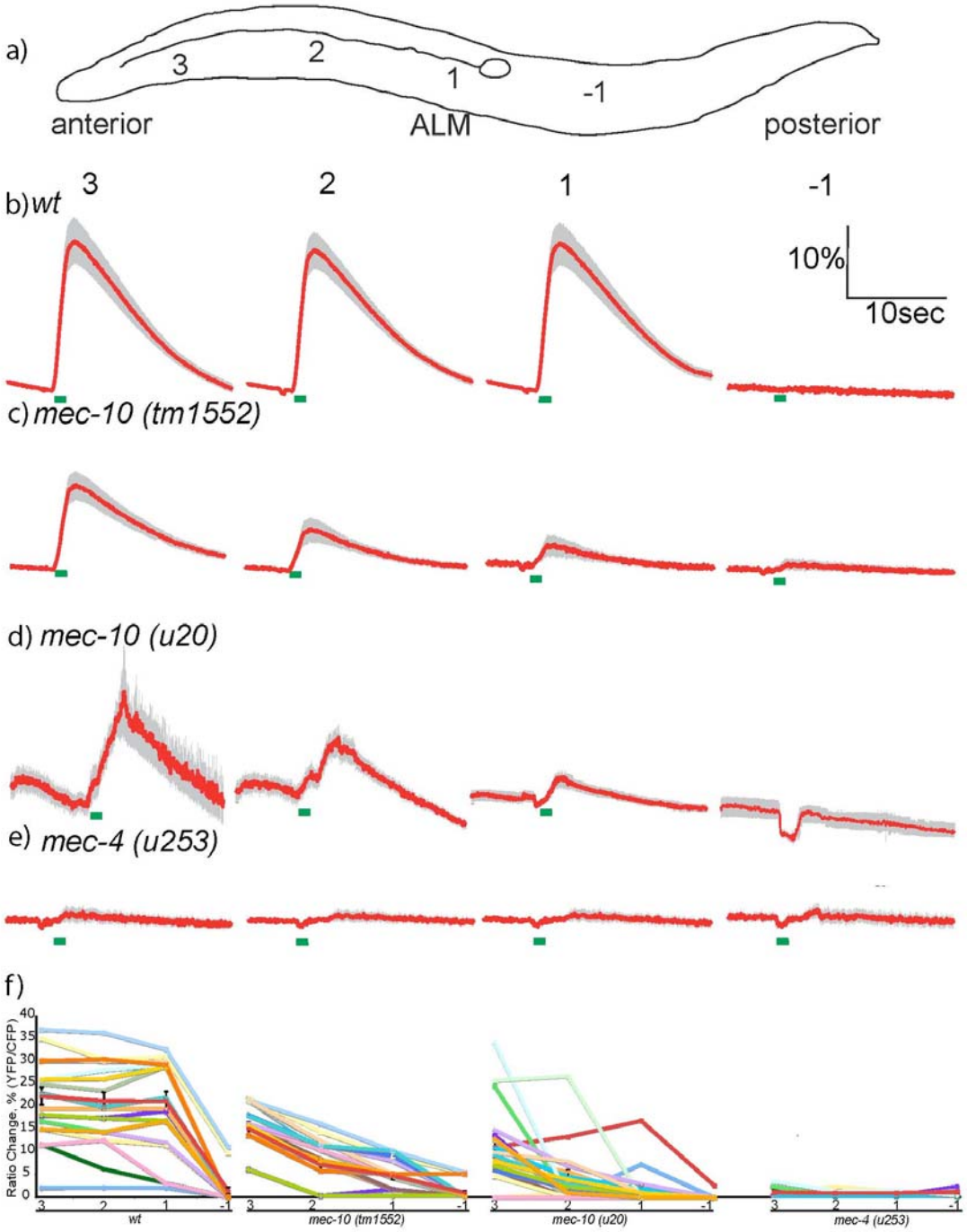

Figure 3.4: *mec-10* mutants have reduced touch-evoked calcium transients in ALM touch neurons.

Figure 3.4: *mec-10* mutants have reduced touch-evoked calcium transients in ALM touch neurons.

(a) Stimulus positions for imaging experiments. Animals expressing cameleon in touch neurons were given a 1-s gentle (buzz) stimulus at the indicated position, as described in Methods.

(b–e) averaged calcium responses of wild-type (b), *mec-10 (tm1552)* (c), *mec-10(u20)* (d), and *mec-4(u253)* (e) mutants. Each red trace represents the average percentage change in R/R_0, where R is the fluorescence emission ratio at a given time point and R_0 is its initial value. The number of individual recordings averaged for each trace were *n* = 27, 23, 22, and 12 (wild-type, positions 3, 2, 1, and -1, respectively); *n* =20, 25, 25, and 8 (*mec-10(tm1552)*, positions 3, 2, 1, and -1, respectively); *n* = 20 [*mec-10(u20)*, all positions]; and *n* = 10, 10, 8, and 8 (*mec-4*, positions 3, 2, 1, and _1, respectively). Grey shading indicates SE of the mean response. The green bar indicates the time of the stimulus. Decreases in the *u20* ratio signal (e.g., at position -1) are not accompanied by reciprocal changes in yellow fluorescent protein (YFP) and cyan fluorescent protein (CFP) emission intensities, suggesting that they are probably motion artifacts.

(**f) Scatter plot of peak calcium responses for each genotype.** Red lines indicate the mean response at each of the 4 stimulus points; error bars indicate SEM. Every other line indicates the response for a single animal. Half the animals were stimulated from anterior to posterior and half from posterior to anterior. One-way ANOVA demonstrated a statistically significant difference in the responses of *mec-10* but not *mec-4* animals at different positions along the anteroposterior axis ($P<0.001$).

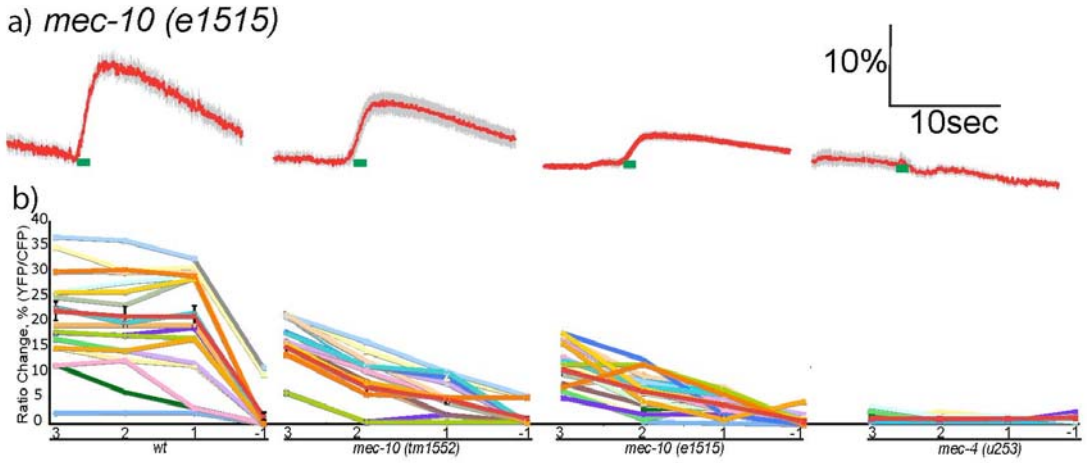

Figure 3.5: Effects of *mec-10(e1515)* on touch-evoked calcium transients in ALM touch neuron.

(a) Averaged calcium response to gentle touch. Each red trace represents the average percentage change in R/R_0, where R is the fluorescence emission ratio at a given time point and R_0 is its initial value. The number of individual recordings averaged for each trace were n=22 (all positions). Grey shading indicates SEM. Scale bars are indicated in upper right. The green bar indicates the time of the stimulus.

(**b) Scatter plot of peak calcium responses.** Red lines indicate the mean response at each of the four stimulus points; error bars indicate SEM. Each other line indicates the response for a single animal. Half the animals were stimulated from anterior to posterior, and half from posterior to anterior. Wild-type, *mec-10(tm1552)* and *mec-4(u253)* data from Figure 3.4 are shown for comparison. One-way analysis of variance (ANOVA) demonstrated a statistically significant difference in the calcium responses of *mec-10(e1515)* animals at different positions along the anteroposterior axis ($p<.001$).

3.3.2 The *mec-10(tm1552)* allele is recessive for behavioural and calcium imaging phenotypes.

To interpret the *mec-10(tm1552)* mutant phenotype, it is important to determine whether the mutant allele leads to a loss or gain of MEC-10 function. Although the *tm1552* allele is a sizable deletion, the deleted gene retains the capacity to encode a transcript that links exon 3 in-frame to exon 7 (details in Figure 3.1). If translated, the deletion transcript would encode a protein lacking 153 amino acids of the extracellular domain, including highly conserved regions known to be critical for function in the DEG/ENaC protein MEC-4 (Hong K et al., 2000).

To assess whether *mec-10(tm1552)* is a loss-of-function allele, I conducted both behavioural and calcium imaging assays. I observed that *mec -10(tm1552)/ +* heterozygotes were indistinguishable from wild-type homozygotes in their sensitivity to gentle touch (Figure 3.6). Likewise, the touch-evoked calcium transients in *mec-10(tm1552)/+* heterozygotes expressing the *bzIs17* cameleon transgene were comparable to those seen in wild-type *bzIs17* animals (Fig. 3.7). I also generated transgenic extrachromosomal arrays expressing the wild-type *mec-10(+)* allele under the control of its own promoter or the touch neuronspecific *pmec-4* promoter. These extrachromosomal arrays rescued the touch-insensitive phenotype of the *mec-10(tm1552)* homozygote at all points of stimulation (Figure 3.6, Figure 3.7, Figure 3.8). These results show that the *mec-10(tm1552)* allele is fully recessive and thus most likely represents a loss-of-function allele.

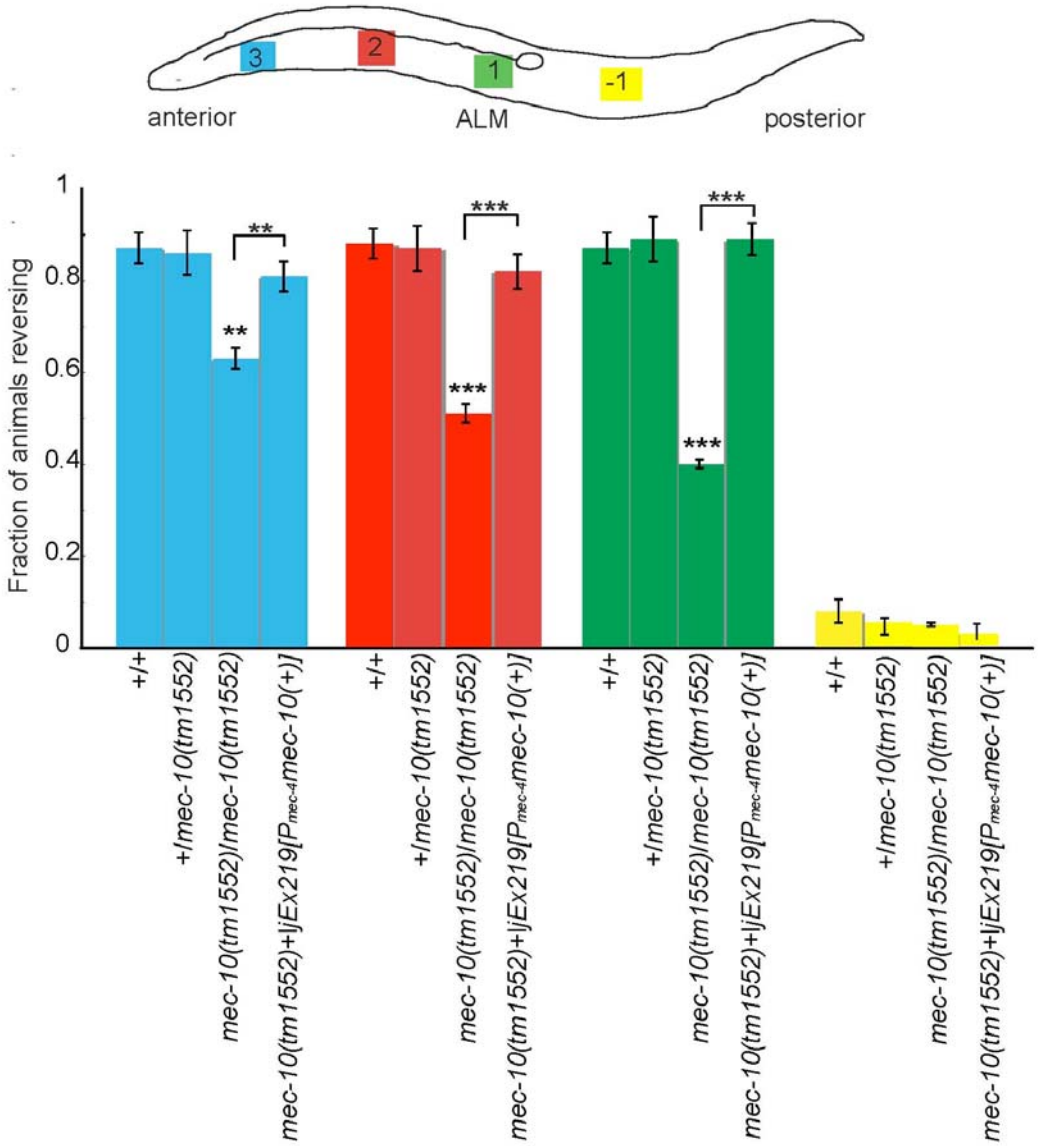

Figure 3.6: *mec-10(tm1552)* is a recessive allele and acts in the touch neurons. Animals were touched with an eyelash at the indicated positions; escape responses (reversals) were scored as described. *mec-10(tm1552)/+* heterozygous animals showed wild-type touch sensitivity at all positions. An extrachromosomal array carrying a *pmec-4::mec-10(+)* transgene rescued the phenotype of the *mec-10(tm1552)* homozygote at all positions; statistical significance (***P* <0.01 at position 3; ****P* <0.001 at positions 1 and 2) is according to the Student's *t*-test (*n*=100 for each genotype over 5 different days).

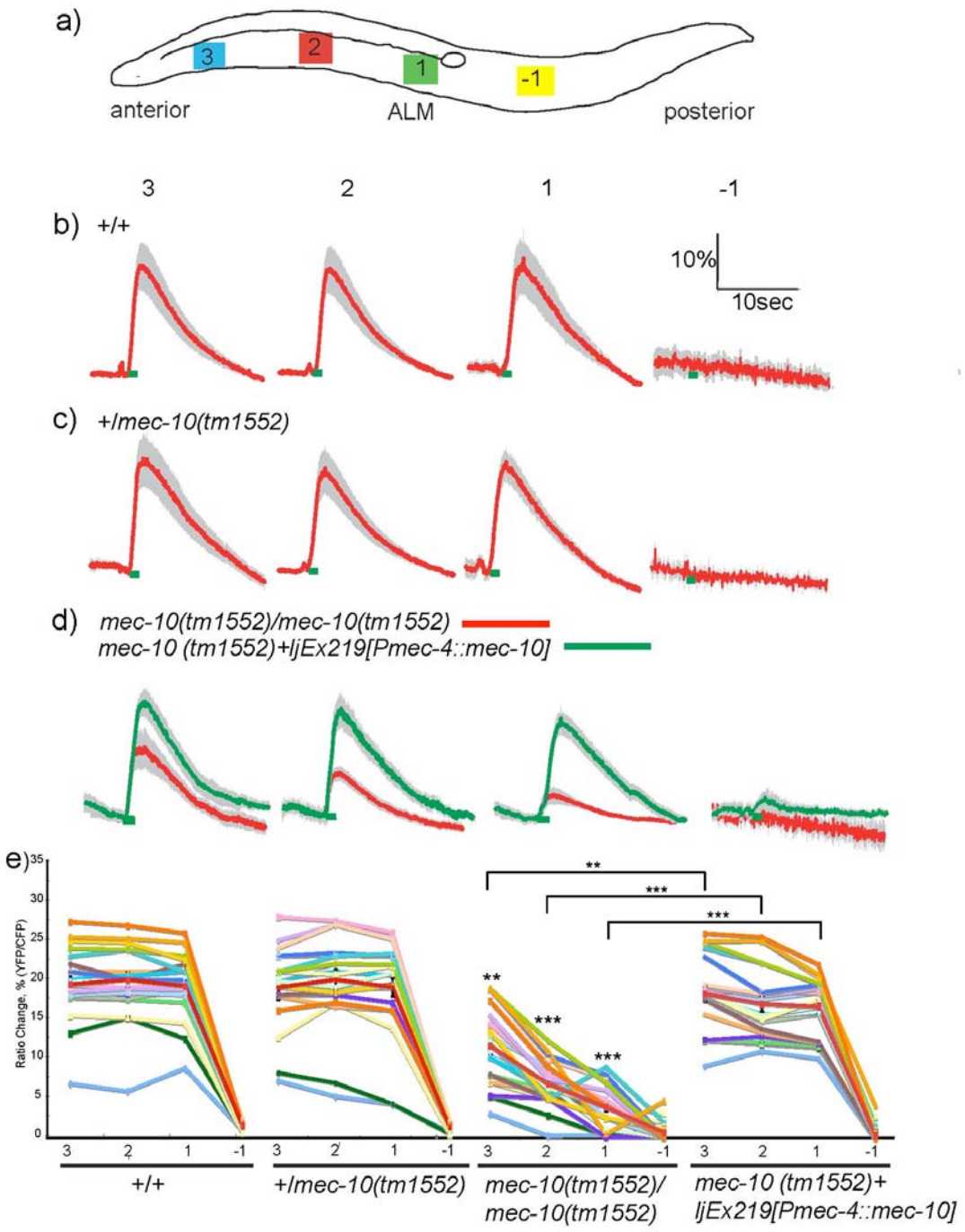

Figure 3.7: *mec-10(tm1552)* dominance tests assayed by calcium imaging.

Figure 3.7: *mec-10(tm1552)* dominance tests assayed by calcium imaging.

(a) Stimulus positions for imaging experiments. Animals expressing cameleon in touch neurons were given a 1-s gentle (buzz) stimulus at the indicated position, as described in methods.

(b–d) Averaged calcium responses of wild-type (b), *mec-10(tm1552)*/+ (c), *mec-10(tm1552)* (d, *red trace*), and *mec-10(tm1552); ljEx228[pmec-4::mec-10;pmyo-2::GFP]* (d, *green trace*) animals. Each trace represents the average percentage change in R/R_0, where R is the fluorescence emission ratio at a given time point and R_0 is its initial value. The number of individual recordings averaged for each trace were *n*=13, 13, 13, and 13 (wild-type, positions 3, 2, 1, and -1, respectively); *n* =13, 13, 13, and 13 [+/*mec-10(tm1552)* heterozygous positions 3, 2, 1, and -1, respectively]; and *n* = 13, 13, 13, and 13 [*mec-10(tm1552)* homozygous, positions 3, 2, 1, and -1, respectively]. Grey shading indicates SEM response. Scale bars are indicated in the top right. The green bar indicates the time of the stimulus.

(e) Scatter plot of peak calcium responses for each genotype. Red lines indicate the mean response at each of the 4 stimulus points; error bars indicate SEM. Every other line indicates the response for a single animal. Statistical significance (***P <0.0005; **P<0.005) is according to the Mann-Whitney rank-sum test (asterisks at stimulus points indicate comparisons to wild-type; asterisks on bars indicate comparisons to the rescue line). Half the animals were stimulated from anterior to posterior and half from posterior to anterior.

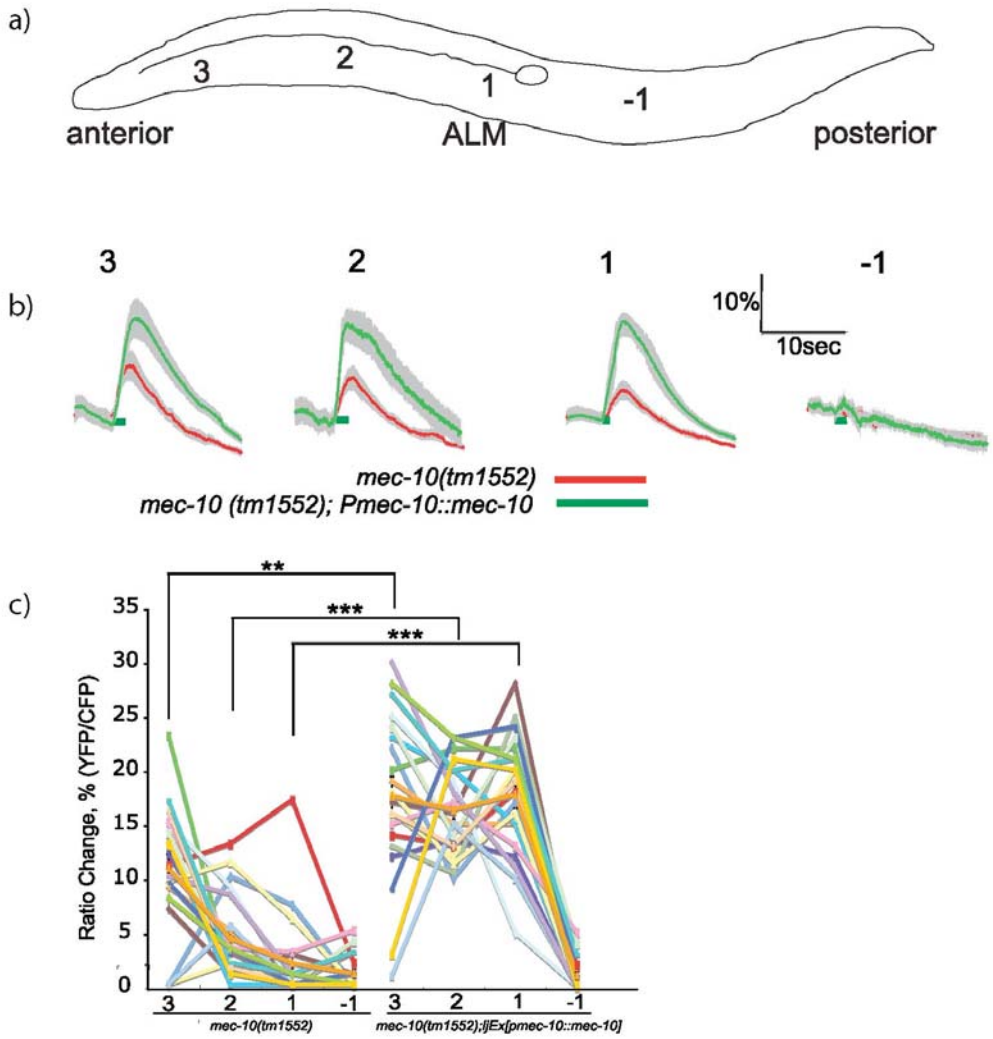

Figure 3.8: Rescue of *mec-10(tm1552)* by *pmec-10::mec-10(+)*.

Figure 3.8: Rescue of *mec-10(tm1552)* by *pmec-10::mec-10(+)*.

(a) Stimulus positions for imaging experiments. Animals were given a 1 second gentle (buzz) stimulus.

(b) Averaged calcium responses of *mec-10(tm1552)* (red trace), and *mec-10(tm1552); Ex[pmec-10::mec-10; pmyo-2::GFP]* (green traces) animals. Each trace represents the average percentage change in R/R_0. The number of individual recordings averaged for each trace were n=13 *mec-10(tm1552)* and n=20 (*pmec-10::mec-10* rescue). Grey shading indicates SEM. Scale bars are indicated in upper right. The green bar indicates the time of the stimulus.

(c) Scatter plot of peak calcium responses for each genotype. Red lines indicate the mean response at each of the four stimulus points; error bars indicate SEM. Each other line indicates the response for a single animal. Statistical significance (*** $p < .0005$; ** $p < .005$) is according to the Mann-Whitney rank sum test. Half the animals were stimulated from anterior to posterior, and half from posterior to anterior.

3.3.3 Gentle touch phenotype of a *mec-10 mec-4* double mutant.

The observation that significant gentle touch responses are seen in *mec-10* but not *mec-4* loss-of-function mutants suggested that touch neuron mechanosensory complexes, particularly those in the distal dendrite, require MEC-4 but not MEC-10. This model would predict that the gentle touch response remaining in *mec-10(tm1552)* deletion mutants would be dependent on MEC-4 and thus absent in a *mec-4* null mutant background. To test this possibility, a *mec- 10(tm1552) mec-4(u253)* double mutant was generated and assayed for its response to gentle touch by behaviour and calcium imaging. I observed that these double mutant animals, like *mec-4(u253)* single mutants, were significantly less sensitive to anterior gentle touch at all stimulus positions as measured in behavioural assays (Figure 3.9). However, at the most distal position, the double mutant did show measurable sensitivity to gentle touch, in contrast to the *mec-4* single mutant, which was completely touch-insensitive. When I measured touch-evoked calcium transients in ALM, I observed a similar result: *mec-10(tm1552) mec-4(u253)* double mutants showed responses that were small but significant compared with baseline and to the *mec-4(u253)* single mutant. Thus the sensitivity to gentle touch remaining in *mec-10(tm1552)* animals is largely but not completely dependent on *mec-4*. The source of the *mec-4*– and *mec-10*–independent touch response in ALM is not known; potentially, loss of both proteins could enhance the normally negligible activity of another ALM-expressed DEG/ENaC channel, possibly DEGT-1 which I have characterized in previous work. Alternatively, indirect touch activation of ALM by other neurons (e.g., ADE/PDE through the PVR interneuron) might be enhanced.

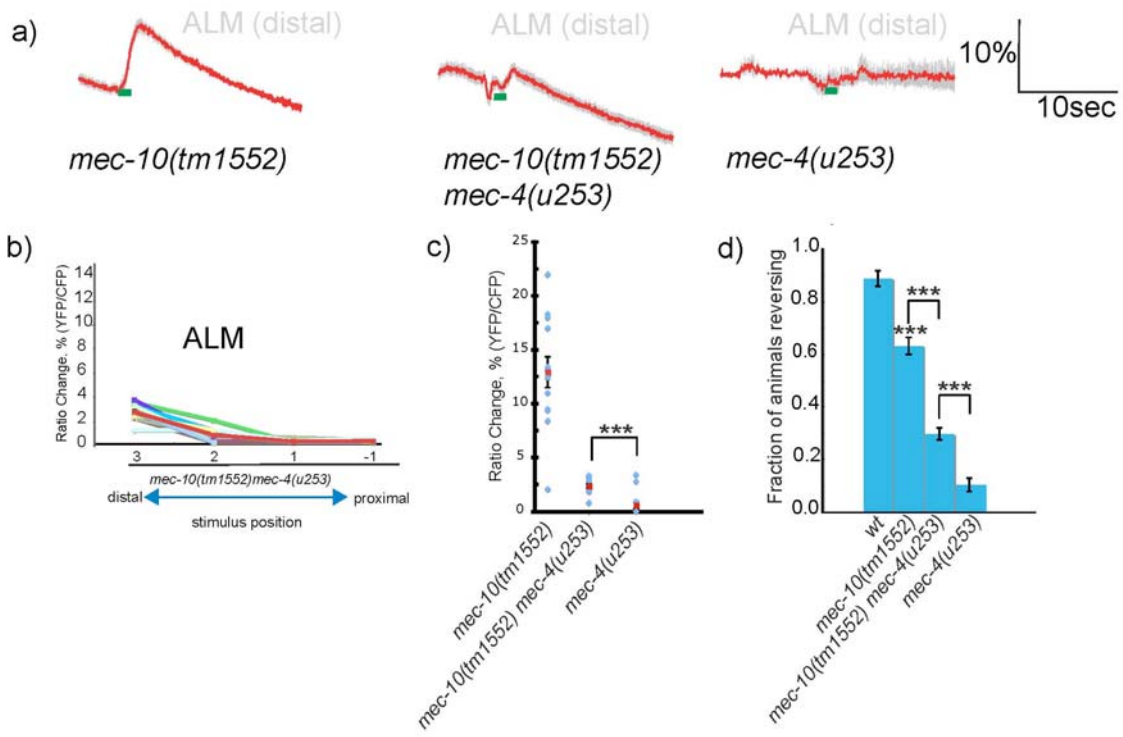

Figure 3.9: Touch phenotype of *mec-10 mec-4* double mutants.

(a) Averaged calcium responses of *mec-10(tm1552)*, *mec-10(tm1552) mec-4(u253)*, and *mec-4(u253)* animals to stimulation of the ALM distal dendrite. Animals were stimulated at position 3. For each genotype 13 animals were imaged.

(b) Scatter plot of peak calcium responses for *mec-10(tm1552) mec-4(u253)* animals with different stimulus positions. Red line indicates the mean response at each of the 4 stimulus points; error bars indicate SEM. Every other line indicates the response for a single animal.

(c) Scatter plot of peak calcium responses for distal stimulation of each genotype. Each point indicates peak calcium response for stimulation at position 3. The double mutant showed significantly more response than *mec-4 (u253)* according to the Mann–Whitney rank-sum test (***P <0.0005).

(d) Avoidance behaviour in response to gentle anterior touch. Over 200 animals were tested for each genotype; statistical significance (P< 0.0005) is according to the Student's *t*-test.

3.3.4 Effects of *mec-10* mutations on PLM posterior touch receptor responses.

C. elegans respond to gentle touch on the posterior body by accelerating forward away from the stimulus; this response is dependent on the left and right PLM neurons. To assess the role of *mec-10* in the PLMs, I assayed avoidance behaviour in response to posterior touch. I used an eyelash to apply gentle stimuli to various points on the posterior half of the body and assayed whether the animals exhibited a forward escape response. I observed that *mec-10(tm1552)* mutants were partially, but not completely, defective in posterior touch avoidance, in contrast to *mec-4(u253)* mutants that were more strongly touch-insensitive. Moreover, I found that *mec-10(tm1552)* mutants were strongly defective in responding to stimuli in areas near the tail (i.e., proximal to the PLM cell body), but responded better to stimuli applied in areas nearer the midbody and further from the PLM cell body (Figure 3.10). As with anterior touch, the *mec-10* phenotypes were all fully recessive in *mec-10(tm1552)*/+ heterozygotes and were rescued by the *pmec-4::mec-10(+)* transgene at all points of stimulation. Thus *mec-10(tm1552)* showed a partial Mec phenotype, more severe at cell body–proximal stimulus points, for both posterior and anterior touch.

I also assayed the effect of *mec-10* on touch-evoked calcium transients in PLM (Figure 3.11). In wild-type animals, stimuli applied anywhere between the midbody and the tail robustly evoked calcium transients in PLM. *mec-10(tm1552)* mutants showed a reduction in the magnitude of touch-evoked calcium transients compared with wild-type and the severity of this defect was significantly greater in response to cell body–proximal stimulation than to distal stimulation (Figure 3.11). As previously observed in ALM, this asymmetry in the severity of the touch response defect was observed in individual mutants as well as across the population of tested animals

(Figure 3.11). Similar results were observed with the *mec-10(e1515)* and *mec-10(u20)* alleles (Figure 3.12). Thus in PLM *mec-10* is also important, but not essential, for gentle touch mechanosensation and its function appears to be more important in proximal regions of the dendrite than in distal regions.

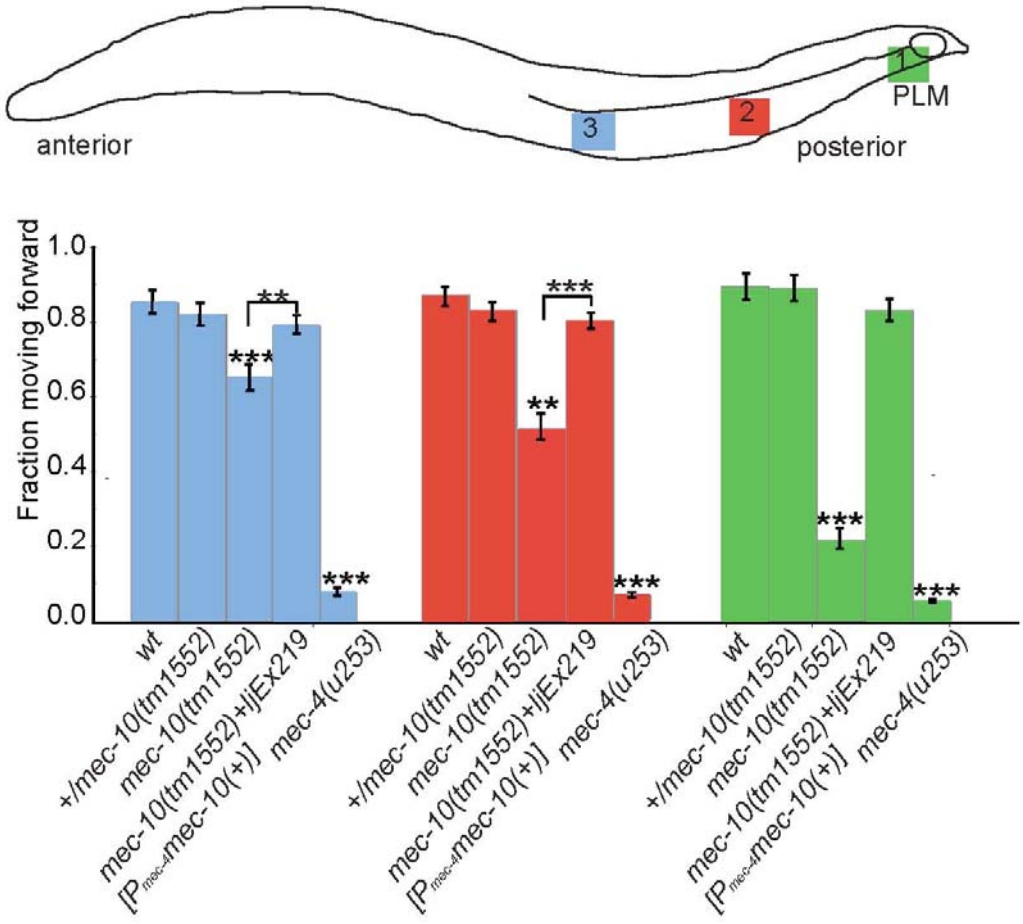

Figure 3.10: Effect of *mec-10* on posterior gentle touch avoidance.

Animals were touched at the indicated positions; forward accelerations were scored as escape responses. One-way ANOVA demonstrated a statistically significant difference in the responses of *mec-10(tm1552)* animals at different positions along the anteroposterior axis (P <0.001). All *mec-10(tm1552)* responses were significantly lower than those of wild-type (P<0.0005). Expression of genomic *mec-10(+)* under the *mec-4* promoter significantly rescues gentle touch in all positions of stimulation (n=100 per position of stimulation).

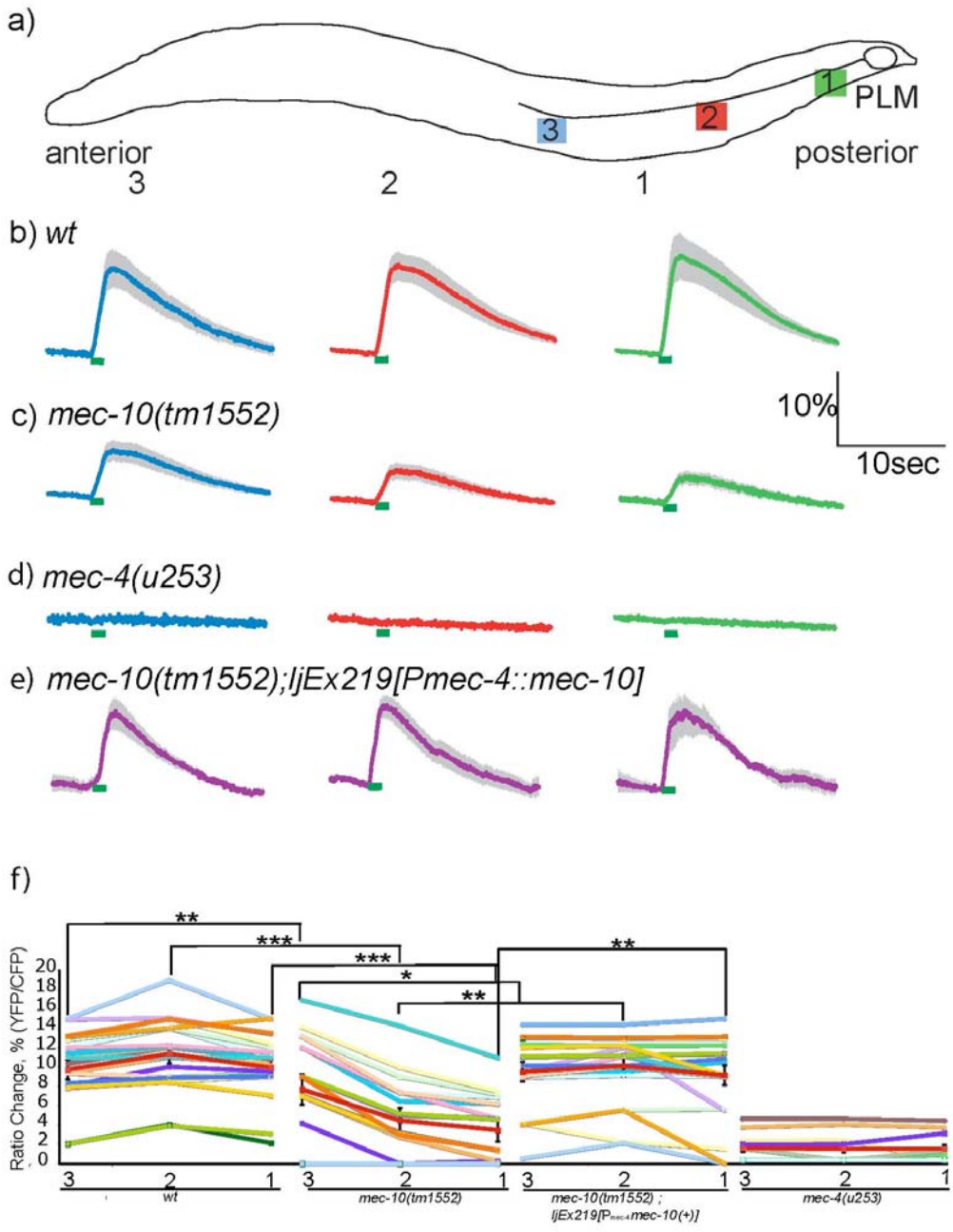

Figure 3.11: *mec-10(tm1552)* mutants have reduced touch-evoked calcium transients in PLM touch neurons.

Figure 3.11: *mec-10(tm1552)* mutants have reduced touch-evoked calcium transients in PLM touch neurons.

(a) Stimulus positions for imaging experiments. Animals were given a 1-s gentle (buzz) stimulus at the indicated position.

(b-e) Averaged calcium responses of wild-type (b), *mec-10(tm1552)* (c), *mec-4(u253)* null mutants (d), and *mec-10(tm1552); ljEx228[pmec-4::mec-10 pmyo-2::GFP]* rescue animals (e). Each trace represents the average percentage change in R/R_0. The numbers of individual recordings averaged for each trace were *n* =22, 22, and 22 (wild-type, positions 3, 2, and 1, respectively); *n*=22, 22, and 22 (*mec-10*, positions 3, 2, and 1, respectively); *n* = 22, 22, and 22 (*mec-10* rescue, positions 3, 2, and 1, respectively); and *n* =10, 10, and 10 (*mec-4*, positions 3, 2, and 1, respectively). Grey shading indicates SEM. Scale bars are indicated in the right. The green bar indicates the time of the stimulus.

(f) Scatter plot of peak calcium responses for each genotype. Red lines indicate the mean response at each of the stimulus points; error bars indicate SEM. Every other line indicates the response for a single animal. Half the animals were stimulated from anterior to posterior and half from posterior to anterior. Statistical significance (***P <0.001; **P < 0.01, *P < 0.05) is according to the Mann–Whitney rank-sum test.

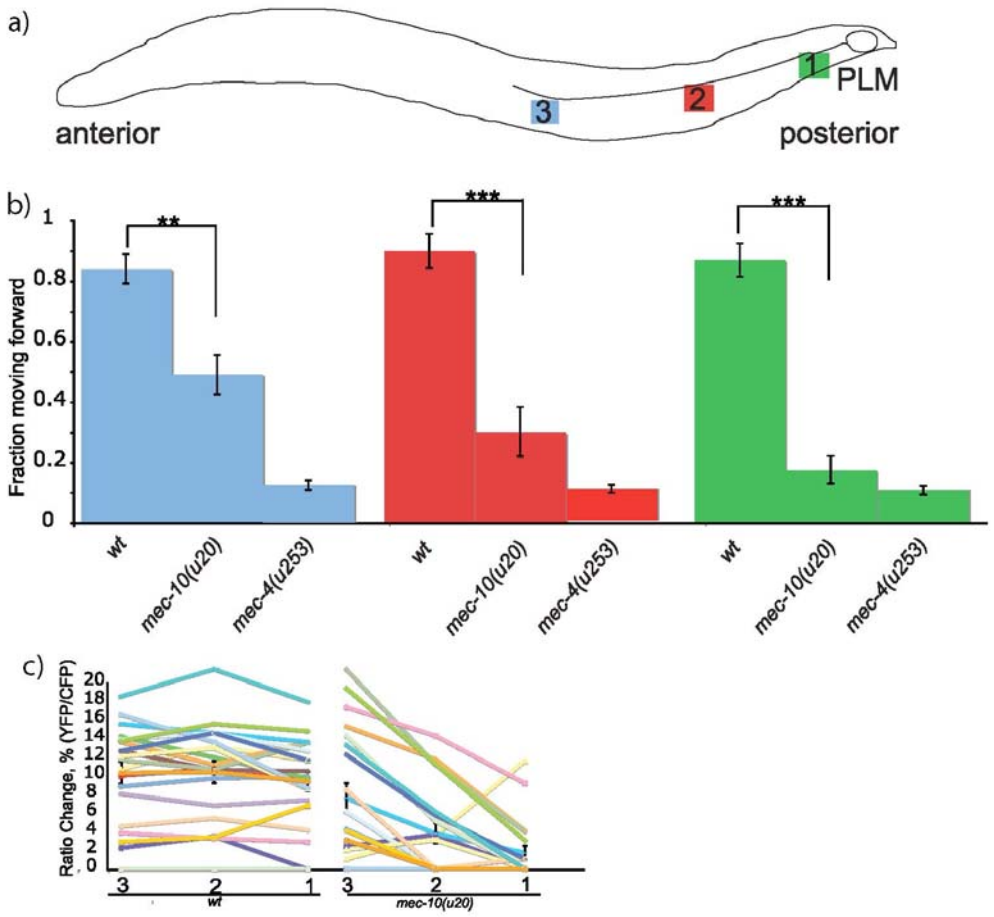

Figure 3.12: Effect of *mec-10(u20)* on posterior touch response.

(**a-b)** Animals were touched with an eyelash at the indicated positions; escape responses (forward accelerations) were scored as described. *mec-10(e1515)* animals were significantly less responsive than wild-type at all positions (***p<.001, **p<.01) according to the Student's t test (n= 100 for each genotype). One-way analysis of variance (ANOVA) demonstrated a statistically significant difference in the responses of *mec-10(u20)* animals at different positions along the anteroposterior axis (p<.001).

(c) Scatter plot of peak calcium responses. Red lines indicate the mean response at each of the four stimulus points; error bars indicate SEM. Each other line indicates the response for a single animal. Wild-type data from Figure 6 are shown for comparison.

3.3.5: Effects of *mec-10* mutations on the potential touch receptor neuron PVM

I also investigated the function of MEC-10 in the PVM neuron. PVM shares the morphology of the gentle body touch neurons ALM, AVM, and PLM and, like these neurons, expresses MEC-10, MEC-4, and other mechanosensory genes. However, unlike these other neurons, PVM is neither necessary nor sufficient for gentle touch avoidance and its role in touch-regulated behaviours has not been characterized (Chalfie M et al., 1985).

To determine whether PVM responds to mechanical stimuli, I used the *bzIs17* line to image touch-induced calcium transients in PVM. I observed that in wild-type animals, PVM generated calcium transients in response to gentle touch stimuli, similar in displacement and speed to those that activated ALM and PLM (Figure 3.13). However, whereas touch stimuli applied between the midbody and the PVM cell body robustly evoked calcium transients in PVM, stimuli applied near the tail did not. Thus the receptive field of PVM correlated closely with the position of the PVM dendrite and was distinct from that of the other gentle body touch neurons. In *mec-10(tm1552)* mutants, the touch-evoked calcium transient was reduced but not eliminated; however, unlike in the other touch neurons, no clear spatial asymmetry was observed in the severity of the phenotype (Figure 3.13). As in ALM, neither the *mec-4* null mutant nor a *mec-10(tm1552); mec-4* double mutant had any detectable response to gentle touch. Thus PVM appears to be a primary gentle touch mechanoreceptor that shares many of the same genetic requirements for touch sensitivity with those (i.e., ALM, AVM, and PLM) involved in the gentle touch escape response.

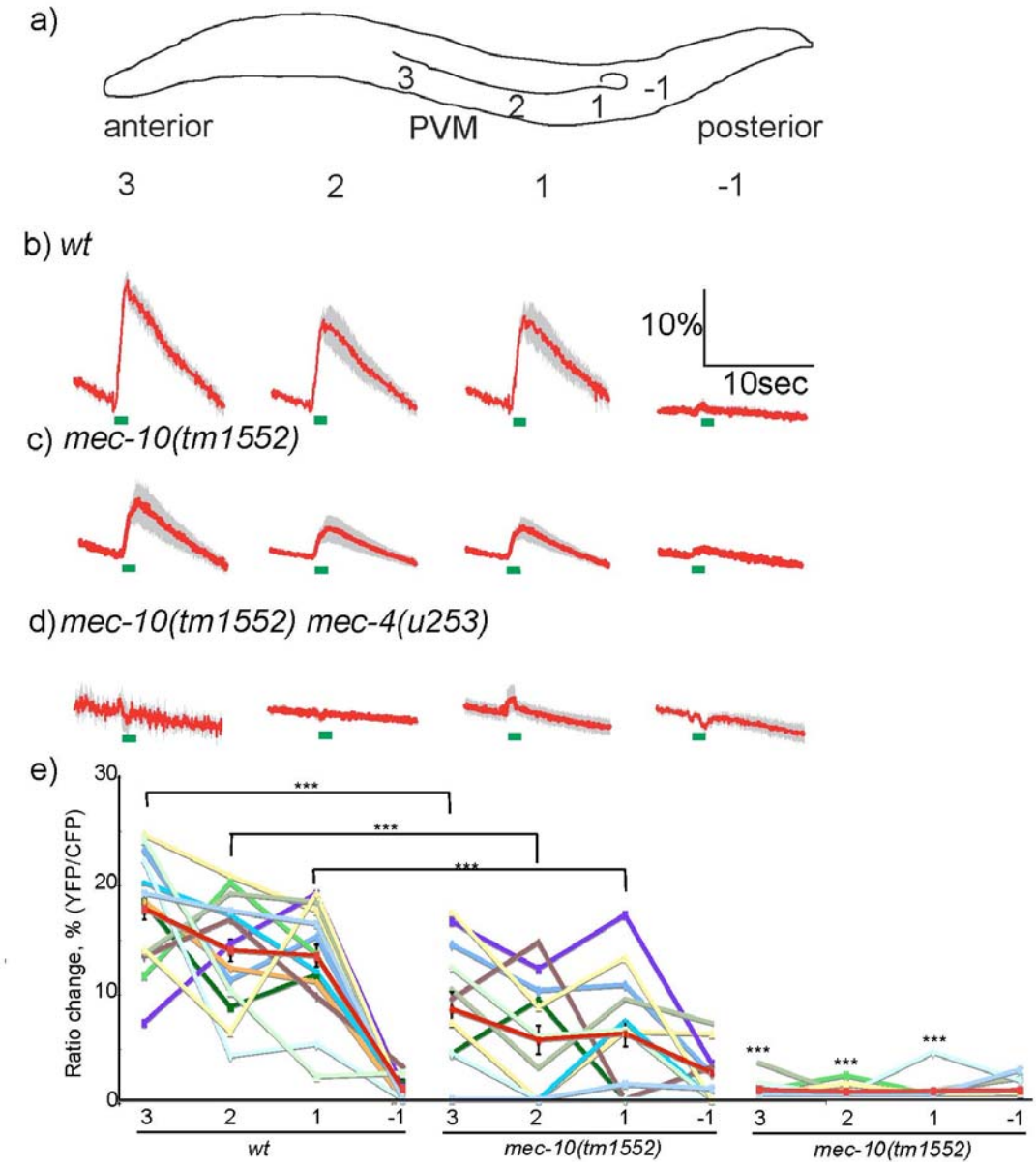

Figure 3.13: *mec-10* mutants have reduced touch-evoked calcium transients in PVM touch neurons.

Figure 3.13: *mec-10* mutants have reduced touch-evoked calcium transients in PVM touch neurons.

(a) Stimulus positions for imaging experiments. Animals were given a 1-s gentle (buzz) stimulus at the indicated position, as described in methods.

(b-d) averaged calcium responses of (b) wild-type, (c) *mec-10(tm1552)*, and (d) *mec-10(tm1552) mec-4(u253)* mutants. Each red trace represents the average percentage change in R/R_0, where R is the fluorescence emission ratio at a given time point and R_0 is its initial value. The number of individual recordings averaged for each trace were *n* =24, 20, 26, and 11 (wild-type, positions 3, 2, 1, and -1, respectively); *n* =19, 18, 17, and 11 (*mec-10*, positions 3, 2, 1, and -1, respectively); and *n*=10, 10, 8, and 8 (*mec-10*; *mec-4*, positions 3, 2, 1, and -1, respectively). Grey shading indicates SEM of the response. Scale bars are indicated in the right. The green bar indicates the time of the stimulus.

(e) Scatter plot of peak calcium responses for each genotype. Red lines indicate the mean response at each of the 4 stimulus points; error bars indicate SEM. Every other line indicates the response for a single animal. Statistical significance (****P*<0.001; ***P* <0.01) is according to the Mann–Whitney rank-sum test.

3.3.6 Localization patterns of *mec-10* and *mec-4* gene fusions in touch neurons

The spatial asymmetry of the *mec-10* touch phenotype raised the possibility that the MEC-10 protein might be asymmetrically localized within the touch neuron dendrites. However, it is also possible that MEC-10 is normally localized throughout the dendrite, but in the *mec-10* mutant MEC-4–containing mechanoreceptors become restricted to the proximal dendrite. To address this question, I generated transgenic lines expressing a full-length gene fusion between the *mec-10* and GFP coding regions under the control of the touch-neuron–specific *pmec-4* promoter. The full-length fusion transgene rescued the gentle touch defect of the *mec-10(tm1552)* deletion (Figure 3.14), suggesting its product is functionally localized within the touch neurons. I compared the fluorescence patterns of these animals with animals expressing a full-length *mec-4::GFP* fusion in the same cells. I observed that MEC-4::GFP fluorescence was distributed in a punctate pattern throughout the ALM and PLM dendrites (Figure 3.15), as reported previously (Cueva JG et al., 2007; Emtage L et al., 2004). In contrast, MEC-10::GFP fluorescence was concentrated in the touch neuron cell bodies and the most proximal regions of the dendrites (Figure 3.15, Figure 3.16). A mutant fusion protein consisting of the *mec-10(tm1552)* deleted polypeptide fused to GFP showed a similar distribution to the wild-type MEC-10::GFP in touch neurons (Figure 3.15c). RNAi of the *degt-1* harsh touch DEG/ENaC channel did not alter the pattern of MEC-10::GFP fluorescence in ALM (Figure 3.16), consistent with the possibility that MEC-10 protein involved in gentle touch is asymmetrically distributed. These results suggest that MEC-10 protein may be selectively localized to mechanotransduction complexes near the touch neuron cell bodies.

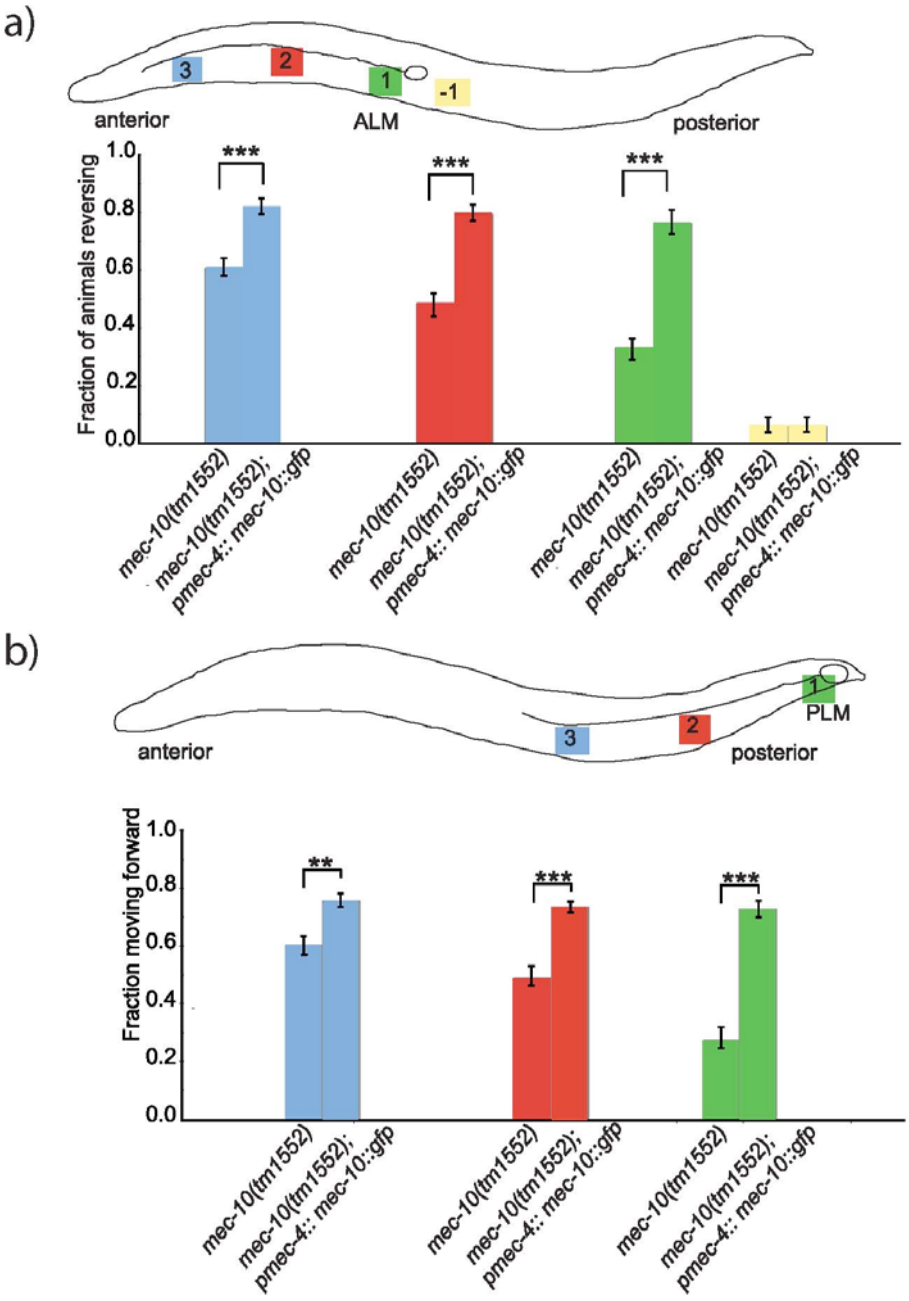

Figure 3.14: Rescue of *mec-10(tm1552)* gentle touch defects by *mec-10::GFP*.

Animals were touched with an eyelash at the indicated positions. Escape responses to anterior (reversals, a) or posterior (forward accelerations, b) were scored as described. *pmec-4::mec-10::gfp* animals were significantly more responsive than non-rescued *mec-10(tm1552)* animals at all positions (***p<.001, **p<.01) according to the Student's t test (n= 100 for each genotype).

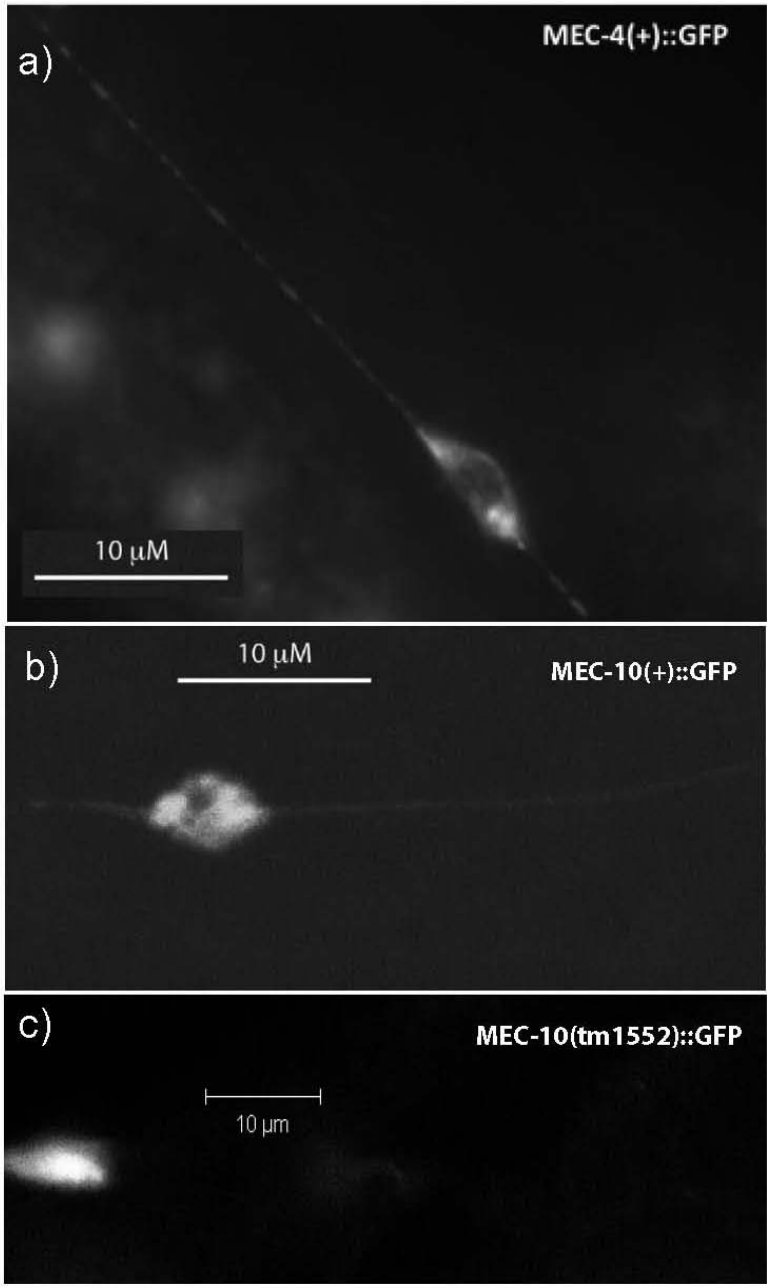

Figure 3.15 Localization of MEC-4 and MEC-10 protein fusions in body touch neurons. Shown are images of MEC-4::GFP (a), MEC-10::GFP (b), and MEC-10(tm1552)::GFP (c) fusions expressed in ALM. MEC-4::GFP normally is distributed in punctae along the touch receptor process. MEC-10::GFP and MEC 10(tm1552)::GFP are found only in the cell body in about 70% of observations; in the rest some staining can be observed in the posterior-projecting dendrite.

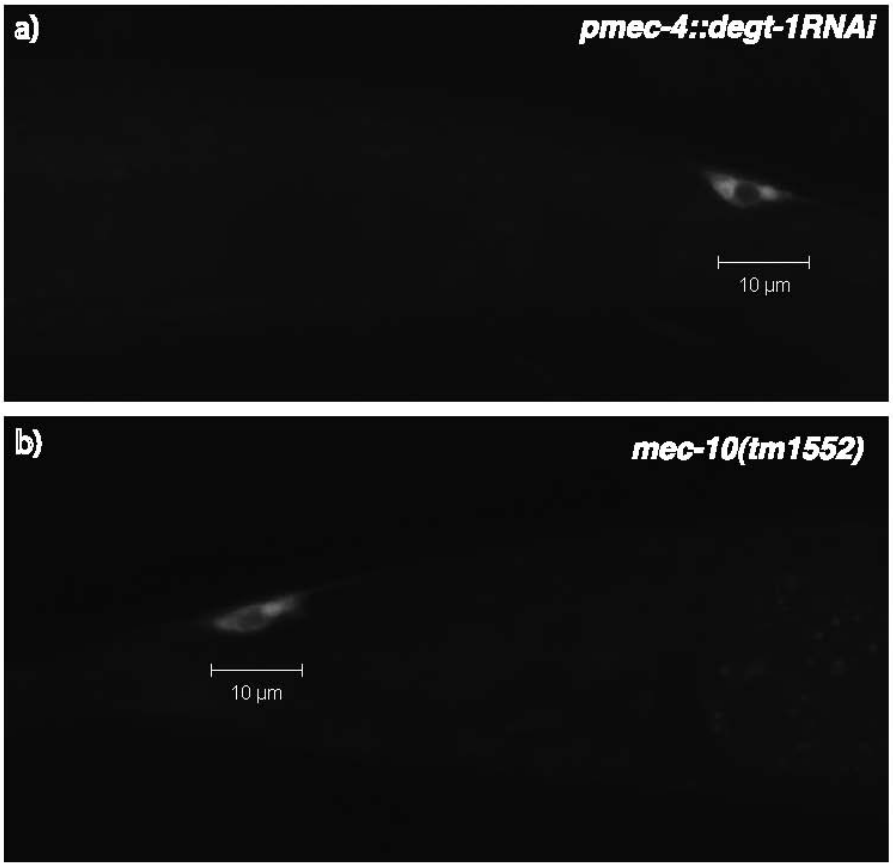

Figure 3.16: Effects of *degt-1::RNAi* and *mec-10(tm1552)* on localization of MEC-10 protein fusions in body touch neurons.

Shown are images of MEC- 10::GFP fluorescence in the ALM neurons of *pmec-4::degt-1RNAi* (a) and *mec-10(tm1552)* (b) animals. MEC-10::GFP fluorescence only in the cell body in about 65% of observations; in the rest some staining can be observed in the posterior-projecting dendrite.

3.4 Discussion

3.4.1 MEC-10 is important but probably not essential for gentle touch response

In recent years, DEG/ENaC channel family members have emerged as central contributors to sensory transduction, although how distinct subunits and complexes contribute to differential perception is poorly understood. In *C. elegans*, the DEG/ENaC channel genes *mec-4* and *mec-10* were identified in screens for mechanosensory (Mec) defects in gentle touch receptor neurons; although *mec-4* appears essential for gentle touch sensation in these neurons, the importance of *mec-10* has not been clearly defined. In this study, I found that although *mec-10* mutations impair the responsiveness of the gentle body touch mechanoreceptors, they do not completely abolish touch responses in these neurons. Indeed, in response to stimulations distal to the cell body, *mec-10* animals exhibit escape behaviour over 60% of the time and the calcium transients evoked in the cell body are nearly half the magnitude of those in wild-type animals. This phenotype contrasts with that of *mec-4*, *mec-2*, and *mec-6* null mutants, which have stronger Mec behavioural phenotypes and whose body touch neurons have no detectable response to gentle touch as measured by calcium imaging (Suzuki H et al., 2003) or electrophysiology (O'Hagan R et al., 2005). Although I cannot be completely certain the *mec-10(tm1552)* deletion allele is a null, based on molecular criteria as well as the results of dominance tests it almost certainly results in a severe loss of *mec-10* function. My results therefore suggest that MEC-10 is not an essential component of the gentle touch mechanosensory complex.

Standard models hypothesize that the mechanosensory complex in the gentle touch neurons consists of a core channel composed of MEC-4 and MEC-10, along with

MEC-2 and MEC-6 as accessory subunits. However, my results suggest that homomeric complexes containing only MEC-4 channel subunits may be capable of functioning as touch receptors. In support of this hypothesis, coexpression of dominantly active MEC-4 with MEC-2 and MEC-6 yields functional channels in *Xenopus* oocytes, and the addition of MEC-10 actually reduces expressed currents in this heterologous system (Goodman MB et al. 2002). Likewise, whereas MEC-4 is required for neurodegeneration induced by gain-of-function alleles of *mec-10*, MEC-10 is not required for *mec-4(gf)*-induced degeneration (Huang M, Chalfie M, 1994). These findings all indicate that MEC-4 can form functional channels without MEC-10 and are consistent with the existence of homomeric mechanotransduction channels. Alternatively, it is possible that MEC-4 may be able to form a gentle touch mechanotransducer by associating with a different, unidentified DEG/ENaC channel subunit. The possibility of a DEG/ENaC protein participating in multiple heteromeric complexes in the same cell is supported by recent evidence that I obtained showing that MEC-10 associates with DEGT-1 to form a harsh touch mechanoreceptor in the ALM neurons. Either of these models suggests a heterogeneous population of mechanosensory complexes might exist in the touch neurons, with only a subset including MEC-10 as a subunit.

3.4.2 Asymmetric requirements for MEC-10 in the gentle touch neurons

I observed an unexpected asymmetry in the requirement for MEC-10 in the ALM and PLM touch neurons. Specifically, in both behavioural and calcium imaging experiments, I observed that *mec-10* null animals were significantly more defective in responding to touch stimuli administered near the neuronal cell body than to stimuli

administered at the distal end of the dendrite. Interestingly, this spatial asymmetry in phenotypic strength resembles what was previously described for weak alleles of *mec-7* (Savage C et al., 1989). Since the imaging experiments measured calcium transients in the cell body, the fact that *mec-10* disproportionately affected responses to stimuli near the cell body is unlikely to reflect a defect in propagation of the mechanoreceptor potential along the process. Rather, MEC-10 may contribute differentially to mechanoreceptor complexes in different regions of the dendrite. Specifically, mechanoreceptor complexes in the cell body–proximal region of the dendrite may require both MEC-4 and MEC-10 subunits, whereas mechanoreceptor complexes in the distal region may require MEC-4 but not MEC-10. This is consistent with the subcellular distribution of the MEC-10::GFP reporter, which was restricted to regions near the touch neuron cell body.

These results may explain the apparent disparity between the relatively mild Mec phenotype observed in this work and a previous electrophysiological study (O'Hagan R et al., 2005), which reported that strong defects in PLM mechanoreceptor potentials were recorded from *mec-10* point mutants. In the latter study, receptor potentials were measured in response to stimuli applied within one length constant of the PLM cell body, about 90 μm. This position, corresponding approximately to stimulus point 1 in Figures 9 and 10, was in the cell body–proximal region of the dendrite, where I observed the strongest requirement for *mec-10*. Thus all data appear to be consistent with the possibility that MEC-10 is an important subunit of cell body–proximal mechanosensory complexes but less important for distal complexes.

3.4.3 PVM is a gentle touch mechanosensory neuron

This study also provides insight into the function of the PVM neuron in *C. elegans*. Although PVM resembles the gentle touch avoidance neurons (ALM, PLM, and AVM) in morphology and gene expression profile, cell ablation studies have failed to provide evidence for a mechanosensory function for this neuron. My calcium imaging results show that PVM responds to mechanosensory stimuli of similar intensity to those that activate the known gentle touch neurons. Moreover, the receptive field of PVM defined by these experiments is distinct from that of any of the gentle touch neurons and correlates precisely with the location of PVM's dendrite. Thus PVM is likely to be a primary mechanosensory neuron responding to gentle touch.

Since PVM is neither necessary nor sufficient for touch-activated escape responses, what role might it play in touchcontrolled behaviours? One possibility is that it might mediate longer-term responses to mechanical stimulation. Repeated or prolonged touch or tap has been implicated in a variety of types of behavioural modulation or plasticity (Rankin CH, Broster BS,1992; Wicks SR and Rankin CH, 1996; Zhao B et al., 2003). The timescales of these effects suggest the involvement of monoamine or neuropeptide modulators released from neurons in mechanosensory circuits (Kindt KS et al., 2007; Sanyal S et al., 2004). Since PVM is known to express at least two neuropeptide genes (*flp-8* and *flp-20*; Kim K and Li C, 2004), it is a plausible candidate for mediating long-term effects of touch on behaviour. Future studies of PVM and PVM-expressed neuropeptides may help to characterize the broader effects of mechanosensory information on *C. elegans* behaviour and to dissect their neural and molecular mechanisms.

3.5 Methods

Transgenic lines

For cloning, I used the MultiSite Gateway Three Fragment Vector Construction Kit. Individual PCR products were cloned into the appropriate pDONOR vector generating pENTRY clones. Subsequently, pENTRY vectors with the promoter and gene of interest as well as an *unc-54* 3'UTR-containing vector were recombined with a pDEST vector to generate an Expression vector. To generate the *pmec-10::mec-10(+)* transgene, a 4.4-kb (kilobase) *mec-10* genomic DNA was amplified using Phusion High- Fidelity DNA Polymerase F-530S from adult genomic DNA using the primers 5'-GTA CAAAAT TCA AAA AAT GAA TCG-3' and 5'-GAA ATA AGA AATTTA TTT TCCG-3'. A 1-kb *mec-4* promoter region was obtained from plasmid pIR13, a gift from I. Rabinowitch from the Schafer lab. The *pmec-4::mec10* construct was injected in *mec-10(tm1552);bzIs17* animals at 70 ng/_l with *pmyo-2::GFP* at 20 ng/µl to generate array *ljEx228[pmec-4::mec-10; pmyo-2::GFP].*

Behavioural assays

For gentle body touch assays, animals were touched by stroking an eyelash hair across the worm's body at different positions. The stimulus was applied at the following positions: anterior body position 3 = behind the terminal bulb of the pharynx, position 2 = between the pharynx and the midbody, and position 1 = at the midbody, -1 = control outside the receptive field; posterior body position 3 =near the anus position, position 2 = halfway between the anus and the vulva, and position 1 near the vulva. Animals were stimulated in each position and were scored for whether

they reversed direction, with a 3-min interval between each stimulus. In some animals, stimuli were applied in a proximal-to-distal direction and in other animals in a distal-to-proximal direction. In all, 100 animals were assayed from each genotype.

Calcium imaging

Optical recordings were performed essentially as previously described (Kerr RA, 2006; Kerr R et al., 2000) on a Zeiss Axioskop 2 upright compound microscope equipped with a Dual View beam splitter and a Uniblitz Shutter. Fluorescence images were acquired using MetaVue 6.2. Filter-dichroic pairs were excitation, 400 – 440; excitation dichroic 455; cyan fluorescent protein (CFP) emission, 465– 495; emission dichroic 505; yellow fluorescent protein (YFP) emission, 520 –550. Individual adult worms (~24 h past L4) were glued with Nexaband S/C cyanoacrylate glue to pads composed of 2% agarose in extracellular saline (in mM: 145 NaCl, 5 KCl, 1 CaCl2, 5 MgCl2, 20 D-glucose, and 10 HEPES buffer; pH 7.2). Worms used for calcium imaging had similar levels of cameleon expression in sensory neurons, as inferred from initial fluorescence intensity. Acquisitions were taken at 28 Hz (35-ms exposure time) with 4 _ 4 or 2 _ 2 binning, using a _63 Zeiss Achroplan water immersion objective.

Gentle body touch stimulation

Gentle body touch stimulation was performed as previously described (Suzuki H et al., 2003), with a standard probe displacement of about 10 μm.

Positions for anterior body touch stimulation were defined as follows:

3 = behind terminal bulb, 2 = midway between the ALM cell body and

terminal bulb, 1 = within 10 μm from ALM cell body, -1_=10 μm posterior of the ALM cell body. For posterior body touch the points of stimulation were 3=within 10μm from the vulva, 2=midway between the vulva and the tip of the tail, 1 =within 10 μm of PLM cell body. For PVM imaging, 3 = 200μm anterior of the ALM cell body, 2= 10μm anterior of the vulva, 1= within 10μm of the PVM cell body, -1 = >10 μm posterior of PVM cell body. Individual worms were stimulated at all sites of interest, with a 5-min interval between each stimulation. Some animals were stimulated at more proximal positions first and then at more distal positions, whereas others were stimulated in the converse order. Some worms were probed only once at one location to exclude a potential artifact due to desensitization of the neuron.

GFP fusions to MEC-4 and MEC-10

I used the *mec-4::GFP* strain ZB154 *zdIs5[pmec-4GFP] I*, described previously (Clark SG, Chiu C, 2003). For the *mec-10::GFP* strain, I used a *pmec-10::mec-10::GFP* plasmid created by introducing a *Pst* I–*Bam* HI fragment, including the *mec-10* promoter and coding sequences except for those encoding the last three AAs, into the pPD95.77 vector, which includes enhanced GFP. The *mec-10(tm1552)::GFP* strain was constructed in the same way, amplifying the same *mec-10* genomic fragment from *tm1552* DNA. Plasmid DNA (50 mg/ml) was coinjected with *myo-2::GFP* cotransformation marker DNA (50 mg/ml) to generate strain ZB2672.

3.6 Experimental Contributions

Laura Grundy helped with the confocal microscopy. Katie Kindt and Wei-Hsiang Lee initiated the project. Monica Driscoll and William Schafer supervised the work.

3.7 References

Bounoutas A, Chalfie M, (2007) Touch sensitivity in *Caenorhabditis elegans*. *Pflu¨gers Arch* 454: 691–702

Chalfie M, Au M, (1989) Genetic control of differentiation of the *Caenorhabditis elegans* touch receptor neurons. *Science* 243: 1027–1033

Chalfie M, Sulston J, (1981) Developmental genetics of the mechanosensory neurons of *Caenorhabditis elegans*. *Dev Biol* 82: 358–370

Chalfie M, Sulston JE, White JG, Southgate E, Thomson JN, Brenner S, (1985) The neural circuit for touch sensitivity in *Caenorhabditis elegans*. *J Neurosci* 5: 956–964

Chelur DS, Ernstrom GG, Goodman MB, Yao CA, Chen L, O'Hagan R, Chalfie M, (2002) The mechanosensory protein MEC-6 is a subunit of the *C. elegans* touch-cell degenerin channel. *Nature* 420: 669–673

Christensen AP, Corey DP, (2007) TRP channels in mechanosensation: direct or indirect activation? *Nat Rev Neurosci* 8: 510–521

Clark SG, Chiu C, (2003) *C. elegans* ZAG-1, a Zn-finger-homeodomain protein, regulates axonal development and neuronal differentiation. *Development* 130: 3781–3794

Colbert HA, Smith TL, Bargmann CI, (1997) OSM-9, a novel protein with structural similarity to channels, is required for olfaction, mechanosensation, and olfactory adaptation in *C. elegans*. *J Neurosci* 17: 8259–8269

Cueva JG, Mulholland A, Goodman MB, (2007) Nanoscale organization of the MEC-4 DEG/ENaC sensory mechanotransduction channel in *Caenorhabditis elegans* touch receptor neurons. *J Neurosci* 27: 14089–14098

Driscoll M, Chalfie M, (1991) The *mec-4* gene is a member of a family of *Caenorhabditis elegans* genes that can mutate to induce neuronal degeneration. *Nature* 349: 588–593

Emtage L, Gu G, Hartwieg E, Chalfie M, (2004) Extracellular proteins organize the mechanosensory channel complex in *C. elegans* touch receptor neurons. *Neuron* 44: 795–807

Garcia-Anoveros J, Corey DP, (1997) The molecules of mechanosensation. *Annu Rev Neurosci* 20: 567–594

Goodman MB, Ernstrom GG, Chelur DS, O'Hagan R, Yao CA, Chalfie M, (2002) MEC-2 regulates *C. elegans* DEG/ENaC channels needed for mechanosensation. *Nature* 415: 1039–1042

Goodman MB, Lumpkin EA, Ricci A, Tracey WD, Kernan M, Nicolson T, (2004) Molecules and mechanisms of mechanotransduction. *J Neurosci* 24: 9220–9222

Goodman MB, Schwarz EM, (2003) Transducing touch in *Caenorhabditis elegans*. *Annu Rev Physiol* 65: 429–452

Hong K, Mano I, Driscoll M, (2000) In vivo structure–function analyses of *Caenorhabditis elegans* MEC-4, a candidate mechanosensory ion channel subunit. *J Neurosci* 20: 2575–2588

Huang M, Chalfie M, (1994) Gene interactions affecting mechanosensory transduction in *Caenorhabditis elegans*. *Nature* 367: 467–470

Huang M, Gu G, Ferguson EL, Chalfie M, (1995) A stomatin-like protein necessary for mechanosensation in *C. elegans*. *Nature* 378: 292–295

Kahn-Kirby AH, Bargmann CI, (2006) TRP channels in *C. elegans*. *Annu Rev Physiol* 68: 719–736

Kerr R, Lev-Ram V, Baird G, Vincent P, Tsien RY, Schafer WR, (2000) Optical imaging of calcium transients in neurons and pharyngeal muscle of C.elegans. *Neuron* 26: 583–594

Kerr RA, (2006) Imaging the activity of neurons and muscles. *WormBook,* edited by. The C. elegans research community. Wormbook, doi/10.1895/wormbook.1.113.1.

Kim K, Li C, (2004) Expression and regulation of an FMRFamide-related neuropeptide gene family in *Caenorhabditis elegans. J Comp Neurol* 475: 540–550

Kindt KS, Quast KB, Giles AC, De S, Hendrey D, Nicastro I, Rankin CH, Schafer WR, (2007) Dopamine mediates context-dependent modulation of sensory plasticity in *C. elegans. Neuron* 55: 662–676

O'Hagan R, Chalfie M, Goodman MB, (2005) The MEC-4 DEG/ENaC channel of *Caenorhabditis elegans* touch receptor neurons transduces mechanical signals. *Nat Neurosci* 8: 43–50

Rankin CH, Broster BS, (1992) Factors affecting habituation and recoveryfrom habituation in the nematode *Caenorhabditis elegans. Behav Neurosci* 106: 239–249

Sanyal S, Wintle RF, Kindt KS, Nuttley WM, Arvan R, Fitzmaurice P, Bigras E, Merz DC, Hebert TE, van der Kooy D, Schafer WR, Culotti JG, Van Tol HH (2004) Dopamine modulates the plasticity of mechanosensory responses in *Caenorhabditis elegans. EMBO J* 23: 473–482

Savage C, Hamelin M, Culotti JG, Coulson A, Albertson DG, Chalfie M, (1989) *mec-7* is a β-tubulin gene required for the production of 15-protofilament microtubules in *Caenorhabditis elegans*. *Genes Dev* 3: 870–881

Suzuki H, Kerr R, Bianchi L, Frokjaer-Jensen C, Slone D, Xue J, Gerstbrein B, Driscoll M, Schafer WR (2003) In vivo imaging of *C. elegans* mechanosensory neurons demonstrates a specific role for the MEC-4 channel in the process of gentle touch sensation. *Neuron* 39: 1005–1017

Tavernarakis N, Driscoll M, (1997) Molecular modeling of mechanotransduction in the nematode *Caenorhabditis elegans*. *Annu Rev Physiol* 59: 659–689

Way JC, Chalfie M, (1989) The *mec-3* gene of *Caenorhabditis elegans* requires its own product for maintained expression and is expressed in three neuronal cell types. *Genes Dev* 3: 1823–1833

Wicks SR, Rankin CH, (1996) The integration of antagonistic reflexes revealed by laser ablation of identified neurons determines habituation kinetics of the *Caenorhabditis elegans* tap withdrawal response. *J Comp Physiol A Sens Neural Behav Physiol* 179: 675–685

Zhang W, Bianchi L, Lee WH, Wang Y, Israel S, Driscoll M, (2008) Intersubunit interactions between mutant DEG/ENaCs induce synthetic neurotoxicity. *Cell Death Differ* 15: 1794–1803

Zhao B, Khare P, Feldman L, Dent JA, (2003) Reversal frequency in *Caenorhabditis elegans* represents an integrated response to the state of the animal and its environment. *J Neurosci* 23: 5319–5328

Chapter 4

Lateral facilitation between primary mechanosensory neurons controls nose touch perception in *C. elegans*.

4.1 Abstract

The nematode *C. elegans* senses head and nose touch using multiple classes of mechanoreceptor neurons that are electrically-coupled through a network of gap junctions. Using *in vivo* neuroimaging, I have found that one sensory neuron class, the multidendritic FLP nociceptors, respond to harsh touch throughout their receptive field but respond to gentle touch only at the tip of the nose. Whereas the FLP harsh touch response depends solely on cell-autonomous mechanosensory channels, gentle nose touch responses require the activities of additional mechanoreceptor classes, OLQ and CEP, which are electrically-coupled to FLP through a gap junction network. Conversely, FLP activity is required to indirectly facilitate nose touch and harsh head touch responses in the OLQs, demonstrating that information flow across the network is bidirectional. Thus, nose touch perception involves a hub-and-spoke network that allows individual sensory neurons to integrate information from multiple interconnected mechanoreceptors.

4.2 Introduction

Somatosensory circuits, which gather sensory information from the skin and body surface, are a feature of most animal nervous systems. A patch of skin typically contains multiple classes of primary somatosensory neurons with dendrites responding to distinct sensory modalities. Somatosensory circuits include thermosensory neurons responding to temperature, touch neurons responding to gentle pressure or motion, proprioceptors responding to body posture, and nociceptors responding to harsh, body-damaging stimuli. Touch neurons, proprioceptors and nociceptors share the property that their activities are controlled by mechanical force.

Most, if not all, primary mechanosensory neurons sense force using ion channels that are directly mechanically gated. Many of these channels, particularly in invertebrates, appear to come primarily from one of two protein superfamilies: the TRP channels and the DEG/ENaC channels (Garcia-Anoveros J, Corey DP, 1997; Goodman MB et al., 2004). TRP channels are non-specific cation channels composed of subunits with six transmembrane α-helices. At least some TRP channels appear to be sufficient by themselves to produce touch- or stretch-evoked currents (Christensen AP; Corey DP, 2007; Kang L et al., 2010). In addition, TRP channels can be activated by G-protein signaling, which has been implicated in other sensory transduction processes including taste, vision and olfaction (Kahn-Kirby AH, Bargmann CI, 2006). In contrast, DEG/ENaC channel subunits have two transmembrane α-helices and form channels that are permeable to sodium and in some cases calcium (Bounoutas A, Chalfie M, 2007). Both families have been implicated in mechanosensory transduction in invertebrates as well as vertebrates.

The process of mechanosensation has been extensively studied in genetically tractable organisms such as *C. elegans* (Arnadottir J, Chalfie M, 2010). Touch is an important sensory modality for *C. elegans*; indeed, over 10% of the neurons in the adult hermaphrodite are thought to be mechanaoreceptors responding to external touch stimuli (White J et al., 1986). The best studied of these are the five neurons (ALML, ALMR, AVM, PLML and PLMR) that sense gentle body touch. These cells sense low-threshold mechanical stimuli using a mechanotransduction complex whose core components include the DEG/ENaC channel proteins MEC-4 and MEC-10 and the stomatin MEC-2 (O'Hagan R et al., 2005). Activation of the ALM and AVM anterior touch neurons triggers a change from forward to backward movement; this escape response appears to depend primarily on gap junctions between the mechanoreceptor neurons and the backward command interneurons that potentiate backward locomotion (Chalfie M et al., 1985). Conversely, activation of PLM posterior body touch receptors activates forward command interneurons that promote accelerated forward locomotion. An additional pair of neurons in the body, the PVD multidendritic nociceptors, is required to generate escape responses to harsh body touch (Way JC, Chalfie M, 1989).

C. elegans also respond to touch stimulation on the nose. When an animal collides with an object head-on, it reverses direction in a manner similar to the anterior touch escape reflex. As many as 20 neurons with sensory endings in or around the nose have been implicated by morphological or functional criteria as potential nose touch mechanoreceptors. Cell ablation experiments indicated that loss of either of two neuron pairs, the ASH and FLP neurons, causes a partial reduction in nose touch response, and elimination of both classes results in a strong nose touch defect (Kaplan

JM, Horvitz HR, 1993). These results led to the conclusion that ASH and FLP are the primary sensory neurons involved in the nose touch escape reflex. The ASH neurons are polymodal nociceptors that respond to chemical and osmotic stimuli in addition to nose touch, and their responses to all these stimuli are dependent on the TRPV channel OSM-9 (Colbert HA et al., 1997). The FLPs have highly branched multidendritic arbours that surround the animal's head, suggesting they may also be nociceptors (Hall D, Altun ZF, 2008). The FLPs express the DEG/ENaC channel MEC-10 (Huang M, Chalfie M, 1994; Chapter 2) as well as the OSM-9 TRPV channel (Colbert HA et al., 1997), though the effects of these molecules on sensation in the FLPs have not been reported.

Additional neurons have been implicated as nose touch mechanosensors, though their importance in nose touch avoidance behaviour is less well established (Figure 4.1a). The four OLQ neurons have ciliated endings in the outer labial sensilla that suggest a function as mechanoreceptors. Ablations of the OLQs alone have little effect on nose touch escape responses, though they enhance the defects of ASH and FLP ablations (Kaplan JM, Horvitz HR, 1993). However, OLQ ablations strongly affect another nose touch-related behaviour, the suppression of lateral “foraging” movements of the head by nose touch (Hart AC et al., 1995). OLQ ablations also affect the rate and amplitude of foraging in unstimulated animals, suggesting a role in mechanosensory feedback for this behaviour. Nose touch evokes calcium transients in the OLQs, which are affected by mutations in the TRPA channel *trpa-1* (Kindt et al., 2007b). The four CEP neurons also have sensory cilia in the nose that indicate a role as mechanoreceptors. Though ablations of the CEPs affect neither nose touch

avoidance or foraging behaviours, they do act with the other dopaminergic neurons to mediate a slowing response to a bacterial lawn, which appears to involve mechanical detection of bacteria (Sawin ER et al., 2000). Gentle nose touch evokes calcium transients in CEP that require the cell-autonomous activity of the TRPN channel TRP-4 (Kindt et al., 2007a). Thus, both the OLQ and CEP neurons appear to sense nose touch; however, their absence primarily affects foraging and slowing behaviours rather than nose touch avoidance.

In this study, I investigated the circuit for *C. elegans* nose touch avoidance in more detail using a combination of neuroimaging and behavioural analysis. I found that the FLP neurons are polymodal nociceptors that respond to harsh touch as well as heat. In addition, the FLPs respond to gentle touch applied to a restricted region of the nose. Whereas harsh head touch is dependent only on the cell-autonomous activity of a MEC-10-containing DEG/ENaC complex, gentle nose touch also requires *mec-10* -independent contributions from other nose touch neurons that are coupled to FLP through gap junctions. Activation of the gentle nose touch neurons thus acts in a circuit-dependent manner to facilitate low threshold responses in the otherwise high-threshold nociceptor neurons. Thus, the FLP neurons exhibited distinct responses to gentle nose touch and harsh head touch.

4.3 Results

4.3.1 The FLP multidendritic nociceptors respond to harsh head touch, gentle nose touch and heat.

The FLP neurons have been implicated by ablation studies in nose touch sensation. In addition, they have a multidendritic morphology characteristic of polymodal nociceptors, suggesting they might respond to touch stimuli on other parts of the head or to other noxious stimuli such as extreme temperatures. To assess the sensory responses of the FLP neurons, I used a transgenic line, *ljEx19,* that expressed the calcium-sensitive fluorescent protein YC2.3 in the FLP neurons under the control of the *egl-46* promoter (Driscoll M, Chalfie M, 1991; Chapter 2). Nose touch behaviour was normal in this line (Figure 4.2a); thus, I applied harsh and gentle touch stimuli by pressing a rounded glass probe to the side of the head in the region of the FLP dendritic lattice (Figure 4.2b) and imaged calcium transients evoked in the FLP cell body. For mechanical stimuli applied directly to the nose, I observed that a small (8 μM) displacement motion stimulus evoked a robust calcium transient similar in dynamics to responses seen in other *C. elegans* nose touch neurons (Kindt et al., 2007a; Kindt et al., 2007b). In contrast, small displacement stimuli applied to the side of the head did not evoke calcium transients in FLP. However, large and long-lasting calcium transients could be evoked by a mechanical stimulus of large (20 μM) displacement and high velocity (Figure 4.1b-d).

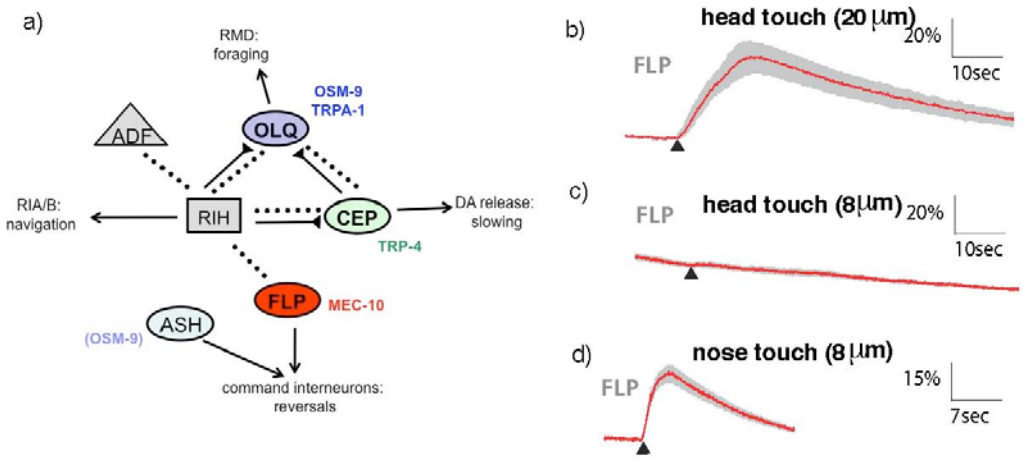

Figure 4.1: The FLP neurons respond to harsh head touch and gentle nose touch.

(a) Connections between nose touch mechanoreceptors Shown are synaptic and electrical connections involving FLP and other nose touch mechanoreceptors. Also indicated are sites of transgenic rescue for genes involved in nose touch behaviour and nose touch-evoked calcium transients in FLP as determined in this study. MEC-10 acts cellautonomously in the FLPs; OSM-9 acts in the OLQs, and TRP-4 acts in the CEPs and other dopaminergic mechanoreceptors. OSM-9 also acts in the ASH neurons to promote nose touch behaviour, though expression here does not affect neural responses to nose touch in FLP (see Figure 4.6).

(b-d) Averaged calcium responses to harsh head touch (a), gentle head touch (b), and gentle nose touch (c). Each red trace represents the average percentage change in R/R_0 for the indicated genotype, where R is the fluorescence emission ratio at a given time point and R_0 is its initial value. The number of individual recordings averaged for each trace were n=24 (harsh head touch), n=21 (gentle head touch), n=12 (gentle nose touch). Grey shading indicates SEM of the mean response. Scale bars are indicated.

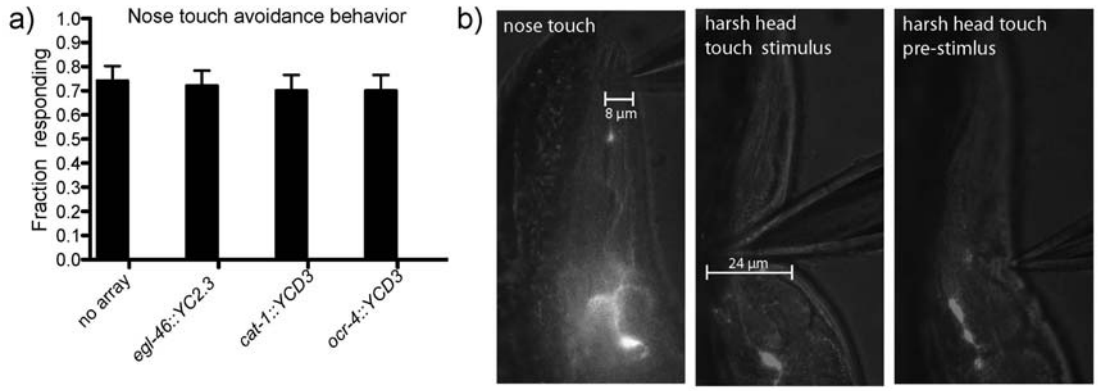

Figure 4.2: Supplemental data for touch-evoked calcium imaging experiments.

(a) Effect of cameleon transgenes on nose touch behaviour. The cameleon imaging lines were assayed for their behavioural response to nose touch as described in methods. Fraction of animals responding is shown; error bars indicate S.E.M. 100 wild-type animals and 50 animals from each cameleon line were tested. (**b) Protocols for nose touch and harsh touch stimulation.** Shown are images of animals receiving the nose touch or harsh head touch stimulus used in calcium imaging experiments. Worms were glued to the tip of the nose without covering the mouth on a 2% agarose pad and are subsequently immersed in extracellular saline. Two types of mechanical stimulation were delivered. The nose touch stimulus, consisted of a 1 second gentle (buzz) stimulus at the edge of the nose of the worm with a final displacement of 8μm. A harsh head touch stimulus was delivered in a more posterior position near the terminal bulb of the pharynx. The probe was displaced a total of 24μm into the worm's head.

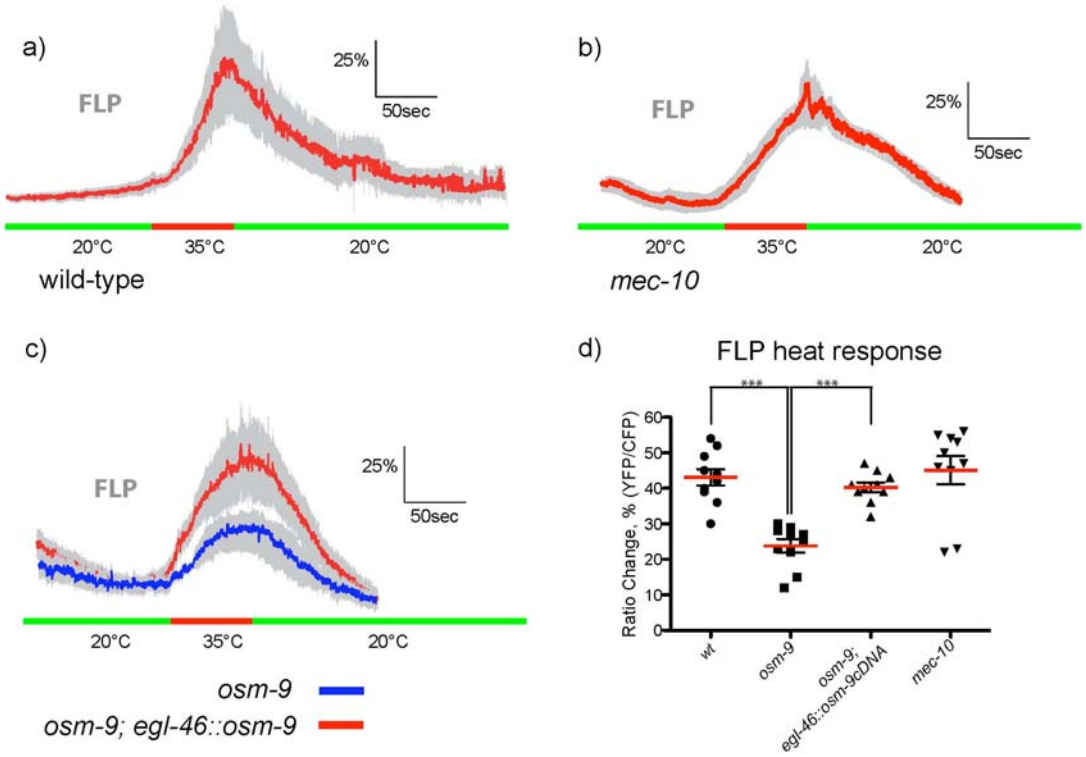

Figure 4.3: FLP heat responses in wild-type and mutant animals.

(a-c) Averaged calcium responses to heat shock stimulus. Each trace represents the average percentage change in R/R_0 for the indicated genotype, where R is the fluorescence emission ratio at a given time point and R_0 is its initial value. The green bar indicates a temperature of 20°C and the red bar indicates a period of stimulation at a temperature of 35°C. 18 wild-type, 10 *mec-10*, 10 *osm-9* and 10 *osm-9; egl 46::osm-9* animals were imaged for these experiments.

(d) Scatter plot of peak calcium responses for each genotype. Statistical significance (*** $p < .0005$) is according to the Mann-Whitney rank sum test.

Since the other multidendritic neurons in *C. elegans*, the PVDs exhibit a response to cold shock (Chapter 2), I tested FLP responses to temperature changes. Rapid increases in temperature from 20º to 35º led to robust calcium transients, indicating that the FLP neurons respond to noxious heat (Figure 4.3) as well as harsh head touch and gentle nose touch and thus they act as polymodal nociceptors.

The FLP neurons express the DEG/ENaC channel MEC-10, which contributes to mechanotransduction channels in other *C. elegans* neurons (Chapters 2 & 3). I tested the effect of a *mec-10* loss-of-function mutation on FLP responses to sensory stimuli. For harsh head touch, the *mec-10(tm1552)* mutant was strongly defective in touch-evoked calcium transients (Figure 4.4a, b). This defect was rescued by expressing the wild-type *mec-10(+)* allele under the control of the *egl-46* promoter (which is FLP-specific when the PVDs are eliminated; a further control experiment showing the specificity of the rescue is shown in Figure 4.5), indicating that MEC-10 functions cell-autonomously in the FLP neurons (Figure 4.4d, e). In contrast, *mec-10(tm1552)* did not affect FLP responses to heat (Figure 4.3b). Thus, MEC-10 does not generally disrupt FLP physiology or excitability, and appears to function specifically in mechanosensation. Finally, I observed that *mec-10(tm1552)* animals showed a partial though significant reduction in the magnitude of the calcium transient evoked by gentle nose touch (Figure 4.6a, b). This defect was rescued by an *egl-46::mec-10(+)* transgene, indicating that the requirement for MEC-10 in FLP nose touch response is cell-autonomous (Figure 4.6b). *mec-10(tm1552)* animals also showed a behavioural defect in nose touch escape response, which was rescued by *egl-46::mec-10(+)* (Figure 4.6d). Thus, whereas responses to harsh head touch are completely MEC-10-dependent, gentle nose touch responses are only partially dependent on MEC-10.

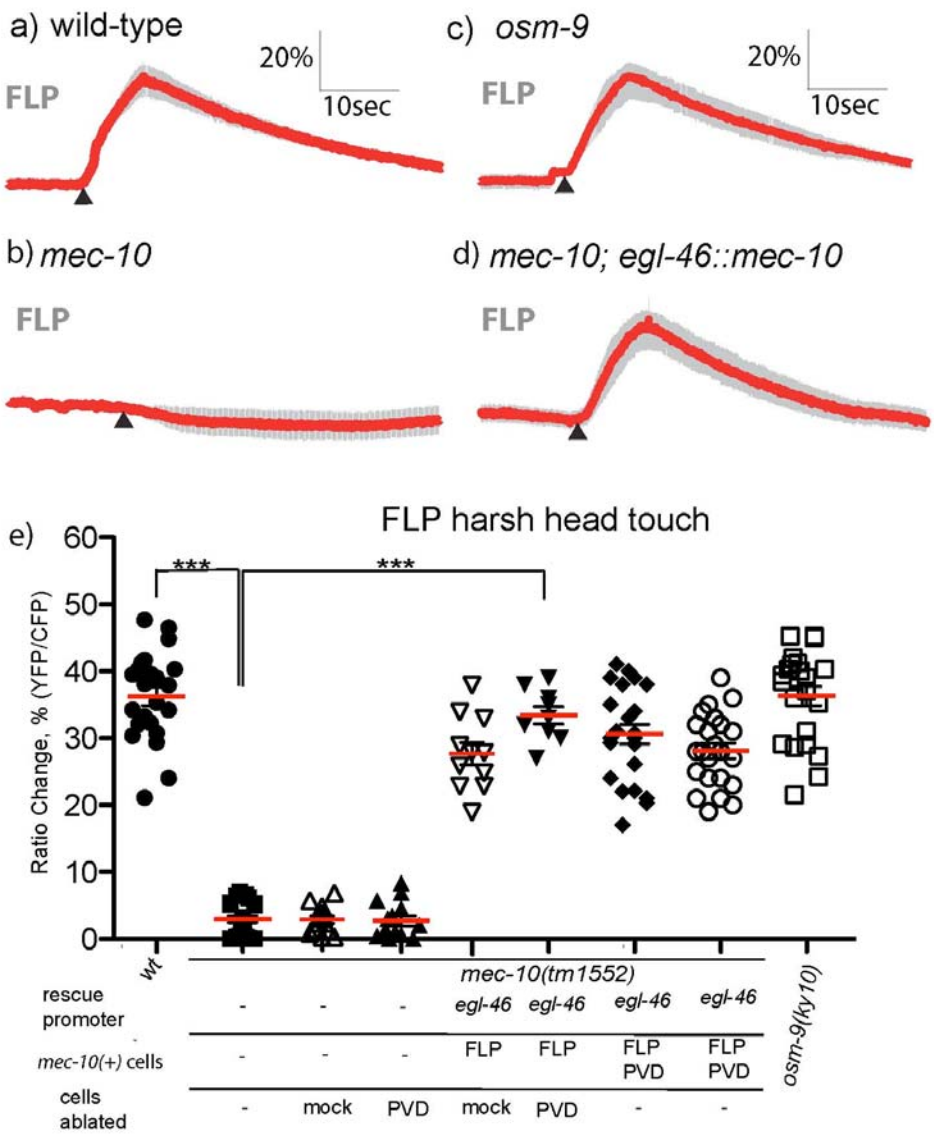

Figure 4.4: MEC-10 is required cell-autonomously for FLP harsh touch response.

Figure 4.4: MEC-10 is required cell-autonomously for FLP harsh touch response.

(a-d) Averaged responses of wild-type (a), *mec-10(tm1552)* (b), *osm-9(ky10)* (c) and *mec-10(tm1552); ljEx220[pegl-46::mec-10(+)]* (d) to harsh head touch stimulation in FLP. Each red trace represents the average percentage change in R/R_0 for 21 (wild-type*, osm-9,* and *mec-10; ljEx220*) or 14 (*mec-10*) individual recordings. Grey shading indicates the SEM. None of these genotypes visibly altered the morphology of FLP or the expression pattern of the cameleon transgene.

(e) Scatter plot of peak calcium responses for each genotype. Statistical significance (*** $p < .0005$) is according to the Mann-Whitney rank sum test. Also shown are data for *mec-10(tm1552);egl-46::mec-10cDNA* (n=23), PVD-ablated *mec-10* (n=14) and *mec-10(tm1552); egl-46::mec-10* (n=9) and mock-ablated *mec-10* (n=11) and *mec-10(tm1552);egl-46::mec-10* (n=14). These results, together with those in Figure 4.5, demonstrate that the transgenic rescue results specifically from expression of *mec-10(+)* in FLP and not PVD.

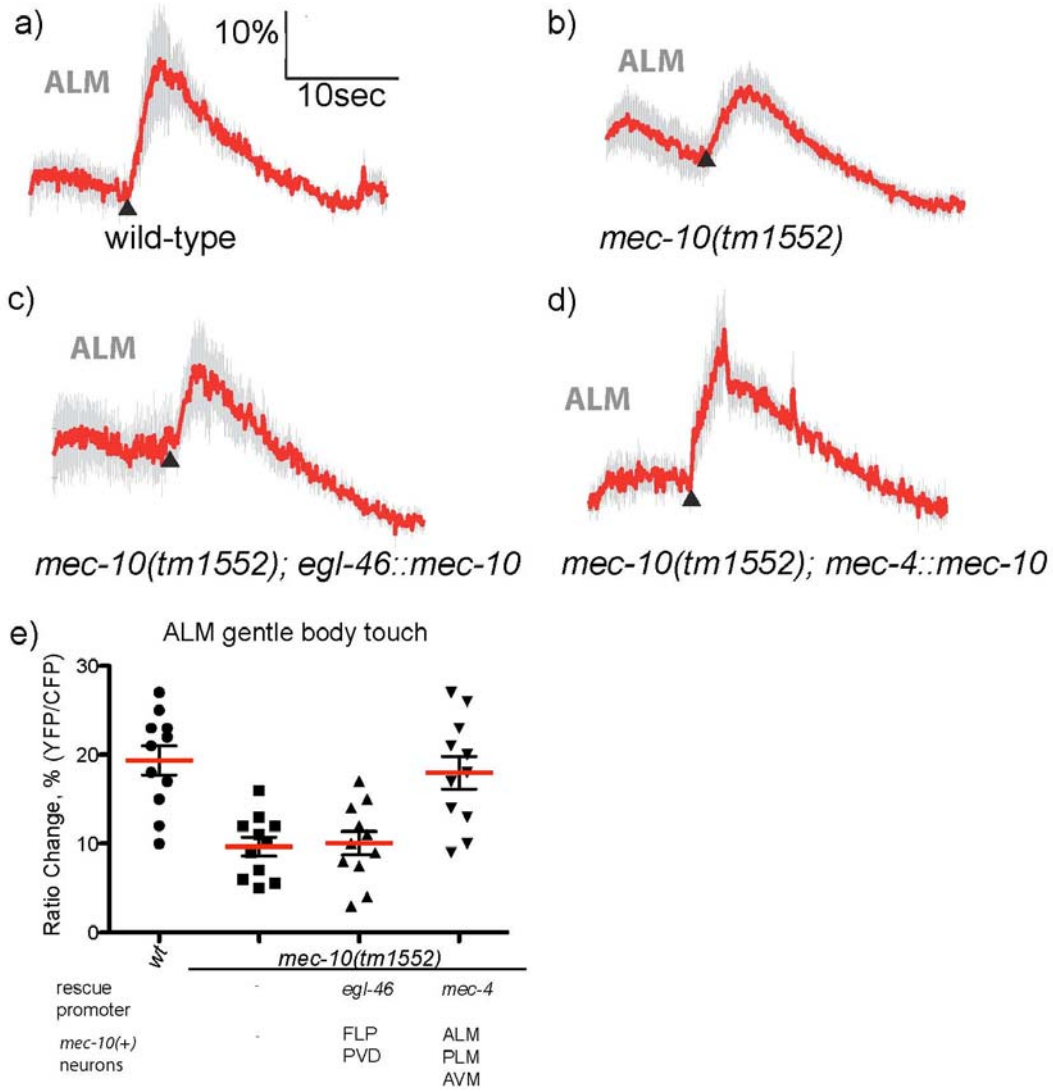

Figure 4.5: *egl-46::mec-10* does not rescue the *mec-10* touch defect in ALM neurons.

(a-d) Averaged calcium responses to gentle body touch in the ALMs. Animals expressing cameleon in the ALM gentle body touch neurons were given a 1 second buzz stimulus on the anterior body as described (Suzuki H et al., 2003). Each red trace represents the average percentage change in R/R_0 for the indicated genotype. 11 animals per genotype were imaged.

(e) Scatter plot of peak calcium responses for each stimulus. The red line indicates mean ratio change; the error bars indicate S.E.M.

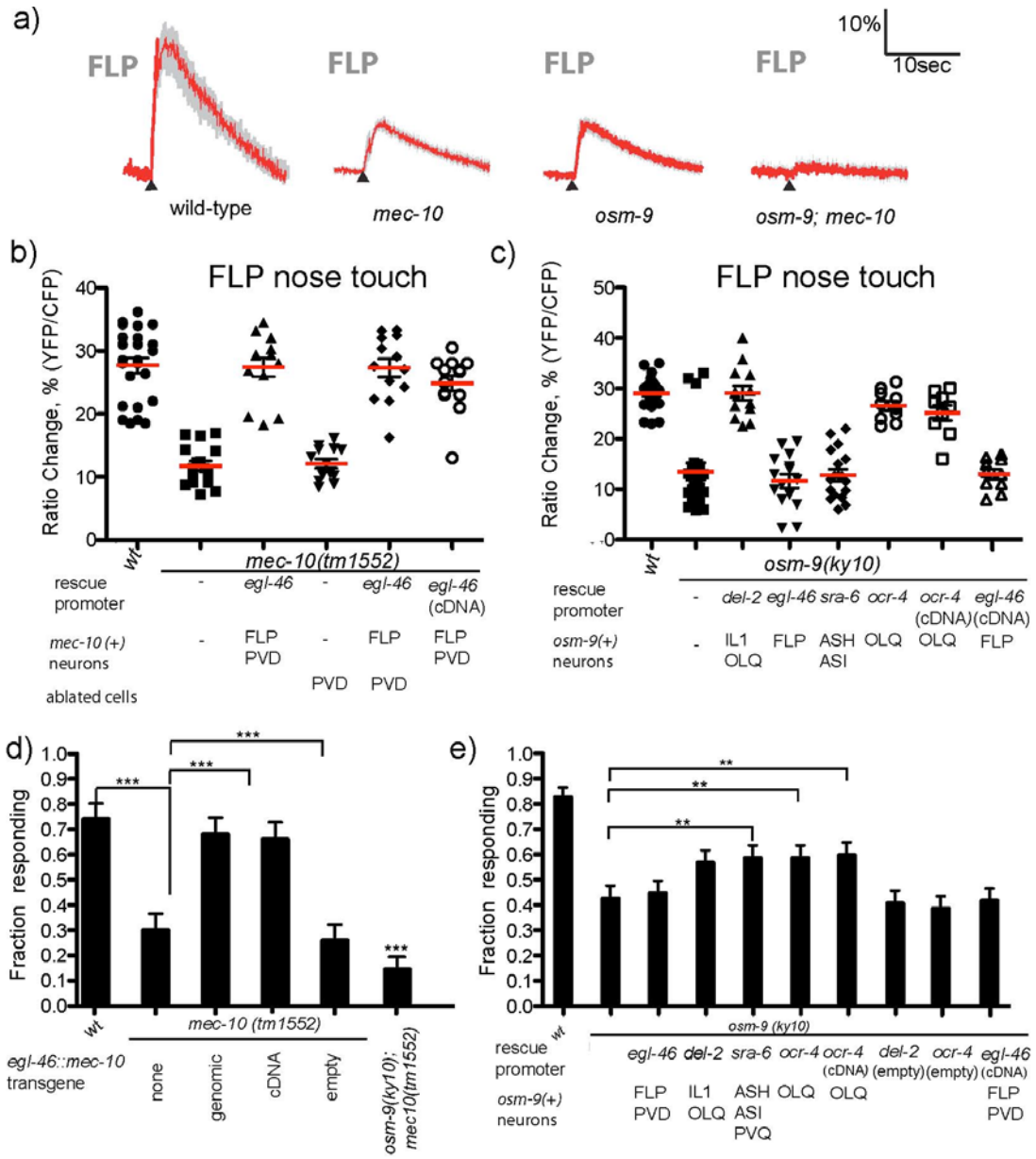

Figure 4.6: MEC-10 is required cell-autonomously and OSM-9 non-autonomously for FLP nose touch response.

Figure 4.6: MEC-10 is required cell-autonomously and OSM-9 non-autonomously for FLP nose touch response.

(a) Averaged responses of wild-type, *mec-10(tm1552)*, *osm-9(ky10)* and *osm-9(ky10); mec-10(tm1552)* to gentle nose touch stimulation in FLP. Each red trace represents the average percentage change in R/R_0 for wild-type (n=24), *mec-10* (n=22), *osm-9* (n=22) and *osm-9;mec-10* (n=13) individual recordings; grey shading indicates SEM.

(b-c) Scatter plot of peak calcium responses for each genotype. In addition to the genotypes in panel **a**, I analyzed *mec-10(tm1552); egl-46::mec-10(genomic)* (n=13) and *mec-10(tm1552); egl-46::mec-10(cDNA)* (n=13) rescue lines in panel **b**, and *osm-9(ky10)* rescue lines expressing *osm-9(+)* under the *del-2* (genomic fragment, n=13), *egl-46* (genomic fragment, n=15; cDNA n=10), *sra-6* (genomic fragment, n=17) or *ocr-4* (genomic fragment, n=10; cDNA, n=9) promoters in panel **c**. For panel **b**, also shown are data for *mec-10* mutant (n=13) and rescue animals (n=13) in which the PVD harsh body touch neurons have been eliminated by laser ablation; these results demonstrate that the transgenic rescue results specifically from expression of *mec-10(+)* in FLP.

(d-e) Effects of *mec-10*, and *osm-9* on nose touch escape behaviour. For all genotypes, at least 50 animals were scored for reversals following nose touch stimulation. Statistical significance (*<0.01 **<0.001 ***<0.0001) is according to the Student's t test.

4.3.2: OSM-9 functions non-autonomously in FLP mechanosensation

To identify the molecules contributing to the MEC-10-independent component of the nose touch response, I assayed additional candidate sensory transduction mutants. In addition to MEC-10, another potential mechanotransduction channel is expressed in the FLP neurons: the TRPV channel OSM-9. To determine whether OSM-9 could contribute to the nose touch response remaining in *mec-10(tm1552)* mutant animals, I imaged FLP responses to nose touch in *osm-9(ky10)* single mutant and *osm-9(ky10); mec-10(tm1552)* double mutant animals. I observed that a null mutation in *osm-9* led to a significant reduction in nose touch-evoked calcium transients in FLP (Figure 4.6a), though it had no effect on response to harsh head touch (Figure 4.3c) and did not alter (Tobin D et al., 2002) FLP morphology or reporter expression (Figure 4.7). Furthermore, an *osm-9(ky10); mec-10(tm1552)* double mutant showed virtually no significant calcium increase in response to nose mechanosensory stimulation in FLP (Figure 4.6a). These results indicate that MEC-10 and OSM-9 contribute additively to the mechanosensory response to nose touch in FLP.

I next carried out cell-specific rescue experiments to determine whether OSM-9, like MEC-10, functions cell-autonomously in the FLP neurons. Unexpectedly, expression of *osm-9(+)* under the FLP-specific *egl-46* promoter did not rescue the nose touch phenotype in FLP (Figure 4.6c, e), though its ability to rescue the defect in responding to heat indicated that it was expressed in the FLP neurons and fully functional (Figure 4.3c, d). Likewise, expression of *osm-9(+)* in the ASH nociceptor neurons did not restore nose touch responses in the FLP neurons, though it did rescue the ASH-mediated *osm-9* osmotic avoidance defect (Figure 4.8). However, an *osm-9(+)* cDNA or genomic fragment robustly rescued the FLP nose touch defect (Figure

4.6c, e) when expressed under the control of either the *del-2* promoter fragment, specific for the OLQ and IL1 labial mechanoreceptors (Kindt KS et al., 2007b), or the OLQ-specific *ocr-4* promoter (Tobin D et al., 2002). These results suggest that OSM-9 functions in the OLQ labial mechanoreceptors to indirectly promote FLP nose touch responses.

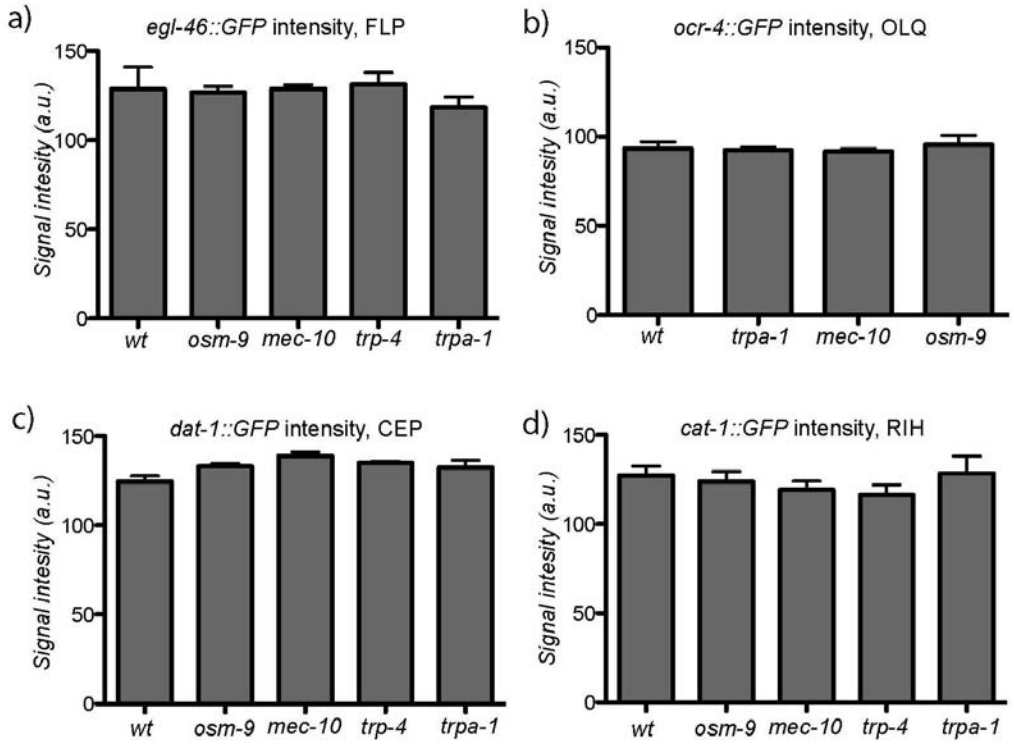

Figure 4.7: Effects of genetic background on expression levels of cameleon and promoter::GFP arrays.

Mean fluorescence intensity was measured for the indicated neuronal cell body using a ZeisLSM 510 Meta confocal microscope with a 40x objective. Images were exported as single TIFF files and fluorescence intensity was quantified using ImageJ. For cameleon lines the same strains used in imaging experiments in the main text were used. At least 5 animals of each genotype were analyzed.

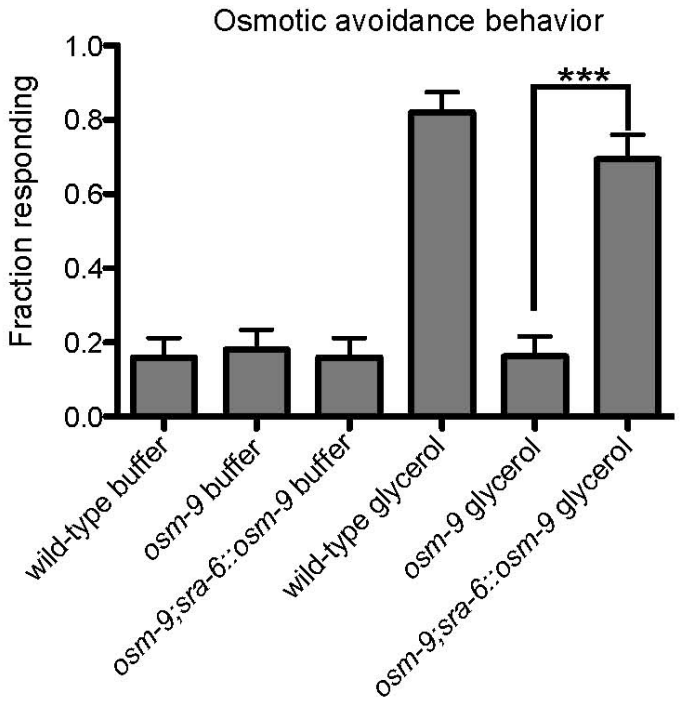

Figure 4.8: *sra-6::osm-9* rescues ASH-mediated osmotic avoidance behaviour.

Wild-type, *osm-9(ky10)*, and *osm-9(ky10); sra-6::osm-9(genomic)* animals were tested for escape behaviour evoked by 1M glycerol as described (Hilliard MA et al., 2002). Each data point represents 50 worms assayed on three independent days. Error bars show S.E.M. *** indicates a significant difference between mutant and rescued strains according to the χ^2 test ($p < 0.001$).

The OLQ neurons have been shown previously to respond to nose touch. To determine whether OSM-9 is required cell-automonously in OLQ for nose touch responses, I imaged nose-touch-evoked calcium transients in OLQ using a previously described *pocr-4::YCD3* cameleon line (Kindt KS et al., 2007b). I found that calcium transients were robustly evoked by gentle nose touch responses in the wild-type OLQ neurons, but were completely absent in the *osm-9(ky10)* mutant background (Figure 4.9a, b). This defect could be rescued by cell-specific expression of *osm-9(+)* under the OLQ specific *ocr-4* promoter (Figure 4.9a, b). Thus, OSM-9 is required cell-autonomously for the OLQs to respond to nose touch. This result suggested the possibility that gentle nose touch sensation by OLQ might indirectly promote nose touch responses in FLP.

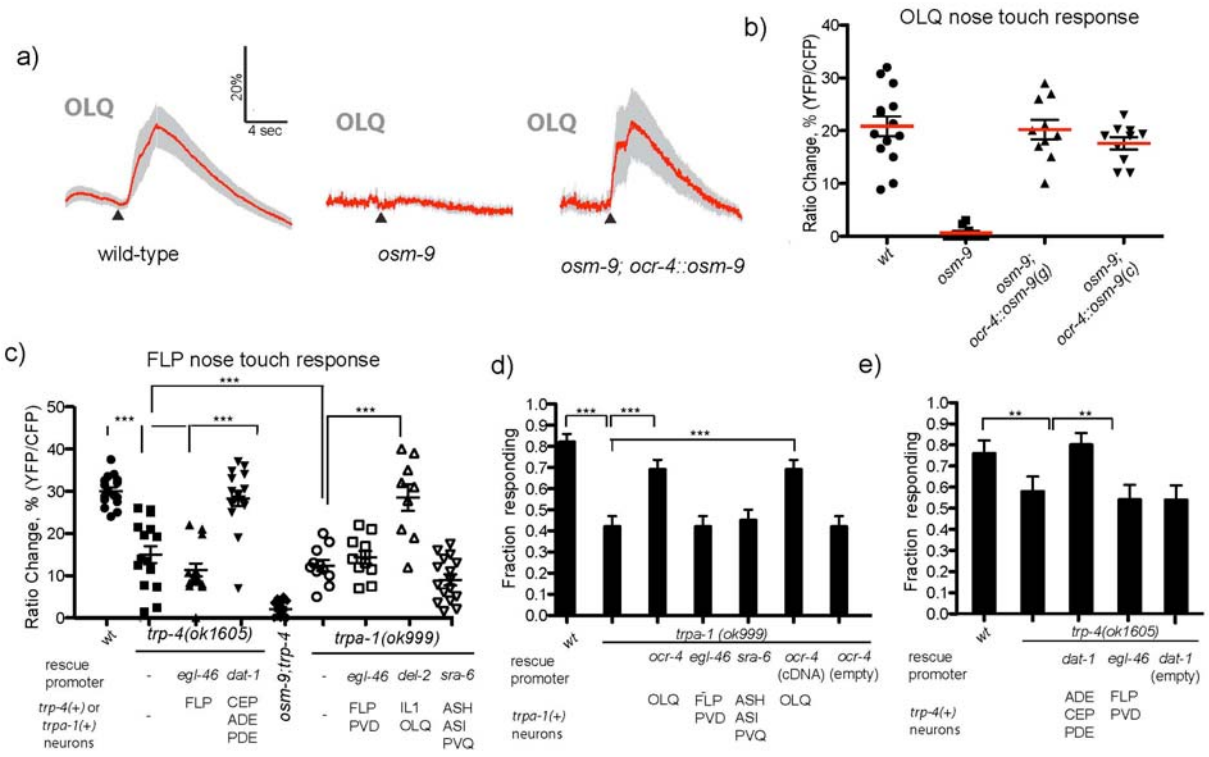

Figure 4.9: Effects of TRP channels in gap junction-coupled neurons on nose touch.

Figure 4.9: Effects of TRP channels in gap junction-coupled neurons on nose touch.

(a) OSM-9 is required cell-autonomously for OLQ nose touch response. Shown are averaged responses of wild-type (n=14), *osm-9(ky10)* (n=10), and *osm-9(ky10); ocr-4::osm-9(+)* (n=10) to nose touch stimulation in OLQ. Grey shading indicates the SEM. None of these genotypes visibly altered the morphology of OLQ or the expression pattern of the cameleon transgene (see Figure 4.7).

(b) Scatter plot of peak OLQ calcium responses for *osm-9* genotypes. In addition to the strains shown in panel **a**, I imaged 10 animals in which *osm-9(ky10)* was rescued by an *ocr-4::osm-9* cDNA transgene.

(c) Effects of *trp-4* and *trpa-1* on FLP nose touch responses. Shown is a scatter plot of peak calcium responses (percentage change in R/R0) for 16 wild-type, 16 *trp-4(ok1605)*, 16 *trp-4; egl-46::trp-4*, 16 *trp-4; dat-1::trp-4*, 16 *osm-9(ky10); trp-4(ok1605),* 11 *trpa-1(ok999)*, 11 *trpa-1; egl-46::trpa-1*, 9 *trpa-1; del-2::trpa-1* and 16 *trpa-1; sra-6::trpa-1* animals. Statistical significance (*** p <.0005) is according to the Mann-Whitney rank sum test.

(d-e) Effect of the *trp-4* and *trpa-1* on nose touch behaviour. For all genotypes, at least 50 animals were scored for reversals following nose touch stimulation. Statistical significance (*<0.01 **<0.001 ***<0.0001) is according to the Student's t test.

4.3.3: A network centred on the RIH interneuron facilitates FLP nose touch responses

How might the OLQ mechanoreceptors facilitate nose touch responses in FLP? The FLP and OLQ mechanoreceptors are both linked by gap junctions to RIH (White J et al., 1986), an interneuron that also makes gap junctions with the dopaminergic CEP mechanoreceptors and the ADF taste chemoreceptors (Figure 4.1a). A similar hub-and spoke network was recently shown to control aggregation behaviour in *C. elegans* (Macosko EZ et al., 2009). I reasoned that this network might allow the OLQ and CEP neurons to facilitate FLP activity through electrical signalling. Consistent with this hypothesis, I observed that loss-of-function mutations in *trpa-1* (which partially reduce OLQ mechanosensation; Figure 4.10, (Kindt KS et al., 2007b)) led to a reduction in nose touch-evoked calcium transients in FLP (Figure 4.9c, d). As was the case for *osm-9*, this defect in FLP calcium response as well as the *trpa-1* nose touch avoidance defect was rescued cell extrinsically by expression of the wild-type transgene in OLQ (Figure 4.9c, d). This provides further evidence that the OLQs facilitate FLP nose touch response, possibly through gap junctions with RIH.

The hub-and-spoke hypothesis predicts that the CEP and RIH neurons should also be important for nose touch responses in FLP. I first tested whether the CEP neurons contribute to FLP nose touch responses. Responses to gentle nose touch in the CEP neurons have been shown to require the TRPN channel TRP-4 (Li W et al., 2006; Kindt KS et al., 2007a; Kang L et al. 2010). When I imaged nose touch responses in FLP, I observed a significant reduction in the nose touch-evoked calcium transient in the *trp-4* null mutant (Figure 4.9c). This defect in FLP calcium response could be rescued by expression of a *trp-4* cDNA in the CEPs under the *dat-1* promoter, but not

by expression of *trp-4* in the FLP neurons themselves (Figure 4.9c). *trp-4* mutants also exhibited a partial defect in nose touch avoidance behaviour, which was rescued by functional expression in the CEPs but not the FLPs (Figure 4.9e). Thus, TRP-4-mediated nose touch responses in CEP, like OSM-9-mediated responses in OLQ, appear to contribute to nose touch responses in FLP. Interestingly, compromising both the OLQ and CEP inputs in an *osm-9; trp-4* double mutant led to a complete loss of nose touch responses in FLP (Figure 4.9c). These results indicate that the OLQ and CEP neurons function additively to promote responses to small-displacement nose touch stimuli in FLP. The model also predicts that the RIH neurons should be activated by nose touch stimuli in a manner dependent on the OLQ and/or CEP neurons. To test this possibility I used the *cat-1::YCD3* transgenic line, which expresses cameleon in RIH, to measure calcium dynamics following nose touch stimulation. I observed (Figure 4.11a) that small-displacement nose touch stimuli indeed evoked large calcium transients in RIH. These transients were similar to the sensory neuron transients in magnitude (28% $\Delta R/R_0$) but were significantly longer in duration, with some responses lasting as long as 25 seconds. Mutations in *osm-9* or *trpa-1*, which eliminate or reduce OLQ nose touch responses, or in *trp-4*, which eliminate CEP nose touch responses, reduced the nose touch-evoked transients in RIH and were rescued cell-specifically in the appropriate neurons (Figure 4.11a, b). Moreover, a *trp-4; osm-9* double mutant, in which OLQ and CEP nose touch responses were both eliminated, showed virtually no nose touch evoked calcium transients in RIH (Figure 4.11a, b). Together, these data indicate that the RIH interneuron is activated by the OLQ and CEP nose touch mechanoreceptor neurons.

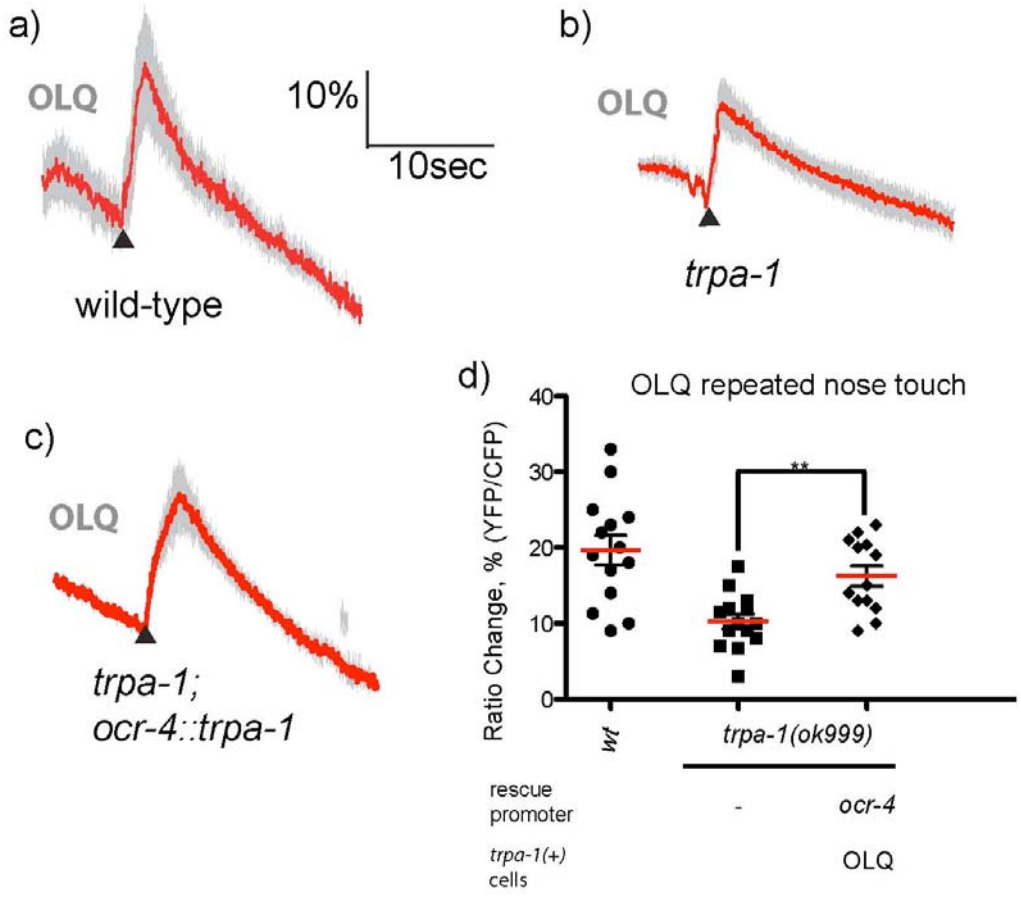

Figure 4.10: *trpa-1* acts cell-autonomously in OLQ to promote nose touch response.

Worms expressing cameleon in OLQ neurons were immobilized to the nose with glue and covered in extracellular saline containing 2mM serotonin. A glass probe delivered a gentle buzzing stimulus to the nose**.**

(a-d) Average traces in OLQ in response to 2nd nose touch stimulation (5-min after the first stimulation) in (a) *wt*, (b) *trpa-1*, (c) *trpa-1* with RIH ablated and (d) *trpa-1; ocr-4::trpa-1*.

(e) Scatter plot quantifying the 2nd OLQ nose touch responses in wild-type (n=14), *trpa-1* (n=14), and *trpa-1;ocr-4::trpa-1* (n=13).

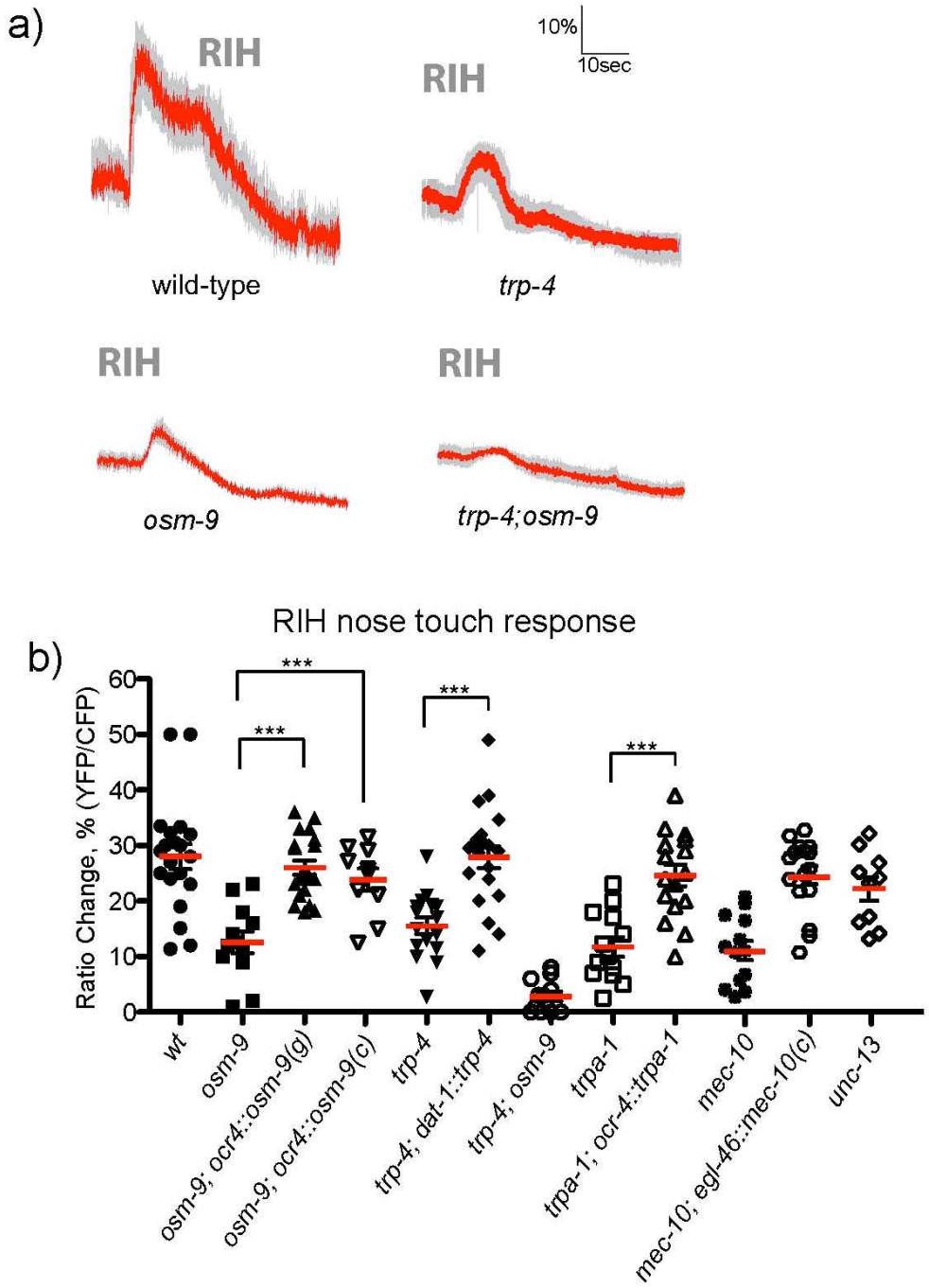

Figure 4.11: The RIH interneuron integrates responses to nose touch.

Figure 4.11: The RIH interneuron integrates responses to nose touch.

(a) Averaged responses of wild-type, *trp-4(ok1605) osm-9(ky10)* and *osm-9(ky10); trp-4(ok1605)* to nose head touch stimulation in RIH. Each solid trace represents the average percentage change in R/R0 for 20 wild-type, 14 *osm-9(ky10)*, 16 *trp-4(ok1605),* and 12*osm-9(ky10); trp-4(ok1605)* individual animals. Grey shading indicates the SEM. None of these genotypes visibly altered the morphology of RIH (data not shown) or the expression pattern of the cameleon transgene (Figure 4.7).

(b) Scatter plot of peak calcium responses for each genotype. In addition to the genotypes in panel a, 10 *unc-13*, 13 *trpa-1*, 16 *trpa-1; ocr-4::trpa-1*, 20 *trp-4; dat-1:: trp-4,* 13 *mec-10,* 16 *mec-10; egl-46::mec-10(cDNA),* 20 *osm-9; ocr-4::osm-9 (genomic)* and 10 *osm-9; ocr-4::osm-9(cDNA)* individual animals were analyzed. Statistical significance (*** p <.0005) is according to the Mann-Whitney rank sum test.

A third prediction of the model is that the RIH neuron should be required for FLP responses to small-displacement nose touch stimuli. To test this prediction, I eliminated RIH through cell-specific laser ablation, and determined the effect of this lesion on calcium transients in FLP. I observed that FLP responses to nose touch were greatly reduced in RIH-ablated animals (Figure 4.12a, c). Behavioural responses to nose touch were likewise impaired in animals lacking the RIH neuron (Figure 4.12d). In contrast, FLP responses to harsh head touch were unaffected by RIH ablation (Figure 4.12b,e). Thus, the RIH interneuron is specifically important for the activation of the FLP neurons in response to nose touch stimulation. Together, these findings indicate that the RIH interneurons facilitate the flow of sensory information from the OLQ and CEP mechanoreceptors to the FLP nociceptor neurons. To specifically assess the involvement of electrical signalling, I assayed the responses of mutants defective in the innexin gene *unc-7*, which encodes a major component of gap junctions in many *C. elegans* neurons (Starich TA et al., 1993; Starich TA et al., 2009). I observed (Figure 4.13) that *unc-7* loss-of-function mutants showed significant defects in nose touch escape behaviour. I also observed that nose touch-evoked calcium transients in RIH were nearly completely absent in *unc-7* mutants (Figure 4.13a, c). Likewise, nose-touch evoked calcium transients in FLP were significantly reduced, resembling in magnitude the responses in the RIH-ablated animals (Figure 4.13b,c); FLP harsh head touch responses, in contrast, were unaffected (Figure 4.12e). These nose touch defects were rescued when a functional *unc-7(+)* transgene was expressed in the nose touch circuit using the *cat-1* (expressed in the CEPs, RIH, and few other neurons) and *egl-46* (expressed in FLP and PVD) promoters (Figure 4.13, Figure 4.14). *unc-7(+)* expression using either promoter

alone did not result in phenotypic rescue (data not shown), suggesting that gap junction formation requires production of the innexin protein in both connected neurons. In contrast, mutations in *unc-13*, which impair synaptic transmission, did not detectably impair RIH nose touch responses (Figure 4.11b). Together, these results support the hypothesis that signalling in the RIH centred nose touch circuit is predominantly if not exclusively mediated by gap junctions.

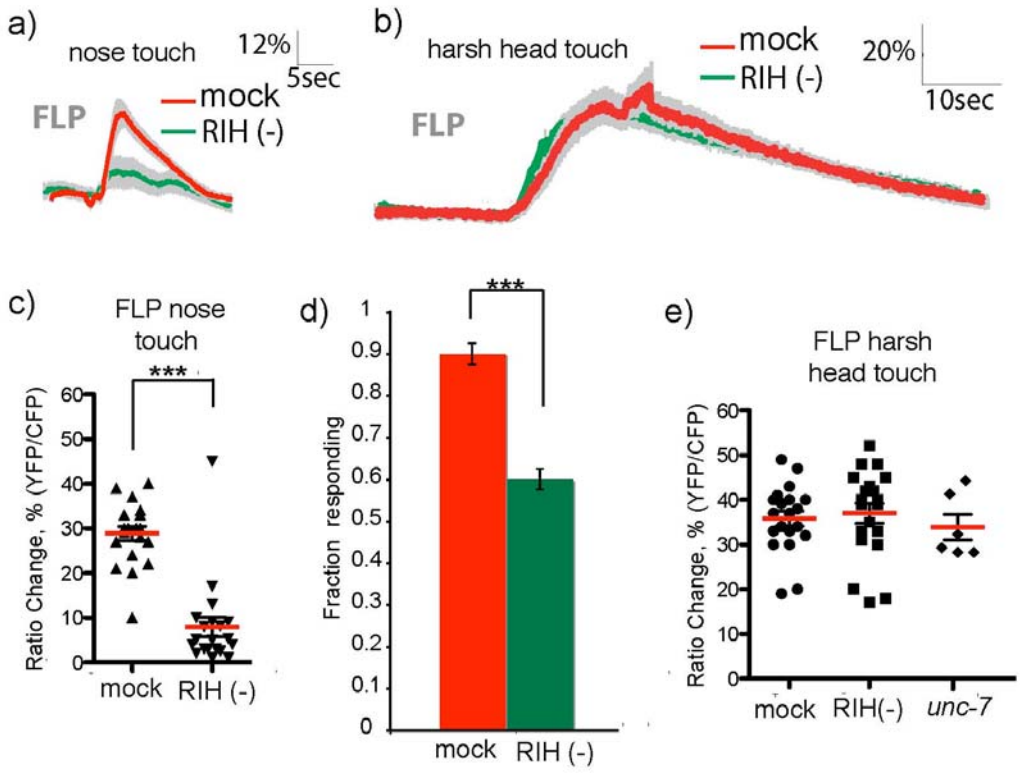

Figure 4.12: The RIH network is important for FLP responses to nose touch but not harsh head touch.

Figure 4.12: The RIH network is important for FLP responses to nose touch but not harsh head touch.

(a) Averaged responses of wild-type and RIH-ablated animals to nose touch stimulation. Each solid trace represents the average percentage change in R/R0 for 24 (mock-ablated, red trace) or 13 (RIH-ablated, green trace) individual recordings. Grey shading indicates SEM of the mean response. Scale bars are indicated above. The green bar indicates the time of the stimulus. Ablation of RIH did not visibly alter the morphology of FLP or RIH or the expression patterns of the cameleon transgenes.

b. Averaged responses of wild-type and RIH-ablated animals to harsh head touch stimulation. Each solid trace represents the average percentage change in R/R_0 for 24 (mock-ablated, red trace) or 13 (RIH-ablated, green trace) individual recordings. Grey shading indicates SEM of the mean response. Scale bars are indicated above.

(c) Scatter plot of peak calcium responses for nose touch stimulation. 20 mock ablated and 20 RIH ablated animals were imaged. Statistical significance (*** p <.0005) is according to the Mann-Whitney rank sum test.

(d) Effect of RIH ablation on nose touch escape behaviour. Animals were touched on the nose and escape responses (reversals) were scored as described. At least 100 animals were tested for each genotype. Statistical significance (*** P < .0005) is according to the Student's t test.

(e) Scatter plot of peak calcium responses for harsh head touch. 20 mock-ablated animals, 20 RIH-ablated animals, and 6 *unc-7* mutant animals were imaged (*unc-7* nose touch responses are in Figure 4.13). Statistical significance (*** p < .0005) is according to the Mann-Whitney rank sum test.

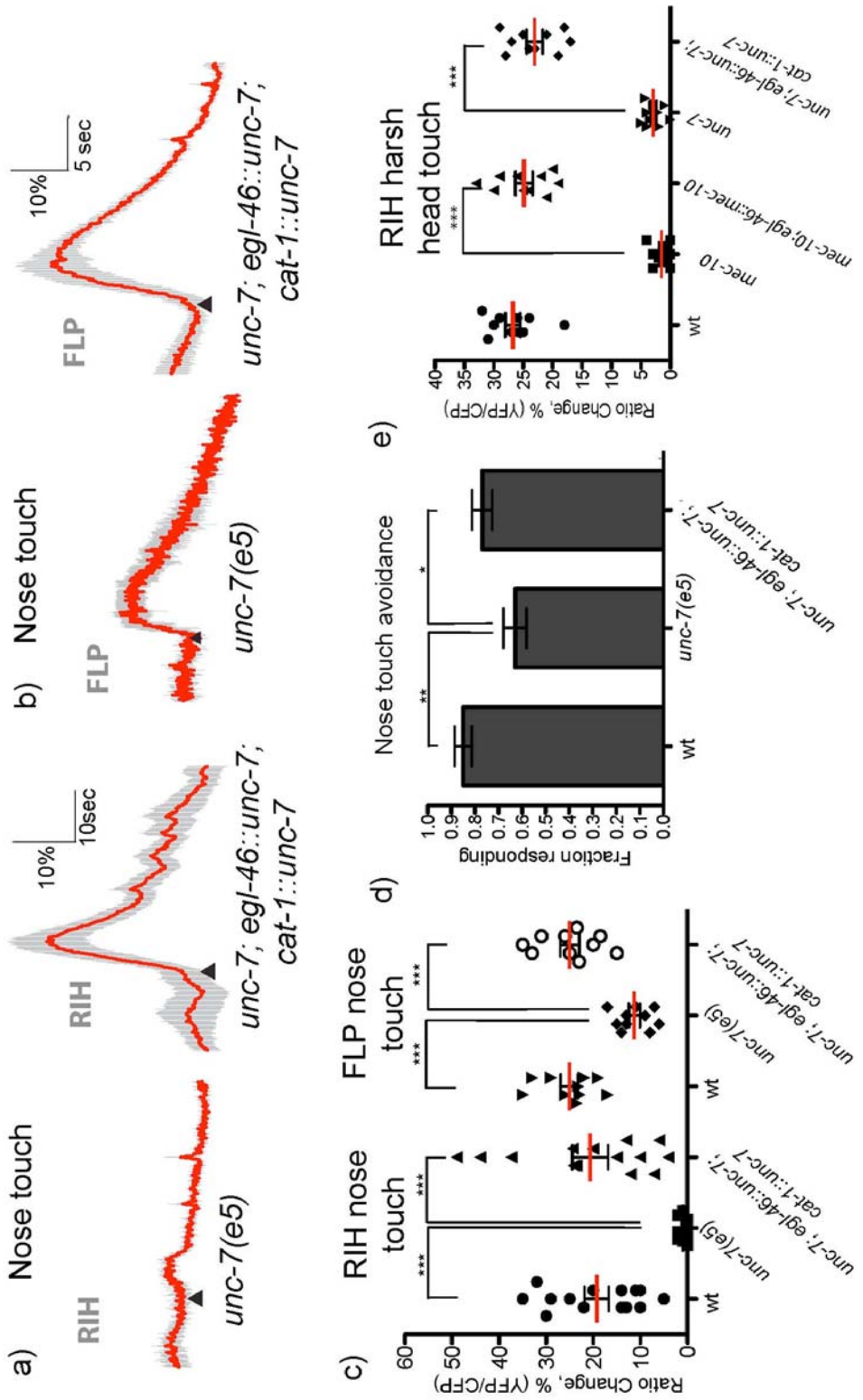

Figure 4.13: Effect of innexin mutations on nose touch responses.

Figure 4.13: Effect of innexin mutations on nose touch responses.

(a) Averaged responses of RIH neurons of *unc-7* innexin mutant and rescued animals to nose touch stimulation. Each solid trace represents the average percentage change in R/R_0 for 10 *unc-7(e5)*,14 animals from an *unc-7; egl-46::unc-7; cat-1::unc-7* rescue line carrying the *cat-1::YCD3* arrays. Grey shading indicates SEM of the mean response. Scale bars are indicated.

(**b) Averaged responses of FLP neurons of *unc-7* innexin mutant and rescued animals to nose touch stimulation.** Each solid trace represents the average percentage change in R/R_0 for 10 *unc-7(e5)* and 10 rescue animals using an *unc-7; egl-46::unc-7; cat-1::unc-7* rescue line carrying the *egl-46::YC2.3* array.

(**c) Scatter plot of peak calcium responses.** Statistical significance (*** $p < .0005$) is according to the Mann-Whitney rank sum test.

(**d) Effect of *unc-7* innexin mutations on nose touch-evoked escape responses.** 100 animals of each genotype were scored for reversals following nose touch stimulation. Statistical significance ($p < 0.005$) is according to the Student's t test.

(**e) Scatter plot of peak RIH calcium responses to harsh touch.** 10 animals were imaged for each genotype. Statistical significance (*** $p < .0005$) is according to the Mann-Whitney rank sum test.

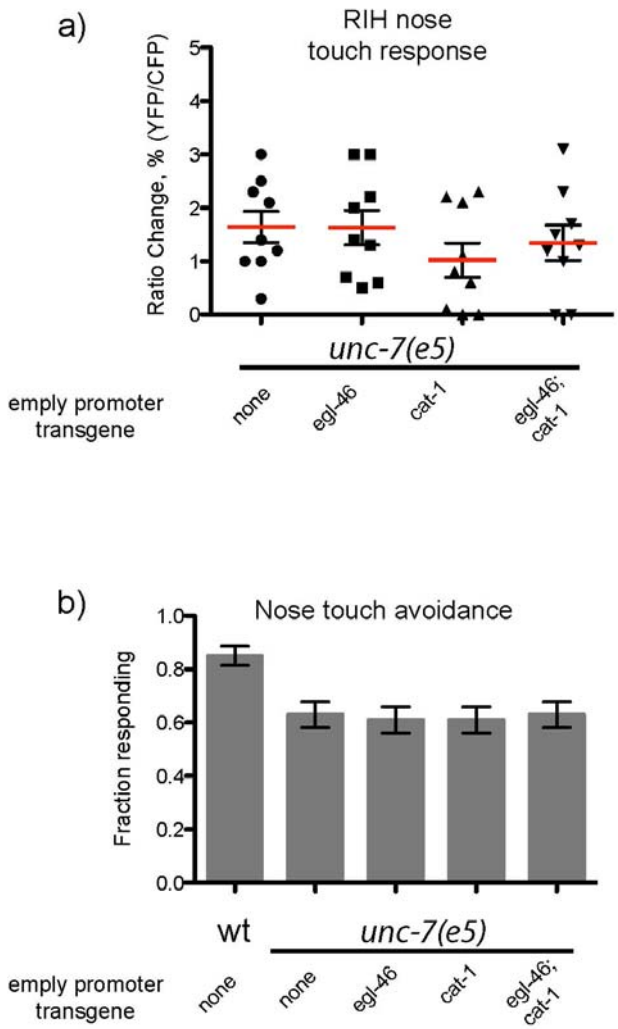

Figure 4.14: Empty vector controls for *unc-7* nose touch rescue.

(a) Scatter plot of responses to nose touch in the RIH neuron. "Empty" plasmids containing only the indicated promoters were injected into *unc-7; cat-1::YCD3* animals at the same concentrations as the rescue constructs in Figure 4.13. 9 animals were imaged for each control strain.

(b) Nose touch escape behaviour "Empty" plasmids containing only the indicated promoters were injected into *unc-7* animals at the same concentrations as the rescue constructs in Figure 4.13. 100 animals were assayed on 3 independent days. Error bars indicate S.E.M.

4.3.4 Information flow through the nose touch network is bidirectional

If signalling in the nose touch circuit is mediated primarily by gap junctions, information flow through RIH might be bidirectional: just as activation of neurons such as OLQ can indirectly excite FLP, FLP activation could be able to excite OLQ. I examined this possibility through both calcium imaging and behavioural analysis. To investigate the influence of FLP on OLQ-dependent behaviour, I analyzed lateral head movements known as foraging. Foraging is controlled by the head motorneuron RMG, which receives synaptic input from OLQ(Hart AC et al., 1995); anterior touch suppresses foraging movements in a process dependent on the tyraminergic RIM interneurons (Alkema MJ et al., 2005). OLQ has been reported to affect both foraging rate and foraging suppression (Driscoll M, Kaplan J, 1997), and I confirmed that OLQ ablation affected both behaviours (Figure 4.15; Figure 4.17). I observed that mutations in the FLP mechanosensory channel *mec-10* also reduced foraging rate as well as touch-evoked suppression of foraging (Figure 4.15; Figure 4.17a). Both phenotypes were rescued by FLP-specific expression of wild-type *mec-10(+)*, indicating that the foraging phenotypes of *mec-10* mutants result from abnormal FLP neurons. Moreover, the effect of *mec-10* on foraging suppression was suppressed by ablation of either the FLP or RIH neurons, further indicating that abnormal FLP activity, conveyed through RIH, suppresses normal foraging behaviour (Figure 4.15). Together, these data support the possibility that the FLP neurons modulate OLQ sensory responses through the RIH circuit.

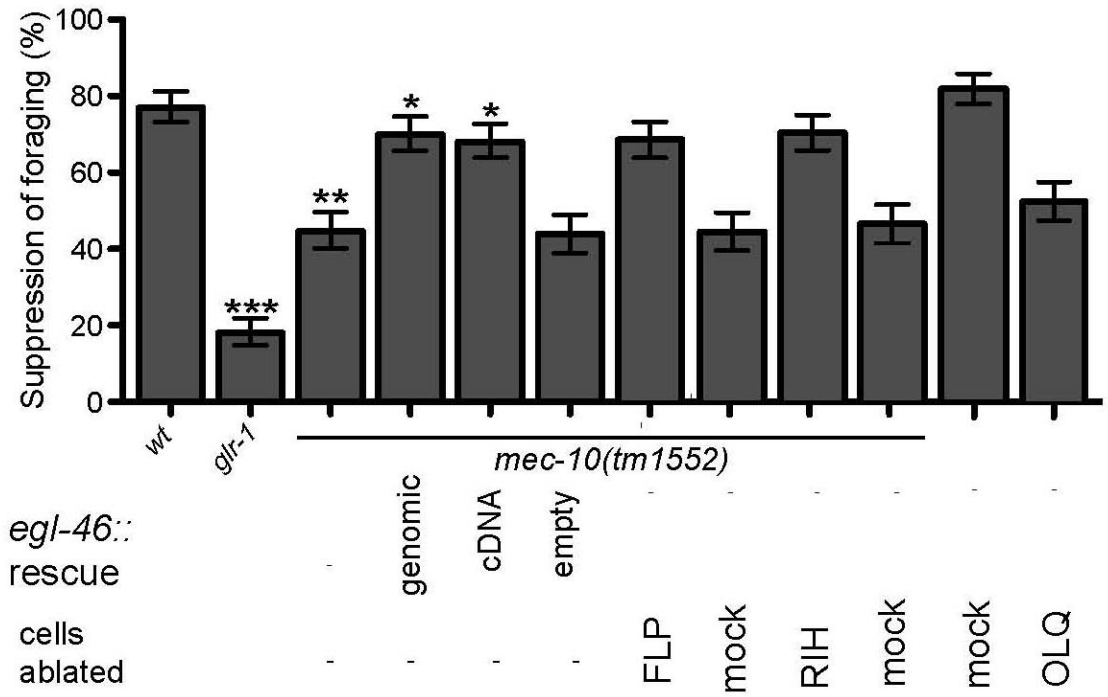

Figure 4.15: Effects of the FLP and RIH neurons on OLQ-dependent foraging behaviour.

mec-10 null mutants are defective in the suppression of foraging head movements while reversing in response to nose touch. This defect is suppressed by ablation of either the FLP or RIH neurons or FLP-specific expression of a *mec-10(+)* transgene in a *mec-10(tm1552)* mutant background. *glr-1* mutants, defective in a glutamate receptor thought to be important for neurotransmission between the OLQ neurons and the RMD motorneuron (Hart et al., 1995), and OLQ-ablated animals were used as controls (n= at least 30 animals on 3 independent days). Asterisks indicate a statistically significant difference between the indicated strain and wild-type (or between two bracketed strains) according to the Student's t test (*<0.01 **<0.001 ***<0.0001). Similar effects were seen on foraging rate (Figure 4.17).

To test the influence of FLP activity on OLQ directly, I imaged OLQ calcium dynamics in response to mechanical stimuli sensed by FLP. I observed that harsh touch applied to the side of the head led to robust calcium transients in OLQ as well as RIH (Figure 4.13e; Figure 4.16a, b). Mutations in the mechanosensory channel *mec-10* eliminated OLQ and RIH responses to harsh head touch, and these responses could be rescued by FLP-specific expression of *mec-10* (Figure 4.13e; Figure 4.17b, c). Moreover, ablation of RIH eliminated the harsh head touch-evoked calcium transients in OLQ (Figure 4.16a, b), indicating that the FLPs indirectly activate the OLQs through the RIH-centred network.

I also tested the effect of the network on nose touch responses in OLQ. Interestingly, a *mec-10* mutation significantly impaired OLQ and RIH calcium responses to nose touch; these defects were rescued by *mec-10(+)* expression in FLP (Figure 4.16a,c). Furthermore, ablation of RIH significantly reduced the responses of the OLQ neurons to nose touch (Figure 4.16a, c). These results indicate that just as the nose touch responses of the FLPs depend on a combination of RIH-mediated network activity and cell-autonomous MEC-10 function, OLQ nose touch responses depend on both RIH-mediated network activity and cell-autonomous OSM-9 function.

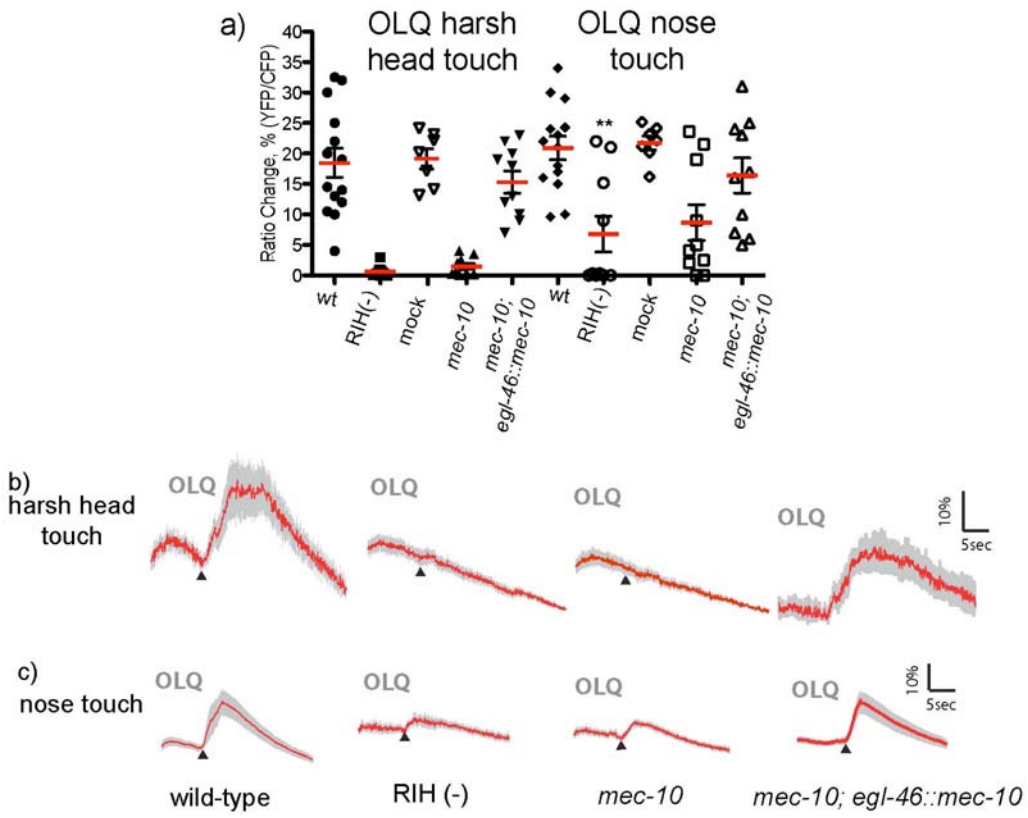

Figure 4.16 The RIH network is important for OLQ responses to nose touch and harsh head touch.

(a) Scatter plot of peak calcium responses to nose touch or harsh head touch in OLQ. For harsh head touch 14 wild-type, 10 RIH-ablated wild-type, 7 mock-ablated wild-type, *10 mec-10(tm1552)* and 10 *mec-10(tm1552); egl-46::mec-10(cDNA)* were imaged. For nose touch 14 wild-type, 10 RIH-ablated wild-type, 7 mock-ablated wild-type, 10 *mec-10(tm1552)* and 10 *mec-10(tm1552); egl-46::mec-10(cDNA)*. Statistical significance (***p < .0005) is according to the Mann-Whitney rank sum test.

(b) Calcium responses in OLQ to harsh head touch. Red traces indicate the average percentage change in R/R_0. Grey shading indicates SEM. None of these genotypes visibly altered the morphology of OLQ or the expression pattern of the cameleon transgene.

(c) Calcium responses in OLQ to nose touch.

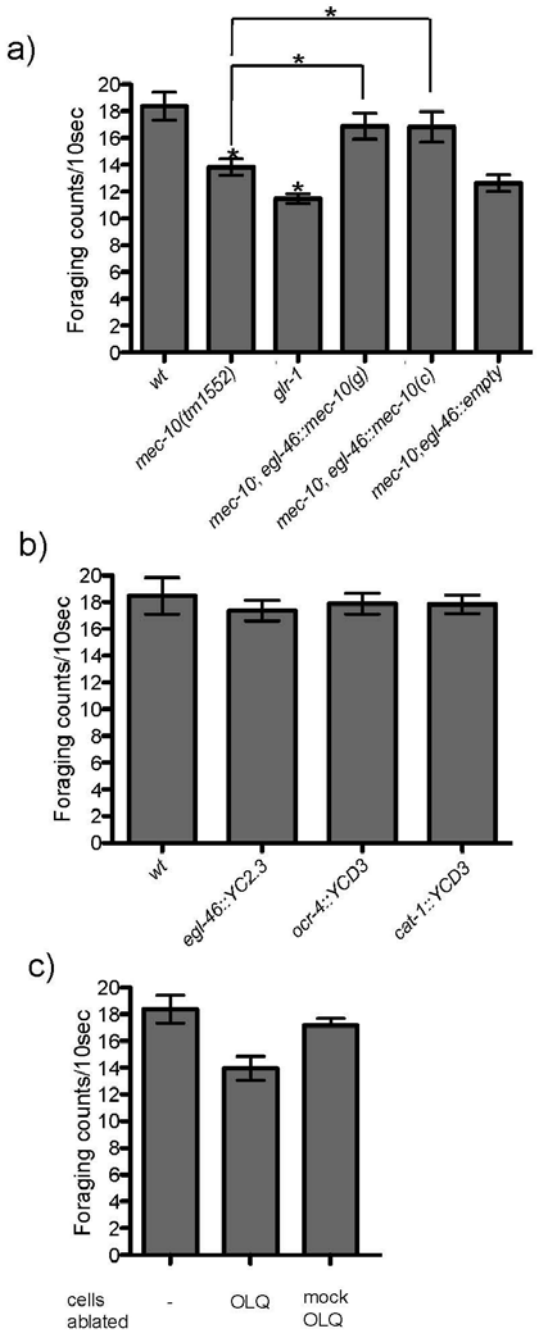

Figure 4.17: Further characterization of the effects of the FLP and RIH neurons on OLQ –dependent behaviour.

Figure 4.17: Further characterization of the effects of the FLP and RIH neurons on OLQ –dependent behaviour.

(a) Effects of *mec-10* on foraging frequency. Foraging rate was scored as described previously (Kindt KS et al., 2007b). Mutant and rescue lines are as described in Figure 4.15; Figure 4.16. Asterisks indicate a statistically significant difference between the indicated strain and wild-type (or between two bracketed strains) according to the Student's t test (*<0.01). At least 19 animals were scored for each genotype.

(b) Cameleon arrays do not alter foraging frequency. The cameleon lines used in other experiments were analyzed as described. At least 19 animals were scored for each genotype.

(c) Effect of cell ablations on foraging frequency. At least 19 ablated or mock-ablated animals were analyzed as described.

4.4 Discussion

I have shown here how a network of interacting mechanosensory neurons detects nose touch stimuli and in response evokes escape behaviour. Two classes of primary nose touch mechanoreceptors, the labial OLQ and cephalic CEP neurons, are required to indirectly facilitate gentle nose touch responses in the FLP head nociceptors. Nose touch activation of OLQ/CEP appears to excite the RIH interneuron through electrical synapses; this in turn depolarizes the FLP nociceptors, allowing these intrinsically high threshold mechanoreceptors to respond to low threshold nose touch stimuli. FLP then activates the backward command interneurons, which evoke reversal behaviour. In a parallel pathway, the ASH polymodal nociceptors also excite the command interneurons in response to nose touch stimulation.

This model represents a significant revision in our understanding of the neural basis of nose touch perception in *C. elegans*. Previous cell killing experiments identified ASH and FLP as the neurons whose ablation led to the most significant nose touch avoidance defects (Kaplan JM, Horvitz HR, 1993); on this basis, these two neuron pairs were thought to autonomously sense most nose touch stimuli (Driscoll M, Kaplan JM, 1997). Because OLQ and CEP ablations had little or no effect on nose touch avoidance, these neurons were thought to be only weakly sensitive to nose touch and relatively unimportant for escape behaviour. My new data indicate that these neurons respond robustly to nose touch, and in doing so contribute to the nose touch response of FLP. Mutations affecting OLQ or CEP mechanosensory molecules significantly compromise nose touch avoidance and reduce nose touch-evoked calcium transients in FLP. Through their RIH-mediated electrical coupling to FLP, active OLQ and CEP neurons appear to facilitate FLP activity, whereas inactive OLQ

and CEP neurons appear to inhibit FLP. Collectively, the RIH-centred nose touch network may act as a kind of coincidence detector, by which coordinated activity of all the inputs facilitates responses throughout the circuit while lack of coordinated activity suppresses responses. These results highlight the importance of combining the use of *in vivo* recordings in combination with ablation experiments in dissecting neural circuit mechanisms.

The nose touch circuit I have defined here is similar in many ways to the recently described hub and spoke network controlling aggregation behaviour in *C. elegans* (Macosko EZ et al., 2009). In both cases, sensory information flows inward from the sensory neurons at the spokes to the integrating neuron at the hub. Processed information also flows outward through the gap junctional connections, with the spoke neurons playing a second role as behaviour-specific outputs of the network. For example, the FLP neurons function both as polymodal nociceptor inputs to the circuit, as well as serving as the primary output from the RIH hub neuron to the command interneurons that execute the reversal reflex. The OLQ and CEP neurons appear to play similar dual roles as gentle touch mechanosensors and outputs for control of foraging and slowing behaviours. In this way, the network acts to couple distinct motor programs and allow their modulation by common sensory inputs.

The bidirectional nature of information flow in the network allows interconnected sensory neurons to modify and fine-tune each other's receptive properties. For example, over most of its receptive field, the FLP neurons respond only to high threshold mechanical stimuli through its cell autonomous MEC-10 harsh touch receptors. However, the electrical connectivity between FLP, OLQ and CEP nose touch mechanoreceptors allows the threshold for touch sensitivity in FLP to be

reduced when the CEP and OLQ neurons are active, facilitating responses to gentle nose touch. Thus, extrinsic network activity defines a gentle touch-sensitive region within the larger receptive field of FLP, which otherwise responds only to harsh touch. In this way, coordinated activity within the nose touch network is able to partially transform the FLPs from harsh touch to gentle touch sensors. Similarly, OLQ responses to nose touch are dependent on both the cell-autonomous activity of the OSM-9 TRPV channel as well as network inputs through RIH. Thus, lateral coupling between head mechanoreceptors allows sensory integration to occur at the most peripheral layer of the nose touch circuit, that of the sensory neurons themselves.

Hub-and-spoke electrical networks present certain problems for information processing by the nervous system. In particular, how can stimuli such as nose touch and harsh touch, which appear to activate most if not all neurons in the circuit, be distinguished? Differences in neuronal dynamics may play an important role; harsh head touch for example appears to evoke longer lasting responses in OLQ and FLP than nose touch. The magnitudes of responses in different neurons also vary; harsh head touch responses are larger than nose touch responses in FLP, but of similar size in OLQ. It will be interesting to explore how these factors influence the behavioural responses to these different stimuli.

The responses of sensory neurons are often considered to reflect the intrinsic properties of a cell and its sensory transduction pathways. However, the importance of interactions between sensory neurons in modifying these properties is becoming increasingly clear. In mammals, chemosensory neurons in taste buds are connected by both electrical and chemical synapses as well as by paracrine signaling (Huang YA et al., 2009; Dando R, Roper SD, 2009). Likewise, extensive gap junction coupling has

been shown to occur between many cell types in the retina, including rod and cone photoreceptors (Nelson R, 1977). In at least some cases, the functions of these connections parallel those in the *C. elegans* nose touch circuit. For example, gap junctions between low-threshold rods and higher threshold cones can facilitate responses in cone cells in low ambient light (Schneeweis DM, Schnapf JL, 1995), just as electrical connectivity in the nose touch circuit can facilitate gentle touch responses in the FLP nociceptors. My finding that electrically-mediated lateral interactions can tune the properties of sensory neurons in the nose touch circuits of *C. elegans* may suggest the existence of similar mechanisms in the nociceptive and somatosensory pathways of larger nervous systems.

4.5 Methods

Generation of FLP/PVD cameleon line *ljEX19*

The *egl-46* promoter region was obtained from plasmid TU#307 (Wu J et al., 2001), a gift from the lab of Martin Chalfie. A 3 kb HinDIII/NotI fragment was fused to cameleon YC2.3 in the vector pPD95.75 (A. Fire). Transgenic lines were obtained by germline injection of a *lin-15(n765)* mutant strain with the *egl-46::YC2.3* plasmid at a concentration of 50 ng/µl along with *lin-15(+)* genomic DNA (30 ng/µl) as a coinjection marker. Once a stable transgenic line was obtained, the *lin-15(n765)* allele was then removed by backcrossing to wild-type (N2) animals.

Transgenic rescue lines:

The *egl-46* promoter was obtained from plasmid TU #307 (Wu J et al., 2001), a kind gift from the Chalfie Lab. Using the primers GGCCTTCTGAAATCAAAACG and AGTTCACGCCAGATGCAAGATG I PCR amplified a 3kb fragment which was cloned into a Gateway 3-way P4-P1R donor vector. The *ocr-4* promoter we used was a 4.8kb fragment previously described by Kindt et al (Kindt KS et al., 2007b). A 3 kb *sra-6* promoter fragment cloned into a Gateway P4-P1R vector was obtained in the form of plasmid MGW1.2, a gift by E. Busch from the de Bono group. The 5ʾ end of the promoter is defined by the sequence 5ʾ-cttttagatataataaatcgaaattg-3ʾ while the 3ʾ end is defined by the sequence 5ʾ-ggcaaaatctgaaataataaatattaaattc-3ʾ adjacent of the start site of *sra-6*. A 2.4kb del-2 promoter was amplified using the following primers 5ʾ-GATTGACATCTAGTAATTTTTAAG-3ʾ and 5-GCTGCAATTGAGTAGAACATGTAG-3ʾ.

A *dat-1* promoter of length 0.8kb was amplified. The 5ʾ sequence was the following

5ʾ-CTCTGAAATGTTTCTAGTCGTTTTTG-3ʾ and

5ʾ- GGCTAAAAATTGTTGAGATTCG-3ʾ adjacent to the start site.

A 4.4kb fragment of *mec-10* genomic DNA was amplified using Phusion High-Fidelity DNA Polymerase F-530S from adult genomic DNA using the primers

5ʾ-GTACAAAATTCAAAAAATGAATCG-3ʾ and

5ʾ-GAAATAAGAAATTTATTTTCCG-3ʾ.

A 6.3kb *osm-9* genomic DNA fragment was amplified from adult genomic DNA using the primers 5ʾ-ATGGGCGGTGGAAGTTCGCGAAAC-3ʾ and

5ʾ-AAGAAAAAAAGTTTTCAAAAAATTAG-3ʾ.

I used a 5.6kb trp-4 cDNA clone from Kindt et al 2007, which was amplified from adult C. elegans RNA using the primers 5ʾ-CCAGATGAATCCCCACACCTCCC-3ʾ and 5ʾ- AAGGGGTTATGCTAAAAACTAGTAGGTACTGC-3ʾ.

I obtained a 2.8kb osm-9 cDNA clone described in (Colbert HA et al., 1997), a gift from the Bargmann lab.

A *trpa-1* 3.6kb cDNA fragment was amplified from a plasmid generated previously (Kindt KS et al., 2007b) using the primers 5ʾ-ATGTCGAAGAAATCATTAGG-3ʾ and 5ʾ-TCAGTTATCTTTCTCCTCAAGT-3ʾ.

A 2.2kb *mec-10* cDNA was amplified using Quiagen OneStep RT-PCR Kit from an RNA library using the primers 5ʾ-ATGAATCGAAACCCGCGAATG-3ʾ and

5`-TCAATACTCATTTGCAGCATTTTC-3`.

In order to generate rescue plasmids, I used the MultiSite Gateway Three Fragment Vector Construction Kit (Invitrogen) to fuse promoter, ORF and an *unc-54* 3'UTR. All fragments generated by PCR were sequenced after cloning, and any mutations that were detected were rectified using the site-directed mutagenesis kit: QuickChange Lightning Site-Directed Mutagenesis Kit, from Stratagene.

I injected the *mec-10(tm1552);ljEx19[egl-46::YC2.3]* worms with *egl-46::mec-10(genomic)* at 80 ng/µl with *unc-122::GFP* at 25 ng/µl to generate array *ljEx220 [egl-46::mec-10].* To generate arrays *ljEx381* and *ljEx382* I injected *mec-10(tm1552)* with *egl-46::mec-10(cDNA)* at 75 ng/µl and *elt-2::RFP* at 25 ng/µl. Two independent arrays were obtained and tested for rescue of the behavioural defect; one of these was subsequently crossed into the various calcium indicator strains that I used for imaging. To genotype the animals that came out of the crosses we used primers in the introns flanking the *tm1552* deletion. The "promoter only" controls for the *egl-46* promoter involved injection into a *mec-10(tm1552)* background in two different combinations. The first was *egl-46* promoter at 80 ng/µl with *unc-122::GFP* at 25 ng/µl and the other was *egl-46* promoter at 80 ng/µl with 25 ng/µl *elt-2::RFP*.

The *sra-6::osm-9* construct was injected in *osm-9(ky10) Ex19[egl-46::YC2.3]* at 50 ng/µl with *unc-122::GFP* at 20 ng/µl to generate array *ljEx222*. Similarly, the *[del-2::osm-9(genomic)]* was injected at 75 ng/µl together with *elt-2::RFP* at 25 ng/µl in *osm-9(ky10)ljEx19[egl-46::YC2.3]* to obtaine array *ljEx235.* To obtain cDNA rescues of *osm-9* in FLP, *osm-9(ky10)* animals were injected with *egl-46::osm-9(cDNA)* at 80ng/µl with 25 ng/µl of *elt-2::RFP*. Two independent arrays *ljEx377* and *ljEx378* were obtained and *ljEx377* was subsequently crossed into the various calcium

indicator lines used for calcium imaging. To genotype the animals that came out of the crosses we used primers in the introns flanking the *ky10* point mutation to generate a PCR fragment which was subsequently sequenced with the primer CTAGGTGGAGGGCTGATTA. In order to obtain the rescue cDNA arrays *ljEx379* and *ljEx380* of *osm-9* in the OLQ neurons I injected *osm-9(ky10)* animals with 90 ng/µl *[ocr-4::osm-9(cDNA)]* and 25 ng/µl *elt-2::RFP*. To image from the rescue lines I crossed *ljEx380* with *osm-9(ky10)ljEx[egl-46::YC2.3].* The "promoter only" controls for the *egl-46* promoter involved injection into an *osm-9(ky10)* background at 80 ng/µl with *elt-2::RFP* at 25 ng/µl and for the *ocr-4* promoter at 90 ng/µl with 25 ng/µl *elt-2::RFP*. The "promoter only" controls were injected as follows: *del-2* promoter was injected at 75 ng/µl with *elt-2::RFP* at 25 ng/µl , *egl-46* promoter involved injection of the promoter at 80ng/µl with 25 ng/µl of *elt-2::RFP* and the *ocr-4* promoter at 90ng/µl with 25 ng/µl of *elt-2::RFP*. All empty promoters were injected in an *osm-9(ky10)* background. The *ocr-4::trpa-1(cDNA)* construct was injected at 80 ng/µl together with *unc-122::GFP* at 25 ng/µl to create *ljEx373* and *ljEx374*. *ljEx374* was subsequently crossed into the various calcium indicator lines used for calcium imaging. *trpa-1(ok999); ljEx115[pdel-2::trpa-1(cDNA);unc-122::gfp]* and *trpa-1(ok999);ljEx119[sra-6::trpa-1(cDNA) unc-122::gfp]* carrying animals (previously described in (Kindt KS et al., 2007b)) were crossed into the *ljEx19[egl-46::YC2.3]* to image from the FLP neurons. To genotype the animals that came out of the crosses we used primers in the introns flanking the *ok999* deletion. The "promoter only" controls were injected as follows: *del-2* promoter was injected at 75ng/µl with *unc-122::GFP* at 25 ng/µl and the *ocr-4* promoter at 80ng/µl with 25 ng/µl of *unc-122::GFP*. All empty promoters were injected in a *trpa-1(ok999)* background.

To determine whether FLP and RIH nose touch defects in *trp-4(ok1605)* mutant worms were rescued by expression of *trp-4* in dopaminergic neurons I crossed *trp-4(ok1605);ljEx19* and *trp-4(ok1605); ljIs104* with *ljEx128[dat-1::trp-4(+); unc-122::GFP]* respectively, an previously described array carrying a *trp-4* cDNA expressed specifically in dopaminergic neurons (Kindt KS et al., 2007a). The "promoter only" control was injected as follows: *dat-1* promoter was injected at 20ng/µl with *unc-122::GFP* at 25 ng/µl in a *trp-4(ok1605)* background.
The *unc-7(e5)* allele was crossed with *ljIs104[cat-1::YCD3]* to image from RIH and with *ljEx19[egl-46::YC2.3].* To generate rescue lines for *unc-7* I co-injected *egl-46::unc-7(cDNA)* and *cat-1::unc-7(cDNA)* to a final concentration of 50 ng/µl each with 25 ng/µl *elt-2::RFP*. Two independent arrays were obtained ljEx375 and ljEx376. ljEx375 was crossed into the appropriate imaging lines. In order to genotype the animals that came out of the crosses we used primers in the introns flanking the *e5* point mutation to generate a PCR fragment which was subsequently sequenced. The "promoter only" controls were injected as follows: *cat-1* promoter was injected at 50 ng/µl with *elt-2::RFP* at 25 ng/µl, the *egl-46* promoter at 50ng/µl with 25 ng/µl of *elt-2::RFP and cat-1;elg-46* at a final concentration of *50* ng/µl with 25ng/µl *elt-2::RFP*. All empty promoters were injected in an *unc-7(e5)* background. To generate the *dat-1::GFP* I injected the construct at 25 ng/µl with 25 ng/µl *unc-122::GFP*.

Cell Ablations

Laser ablations were carried out using a standard protocol (Bargmann CI, Avery L, 1995). The RIHs, OLQs and FLPs were ablated in the early L1 stage, usually with 3-4hr post hatching; the PVD cells were ablated at a slightly later stage near the end of L1. Loss of the ablated cell was confirmed by observing loss of cameleon fluorescence in the adult animal.

Calcium Imaging

Optical recordings were performed essentially as described (Kerr R et al., 2000; Kerr, RA, 2006) on a Zeiss Axioskop 2 upright compound microscope equipped with a Dual View beam splitter and a Uniblitz Shutter. Fluorescence images were acquired using MetaVue 6.2. Filter-dichroic pairs were excitation, 400–440; excitation dichroic 455; CFP emission, 465–495; emission dichroic 505; YFP emission, 520–550. Individual adult worms (~24h past L4) were glued with Nexaband S/C cyanoacrylate glue to pads composed of 2% agarose in extracellular saline (145 mM NaCl, 5 mM KCl, 1 mM CaCl2, 5 mM MgCl2,20 mM D-glucose, 10 mM HEPES buffer, pH 7.2). 5 mM serotonin was also added for nose touch imaging experiments. Worms used for calcium imaging had similar levels of cameleon expression in sensory neurons as inferred from initial fluorescence intensity. Acquisitions were taken at 28Hz (35ms exposure time) with 4x4 or 2x2 binning, using a 63x Zeiss Achroplan water immersion objective. Thermal stimulation was applied as described in Chapter 2.

Nose touch stimulation

The nose-touch stimulator was a needle with a 50-μm diameter made of a drawn glass capillary with the tip rounded to ~10 μm on a flame. I positioned the stimulator using a motorized stage (Polytec/PI M-111.1DG microtranslation stage with C-862 Mercury II controller). The needle was placed perpendicular to the worm's body at a distance of 150μm from the side of the nose. In the on phase, the glass tip was moved toward the worm so that it could probe ~8 μm into the side of the worm's nose on the cilia and held on the cilia for 1 second, and in the off phase the needle was returned to its original position.

Harsh head touch stimulation

To visualize the harsh head touch response in FLP, the same nose touch setup was used but the probe was aligned in a more posterior position between the two bulbs of the pharynx. The probe was displaced ~24μm at a raised speed of 2.8mm/s. The stimulus was a buzz (i.e. the probe was displaced 2.5 μm in and out for the duration of the stimulus) lasting ~1 second.

Microscopy for still images

To obtain single images we used a ZeisLSM 510 Meta confocal microscope with a 40x objective. Images were exported as single TIFF files. To measure the intensity of the fluorescence we imported the TIFF image in ImageJ. I generated a region of interest around the cell body of the neuron of interest and measure the mean intensity using a scale between 0 and 255 arbitrary units.

Behavioural Assays

Nose touch

For nose touch, assay plates were prepared fresh within 4 h of use by spreading one drop of a saturated *E. coli* strain OP50 culture onto nematode growth medium plates. Two plates of ten worms each per genotype were allowed to move forward into an eyelash in the path of the worm. I recorded either a reversal response or null response. I scored the assay blinded and repeated it on at least five independent days. The nose-touch insensitive mutant *glr-1(n2461)* was used as a control.

Foraging

Foraging behaviour was scored by recording videos using an automated tracking system recording at 30fps. The worm tracker maintained the worm in view during the 2 minute recording following a period of 10 minutes in which the worms were allowed to recover after being transferred to fresh, thinly seeded OP50 plates. The videos were scored blind, counting the number of foraging movements in 10 second intervals during which the worm was moving in a forward direction. A foraging movement was defined as a complete cycle of movement from the tip of the nose from the ventral side through the dorsal side or vice versa. I quantified three 10-s intervals for each worm assayed and scored at least 30 worms per strain in three different days. In order to assay inhibition of foraging in response to nose touch, I used plates and hair picks prepared as for the nose-touch assay. Nose touch in this case was applied during forward movement to the nose of the worm. I defined inhibition of foraging as least two consecutive head bends without foraging during backward movement. I blindly scored more than 30 worms per strain on each trial.

4.6 Experimental Contributions

I conducted all the experiments presented in Chapter 4 under the guidance and supervision of William R Schafer.

4.7 References

Alkema MJ, Hunter-Ensor M, Ringstad N, Horvitz H R (2005). Tyramine functions independently of octopamine in the *Caenorhabditis elegans* nervous system. Neuron *46*, 247-260

Arnadottir J, Chalfie M (2010) Eukaryotic mechanosensitive channels. Annu Rev Biophys *39*, 111-137

Bargmann CI, Avery L (1995). Laser killing of cells in *Caenorhabditis elegans.* *Meth Cell Biol 48*, 225-250

Bounoutas A, Chalfie M (2007). Touch sensitivity in *Caenorhabditis elegans.* Pflugers Arch *454*, 691-702

Chalfie M, Sulston JE, White JG, Southgate E, Thomson JN, Brenner S (1985) The neural circuit for touch sensitivity in *Caenorhabditis elegans*. J Neurosci *5*:956-964

Christensen AP, Corey DP (2007) TRP channels in mechanosensation: direct or indirect activation? Nat Rev Neurosci *8*, 510-521

Colbert HA, Smith TL, Bargmann CI (1997) OSM-9, a novel protein with structural similarity to channels, is required for olfaction, mechanosensation, and olfactory adaptation in *C. elegans*. J Neurosci *17*:8259-8269

Dando R, Roper SD (2009). Cell-to-cell communication in intact taste buds through ATP signalling from pannexin 1 gap junction hemichannels. J Physiol *587*: 5899-5906

Driscoll M, Chalfie M (1991). The *mec-4* gene is a member of a family of *Caenorhabditis elegans* genes that can mutate to induce neuronal degeneration. Nature *349*:588-593

Driscoll M, Kaplan J (1997) Mechanotransduction. In *C. elegans* II, D. L. Riddle, T. Blumenthal, B. J. Meyer, and J. R. Priess, eds. (Cold Spring Harbor, NY, Cold Spring Harbor Press)

Garcia-Anoveros J, Corey DP (1997) The molecules of mechanosensation. Annu Rev Neurosci *20*, 567-594

Goodman MB, Lumpkin E A, Ricci A, Tracey WD, Kernan M, Nicolson T (2004) Molecules and mechanisms of mechanotransduction. J Neurosci *24*, 9220-9222

Hall D, Altun Z F (2008) *C. elegans* atlas (Cold Spring Harbor, NY, Cold Spring Harbor Laboratory Press)

Hart AC, Sims S, Kaplan JM (1995) Synaptic code for sensory modalities revealed by *C. elegans* GLR-1 glutamate receptor. Nature *378*: 82-85

Hilliard MA, Bargmann CI, Bazzicalupo P (2002) *C. elegans* responds to chemical repellents by integrating sensory inputs from the head and the tail. Curr Biol *12*: 730-734

Huang M, Chalfie M (1994) Gene interactions affecting mechanosensory transduction in *Caenorhabditis elegans*. Nature *367*: 467-470

Huang YA, Dando R, Roper SD (2009) Autocrine and paracrine roles for ATP and serotonin in mouse taste buds. J Neurosci *29*:13909-13918

Kahn-Kirby AH, Bargmann CI (2006) TRP channels in *C. elegans.* Annu. Rev. Physiol. 68:719–36

Kang L, Gao J, Schafer WR, Xie Z, Xu XZ (2010) *C. elegans* TRP family protein TRP-4 is a pore-forming subunit of a native mechanotransduction channel. Nature 67(3):349-51

Kaplan, JM, Horvitz HR (1993) A dual mechanosensory and chemosensory neuron in *Caenorhabditis elegans*. Proc. Natl. Acad. Sci. USA 90, 2227–2231

Kerr R, Lev-Ram V, Baird G, Vincent P, Tsien RY, Schafer WR (2000) Optical imaging of calcium transients in neurons and pharyngeal muscle of *C. elegans.* Neuron 26(3):583-94

Kerr RA (2006). Imaging the activity of neurons and muscles. WormBook, 1-13

Kindt KS, Quast KB, Giles AC, De S, Hendrey D, Nicastro I, Rankin CH, Schafer WR (2007a) Dopamine mediates context-dependent modulation of sensory plasticity in *C. elegans*. Neuron 55(4):662-76

Kindt KS, Viswanath V, Macpherson L, Quast K, Hu H, Patapoutian A, Schafer WR (2007b) *Caenorhabditis elegans* TRPA-1 functions in mechanosensation. Nature Neurosci. 10: 568-577

Li W, Feng Z, Sternberg PW, Xu XZ (2006) A *C. elegans* stretch receptor neuron revealed by a mechanosensitive TRP channel homologue. Nature 440:684–687

Macosko EZ, Pokala N, Feinberg EH, Chalasani SH, Butcher RA, Clardy J, Bargmann CI (2009) A hub-and-spoke circuit drives pheromone attraction and social behaviour in *C. elegans*. Nature *458*: 1171-1175

Nelson R (1977). Cat cones have rod input: a comparison of the response properties of cones and horizontal cell bodies in the retina of the cat. J Comp Neurol *172*: 109-135

O'Hagan R, Chalfie M, Goodman MB (2005) The MEC-4 DEG/ENaC channel of *Caenorhabditis elegans* touch receptor neurons transduces mechanical signals. Nat Neurosci 8:43–50

Sawin ER, Ranganathan R, Horvitz HR (2000) *C. elegans* locomotory rate is modulated by the environment through a dopaminergic pathway and by experience through a serotonergic pathway. Neuron 26:619–631

Schneeweis DM, Schnapf JL (1995) Photovoltage of rods and cones in the macaque retina. Science *268*, 1053-1056

Starich TA, Herman RK, Shaw JE (1993) Molecular and genetic analysis of unc-7, a *Caenorhabditis elegans* gene required for coordinated locomotion. Genetics *133*: 527-541

Starich TA, Xu J, Skerrett IM, Nicholson BJ, Shaw JE (2009) Interactions between innexins UNC-7 and UNC-9 mediate electrical synapse specificity in the *Caenorhabditis elegans* locomotory nervous system. Neural Dev *4*, 16.

Suzuki H, Kerr R, Bianchi L, Frokjaer-Jensen C, Slone D, Xue J, Gerstbrein B, Driscoll M, Schafer WR (2003) In vivo imaging of *C. elegans* mechanosensory neurons demonstrates a specific role for the MEC-4 channel in the process of gentle touch sensation. Neuron 39:1005–1017

Tobin D, Madsen D, Kahn-Kirby A, Peckol E, Moulder G, Barstead R, Maricq A, Bargmann C (2002) Combinatorial expression of TRPV channel proteins defines their sensory functions and subcellular localization in *C. elegans* neurons. Neuron 35:307–318

Way JC, Chalfie M (1989) The *mec-3* gene of *Caenorhabditis elegans* requires its own product for maintained expression and is expressed in three neuronal cell types. Genes Dev 3:1823–1833

White JG, Southgate E, Thomson JN, Brenner S (1986) The structure of the nervous system of the nematode *Caenorhabditis elegans.* Philos Trans R Soc Lond 314:1–340

Wu J, Duggan A, Chalfie M (2001) Inhibition of touch cell fate by *egl-44* and *egl-46* in *C. elegans*. Genes Dev. 15(6):789-802

Chapter 5

Conclusions

5.0 Conclusions

In the previous chapters I presented and discussed results that I obtained in the three main projects that I pursued during my PhD. My work has mostly focused on mechanosensation and thermosensation in the nematode *C. elegans*. Through the study of these sensory modalities, I also tried to gain further insight into the molecular and cellular basis of nociception.

5.1 The PVD neurons as a model for studying nociception.

5.1.1 The PVDs are mutlimodal nociceptive neurons.

My work largely focused on the PVD neurons and their ability to respond to harsh mechanical and cold stimuli. This pair of neurons had received little attention in comparison to the touch circuit neurons when I started my PhD. The PVDs were implicated by a series of ablation experiments in the sensation and avoidance of harsh body touch (Way JC, Chalfie M, 1989) as well as in the tap withdrawal reflex (Wicks SR, Rankin CH, 1995). In addition the Chalfie lab had made a number of interesting observations. They identified the elaborate ultrastructure of the PVD neurons, resembling that of mammalian mechanoreceptors and they showed that the homeo-box-containing gene *mec-3* was essential for the development and function of the PVDs (Way JC, Chalfie M, 1989; Way JC et al, 1992). More so they were able to confirm the expression of some but not all of the components of the mechanosensory complex expressed in the touch receptor neurons (Huang M, Chalfie M, 1994; Du H et al, 1996). My collaborator Millet Treinin had also made unpublished observations that elimination of the PVDs via genetic ablation resulted in a strong defect in

noxious cold avoidance. Surprisingly very little was known about the cells and molecules that mediate the response of worms to either noxious heat or noxious cold. A single study regarding the response of *C. elegans* to noxious heat had reported that thermal nociceptors are located in the head and the tail, that nociceptive heat responses use a different neural circuit than thermotaxis and finally that the thermal avoidance response is modulated by glutamate and neuropetides (Wittenburg N, Baumeister R, 1999).

My work confirmed that the PVD neurons respond to both harsh touch and noxious cold and that these neurons are required for the escape responses to these stimuli.

5.1.2 The DEG/ENaC proteins MEC-10 and DEGT-1 are subunits of a mechanosensitive channel.

I identified the DEG/ENaC protein MEC-10 as essential for the responses to harsh touch, while I showed that a second novel DEG/ENaC channel, namely DEGT-1 is required for harsh touch transduction.

The identity of the harsh touch mechanosensory complex both in mammals and in *C. elegans* was previously unknown. The best-studied mechanoreceptors in mammals are located in the skin. Some of the cutaneous fibre endings are classified as high-threshold receptors (HTMs) and are excited by injurious mechanical forces. These can be either mechanosensitive or polymodal neurons (Delmas P et al., 2011). Excitatory mechanosensory currents recorded in response to strong mechanical stimuli have yet to be matched to a particular candidate channel. My results suggest that two DEG/ENaC proteins, MEC-10 and DEGT-1 act in a harsh touch mechanosensory complex possibly acting as the pore forming subunits. Based on my findings and

recent work from D. melanogaster (Zhong L et al, 2010) it is possible to suggest as plausible candidates one or more DEG/ENaC channels.

5.1.3 The TRP channel TRPA-1 is a cold sensor.

Genetic studies of thermosensation *in C. elegans* mostly focused on thermotaxis had failed to provide evidence of direct temperature regulation of ion channels, while a cGMP-dependent molecular network regulating the TAX-4 and TAX-2 ion channels was shown to regulate the amazing thermosenstivity of the AFD neurons (Coburn C, Bargmann CI, 1996; Komatsu H et al, 1996, Komatsu H et al, 1999, Ramot D et al, 2008a, reviewed in Garrity PA et al, 2010). This was rather surprising since the *C. elegans* genome is predicted to encode at least 24 TRP channels, including relatives of insect and mammalian temperature-sensitive TRPs (Goodman MB, Schwarz EM, 2003). My work identified TRPA-1 as the first worm TRP channel to be involved in thermosensation. *C. elegans* TRPA-1 is activated by cooling. This is in agreement with observations made in mammalian systems where TRPA1 is activated by cooling with a threshold of approximately 17°C. However this is in contrast to the *D. melanogaster* orthologue of TRPA1 namely dTRPA-1, which is activated by warming rather than by cooling. The mechanistic basis for this opposite thermosensitivity is still an open question.

My results may also indirectly affect an ongoing debate as to whether TRPA1 is really activated by cold. There is evidence arguing both ways (Jordt et al., 2004; Nagata et al., 2005; Story GM et al., 2003; Kwan KY et al., 2006; Fajardo O et al., 2008). However I have shown that the *C. elegans* orthologue of the mammalian TRPA1 is able to sense cold *in vivo* and is capable of forming cold-activated channels

in heterologous cells producing cold-activated cation currents. More so the cold sensing defect of *trpa-1* mutant worms can be rescued by the expression of the mammalian TRPA1 in the PVD neurons.

5.1.4 Future directions: Identification of other proteins required for mechanosensation and cold sensation in PVD.

Around the time my work on the PVDs was published a number of papers came out further characterizing these neurons. In particular four papers addressed the molecular basis of the elaborate branching pattern of these mutlidendritic neurons (Oren-Suissa M et al., 2010; Smith CJ et al., 2010; Alberg A et al., 2010; Aguirre-Chen C et al., 2011). Smith CJ and co-workers provided a very detailed expression profiling study identifying a variety of genes that could be involved in the development and function of the PVDs (Smith CJ et al., 2010). Stomatins are particularly important for mechanosensory complexes and while MEC-2 the stomatin associated with the gentle touch mechanosensory complex is absent in PVD two uncharacterized stomatins are enriched in the expression profile of PVD and may function in the harsh touch mechanosesory complex. Notably, the homologue of a protein implicated in hereditary human deafness namely TMC1 was also enriched in the PVD expression profiling. The mechanism of action of TMC1 in mammalian auditory mechanotransduction remains unknown and the worm could provide important insight. Since harsh touch –evoked neural activity and behaviour can be assayed with relative ease it would be interesting to identify further molecules involved in the harsh touch mechanosensory complex using forward mutant screens and reverse genetics candidate gene approaches. Further screens can also be designed to investigate the

molecular mechanism by which the PVD neurons respond to noxious cold.

5.1.5 Future directions: Using the PVD polymodal nociceptors as a model to investigate analgesia.

Mammalian pain pathways are modulated by opioids (Dores RM et al., 2002). They have many effects on neuronal physiology. For example TRP channels are though to be potential targets of opioid signalling. However the mechanism of analgesia is not well-understood. I have carried out preliminary experiments showing that opioids can affect noxious cold and heat responses in *C. elegans*, as well as avoidance to noxious chemicals. Using *in vivo* neuroimaging I have found that the responses of the PVDs to noxious cold can be modulated by opioids. Moreover, I have found that a mutation in a G-Protein Coupled Receptor (GPCR) suppresses the effects of morphine and endomorphins on the heat and cold responses of the worm. This finding suggests that opioids may affect anelgesia via GPCRs in C. elegans, similarly to higher animals (Dores RM et al., 2002; Dreborg S et al., 2008). Further work on this topic may identify additional molecules involved in this process which will strengthen the importance of the PVDs as a model for the study of nociception and analgesia.

5.2 Investigating the mechanism of Gentle-touch mechanosensation

A number of different types of channels, such as DEG/ENaC, TRP, K_{2P}, and MscS-like, are thought to be mechanically-gated in eukaryotic sensory systems. These candidates are the result of forward and reverse genetic screens in a variety of model organisms and they have been identified on the basis of the phenotype of mutant animals, the *in vivo* expression of the channel proteins in mechanosensory cells and by *in vitro* experiments. The most substantial and convincing body of evidence comes from the MEC-4/MEC-10 channel in *C. elegans* and the TRPY1 channel in yeast. In *C. elegans* the gentle touch transduction complex pore is composed of the well-studied MEC-4 pore subunit, which is essential for gentle touch sensation and MEC-10 whose importance is poorly defined. They are thought to associate with two other proteins: MEC-2 and MEC-6. These four proteins have been hypothesized to form a complex given that they interact genetically, they coimmunoprecipitate each other, they colocalize in puncta along the touch neuron processes (with the exception of MEC-10 which had not been tested at the start of my PhD) and they interact electrtophysiologically when expressed in *Xenopus* oocytes (Chelur DS, et al, 2002; Goodman MB et al, 2002; Zhang S et al, 2004).

5.2.1 MEC-10 is important for mechanosensory channels near the cell body.

My behavioural and *in vivo* neuroimaging studies of a deletion and two point mutants of *mec-10* have led me to the conclusion that MEC-10 is important but not essential for gentle touch responses in the touch receptor neurons. Moreover, it came as a surprise to me to observe an asymmetric requirement for MEC-10, that is, it only seems to be required proximally to the cell body. The response of *mec-10* mutants

was very strong distally from the cell body but very poor proximally to the cell body of the touch receptor neurons. I tested the subcellular localization of a rescuing MEC-10::GFP translational fusion and found it to be restricted to the neuronal cell body and the proximal dendrite. This observation was consistent with the rest of my data. However, these observations are in contrast with the phenotypes of *mec-4*, *mec-2* and *mec-6* null mutants, which have very strong mechanosensory defects and translational GFP and RFP fusions of these MEC proteins localize all along the process of the touch receptor neurons.

The current model in literature hypothesizes that the gentle touch mechanosensory complex in the touch receptor neurons is composed of a heteromeric channel of MEC-4 and MEC-10 complimented by MEC-2 and MEC-6 in an accessory role. My results suggest that it is possible to form complexes with a homomeric channel pore composed of just MEC-4 channel subunits. This hypothesis is supported from *Xenopus* oocyte experiments. In these experiments a dominant active version of MEC-4 coexpressed with MEC-2 and MEC-6 is able to generate functional currents, which are reduced upon the addition of a MEC-10 subunit (Goodman MB et al, 2002). More so, when gain of function alleles of *mec-4* and *mec-10* were assayed for a degeneration phenotype in the touch receptor neurons it was found that *mec-4(gf)* - induced degeneration does not require the presence of MEC-10, in contrast to *mec-10(gf)*- induced degeneration which is not possible in the absence of MEC-4. An alternative possibility is that MEC-4 forms heteromeric channels with another DEG/ENaC channel. The asymmetric phenotype of MEC-10 that I described in Chapter 3 largely resembles the phenotype described for weak alleles of *mec-7* (Savage C et al, 1989). One cannot exclude the possibility that *mec-10* mutant animals

are defective in propagation of the mechanoreceptor potential (MCR) along the process given that I am imaging from the cell body of the touch receptor neurons, however I believe that MEC-10 contributes to the mechanosensory complexes near the cell body and not those located more distally. Electrophysiology experiments by O'Hagan et al suggest that mec-10 point mutants exhibit severe defects when the PLM neurons are stimulated about 90μm away from the PLM cell body(O'Hagan R et al, 2005). This position corresponds to position 1 in my experiments and the results are compatible with my calcium imaging data. Of course it would be particularly useful to obtain electrophysiology results for *mec-10* mutants when they are probed at more distal positions, to determine whether one can obtain a similar asymmetric phenotypes to the one I have observed. More so, given that some alleles of *mec-7* have been reported to show a similar behavioural phenotype to *mec-10* it would be interesting to investigate their calcium responses and to establish the genetic interactions that may lead to the asymmetric phenotype observed in some *mec* mutants.

5.2.2 PVM is required for gentle touch sensation

An interesting finding presented in Chapter 3 is the fact that contrary to laser ablation experiments which have failed to demonstrate a role for PVM in gentle touch sensation, *in vivo* neuroimaging from PVM shows it is able to respond to mechanical stimuli. Even though it may not be required for escape responses to gentle touch stimulation it may be required for the neuropeptidergic modulation of the touch circuit. Indeed it has been shown that repeated stimulation of animals by touch and/or

taping has pronounced effects on behavioural modulation and plasticity (Rankin CH, Broster BS,1992; Wicks SR and Rankin CH, 1996; Zhao B et al., 2003). The time-scale of these effects is compatible with the involvement of monoamine and neuropeptide modulators, which could be released by the mechanosensory neurons. PVM expresses both *flp-8* and *flp-20* and therefore it could be a modulator of the excitability of the touch circuit (Kim K and Li C, 2004). In the future it should be possible to study the responses of PVM to multiple stimulations by neuroimaging and to assess the effects of PVM-expressed neuropetides on the other touch circuit neurons both behaviourally and by calcium imaging.

5.3 Investigating the Nose Touch Circuit

In Chapter 4 I presented a study of the nose touch circuit. I used a combination of laser ablations, calcium imaging and behavioural assays to investigate in greater detail the interactions between the neurons contributing to the nose touch response. The current scientific literature suggested that the nose touch response was mediated largely by the ASH and FLP neurons. ASH was a known polymodal neuron, however little was known about the nature of the FLP neurons.

5.3.1 The FLP neurons are polymodal nociceptors

Similar to the PVDs the FLP neurons are multidendritic head neurons covering most of the animal's head. I investigated whether they were capable of robustly responding to multiple sensory cues. In particular I found that they were responsive to the gentle nose touch stimulation at the tip of the nose, to harsh head touch and to noxious heat. The ability of these neurons to generate robust responses to a number of distinctive

stimuli suggests that they are polymodal nociceptors. I subsequently investigated the molecular basis of these responses in the FLPs. I found that while harsh head touch is dependent on the autonomous activity of MEC-10, gentle nose touch responses require both MEC-10 as well as other, MEC-10 independent contributions from two other neuron classes, the OLQs and CEPs.

5.3.2 The TRPN channel TRP-4 acts in the CEP neurons and the TRPV channel OSM-9 acts in the OLQ neurons.

I investigated which transduction mutants affected cell-specifically the nose touch responses in the CEPs and the OLQs. I confirmed that TPR-4 is the transducer of mechanical stimuli in CEP. Previous work on the OLQs by Katie Kindt in the lab showed that animals mutant for another TRP channel, TRPA-1 were defective in repeated nose touch stimulation (Kindt KS et al, 2007b). However, Kindt et al did not examine the TRPV channel OSM-9, which is expressed in the OLQ neurons. OSM-9 has been shown to mediate nose touch responses in ASH. An *osm-9* null allele eliminates OLQ nose touch responses. Both TRP-4 and OSM-9 act in a cell-autonomous fashion to generate nose touch evoked calcium transients.

5.3.3 A Hub and Spoke Circuit controls nose touch.

The OLQs and CEPs are connected to FLP via a single interneuron, namely RIH by means of gap junctions. Mutations that disrupt sensory transduction in these neurons affect the ability of FLP to respond to nose touch. Therefore it appears that activation of the gentle nose touch neurons acts via a bidirectional flow of information in the circuit in order to facilitate low threshold responses in FLP, which is otherwise a

high-threshold nociceptor. The circuit I have explored has a number of similarities to the recently described hub and spoke circuit that controls aggregation behaviour in *C. elegans* (Macosko EZ et al., 2009). In either system, sensory information flows from the sensory neurons to the interneuron that integrates the information and acts as the hub. In addition information processed in RIH flows out to the sensory neurons, which function as behaviour specific outputs of the network. The FLP neurons function as polymodal nociceptors and also relay information to the command information in order to execute the reversal reflex. Similarly the OLQ and CEP neurons are responsible for foraging and the slowing response to food respectively. Neuroscientists often consider the responses of sensory neurons as being a direct reflection of the intrinsic properties and the external sensory cues it receives via sensory transduction pathways. The current thinking is being revised in order to incorporate the interactions between sensory neurons in modifying their properties.

Examples of networks where neurons are coupled electrically include the AB and PD cells in the stomatogastric ganglion of the lobster, which are electrically coupled by gap junctions, thus firing in synchrony and the postural network of the lamprey where the reticulospinal neurons transmitting commands from the brain to the spinal cord connect via gap junctions to the pattern generating neurons contributing to their excitation (Miller JP, Selverston AI, 1982). Notably, the role of gap junctions is not only to make just two neurons behave like one. Large populations of non-synchronized neurons have been found to connect via gap junctions. In these cases action potentials can echo through the network allowing the generation of a sustainable burst, until all the neurons have been eventually synchronized. Such a burst underlies the activity of neurons in the command system for escape swimming

reflex in the sea slug *Tritonia*. A number of examples can also be found in mammalian systems. For example chemosensory neurons in taste buds talk to each other via electrical and chemical synapses as well as by paracrine signaling (Huang YA et al., 2009; Dando R, Roper SD, 2009). In a similar fashion, extensive gap junction coupling occurs between many cell types in the retina, including rod and cone photoreceptors (Nelson R, 1977). One can parallel the functions of these connections to those in the *C. elegans* nose touch circuit. Notably, gap junctions between low-threshold rods and higher threshold cones can facilitate responses in cone cells in low ambient light (Schneeweis DM, Schnapf JL, 1995), just as electrical connectivity in the nose touch circuit can facilitate gentle touch responses in the FLP nociceptors.

However the identification of a second hub and spoke circuit in the *C. elegans* nervous system raises a number of questions. For example how does the structure of a hub and spoke network affect sensory responses and how is it that such a circuitry is more advantageous in comparison to simpler circuits with fewer neurons? One could imagine that the hub and spoke circuit is the ancestor of the structure of the neo-cortical neuron. I would describe the hub as being equivalent to the soma and the spokes as being equivalent to the dendritic branches. The gap junctions can be paralleled to the axial resistance that is observed on the dendritic tree of the elaborate cortical neurons. Alternatively one can imagine that a hub and spoke network, may act as an adaptation to overcome the down sides of iso-potential neurons. The use of mathematical modelling and the manipulation of the nose touch circuit with the use of optogenetic tools would certainly allow an extensive examination of the properties of the hub and spoke motif. This way I hope that it will soon be possible to understand

how these networks evolved and what are the computational novelties they introduced to the worm's simple nervous system.

5.4 General Conclusions

Polymodal nociceptors are capable of detecting noxious stimuli, including harsh touch, toxic chemicals and extremes of heat and cold. The molecular mechanisms by which nociceptors are able to sense multiple qualitatively distinct stimuli are not well understood. My results suggest that *C. elegans* nociceptors respond to thermal and mechanical stimuli using distinct sets of molecules and identify DEG/ENaC and TRPA-1 channels as potential receptors for mechanical pain and cold respectively.

Somatosensory circuits that gather sensory information from the skin are a feature of most animal nervous systems. These circuits include, touch neurons, proprioceptors, nociceptors and thermosensory neurons. How these neurons interact with each other to modify their properties is subject to intense investigation. My results shows that electrically-mediated lateral interactions can tune the properties of sensory neurons in the nose touch circuit of the worm. This finding suggests the existence of similar mechanisms in the nociceptive and somatosensory pathways of larger nervous systems.

5.5 References

Aguirre-Chen C, Bülow HE, Kaprielian Z (2011) C. elegans bicd-1, homolog of the Drosophila dynein accessory factor Bicaudal D, regulates the branching of PVD sensory neuron dendrites. Development 138(3):507-18

Albeg A, Smith CJ, Chatzigeorgiou M, Feitelson DG, Hall DH, Schafer WR, Miller DM 3rd, Treinin M (2011) *C. elegans* multi-dendritic sensory neurons: morphology and function. Mol Cell Neurosci. 46(1):308-317

Chelur DS, Ernstrom GG, Goodman MB, Yao CA, Chen L, O'Hagan R, Chalfie M, (2002) The mechanosensory protein MEC-6 is a subunit of the *C. elegans* touch-cell degenerin channel. *Nature* 420: 669–673

Coburn C, Bargmann CI (1996) A putative cyclic nucleotidegated channel is required for sensory development and function in *C. elegans*. Neuron 17: 695–706

Dando R, Roper SD (2009). Cell-to-cell communication in intact taste buds through ATP signalling from pannexin 1 gap junction hemichannels. J Physiol *587*: 5899-5906

Delmas P, Hao J, Rodat-Despoix L (2011) Molecular mechanisms of mechanotransduction in mammalian sensory neurons. Nat Rev Neurosci. 12(3):139-53

Dores RM, Lecaudé S, Bauer D, Danielson PB (2002) Analyzing the evolution of the opioid/orphanin gene family. Mass Spectrom Rev. 21(4):220-43

Dreborg S, Sundström G, Larsson TA, Larhammar D (2008) Evolution of vertebrate opioid receptors. Proc Natl Acad Sci U S A 7;105(40):15487-92

Du H, Gu G,William CM, Chalfie M (1996) Extracellular proteins needed for *C. elegans* mechanosensation. Neuron 16:183–194

Fajardo O, Meseguer V, Belmonte C, Viana F (2008) TRPA1 channels mediate cold temperature sensing in mammalian vagal sensory neurons: pharmacological and genetic evidence. 28(31):7863-75

Garrity PA, Goodman MB, Samuel AD, Sengupta P (2010) Running hot and cold: behavioral strategies, neural circuits, and the molecular machinery for thermotaxis in *C. elegans* and *Drosophila*. Genes Dev. 2010 Nov 1;24(21):2365-82

Goodman MB, Ernstrom GG, Chelur DS, O'Hagan R, Yao CA, Chalfie M, (2002) MEC-2 regulates *C. elegans* DEG/ENaC channels needed for mechanosensation. *Nature* 415: 1039–1042

Goodman MB, Schwarz EM. 2003. Transducing touch in *Caenorhabditis elegans*. Annu Rev Physiol 65: 429–452

Huang M, Chalfie M (1994) Gene interactions affecting mechanosensory transduction in *Caenorhabditis elegans*. Nature 367:467–470

Jordt SE, Bautista DM, Chuang HH, McKemy DD, Zygmunt PM, Högestätt ED, Meng ID, Julius D (2004) Mustard oils and cannabinoids excite sensory nerve fibres through the TRP channel ANKTM1. *Nature* 427(6971):260–65

Kim K, Li C, (2004) Expression and regulation of an FMRFamide-related neuropeptide gene family in *Caenorhabditis elegans*. *J Comp Neurol* 475: 540–550

Kindt KS, Viswanath V, Macpherson L, Quast K, Hu H, Patapoutian A, Schafer WR (2007b) *Caenorhabditis elegans* TRPA-1 functions in mechanosensation. Nature Neurosci. 10: 568-577

Komatsu H, Mori I, Ohshima Y (1996). Mutations in a cyclic nucleotide-gated channel lead to abnormal thermosensation and chemosensation in *C. elegans*. Neuron 17: 707–718

Komatsu H, Jin YH, L'Etoile N, Mori I, Bargmann CI, Akaike N, Ohshima Y (1999) Functional reconstitution of a heteromeric cyclic nucleotide-gated channel of *Caenorhabditis elegans* in cultured cells. Brain Res 821: 160–168

Kwan KY, Allchorne AJ, Vollrath MA, Christensen AP, Zhang DS, Woolf CJ, Corey DP (2006) TRPA1 contributes to cold, mechanical, and chemical nociception but is not essential for hair-cell transduction. Neuron 50(2):277-89

Miller JP, Selverston AI (1982) Mechanisms Underlying Pattern Generation in Lobster Stomatogastric Ganglion as Determined by Selective Inactivation of Identified Neurons. II. Oscillatory Properties of Pyloric Neurons. J. Neurophysiology 48(6): 1378-1391

Nagata K, Duggan A, Kumar G, Garcia-Anoveros J (2005) Nociceptor and hair cell transducer properties of TRPA1, a channel for pain and hearing. *J. Neurosci.* 25(16) :4052–61

Nelson R (1977). Cat cones have rod input: a comparison of the response properties of cones and horizontal cell bodies in the retina of the cat. J Comp Neurol *172*: 109-135

O'Hagan R, Chalfie M, Goodman MB, (2005) The MEC-4 DEG/ENaC channel of *Caenorhabditis elegans* touch receptor neurons transduces mechanical signals. *Nat Neurosci* 8: 43–50

Oren-Suissa M, Hall DH, Treinin M, Shemer G, Podbilewicz B (2010) The fusogen EFF-1 controls sculpting of mechanosensory dendrites. Science 328(5983):1285-8

Ramot D, MacInnis BL, Goodman MB (2008a) Bidirectional temperature-sensing by a single thermosensory neuron in *C. elegans*. Nat Neurosci 11: 908–915

Rankin CH, Broster BS, (1992) Factors affecting habituation and recoveryfrom habituation in the nematode *Caenorhabditis elegans. Behav Neurosci* 106: 239–249

Savage C, Hamelin M, Culotti JG, Coulson A, Albertson DG, Chalfie M, (1989) *mec-7* is a β-tubulin gene required for the production of 15-protofilament microtubules in *Caenorhabditis elegans. Genes Dev* 3: 870–881

Schneeweis DM, Schnapf JL (1995) Photovoltage of rods and cones in the macaque retina. Science *268*, 1053-1056

Smith CJ, Watson JD, Spencer WC, O'Brien T, Cha B, Albeg A, Treinin M, Miller DM 3rd (2010) Time-lapse imaging and cell-specific expression profiling reveal dynamic branching and molecular determinants of a multi-dendritic nociceptor in *C. elegans*. Dev Biol. 345(1):18-33

Story GM, Peier AM, Reeve AJ, Eid SR, Mosbacher J, Hricik TR, Earley TJ, Hergarden AC, Andersson DA, Hwang SW, McIntyre P, Jegla T, Bevan S, Patapoutian A (2003) ANKTM1, a TRP-like channel expressed in nociceptive neurons, is activated by cold temperatures. Cell 112(6):819-29

Way JC, Chalfie M (1989) The *mec-3* gene of *Caenorhabditis elegans* requires its own product for maintained expression and is expressed in three neuronal cell types. Genes Dev 3:1823–1833

Way JC, Run JQ, Wang AY (1992) Regulation of anterior cell-specific mec-3 expression during asymmetric cell division in *C. elegans*. Dev Dyn 194(4):289-302

Wicks SR, Rankin CH (1995) Integration of Mechanosensory Stimuli in Caenorhabditis elegans. J Neurosci 15(3 Pt 2):2434-44

Wicks SR, Rankin CH, (1996) The integration of antagonistic reflexes revealed by laser ablation of identified neurons determines habituation kinetics of the *Caenorhabditis elegans* tap withdrawal response. *J Comp Physiol A Sens Neural Behav Physiol* 179: 675–685

Wittenburg N, Baumeister R (1999) Thermal avoidance in *Caenorhabditis elegans*: An approach to the study of nociception. Proc Natl Acad Sci USA 96(18):10477-82

Zhang S, Arnadottir J, Keller C, Caldwell GA, Yao CA, Chalfie M (2004) MEC-2 is recruited to the putative mechanosensory complex in *C. elegans* touch receptor neurons through its stomatin-like domain. Curr Biol. 14(21):1888-96

Zhao B, Khare P, Feldman L, Dent JA, (2003) Reversal frequency in *Caenorhabditis elegans* represents an integrated response to the state of the animal and its environment. *J Neurosci* 23: 5319–5328

Zhong L, Hwang RY, Tracey WD (2010) Pickpocket is a DEG/ENaC protein required for mechanical nociception in *Drosophila* larvae. *Curr. Biol.* 20:429-434

Appendices

The following pages contain appendices relevant to each results chapter (Chapter 2-5). Each appendix is named according to the chapter.

Chapter 2 Appendix 1

Strains used in experiments described in Chapter 2

AQ2145 *ljEx19[pegl-46::YC2.3; lin-15(+)]*

AQ2124 *mec-10 (tm1552) mec-4(u231); ljEx19*

AQ2125 *trpa-1(ok999); ljEx19*

AQ2146 *mec-10(tm1552) mec-4(u253); ljEx19*

AQ2126 *mec-10(tm1552); ljEx19*

AQ2148 *osm-9(ky10); ljEx19*

AQ2143 *del-1(ok1500); ljEx19*

AQ2144 *unc-8(n491n1192); ljEx19*

AQ2284 *trp-4(ok1605); ljEx19*

NC279 *del-1(ok150)*

MT2611 *unc-8(n491n1192*)

AQ906 *bzIs17[pmec-4::YC2.12; lin-15(+)]*

AQ908 *mec-4(u253); bzIs17*

AQ1413 *mec-10(tm1552); bzIs17*

AQ2150 *mec-10(tm1552) mec-4(u253); bzIs17*

AQ2285 *unc-8(n49n1192); mec-4(u231)*

AQ2286 *del-1(ok150); mec-4(u231); ljEx19*

AQ2287 *asic-1(ok415); mec-4(u231)*

AQ2288 *asic-1(ok415); ljEx19*

AQ2270 *mec-10(tm1552); ljEx19; ljEx220[pegl-46::mec-10(+);punc-122::GFP]*

AQ2272 *mec-10(tm1552); ljEx19;ljEx221[pser-2prom3::mec-10(+);punc-122::GFP]*

AQ2273 *mec-10(tm1552); ljEx19; ljEx221*

AQ2280 *ljEx19; ljEx224[pegl-46::degt-1RNAi (Kamath); pmyo-2::GFP]*

AQ2282 *ljEx19; ljEx225[pser-2prom-3::degt-1RNAi (Kamath); pmyo-2::GFP]*

AQ2348 *ljEx246[pegl-46::trpa-1(+)]*

AQ2349 *ljEx247[pegl-46::mTRPA1]*

NC1687 *wdIs52[PF49H12.4::GFP; unc-119(+)]*

AQ2396 *ljEx250[pser-2prom3::mec-10::GFP; pmyo-2::GFP]*

AQ2400 *ljEx254[pser-2prom3::degt-1::GFP; pmyo-2::GFP]*

AQ2402 *ljEx256[pser-2prom3::degt-1::mCherry-RFP; pmyo-2::GFP]*

AQ2404 *ljEx258[pser-2prom3::degt-1RNAi(Sonnichsen); pmyo-2::GFP]; ljEx19*

AQ2405 *ljEx259[pser-2prom3::asic-1RNAi; pmyo-2::GFP]; ljEx19*

AQ2406 *ljEx260[pser-2prom3::unc-8RNAi; pmyo-2::GFP]; ljEx19*

AQ2407 *ljEx225; ljEx19; ljEx261[pser-2prom3::Cbr-degt-1; punc-122::GFP]*

AQ2408 *ljEx19; ljEx262[pegl-46::mTRPA-1; pmyo-2::GFP]*

AQ2409 *bzIs17*;*ljEx263[pmec-4::trpa-1(+); pmyo-2::GFP]*

AQ2410 *ljEx19; ljEx264[pegl-46::degt-1RNAi (Sonnichsen); pmyo-2::GFP]*

AQ2411 *ljEx258; ljEx19; ljEx261*

AQ2412 *ljEx234; ljEx19; ljEx261*

AQ2413 *ljEx266[pmec-4::Cbr-degt-1; punc-122::GFP]*

AQ2414 *bzIs17; ljEx265[pmec-4::degt-1RNAi (Sonnichsen); pmyo-2::GFP]*

AQ2415 *bzIs17; ljEx265; ljEx266*

AQ2416 *bzIs17; ljEx240[pmec-4::degt-1 RNAi(Kamath); pmyo-2::GFP]; ljEx266*

AQ2417 *mec-10(tm1552); ljEx19; ljEx230[pser-2prom-3::mec-10(cDNA)]*

AQ1044 *ljEx95 [psra-6::yc2.12; lin-15(+)]*

AX1907 *[pgcy32::YC3.60]*

AQ2427 *ljEx250; ljEx256*

AQ2428 *ljEx267[pser-2prom3::trpa-1::GFP; pmyo-2::GFP]*

AQ2437 *bzIs17; ljEx240*

AQ2435 *bzIs17; ljEx268[pmec-4::degt-1(+); pmyo-2::GFP]*

AQ2436 *mec-10(tm1552) mec-4(u2530; bzIs17;ljEx228[pmec-4::mec-10(+) pmyo-2::GFP]*

Chapter 3 Appendix 1

Strains used in experiments described in Chapter 3

AQ906 *bzIs17[pmec-4::YC2.12; lin-15(+)]*

AQ908 *mec-4(u253); bzIs17*

AQ1413 *mec-10(tm1552); bzIs17*

AQ2150 *mec10(tm1552) mec-4(u253) bzIs17*

AQ2268 *mec-10(tm1552); bzIs17; ljEx228[pmec-4::mec-10; pmyo-2::GFP]*

AQ2436 *mec-10(tm1552) mec-4(u253); bzIs17; ljEx228[pmec-4::mec-10(+); pmyo-2::GFP]*

ZB154 *zdIs5[mec-4::GFP] I, ZB2672 bzEx[mec-10::GFP; pmyo-2::GFP]*

Chapter 4 Appendix 1

Strains used in experiments described in Chapter 4

AQ2145 *ljEx19[egl-46::YC2.3; lin-15(+)]*

AQ2045 *ljIs104[cat-1::YCD3]*

AQ906 *bzIs17[mec-4::YC2.12]*

AQ1490 l*jEx130[ocr-4::YCD3]*

AQ2695 *unc-13(e51); ljIs104[cat-1::YCD3]*

AQ2126 *mec-10(tm1552); ljEx19*

AQ2270 *mec-10(tm1552); ljEx19; ljEx220[egl-46::mec-10(genomic); unc-122::GFP]*

AQ2692 *mec-10(tm1552); ljEx381[egl-46::mec-10(cDNA); elt-2::RFP]*

AQ2693 *mec-10(tm1552); ljEx382[egl-46::mec-10(cDNA); elt-2::RFP]*

AQ2694 *mec-10(tm1552); ljEx381; ljEx19[egl-46::YC2.3; lin-15(+)]*

AQ2697 *mec-10(tm1552); ljIs104 [cat-1::YCD3]*

AQ2698 *mec-10(tm1552); ljEx381; ljIs104 [cat-1::YCD3]*

AQ2699 *mec-10(tm1552); ljEx130 [ocr-4::YCD3]*

AQ2700 *mec-10(tm1552); ljEx381; ljEx130 [ocr-4::YCD3]*

AQ2481 *mec-10(tm1552);bzIs17; ljEx275[mec-4::mec-10(cDNA)]*

AQ1413 *mec-10(tm1552);bzIs17*

AQ2701 *mec-10(tm1552);bzIs17; ljEx381*

AQ2125 *trpa-1(ok999); ljEx19*

AQ1491 *tpra-1(ok999); ljEx130[ocr-4::YCD3]*

AQ2679 *trpa-1(ok999); ljEx373[ocr-4::trpa-1(cDNA);unc-122::GFP]*

AQ2680 *trpa-1(ok999); ljEx374[ocr-4::trpa-1(cDNA);unc-122::GFP]*

AQ2696 *trpa-1(ok999); ljEx374; ljEx130[ocr-4::YCD3]*

AQ2681 *trpa-1(ok999); ljEx374; ljEx19[egl-46::YC2.3]*

AQ2682 *trpa-1(ok999); ljEx374; ljIs104[cat-1::YCD3]*

AQ2702 *trpa-1(ok999); ljIs104[cat-1::YCD3]*

AQ1492 *trpa-1(ok999); ljEx115[pdel-2::trpa-1(cDNA);unc-122::GFP]; ljEx130*

AQ2265 *trpa-1(ok999); ljEx115; ljEx19[egl-46:;YC2.3]*

AQ2262 *trpa-1(ok999); ljEx19; ljEx119[sra-6::trpa-1(cDNA) unc-122::GFP]*

AQ2574 *unc-7(e5); ljIs104[cat-1::YCD3]*

AQ2683 *unc-7(e5); ljEx375[egl-46::unc-7(cDNA);cat-1::unc-7(cDNA);elt-2::RFP]*

AQ2684 *unc-7(e5); ljEx376[egl-46::unc-7(cDNA);cat-1::unc-7(cDNA);elt-2::RFP]*

AQ2685 *unc-7(e5); ljEx384; ljIs104[cat-1::YCD3]*

AQ2703 *unc-7(e5); ljEx19[egl-46::YC2.3]*

AQ2707 *unc-7(e5); ljEx384; ljEx19[egl-46::YC2.3]*

AQ2148 *osm-9(ky10); ljEx19[egl-46::YC2.3]*

AQ2149 *osm-9(ky10); mec-10(tm1552); ljEx19[egl-46::YC2.3]*

AQ2274 *osm-9(ky10); ljEx19; ljEx222[sra-6::osm-9(genomic);unc-122::GFP]*

AQ2294 *osm-9(ky10); ljEx19; ljEx235[del-2::osm-9(genomic);elt-2::RFP]*

AQ2686 *osm-9(ky10); ljEx377[egl-46::osm-9(cDNA);elt-2::RFP]*

AQ2687 *osm-9(ky10); ljEx378[egl-46::osm-9(cDNA);elt-2::RFP]*

AQ2688 *osm-9(ky10); ljEx377; ljEx19[egl-46::YC2.3]*

AQ2689 *osm-9(ky10); ljEx379[ocr-4::osm-9(cDNA);elt-2::RFP]*

AQ2690 *osm-9(ky10); ljEx380[ocr-4::osm-9(cDNA);elt-2::RFP]*

AQ2691 *osm-9(ky10); ljEx380; ljEx130[ocr-4::YCD3]*

AQ2284 *trp-4(ok1605); ljEx19[egl-46::YC2.3]*

AQ2266 *trp-4(ok1605)ljEx19; ljEx128[dat-1::trp-4(+); unc-122::GFP]*

AQ2704 *trp-4(ok1605);osm-9(ky10); ljEx19[egl-46::YC2.3]*

AQ2705 *trp-4(ok1605); ljEx128; ljIs104[cat-1::YCD3]*

AQ2706 *ljEx383; Ex[dat-1::GFP]*